Characteristics and Ore Genesis of the Mount Cuthbert Deposit, Kalkadoon-Leichardt Belt, Mt Isa Inlier, North West Queensland.

Thesis submitted in accordance with the requirements of the University of Adelaide for an Honours Degree in Geology

Callum Murison

November 2015

THE UNIVERSITY of ADELAIDE

ABSTRACT

The Mount Cuthbert mine is situated ~100km NE of Mt Isa near the eastern edge of the Kalkadoon Leichhardt Belt (KLB); a Proterozioc block of the Mt Isa Inlier that divides the world class mineral regions of the IOCG-style Eastern Fold Belt (EFB) and the Mount Isa style copper deposits of the Western Fold Belt (WFB). KLB hosted deposits display characteristics related to both the EFB and WFB style of mineralisation; however mineralisation at Mount Cuthbert is indicative of a genesis for KLB hosted deposits related to metasomatic and tectonic events responsible for mineralisation in the EFB.

The Mount Cuthbert mine is a low tonnage-high grade, shear controlled, retrograde chalcopyrite-pyrite-pyrrhotite deposit hosted within silica-dolomite and biotite-chlorite altered schists and felsic volcanic units of the Leichhardt Volcanics. The paragenetic alteration sequence is composed of 5 alteration stages: Stage 1) sodic alteration (albite + quartz); Stage 2) K-Fe-Ca alteration (siderite + calcite + dolomite+ quartz + biotite ± magnetite ± ilmenite ± apatite ± pyrite); Stage 3) mineralisation (chalcopyrite + quartz ± pyrite ± pyrrhotite ± calcite ± chlorite); Stage 4) major chloritisation; Stage 5) oxidation and localised enrichment to chalcocite. The alteration halo within the deposit is characterised by a proximal alteration envelope (<50m) consisting of chalcopyrite, pyrite, quartz, dolomite and chlorite, an intermediate alteration envelope (50-500m) described by quartz-carbonate veining with minor chalcopyrite, pyrite and pyrrhotite, in addition to extensive biotite and chlorite alteration and minor magnetite alteration. A distal alteration envelope (>500m) is identified tentatively as albite dominant.

The trace geochemistry of the main chalcopyrite ± pyrite ore phase reveals elevated Ni, Zn, Cd and Hg in pyrite and elevated Sn, Pb, Se, V, Cr, Te, Ga, As, Cd, Mo, Ga, Bi and Sb in chalcopyrite. Differing elemental trends within the ore minerals supports paragenetic evidence suggesting several phases of sulphide growth.

The characteristics and features of the Mount Cuthbert deposit outlined in this study show the greatest number of similarities to other low tonnage-high grade, shear hosted deposits present in the KLB (i.e. Mighty Atom, Orphan). This suggests that despite having a genesis related to that of the EFB, KLB deposits are uniquely their own style of mineralisation. This supports a shear-zone associated exploration model that is specific to the KLB.

KEYWORDS

Mount Isa Inlier, Kalkadoon-Leichhardt Belt, Mount Cuthbert, ore genesis, ore geochemistry

TABLE OF CONTENTS

LIST OF FIGURES AND TABLES

INTRODUCTION

The Mount Isa Inlier in North West Queensland is a region abundant in Proterozoic Cu (-Au) ore deposits that share a common geodynamic and metallogenic history (i.e. Van Dijk, 1991; Oliver, 1995; Ford & Blenkinsop, 2008). It is comprised of 3 distinct Proterozoic blocks that make up an area >200,000km^2 (Betts et al., 2006): the Eastern Fold Belt (EFB), the Western Fold Belt (WFB) and the central Kalkadoon-Leichhardt Belt (KLB) (Figure 1, inset). Each block hosts a number of broadly coeval ore deposits which despite their shared history, display unique characteristics and styles of mineralisation. At present, related mineralisation styles are generally separated into Iron Oxide Copper Gold (IOCG) deposits of the Eastern Fold Belt and metasediment hosted breccia deposits of the Western Fold Belt (Betts et al. 2006). Research in regards to KLB hosted deposits is not extensive, and at this stage it has not been conclusively proven whether copper deposits of the KLB are more related to those of the highly metasomatised EFB, or the relatively undeformed WFB.

The Mount Cuthbert mine is situated towards the eastern edge of the KLB in the northern half of the Mount Isa Inlier (Figure 1). It is a historic copper mine recently recommissioned by Malaysian owned Malaco Leichhardt Pty Ltd as part of a tenement package that covers 856km^2, and consists of 50 granted exploration, mining and water licenses with a further 11 applications for exploration permits (malaco.com.my). The copper mineralisation at Mount Cuthbert-Kalkadoon appears to have characteristics aligned with both the EFB and WFB style of mineralisation (Rypkema, 1986) however; in regards to geochemistry, petrology, and its resemblance to other copper deposits within the Mount Isa Inlier there has been little previous research.

The project uses field and petrographic observations and geochemical data to detail the host rocks, mineralisation and alteration around the Mount Cuthbert deposit. An understanding of the controls on mineralisation will test the hypothesis that Mount Cuthbert style mineralisation can be categorised within the context of the characteristic mineralisation styles of the EFB, WFB and KLB hosted copper deposits. This work is proposed with the aim of developing a genetic model for deposits within the Kalkadoon-Leichhardt Belt in order to guide exploration strategy within Malaco Mining's exploration tenure, and within the Kalkadoon-Leichardt Belt.

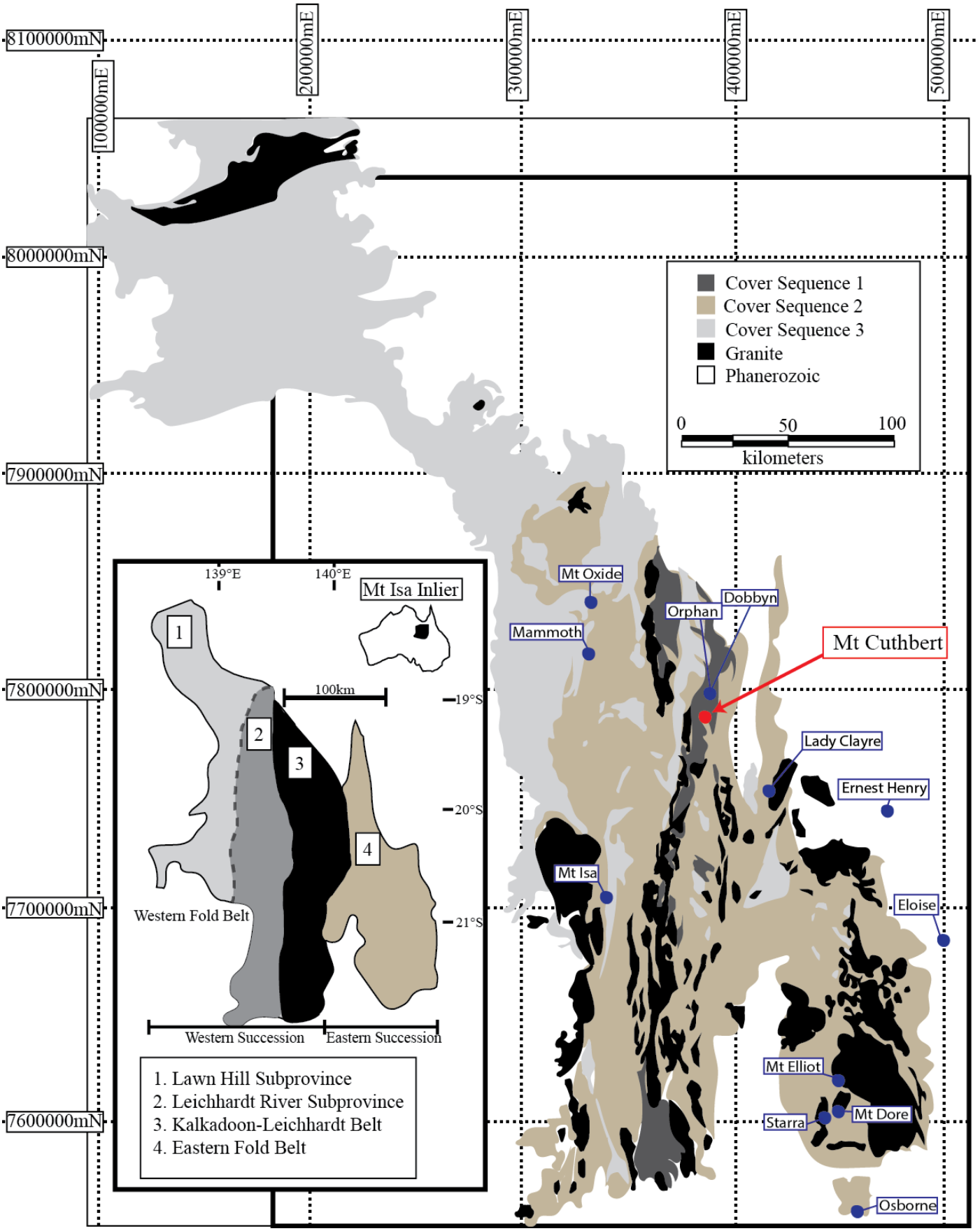

Figure 1: Map describing the separate blocks of the Mt Isa Inlier and the location of Mount Cuthbert. Modified from Queensland Department of Mines and Energy et al. (2000).

REGIONAL AND LOCAL DEPOSIT GEOLOGY

Mount Isa Inlier; Regional Geology and Formation

The Mount Isa Inlier is characterised by Palaeo- to Mesoproterozoic metasedimentary and meta-volcanic rocks, with widespread I- and A-type granitoids. Basement formation and subsequent deformation occurred during the Paleoproterozic Barramundi Orogeny (1890-1840 Ma) (Bierlein et al. 2011). These ca. 1870-1850 Ma basement rocks are commonly referred to as Cover Sequence 1 (CS1) and consist mainly of the felsic volcanics and coeval granites of the Leichhardt Volcanics and the Kalkadoon Batholith
(
Figure 2) that now comprise the majority of the KLB (Figure 1)(Murphy et al. 2011). Three major stacked superbasins followed the cessation of the Barramundi Orogeny in what is believed to be a back-arc setting (Blake et al. 1992). These include the ca. 1800-1750 Ma Leichhardt Superbasin and the ca. 1730-1690 Ma Calvert Superbasin of Cover Sequence 2 (CS2), as well as the ca. 1665-1575 Ma Isa Superbasin of Cover Sequence 3 (CS3) (Figure 1,
Figure 2). The deposition of these cover sequences was accompanied by significant (usually bimodal) igneous activity that immediately preceded and often overlapped with the beginning of each period of sedimentary accumulation (Murphy et al. 2011). Deposition was terminated by the ca. 1610-1500 Ma Isan Orogeny (and accompanying felsic magmatism in the EFB), which resulted in multiple deformation, metamorphic and metasomatic events as well as the formation of the majority of mineralisation in the Mount Isa Inlier (Page and Bell 1986).

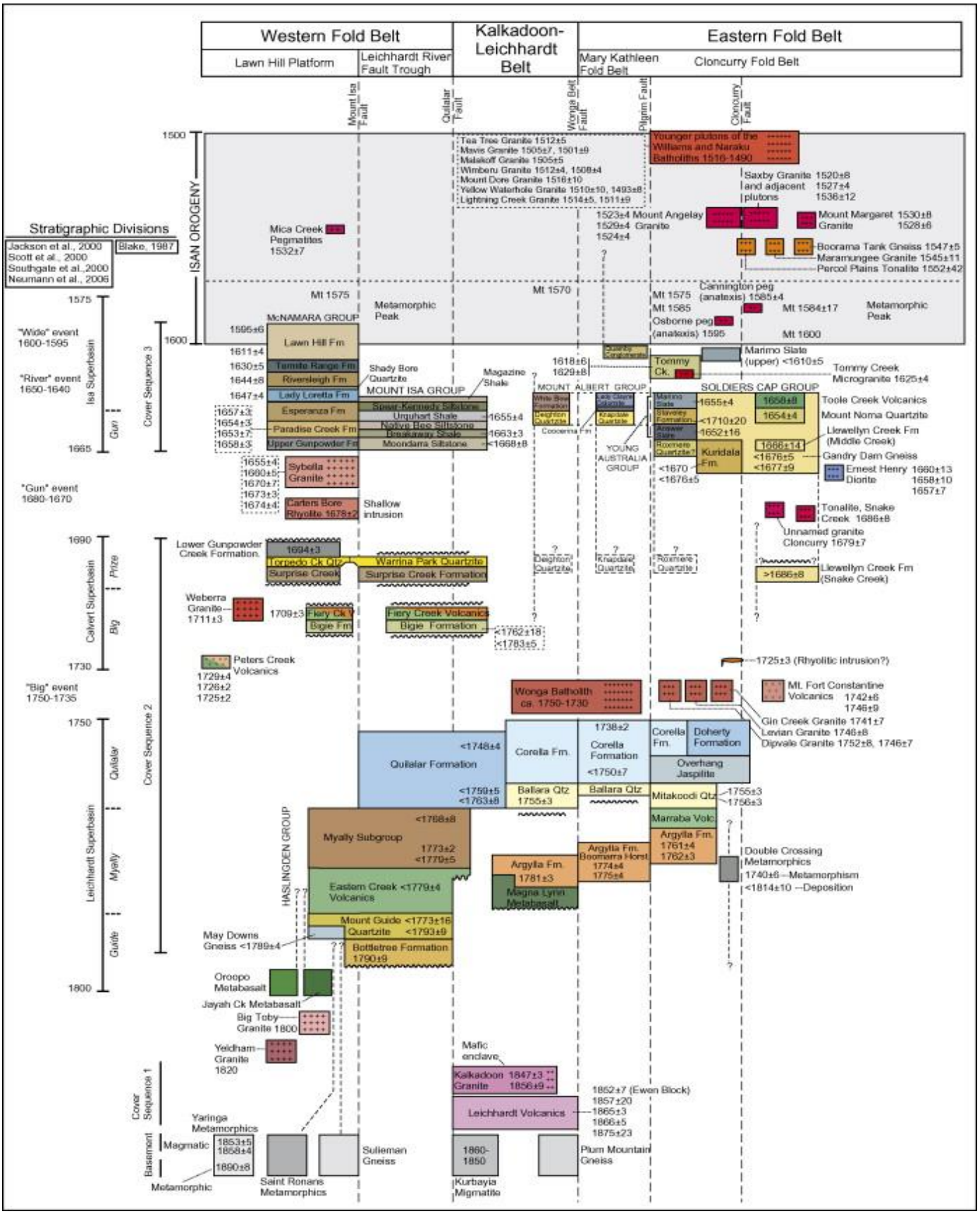

Figure 2: Chronostratigraphic framework of the Mount Isa Inlier showing cover sequence deposition, and orogenic events. On the left side superbasin and cover sequence units are grouped, and the top of the image divides lithological units into the separate blocks of the Mount Isa Inlier. The Isan orogeny, including the timing of peak metamorphism, is shaded in purple. From Foster and Austin (2008)

Alteration and Mineralisation

Although temporally related, the deformation, metamorphic and metasomatic events responsible for mineralisation have materialised with distinct characteristics in the separate blocks that comprise the Mount Isa Inlier (Betts et al. 2006, Ford and Blenkinsop 2008, Murphy et al. 2011).

EASTERN FOLD BELT

Eastern Succession copper deposits are intensely metasomatised, structurally controlled and tend to be associated with Fe oxides (Betts et al. 2006). Common feature shared between the EFB deposits are summarised in Table 1. Genesis of the EFB deposits is described by multi-staged Na(-Ca) alteration accompanied by moderate-minor K-Fe alteration (Murphy et al. 2011) that occurred over several hundred million years prior to and during the Isan Orogeny. Betts et al. (2006) attribute the earliest alteration event to ca. 1750-1730 Ma Na(-Ca) alteration, however the most extensive Na(-Ca) alteration phase is associated with granite intrusions of the Williams-Naraku Batholith (ca. 1555-1485 Ma) (Oliver 1995, Laukamp et al. 2011, Hutton et al. 2012). This regional Na-Ca alteration event was widely overprinted by moderate-minor K-Fe alteration (Laukamp et al. 2011), often in assemblages comprised of biotite, k-feldspar, hematite, pyrite and quartz, and which is associated with extensive Cu-Au mineralisation (Wyborn 1998).

(Cu) Mineral Systems	IOCG, Cu(-Au)
Host Rocks	Ironstones, carbonaceous siltstones, volcaniclastics, carbonates, mafic sills and dykes
Structural Style	Shear zone and fracture controlled deposits (i.e. Ernest Henry); Ironstone hosted stratiform deposits (i.e. Osborne, Starra)
Alteration	Na-Ca - Albite, scapolite, carbonate; K-Fe - Biotite, magnetite, hematite, k-feldspar; Sporadic sericite and silicification often limited to dilational fractures
Fluid Type	Dominant magmatic fluid: high temperature (>300-500°C), highly saline (>26-70 wt% $NaCl_{equiv}$), generally CO_2 bearing magmatic fluids that underwent fluid mixing with less prevalent sedimentary and metamorphic fluid
Other Features	Wide range in Cu:Au ratios, intensely metasomatised, associated with Fe-oxides, spatially associated to plutonic igneous rocks
References	Oliver (1995), Williams (1998), (Rubenach 2005), Mark et al. (2006), Duncan et al. (2011), Murphy et al. (2011)

Table 1: Table depicting characteristic features of EFB-hosted copper deposits

WESTERN FOLD BELT

Western Succession copper deposits are generally vein or breccia hosted quartz-copper-carbonate deposits in which formation is suggested to be due to the circulation of low-moderate temperature (270-350°C), Sulphur-enriched, hydrothermal brines derived from evaporites, and enriched by the Cu-bearing mafic rocks of the Eastern Creek Volcanics (ECV). Common feature shared between the WFB deposits are summarised in Table 2.

Waring et al. (1998) infer from their WFB based study of $\delta^{13}C$ and $\delta^{18}O$ isotopes in quartz and carbonate veins that many of the WFB deposits had formed from the same style of Cu-bearing hydrothermal fluid-host rock interactions that occur at the Mt Isa Mine. Their study also reveals an alteration envelope depleted in K_2O/K_2O+Na_2O that surrounds the Mt Isa copper orebody, as well as a mineralisation vector defined by

dolomite ± chalcopyrite veins that increase in intensity and abundance towards a massive sparry dolomite-ankerite-quartz-chalcopyrite core.

The relationship between WFB deposits is supported by the similarities in the nature of WFB deposit host rocks (commonly silica-dolomite) as well as their tendency to be spatially association to the ECV (i.e. Mt Isa, Mount Oxide, Lady Annie, Mammoth) (Blake 1987, Van Dijk 1991)). A WFB exploration model may therefore be described by K_2O/K_2O+Na_2O depletion in the surrounding rock, and where there is also evidence of the gradation of dolomite ± chalcopyrite veins towards a mineralised point that is abundant in carbonaceous material and located proximal to the ECV.

(Cu) Mineral Systems	Cu (Au poor)
Host Rocks	Units of the Mt Isa Group (i.e. siltstones and shales); Whitworth Quartzite of the Myally Subgroup (i.e. Mammoth)
Structural Style	Sediment hosted vein or breccia (i.e. Mt Isa)
Alteration	Silica-dolomite, no or minor syn-ore Fe-oxides
Fluid Type	Dominant metamorphic: low-moderate temperature, low salinity
Other	Low redox systems that contain elevated Co and As, spatial association to the Eastern Creek Volcanics (ECV)
Referenecs	Blake (1987); Van Dijk (1991), Waring et al. (1998), Williams (1998), Murphy et al. (2011)

Table 2: Table depicting characteristic features of WFB-hosted copper deposits

KALKADOON LEICHHARDT BELT

Previous workers indicate that Cu ± Au deposits of the KLB are generally small and occur as single or multiple vein lodes within shear zones and faults (Raymond 1992). Their occurrence is reasonably abundant; however their small size makes many prospects uneconomic in today's market. Adding to the comparatively low number of

operating sites in the KLB is the historic small-scale "gouger" copper mining industry of the early 1900s, which has removed much of the most easily extracted metals in the region (Hutton et al. 2012). The result of this is a lack of recorded research on deposits of the KLB; however some similarities between KLB deposit characteristics can be discerned from the few available sources (Carter et al. 1961, Krosch and Sawers 1974, Brooks 1977, Derrick and Wilson 1982).:

Host Rock	Carbonaceous and pyritic schists, calc-silicate rocks, metabasalts, felsic volcanics and felsic igneous rocks
Host Unit	Argylla Formation (i.e. Mount Hope, Mighty Atom, Wee MacGregor), Leichhardt Volcanics (i.e. Dobbyn, Orphan)
Style	Deposits are shear zone and fracture hosted vein deposits
Alteration	Silicification, biotisation and chloritisation, minor magnetism
Metamorphism	Lower amphibolite and greenschist facies
Secondary enrichments	Gold, silver, bismuth

Table 3: Summary of common features shared by Cu-deposits hosted by the Kalkadoon-Leichhardt Belt (Carter et al. 1961, Krosch and Sawers 1974, Brooks 1977, Derrick and Wilson 1982).

MOUNT CUTHBERT LOCAL GEOLOGY

The area that makes up the mine area of the Mount Cuthbert mine is a merger of the historic workings of the Mount Cuthbert open pit in the South and the Kalkadoon underground workings in the North. The lithology is comprised predominantly of greenschist facies biotite/chlorite-quartz schists (Marlow, 1977, Williams, 1998), separated from a large porphyritic granodiorite body by an intensely chloritised N-S shear zone (Figure 3) (Rypkema, 1986). Previous workers (i.e. Marlow, 1977; Rypkema, 1986) have not reached agreement on whether the host rocks that contain the Mount Cuthbert deposit belong to Leichhardt Volcanics and comagmatic felsic

intrusions of the Kalkadoon Batholith (ca. ~1845 - ~1898 Ma; Foster and Austin 2008), or to the felsic volcanics of the Argylla Formation (ca. 1762 Ma; Page and Bell 1986). Mineralisation is controlled by the N-S shear zone and has been suggested to plunge steeply towards the South (Cavaney, 1970). Sulphides occur predominantly as chalcopyrite-pyrite-pyrrhotite and are primarily hosted in a brecciated quartz-dolomite gangue, commonly in association with biotite and retrograde chlorite alteration.

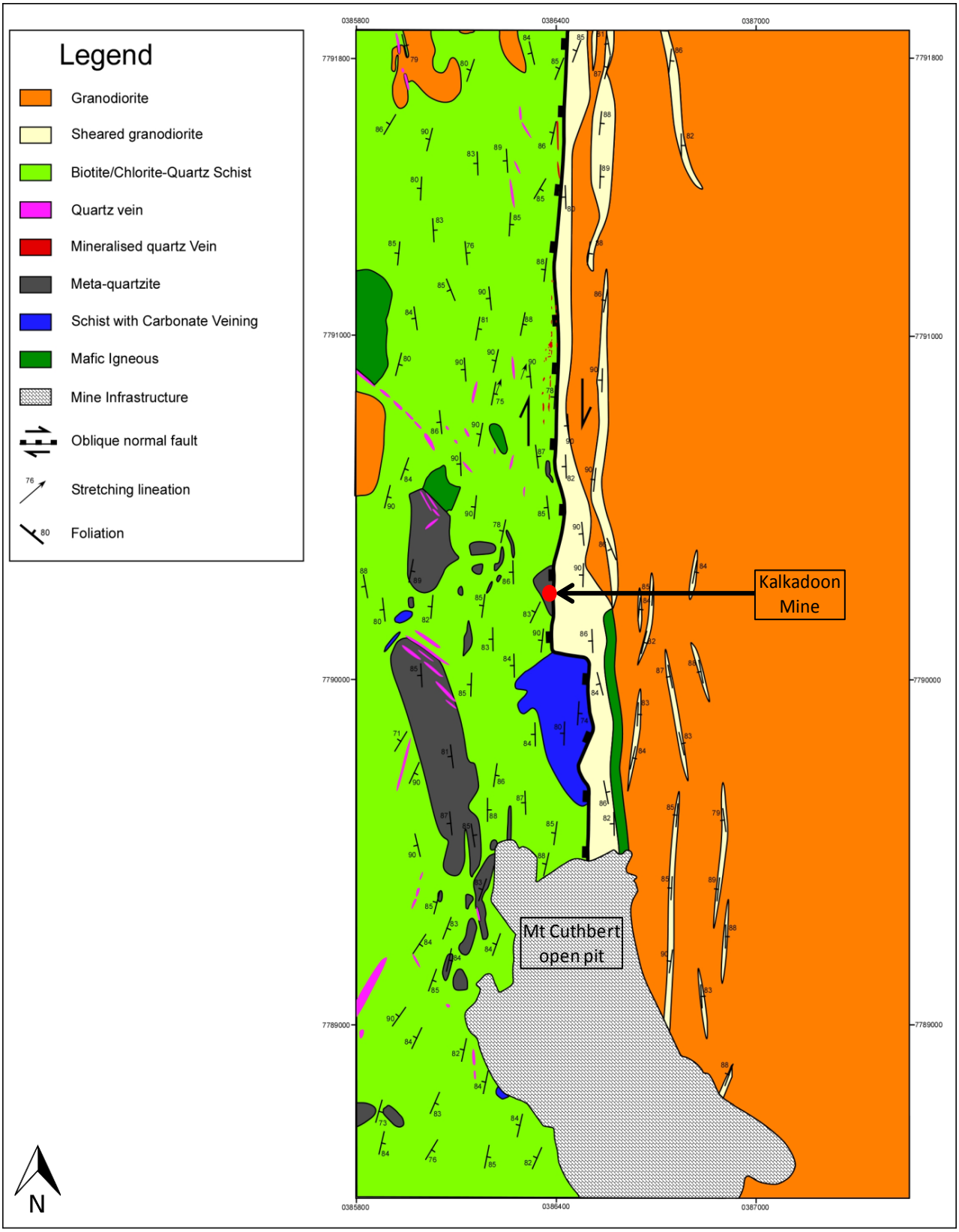

Figure 3: Structural map of the Mount Cuthbert mine (*pers. comm.* Christie et al., 2015).

METHODS

Sampling

Drill core logs were produced for 24 holes representing a North-South section between the Mount Cuthbert and Kalkadoon workings (Figure4). These include 3 recently drilled 63.5mm HQ diamond drill core and 21 stored at the Geological Survey of Queensland's Mount Isa core store including historical HQ, NQ diamond drill core and rock chips from Reverse Circulation (RC) drilling.

Drill core was logged for lithology, alteration and sulphides as well as vein abundance, style and mineral constituents. HQ diamond drill core was logged in 0.5m intervals, whereas the historical core (often degraded and weathered) was logged in intervals representing one lithology type. The data for each drill core was later reformatted using the MapInfo program and augmented through the addition of assay data where available, and displayed in a vertical striplog.

From these drill holes a total of 108, ~10cm quarter core samples representative of mineralisation, host rocks, veining and alteration were selected for detailed analysis at the hand sample scale. The most representative 29 samples were selected to be made into thin sections for petrology and 9 of these were sent to Roger Taylor of R G Taylor, Geological Services (Appendix A). Roger Taylor provided preliminary petrology and paragenesis reports that served as a basis for more in depth thin section analysis. The remaining thin sections underwent optical microscopy on the Nikon Eclipse LV100

POL Petrographic Microscope to assess host rock petrology, ore zone mineralogy and paragenesis.

SEM

The Philips XL-30 Scanning Electron Microscope (SEM) was used for textural and mineralogical analysis of Mt Cuthbert ore mineralogy. The SEM was equipped with an energy-dispersive X-ray spectrometer and was used to identify accessory minerals within the sample. Back-scattered electron (BSE) imaging was also used to select areas for further trace element analysis.

LA-ICPMS

In situ Laser Ablation-Inductively Coupled Plasma -Mass Spectrometry (LA-ICP-MS) on a UP-213 NdYag New Wave pulsed solid state laser (UP-213 New Wave) coupled to an Agilent 7500cx ICP- Quadrupole Mass Spectrometer was utilised to broadly target major sulphides in the deposit for trace element composition and zonation. Sulphide size and morphology varied in order to maximise the potential for trace element detection and care was taken where possible to avoid mineral inclusions within the sulphides. Further details of analytical methods, standards and calibration are given in Cook et al. (2013b). Data was reduced using the GLITTER data reduction software and compiled into tables using Microsoft Excel (Appendix B).

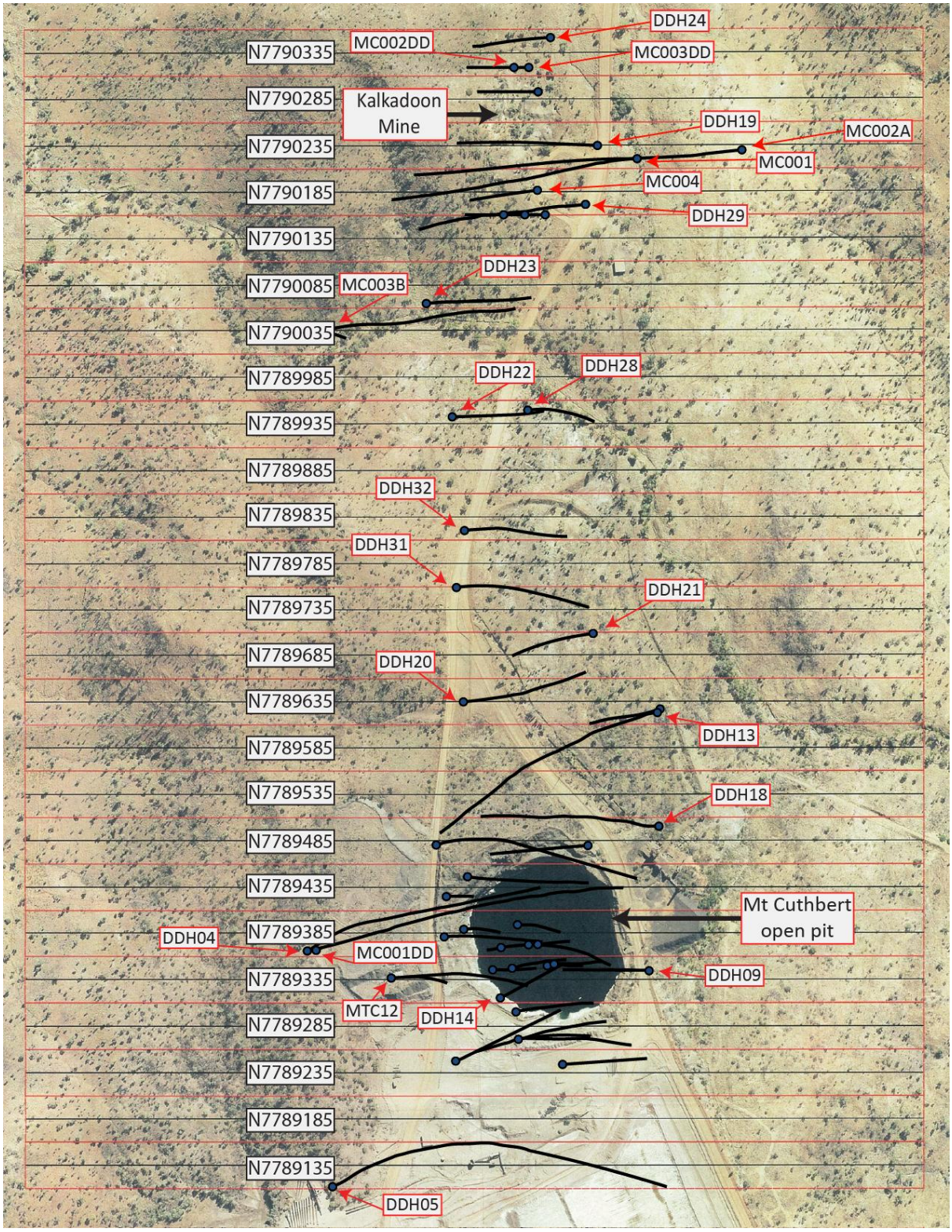

Figure 4: Plan view depicting drill holes for 24 holes representing a North-South section between the Mount Cuthbert and Kalkadoon workings.

OBSERVATIONS AND RESULTS

Host Rocks

Field observation, petrology and SEM work indicate 3 main lithology types comprising the majority of the local geology of the Mount Cuthbert ore deposit. These include:

- Biotite/quartz schist ± chlorite alteration
- Felsic metavolcanics (including volcanic ash deposits) and,
- Porphyritic granodiorite

In addition to these several minor lithology types were also identified. These include:

- Mafic metavolcanics
- Coarse grained felsic igneous rocks including granite and granodiorite
- Quartzite, chert, siltstone

See Appendix C for further petrological remarks.

BIOTITE/QUARTZ SCHIST ± CHLORITE ALTERATION

Strongly foliated schist is the most abundant lithology type within the Mount Cuthbert mine area. It occurs in a variety of styles due to the differing proportions of biotite, quartz and chlorite alteration. Where chlorite alteration is most intense, rock has a light to deep green appearance, and is extremely soft. Where biotite + quartz ± chlorite occur in more even proportions the rock displays intense green and black banding, 1-5mm in thickness (Figure 5, a) that cross cut the quartz-rich host rock.

Petrological and SEM analysis of biotite/quartz schists highlight the strong fabric of biotite/chlorite bands that cut through the fine grained quartz groundmass.

Biotite/chlorite crystals average 50-100μm in diameter and quartz <100μm in diameter,

however the quartz crystals amass together to form larger pod like aggregates between foliated biotite/chlorite (Figure 6, d). The rock is comprised of approximately equal proportions of biotite + chlorite:quartz.

FELSIC METAVOLCANICS AND VOLCANICLASTIC ASH FALL DEPOSITS

The felsic metavolcanics are a group of fine grained, quartz rich volcanics that display a wide range of volcanic textures. The rocks were given the field names ‘felsic metavolcanic’, ‘volcaniclastic ash deposit’ or ‘ignimbrite’, ‘biotite-rich ignimbrite’, and ‘compositionally banded metavolcanic’; however petrology suggests these are related rock types based on the fine groundmass (<10µm) consisting of quartz ± albite ± k-feldspar that is the shared feature of these rock types.

At the hand sample scale, the groundmass takes on a light grey to purple-grey colouration (Figure 5, d). It is comprised of an amalgamation of fine minerals (<25µm in diameter) consisting of 60-70% quartz, ~20% k-feldspar and albite, and <10% biotite and a glassy aggregate of minerals that are indistinguishable under optical microscopy (Figure 6, f).

In some areas this groundmass comprises ~100% of the rock; however these areas often grade (both softly and sharply) into a porphyritic rock interpreted to be a volcaniclastic ash deposit. These ash fall units consist of angular-subangular phenocrysts that comprise 0-30% of the rock area (Figure 5, b), and occasionally display smearing (light and dark banding) due to shearing of the rock. Petrology reveals that phenocrysts are comprised of quartz, plagioclase and k-feldspar (500-2000µm) and clusters of biotite/chlorite (1000-3000µm) (Figure 6, e). Biotite/chlorite clusters are often elongated and display a common orientation.

Another style of felsic metavolcanic was given the field term ‘coarse metavolcanic’ (Figure 5, c). The coarse metavolcanic is comprised of ~50% phenocrysts of fine-medium size (~500 µm) and a mosaic textured groundmass comprised of quartz (60%), k-feldspar (20%) and albite (40%) that ranges in size from 100-200µm. Quartz phenocrysts comprise 40-50% of the rock with smaller portions of albite (~35%) and k-feldspar (~15%). In addition the rock contains elongate wispy brown biotite crystals that occupy ~5-10% of the rock.

FELSIC IGNEOUS ROCKS

Felsic igneous rocks refer to granite, granodiorite and the porphyritic granodiorite that is a major unit within the Mount Cuthbert mine area.

Granite consists of 40% potassium feldspar, 35% quartz, 20% plagioclase and minor chlorite. These minerals show strong grain contacts and have an average size of 1-1.5cm. (Figure 5, g). K-feldspar, quartz and plagioclase show strong grain contacts and have an average size of 1cm. Biotite/chlorite alteration is fine grained (<100 µm) and occasionally forms along grain boundaries of larger grains or as clustered crystals. K-feldspar has a perthitic texture and is evident as microcline in many cases (Figure 6, c).

Granodiorite is comprised of coarse grained quartz (25%), feldspar (25%), plagioclase (30%) and biotite (15%) and show strong grains contacts, averaging 1cm in size (Figure 5, h). Biotite/chlorite alteration occasionally forms along grain boundaries and feldspars are frequently overprinted by sericite alteration (Figure 9, b).

Porphyritic granodiorite is comprised predominantly of coarse quartz and potassium feldspar phenocrysts with minor plagioclase phenocrysts. These phenocrysts lay in a dark grey groundmass comprised of coarse biotite, fine grained, intergrown biotite and muscovite, and fine grained quartz (Figure 6, a). The porphyritic granodiorite displays a

phenocryst supported texture and can be distinguished from the porphyritic felsic metavolcanics by the colour and components of the groundmass and the size and abundance of the phenocrysts, which often reach 1cm in diameter. (Figure 5, e).

MAFIC METAVOLCANICS

The mafic metavolcanic is a porphyritic rock that consists of 50% elongate albite phenocrysts (1-3mm) with no common orientation in a medium to fine grained, black groundmass (<100 μm). The groundmass contains mostly biotite (35% of the total rock) with <10% magnetite and quartz, and <5% spinel, calcite, ilmenite (Figure 5, f; Figure 6, b) and a lime green granular mineral tentatively identified as epidote.

QUARTZITE, CHERT, SILTSTONE.

These sedimentary rocks occur infrequently within the Mount Cuthbert mine area. Quartzite is present as fine-grained interlocking quartz that occurs in rare packages up to 5m in thickness. Chert was recognised in one 10m package in the core logging. It is extremely fine, displays a purple colouration, and has high hardness that gives a polished look to the rock. Siltstone displays fineness similar to chert however remnants of fine banding suggesting clastic deposition and a slightly darker colour allow differentiation. It was recognised in rare instances in packages up to 5m in thickness. These units did not undergo petrological analysis.

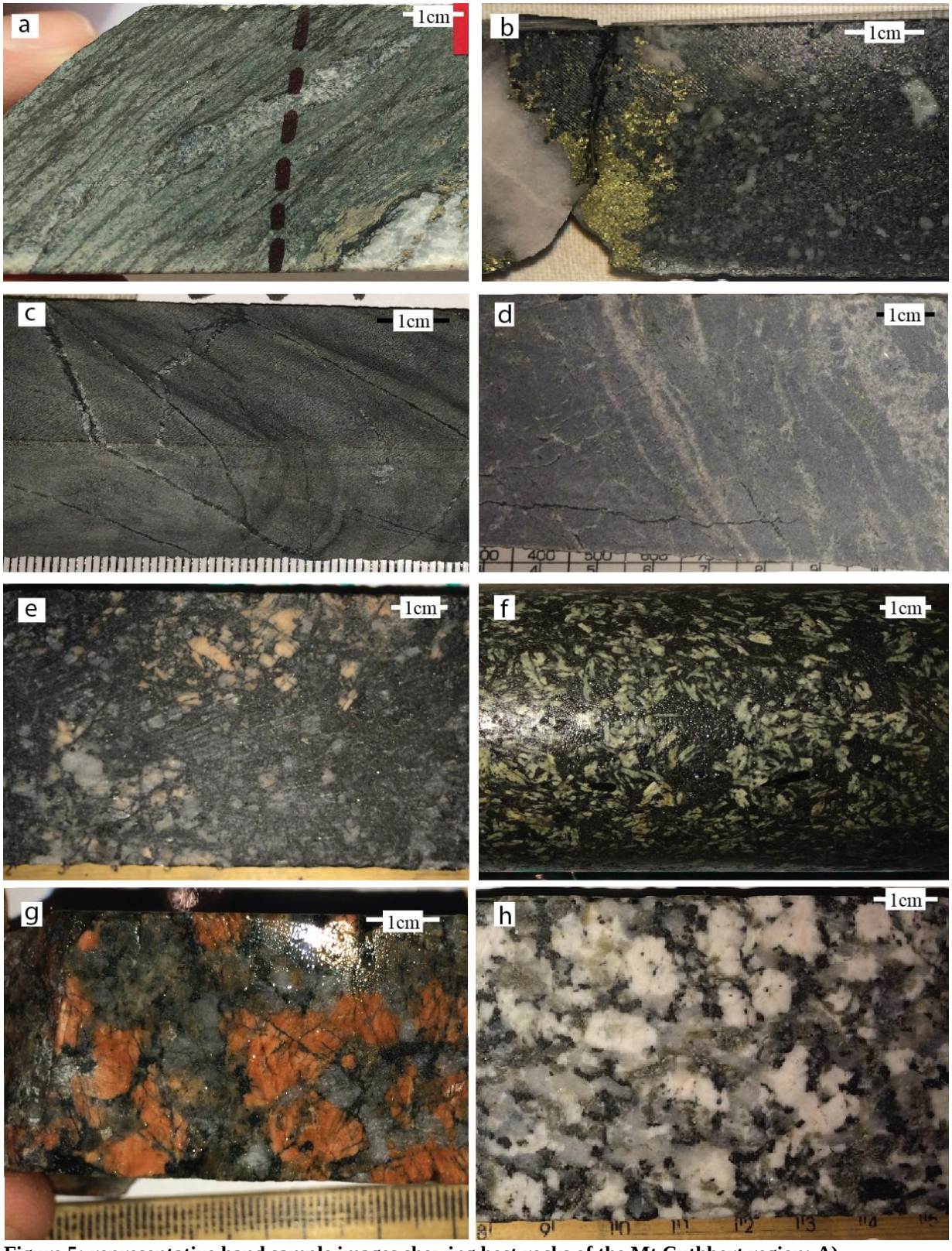

Figure 5: representative hand sample images showing host rocks of the Mt Cuthbert region: A) from hole MC001DD - shows biotite/quartz schist with moderate chlorite alteration; B) coarse grained metavolcanic from hole MC001DD; C) banded metavolcanic from hole MC001DD; D) one example of the fine grained, quartz rich groundmass with no phenocrysts; E) from hole MC001 - depicts the porphyritic granodiorite; F) elongate plagioclase grains in the mafic metavolcanic from hole MTC12; G) granite from hole MC003B; H) granodiorite from hole MC001.

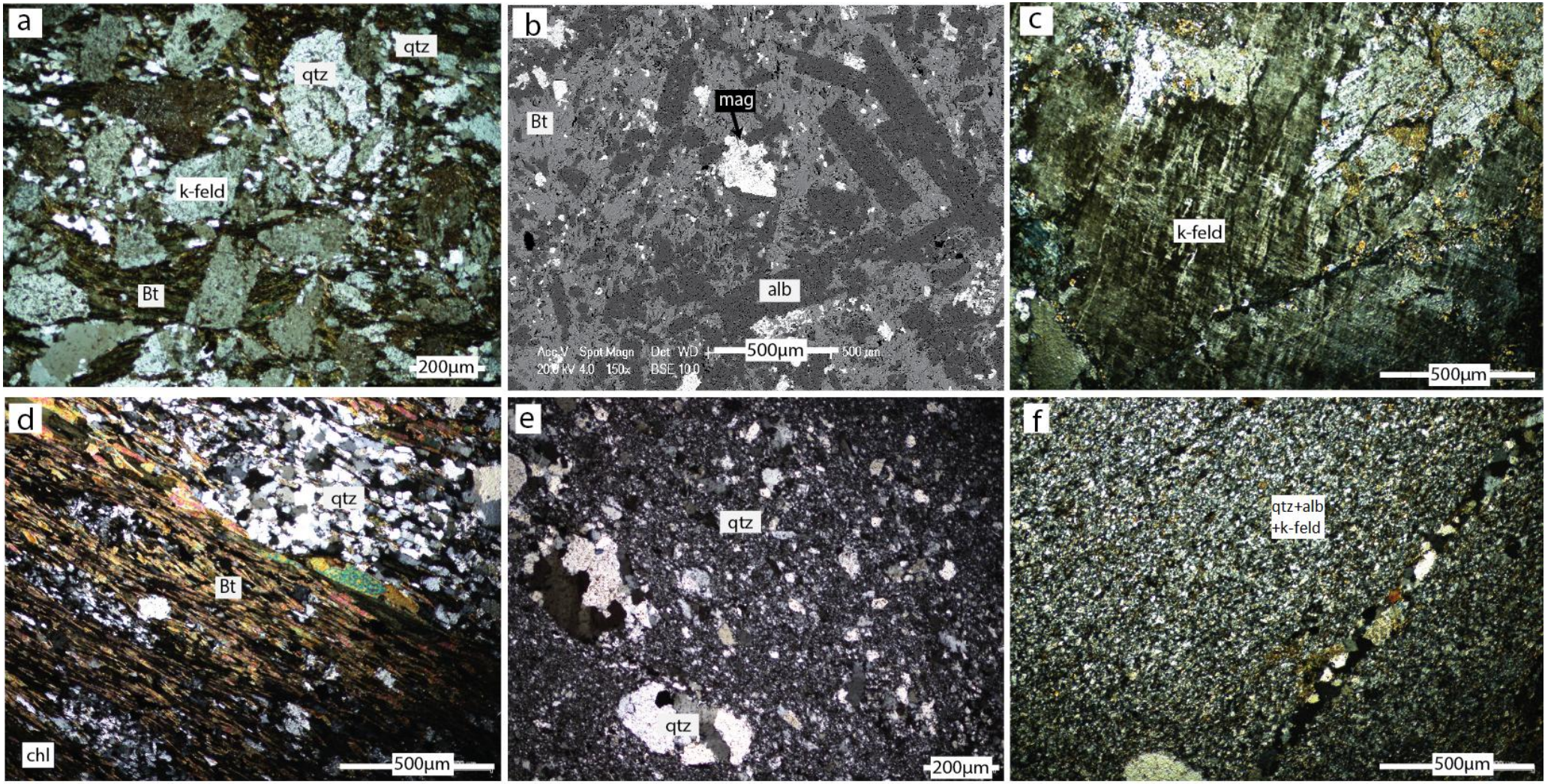

Figure 6: representative images of: A) porphyritic grandiorite displaying coarse quartz and k-feldspar phenocrysts in a fine biotite-quartz groundmass; B) SEM image of elongate albite overprinted by magnetite in a biotite groundmass from the mafic metavolcanic; C) perthitic texture of k-feldspar in granite; D) strong fabric in biotite/chlorite-quartz schist; E) quartz phenocrysts and the fine groundmass that typifies the felsic volcaniclastics; F) fine, quartz-albite-kfeld groundmass in the felsic metavolcanic.

Alteration and veining

Alteration within the Mount Cuthbert mine area reaches high intensity and produces a set of alteration types comprised of dolomite, silica, biotite, chlorite, magnetite, albite, red rock and sericite alteration along with quartz, calcite and dolomite veins.

DOLOMITE

Within the Mount Cuthbert mine area dolomite is the main host for sulphides. It occurs in massive sequence up to 65m in thickness (Figure 13) and also in smaller, irregular pods and veins that range from 10s of meters in thickness to the mm scale (Figure 7, e). The thickest package of dolomite occurs at the northern end of the Mount Cuthbert mine area, with the thickest sequences occurring between ~50-150m depth (Figure 13). Where present as veins it commonly has variable percentages of quartz (1-40%) that occur within the dolomite matrix. Dolomite veins are also associated with intense chlorite alteration.

Semi-quantitative data from SEM analysis indicate Fe-Mg zonation within the dolomite mineral structure (Figure 9, i) suggesting dolomite-ankerite zonation. Dolomite also contains early, elongate siderite prisms that have been overprinted by dolomite, chalcopyrite and pyrite. Under petrological analysis dolomite is observed to consist primarily of coarse interlocking mosaic crystals ranging from 100 μm to 1mm in diameter with varying percentages of quartz (up to 40%) as infill and as fine grained growth at dolomite crystal boundaries.

SILICIFICATION AND QUARTZ VEINING

Silica alteration is moderately abundant within the Mount Cuthbert mine area and occurs most notably as a translucent grey overprinting of dolomite (Figure 7, f; Figure 8, g), and as a major constituent of the breccia matrix in brittle fractured rocks. Outside of dolomite it occurs in small, irregular patches that result in a lightening of the rock colour as well as an increase in hardness.

At the microscopic level silicification is an extremely fine (<10μm) aggregate of quartz ± albite crystals that grow in the rock matrix between larger phenocrysts (Figure 9, d), often along grain boundaries, as well as around biotite/quartz veins as an alteration product. The fine quartz aggregates display elongation and ductile shear textures where they have been forced between larger phenocrysts (Figure 6, a).

Silicification is also present as quartz veining. Quartz veins range in thickness from 1mm-1m and display a wide variation in texture. They are common as sharp, defined veins that clearly cross-cut the host rock (Figure 7, c), as strongly foliated masses that have been overprinted by later stages of alteration (Figure 7, d) and as rounded pools that share a diffusive boundary with the host rock suggesting a ductile nature of deformation (Figure 7, a). Quartz veins are commonly made up of varying percentages of coarse calcite (1-20%) and often contain biotite in veins (Figure 19, f).

BIOTITE ALTERATION

Biotite alteration is abundant throughout the mine area where it occurs most often as fine foliated strands that crosscut existing host rock, commonly resulting in the formation of biotite-quartz schists. In the most intensely biotite altered zones biotite complete replaces pre-existing rock to form foliated bands up to 5cm in thickness

(Figure 8, f). In other instances it forms a vital part of the rock matrix, where it may form localised anastomosing meshwork patterns (Figure 9, a).

Biotite is also present commonly as an infill product in quartz veins (Figure 19, f), and as alteration surrounding both quartz veins (Figure 8, a) and dolomite veins (Figure 19, g), however it is more common to see chlorite alteration around veins, where it is assumed that retrograde replacement of biotite has occurred in later alteration events.

Biotite is also the main host to accessory minerals within the mine area. The most abundant include magnetite, ilmenite, apatite, zircon and monazite (generally monazite-Ce) with rarer bastnasite-Ce and Ti-oxide. Biotite also contains trace quantities of unidentified REE-enriched minerals such as Ca-Y-F-Oxide, Ce-F-oxide, Ce-oxide, As-Cu-Fe-Sulphide and Ni-As-Sulphide.

CHLORITE ALTERATION

Chlorite alteration occurs abundantly throughout the mine area. It is most common as a replacement product of biotite (Figure 21, e) and of actinolite (Figure 9, f). At low intensities it is present as an infill product in brittle micro-fractures (<1mm in width), as a subtle diffusive spread through the host rock restricted to small areas that are often spatially related to sulphides (Figure 11, c) and as alteration around quartz and dolomite veins (Figure 19, g). At moderate intensities it is found as fine veins, 1-5mm in thickness (Figure 5, a) that occur in association with biotite and cross cut the host rock. In the most intense cases chlorite permeates through the rock creating a nearly pure chlorite fabric (Figure 8, c; Figure 9, e) and which may overprint mineralisation and host rock constituents in an amalgamation of fine fibrous stands (<10μm in width) (Figure 21, d). The most intense chlorite alteration appears to be spatially related to dolomite.

Semi-Quantitative Analysis of chlorite reveals that the solid solution series between Fe^{2+} and Mg^{2+} in the chlorite chemical structure ($(Mg, Fe)_3(Si,Al)_4O_{10}$) tends to the Fe-rich side of the exchange. In rare instances, where chlorite comes into contact with pyrite, pyrrhotite and chalcopyrite, a Fe-rich mineral tentatively identified as Chamosite overprints the existing rock constituents (Figure 19, e; Figure 21, f).

MAGNETITE ALTERATION

Low concentrations of magnetite are present in small patches throughout the study area. It occurs as isolated crystals, scattered through the host rock, with a euhedral to subhedral shape and a diameter that reaches 1mm in size (Figure 8, b). Magnetite is frequently found as phenocrysts within finer grained biotite and chlorite, but despite its association to these strongly foliated minerals magnetite displays no evidence of strain or stress to its structure (Figure 18, d). In zones of supergene alteration proximal to the surface magnetite has been altered to hematite. SEM Semi-quantitative analysis indicates the presence of rare Fe-oxides with element ratios that suggest the reduction of magnetite to wustite, a mineral that occurs in highly reducing environments (Boctor et al. 1982).

ALBITE (± HEMATITE, K-FELDSPAR, QUARTZ, ILMENITE AND APATITE) ALTERATION

At the hand sample scale albite alteration is recognisable as a smeared colouration that ranges from brown to deep purple (Figure 7, g; Figure 8, d, f) and can be both pervasive through the host rock or present as small, intense patches. The deep purple colouration is due to variations in the abundance of extremely fine opaque minerals (Figure 9, c). SEM semi-quantitative analysis (Figure 22, a; b) suggests these opaque minerals consist

predominantly of hematite and ilmenite that occur contemporaneously with equally fine albite, K-feldspar, quartz and apatite. Coarser albite (200-500µm) frequently occurs with quartz as infill in veins (Figure 18, a) and as a fine quartz-albite groundmass. It is common to see albite alteration occurring concurrently with red-rock alteration.

RED-ROCK ALTERATION (K-FELDSPAR + ALBITE + FINE GRAINED QUARTZ ± HEMATITE ±SERICITISATION OF FELDSPARS)

Red-rock alteration is moderately abundant within the Mount Cuthbert mine area. It is most commonly found as weakly-moderately pervasive patches spread diffusely throughout the host rock (Figure 7, c; Figure 8, e) with a colour that ranges from deep red to pink. It occurs at greater intensity with the intrusion of calcite or quartz veins (Figure 8, e) and is commonly found in association with silicification and albitisation (Figure 9, c).

Petrological analysis of red-rock alteration indicates that alteration is a result of intergrown k-feldspar, albite and quartz crystals (~100µm) as well as ~10% of extremely fine (<10µm) hematite (Figure 9, h).

Sericite alteration is also present frequently in red-rock altered areas where it is found as extremely fine needle-like aggregates, usually in the core of albite and k-feldspar grains (Figure 9, b). It is also found as a matrix product with fine quartz crystals or as alteration around veins (Figure 9, d).

CALCITE VEINING

The Mount Cuthbert mine area also contains discrete zones of calcite alteration that occur in the most concentrated areas as fine stockwork veining and breccias (Figure 7, b; Figure 8, e) that are comprised of calcite infill with medium-coarse sized,

interlocking crystals (250μm to 1mm). This stockwork style veining is rare, and appears to be confined to a small area of fine felsic metavolcanic in the southern part of the mine area. It is more common to see calcite + quartz as isolated veins from 1mm-20cm in thickness. Calcite veins are also present in minor amounts as small fractures through dolomite (Figure 8, g). Calcite veining is associated with red-rock and albite alteration.

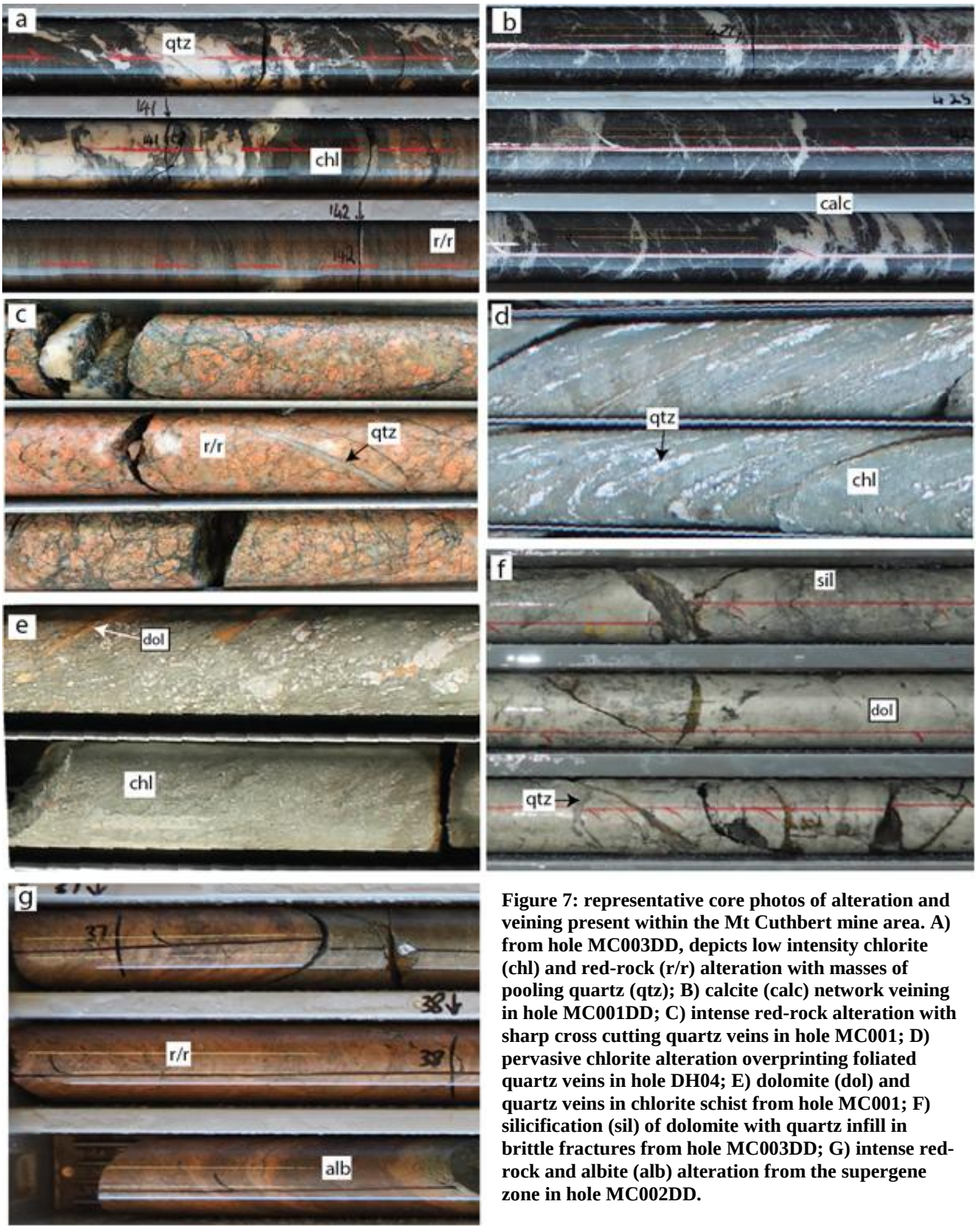

Figure 7: representative core photos of alteration and veining present within the Mt Cuthbert mine area. A) from hole MC003DD, depicts low intensity chlorite (chl) and red-rock (r/r) alteration with masses of pooling quartz (qtz); B) calcite (calc) network veining in hole MC001DD; C) intense red-rock alteration with sharp cross cutting quartz veins in hole MC001; D) pervasive chlorite alteration overprinting foliated quartz veins in hole DH04; E) dolomite (dol) and quartz veins in chlorite schist from hole MC001; F) silicification (sil) of dolomite with quartz infill in brittle fractures from hole MC003DD; G) intense red-rock and albite (alb) alteration from the supergene zone in hole MC002DD.

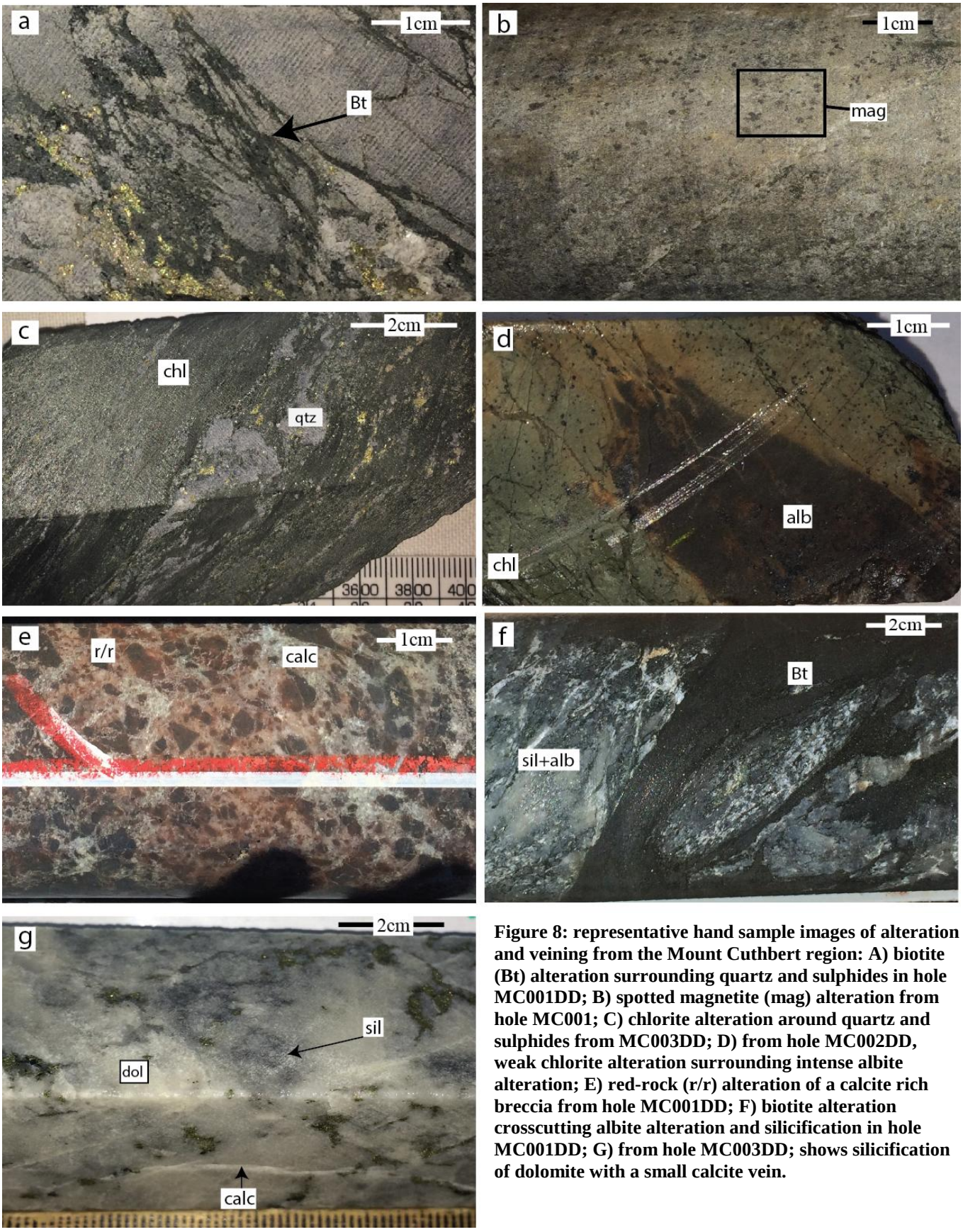

Figure 8: representative hand sample images of alteration and veining from the Mount Cuthbert region: A) biotite (Bt) alteration surrounding quartz and sulphides in hole MC001DD; B) spotted magnetite (mag) alteration from hole MC001; C) chlorite alteration around quartz and sulphides from MC003DD; D) from hole MC002DD, weak chlorite alteration surrounding intense albite alteration; E) red-rock (r/r) alteration of a calcite rich breccia from hole MC001DD; F) biotite alteration crosscutting albite alteration and silicification in hole MC001DD; G) from hole MC003DD; shows silicification of dolomite with a small calcite vein.

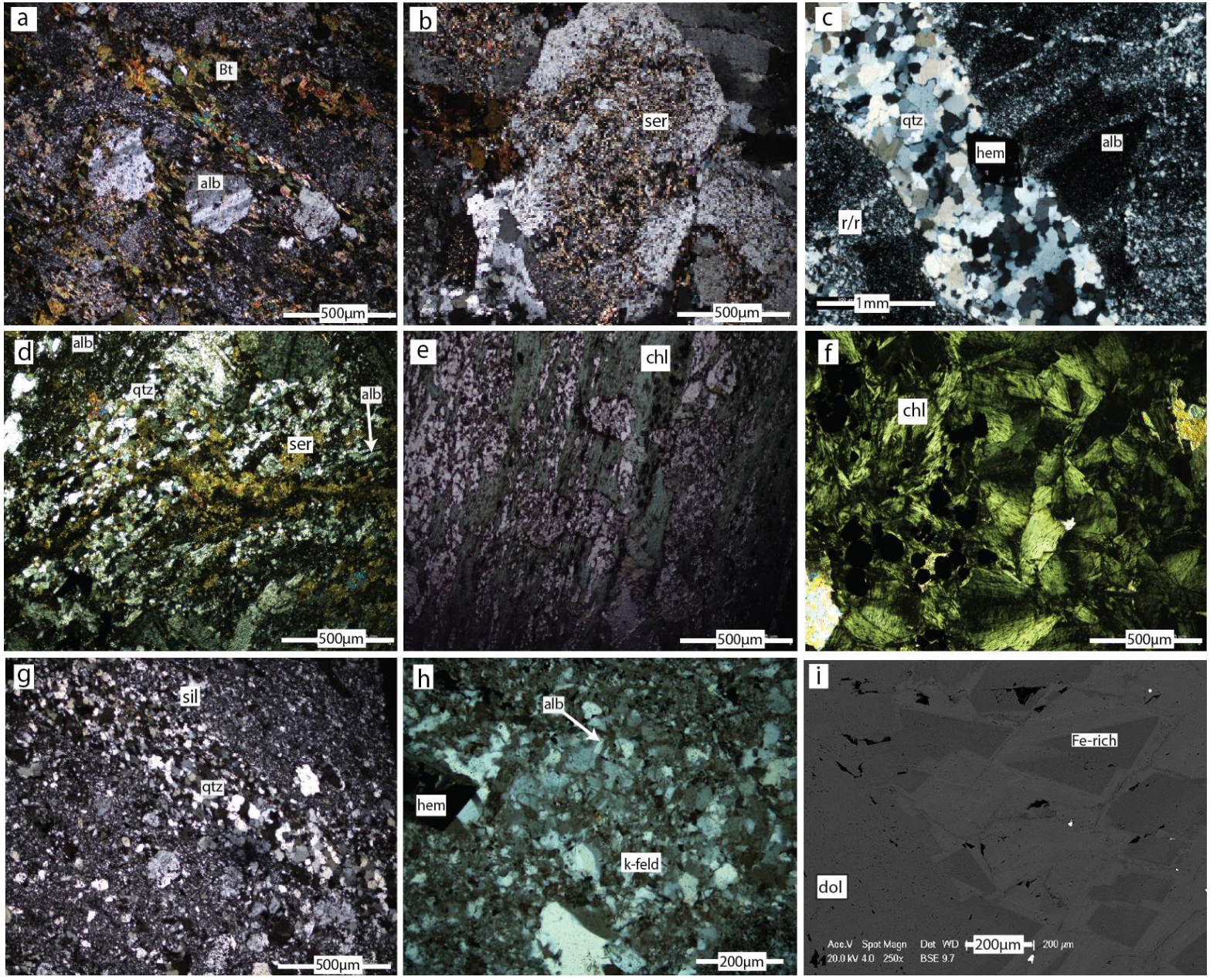

Figure 9: Petrology images representative of alteration within the Mt Cuthbert mine area: A) from MC004, depicts biotite alteration through the matrix; B) from MC003B, sericite alteration of feldspar; C) from MC002DD, shows both purple albite alteration and red-rock alteration as well as a late quartz vein; D) sericite and silicification through the matrix from MC003DD; E) pervasive chlorite alteration from MC001DD; F) chlorite pseudomorphing actinolite in MC001DD; G) silicification in MC001; H) red rock alteration from MC002DD; I) zonation in dolomite, the dark grey contains higher iron content than the surrounding light grey colour

Ore Minerals; Textures and Relationships

Ore minerals within the Mount Cuthbert mine area consists of chalcopyrite-pyrite-pyrrhotite assemblages with minor marcasite and chalcocite. The dominant ore phase is comprised of chalcopyrite + quartz ± pyrite and is most abundant in the northern section of the mine hosted by ~65m of silica altered dolomite. Mineralisation is also present at lower concentrations outside of the dolomitic unit. Similar to within the dolomite it shows spatial association to quartz/carbonate veining and can be found as a constituent of the vein, or disseminated through the surrounding rock.

SILICA-DOLOMITE HOSTED ORE

Within the silica-dolomite host, chalcopyrite ± pyrite assemblages are found as disseminated flakes within the dolomite, as infill in veins and fractures and as breccia matrix, with the most concentrated areas of mineralisation associated with the most intense silicification. The chalcopyrite:pyrite ratio heavily favours chalcopyrite, with pyrite present at low concentrations generally as euhedral crystals that lay within a chalcopyrite matrix (Figure 10, b).

The style of deposition is most commonly as chalcopyrite + quartz ± pyrite as infill in veins that cross cut the dolomite host. In the most extreme cases dolomite has been removed from the wall rock and embedded as dolomite clasts (Figure 10, a) in a chalcopyrite + quartz ± pyrite breccia matrix spanning up to 0.5m of core. Dolomite clasts are angular, subangular and sub-rounded and vary in size from 0.5-10cm. In some cases clasts show evidence of dissolution, as indicated by textural complexity at the boundary of the clasts. The matrix:clast ratio heavily favours the matrix and clasts show both evidence of minor transportation, often maintaining a similar shape to gouges in

nearby wall rock, and evidence of more significant transportation suggested by the rotation of clasts. This textural evidence has been interpreted as a hydrothermal style of breccia (Taylor and Pollard, 2006).

Chalcocite is present in 2 samples at 59.5m and 130.8m (hole MC003DD, sample #10 and #17), where it is found as fine margins that occur at the edge of some chalcopyrite crystals (Figure 10, d). The extent of the chalcocite enrichment is unclear, however the lack of chalcocite enrichment in any of the other samples from the silica-dolomite zone suggests that enrichment may be localised to small areas of the rock.

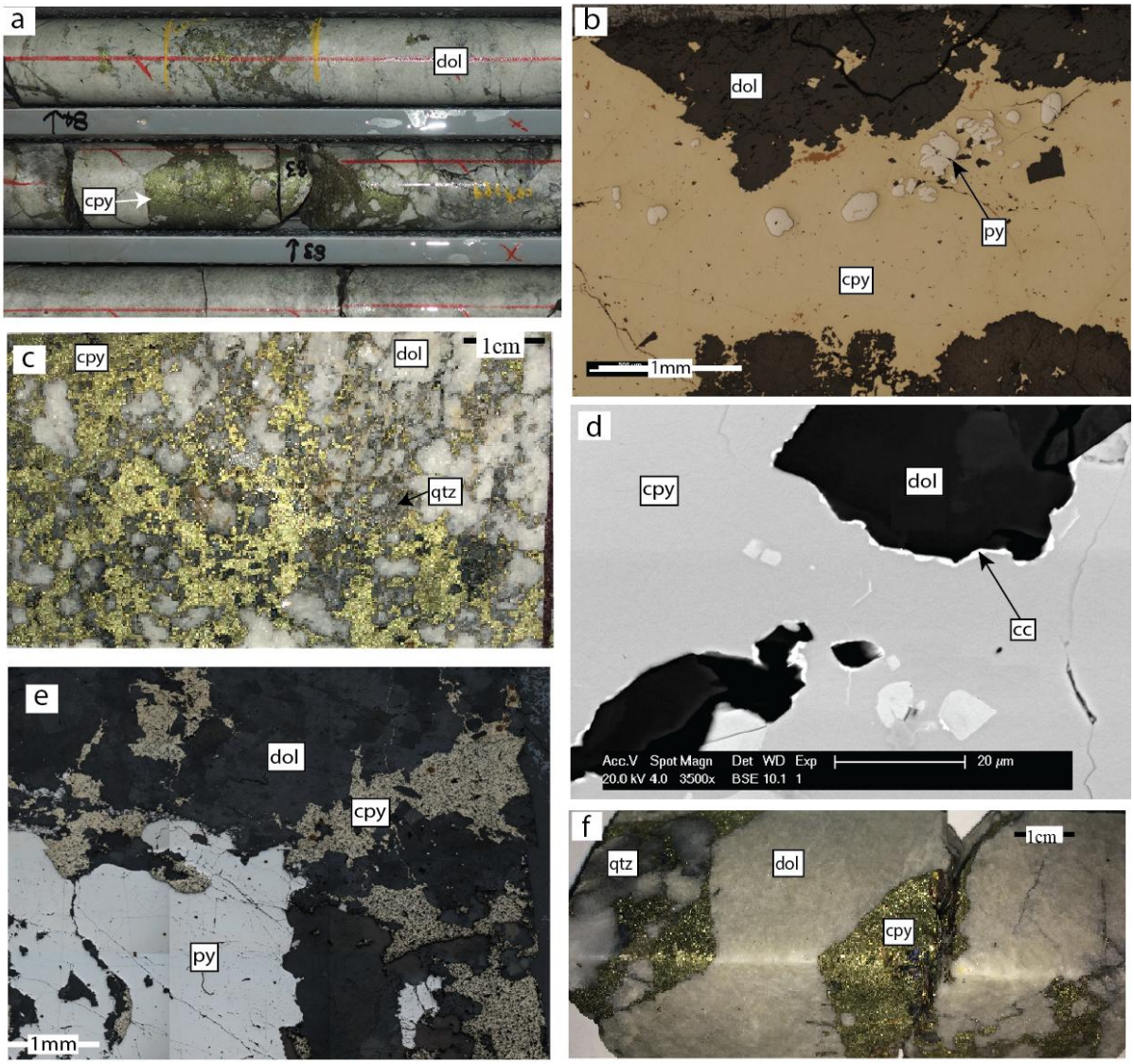

Figure 10: Representative hand sample, optical microscopy and SEM images of silica-dolomite hosted mineralisation; A) chalcopyrite rich breccia in dolomite. Subtle silicification is visible on the central right side of the image; B) early euhedral pyrite crystals in chalcopyrite infill; C) chalcopyrite + quartz as a fine breccia matrix in dolomite; D) supergene enrichment of chalcopyrite to chalcocite at crystal edges; E) coarse pyrite and surrounding chalcopyrite display an uncoupled texture in which there is no interaction between the sulphides, and chalcopyrite is deposited within depressions of the sulphide; F) chalcopyrite deposited in the neck of boundinaged dolomite.

MINERALISATION OUTSIDE THE SILICA-DOLOMITE ZONE

Outside of the silica-dolomite zone the chalcopyrite:pyrite ratio is more even. Mineralisation is present most commonly as infill in quartz-carbonate veins that crosscut the host rock and is often accompanied by chlorite alteration (Figure 11 a, c, e). It is common to see mineralisation at the outer edge of veins (Figure 11, d, h) and within the host rock adjacent to veins, where it is found as discontinuous crack style veinlets, irregular blebs and as stringers and lenses along the foliation of the host rock (Figure 11 a – left side). Coarse, euhedral-subhedral pyrite crystals are frequently found in isolation (Figure 11, c), or surrounded by anhedral chalcopyrite (Figure 11, i). In other instances chalcopyrite ± pyrite is emplaced in zones of localised extension such as within and around the neck of boundinaged dolomite (Figure 10, f) and quartz veins. Mineralisation is also deposited in deformed zones such as along the tails of (rare) sigma clasts (Figure 11, e).

A secondary, minor ore phase is chalcopyrite + pyrrhotite ± pyrite. The chalcopyrite-pyrrhotite phase displays an intergrown symplectic growth style (Figure 10, f). It is associated with calcite ± quartz veining, and occurs both within veins and in the surrounding host rock. Within chalcopyrite-pyrrhotite hosting veins chalcopyrite is present in greater abundance as infill within the vein, whereas pyrrhotite is more abundant within the host rock (Figure 10, d).

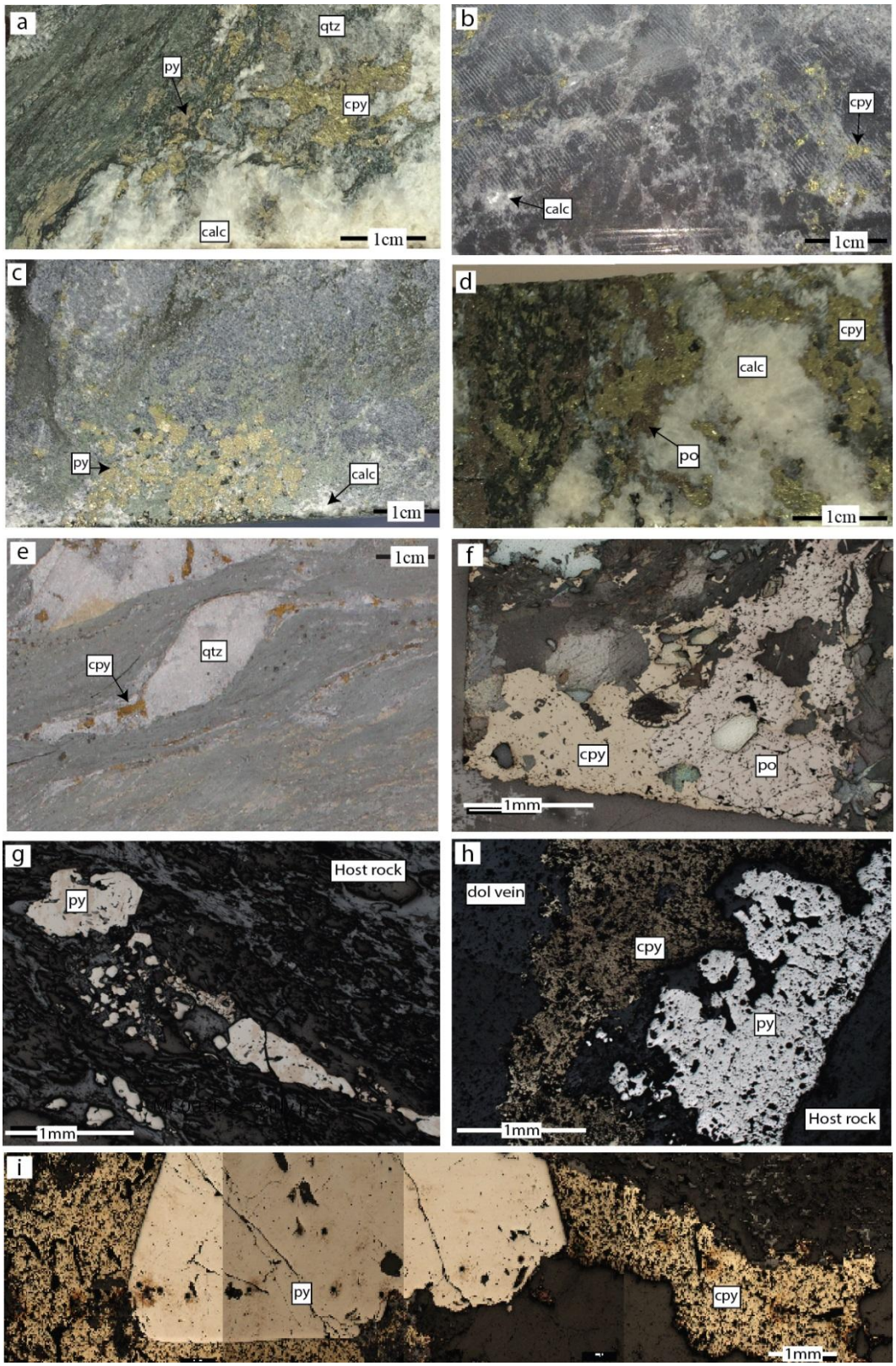

Figure 11: Representative hand sample, optical microscopy and SEM images of mineralisation outside the silica-dolomite zone: A) chalcopyrite overprinting host rock (right side) and chalcopyrite + pyrite deposited along the foliation of existing rock (left side); B) fine stockwork veining of calcite and minor chalcopyrite; C) clustered, euhedral pyrite crystals with surrounding chlorite-calcite alteration; D) intergrown pyrrhotite-chalcopyrite in a calcite vein. Pyrrhotite is in greater quantity on the host rock side of the vein; E) chalcopyrite deposited along the tails of a sigma clast; F) chalcopyrite and pyrrhotite displaying a coupled texture suggesting simultaneous growth; G) sheared pyrite; H) pyrite and chalcopyrite growth at the edge of a dolomite vein. Pyrite lies closest to the host rock, while chalcopyrite is placed towards the centre of the vein; I)) coarse pyrite and surrounding chalcopyrite, the dark box is a machine error due to the automatic contrast function, however it is still representative of pyrite texture

Textures and relationships

Chalcopyrite is frequently present as anhedral masses with a dirty appearance due to abundant inclusion within the chalcopyrite matrix. Inclusions are most commonly comprised of quartz and dolomite; however rare instances of unidentified Fe-silicates and exotic minerals including an unidentified Co-As-sulphide were documented also. Chalcopyrite also occurs with a clean, texture (Figure 10, b).

Similarly, pyrrhotite is also found frequently with this inclusion-rich texture (Figure 11, f) and is intimately associated with chalcopyrite in an intergrown symplectic manner (Figure 20, e). This is in contrast to pyrite, which most often maintains a clean surface (Figure 10, e; Figure 11, i), and tends to be less coupled to chalcopyrite than pyrrhotite (Figure 10, e; Figure 11, i). Pyrite ranges in size from <100µm – 1cm and displays several phases of pyrite growth as evidenced by its deformation (Figure 11, g) and recrystallization (Figure 11, h).

Trace mineral inclusions identified in pyrite include Te + Bi, monazite-Ce, Co-As-Sulphide and Sn. Trace mineral inclusions identified in chalcopyrite include U-Fe-Y-oxide, PbS, ZnS, Pb + Se, Zr, copper carbonate, Ag, Tc and chromium carbonate.

Core Logging and Alteration Envelopes

A proximal (<50m) alteration halo to the main mineralised zone is portrayed in Figure 13. There are several trends evident:

- Silica-dolomite hosts major mineralisation (up to 8% Cu)
- Quartz veining inside and around the dolomite body is abundant
- The copper hosting dolomite body is surrounded by rock that has been intensely chlorite altered (80-100% chlorite alteration)

- Sporadic occurrences of magnetite, albite and red-rock alteration occur
- Assay data describes peaks in Au, Co, Ni, Se, Sb, Te and Ag that correspond with peaks in Cu

Intermediate alteration (Figure 12) refers to alteration that occurs within the Mount Cuthbert shear zone, but outside of the main copper zone, from 50-500m distant. There are several trends evident:

- Mineralisation outside of the main silica dolomite zone displays an association with quartz and calcite veining. Biotite and chlorite alteration are extensive and albite and magnetite alteration are sporadic. K (%) elevated at ~3-5x average crustal levels (Rudnick and Gao 2003) throughout the core
- Pyrrhotite is closely associated with calcite veining and increased K (%) (due to biotite and red-rock alteration)
- Co, Ni, Sb, Se and Te maintain elevated values outside of the copper-rich areas, although their greatest concentration is spatially associated with copper.

Log for MC001DD

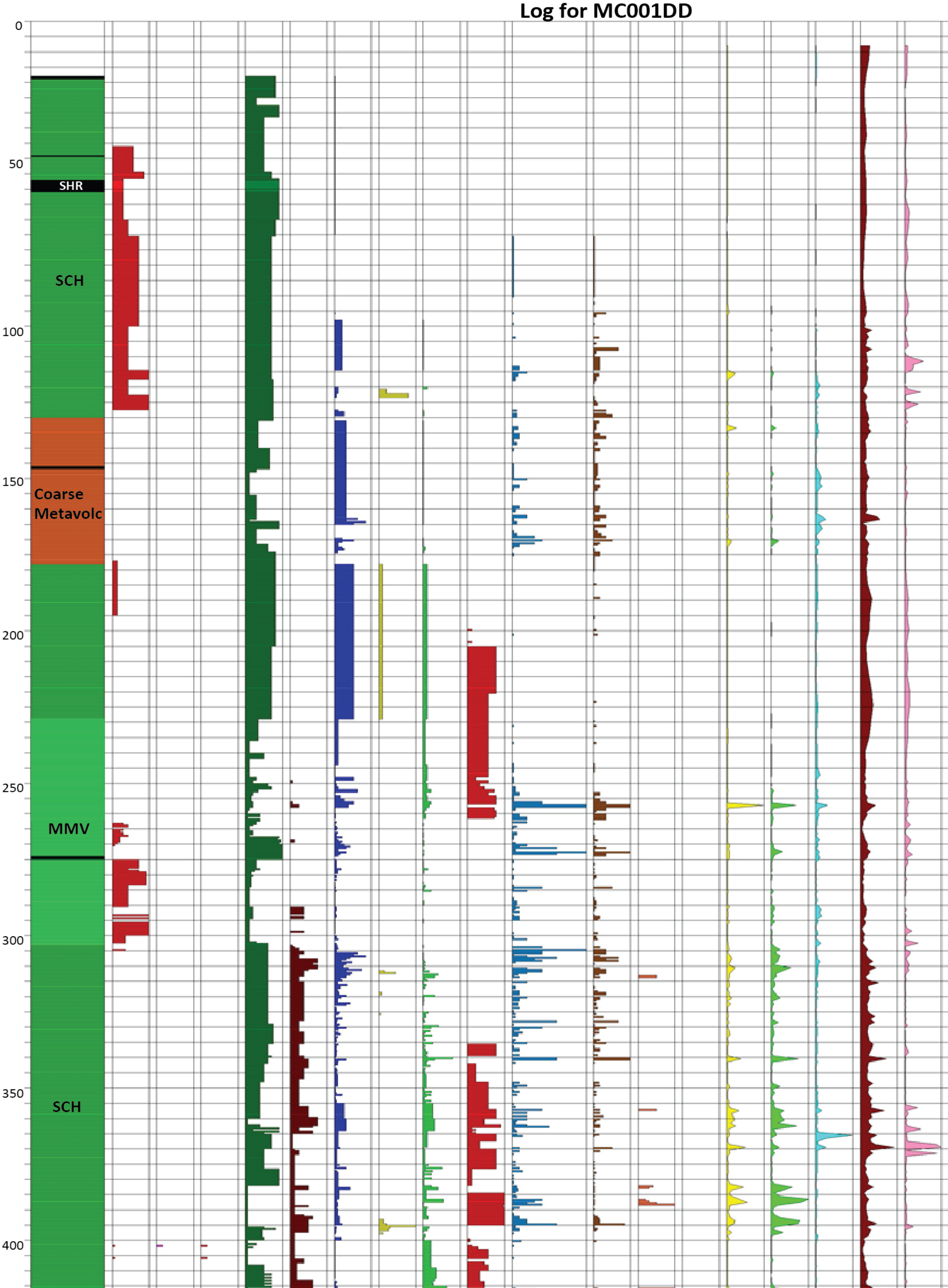

Log for MC003DD

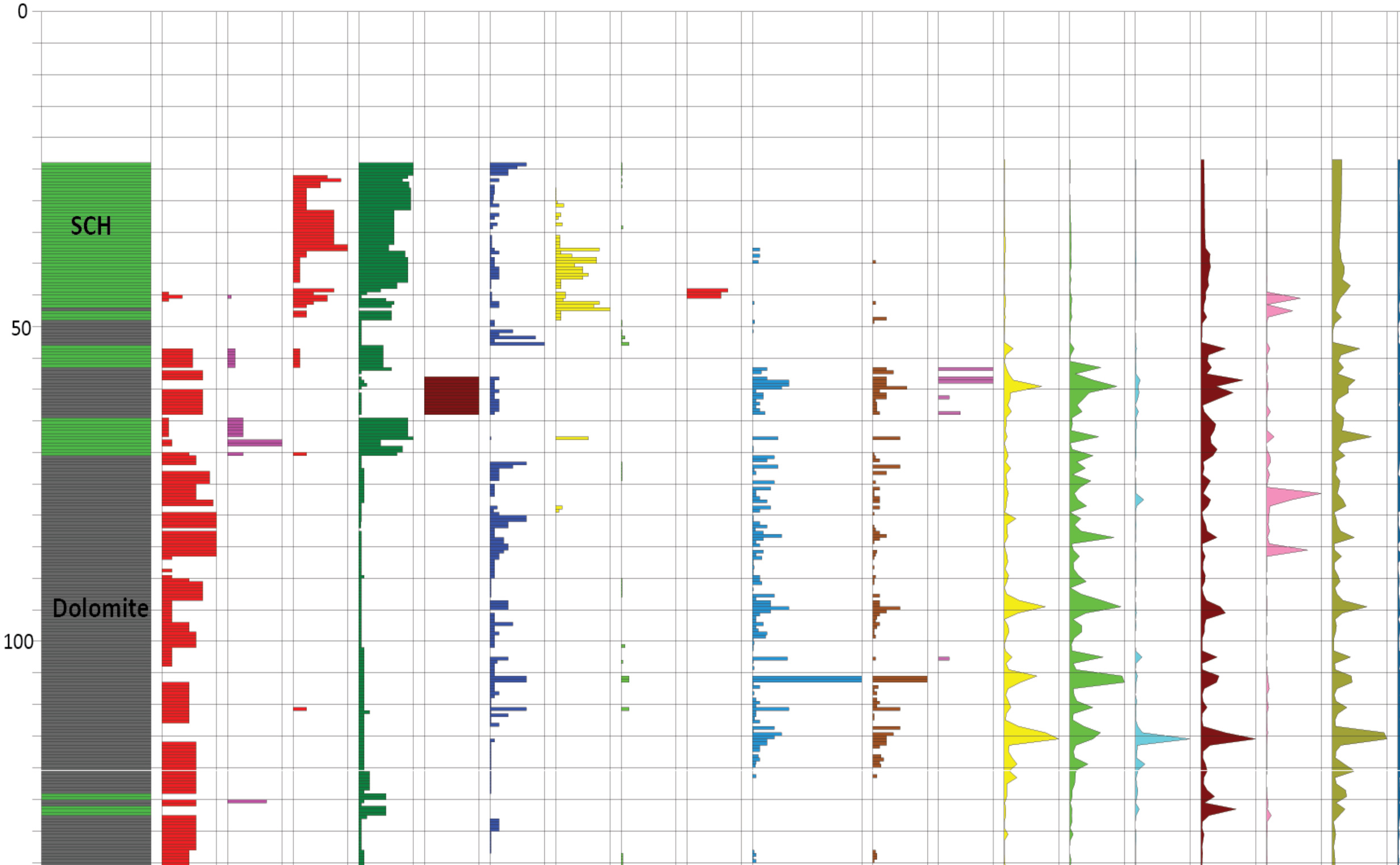

Trace geochemistry

TRACE GEOCHEMISTRY OF PYRITE

Trace geochemistry of pyrite reveals 2 trends. Trend 1 occurs in pyrites from the main silica-dolomite hosted orebody and contains elevated in Ni, Zn, Cd and Hg (pink field; Figure 14, a, b, e, f). The second trend occurs in pyrites located outside of the silica-dolomite zone. These pyrites are elevated in As, Se and Co, with a moderate elevation in Ni (green and blue fields; Figure 14, c, d, g, a).

The pyrite from MC003B (blue field; Figure 14) represents early pyrite that grew post deformation (i.e. Figure 11, g) whereas pyrites from MC001DD (green field; Figure 14) grew during the main mineralisation event. These pyrites share comparable geochemistry, however the early pyrite shows elevated Se and Co and depleted As (Figure 14, d, g, c) in comparison to the pyrites that grew during the main mineralisation event. See Appendix B for pyrite images representative of different trends.

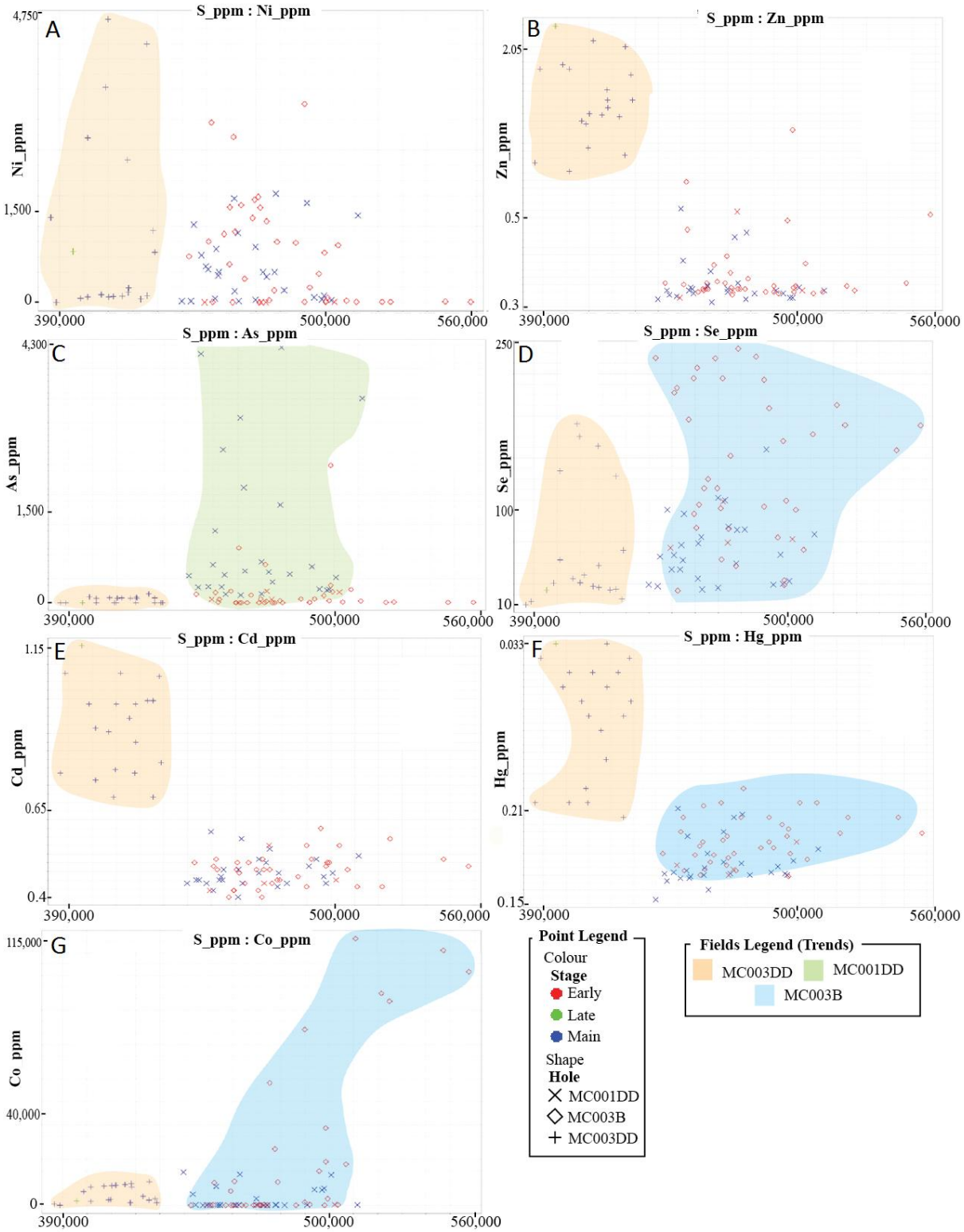

Figure 14: Graph depicting trace concetration in pyrite: A) Ni v S, elevated Ni in pyrites fromthe main mineralised zone (pink field); B) Zn v S, elevated Zn in pyrites from the main mineralised zone (pink field); C) As v S, elevated As in pyrites outside of the main mineralised zone (green field); D) Se v S, elevated Se in early pyrite (blue field), moderately elevated Se in pyrites from the main mineralised zone (pink field); E) Cd v S, elevated Cd in pyrites from the main mineralised zone (pink field); F) Hg v S, elevated Hg in pyrites from the main mineralised zone (pink field); G) Co v S, elevated Co in early pyrite (blue field).

TRACE GEOCHEMISTRY OF CHALCOPYRITE

The trace geochemistry of chalcopyrite depicts 3 trends. Trend 1 displays elevated Ga, Sn, In, Zn, Bi, Pb, Se and S in comparison to the other trends (pink field; Figure 15., d, g, I, m, n, o, p, q). This trend occurs in chalcopyrites throughout the mine area that display a clean texture with no or minor inclusions present..

The 2nd trend (purple field; Figure 15, a, b, c, d, e, f, h) has elevated V, Cr, Te, Ga, As, Cd and Mo. The chalcopyrites that comprise trend 2 are from the main mineralised zone as well as outside the mineralised zone. These chalcopyrite crystals have a high abundance of inclusions.

The 3rd trend (green field; Figure 15, j, k, l, m) shows elevated Co, Ni, Ag and Zn and occurs in chalcopyrite crystals that occur in association with pyrrhotite outside of the main mineralised zone.

See Appendix B for chalcopyrite images representative of different trends.

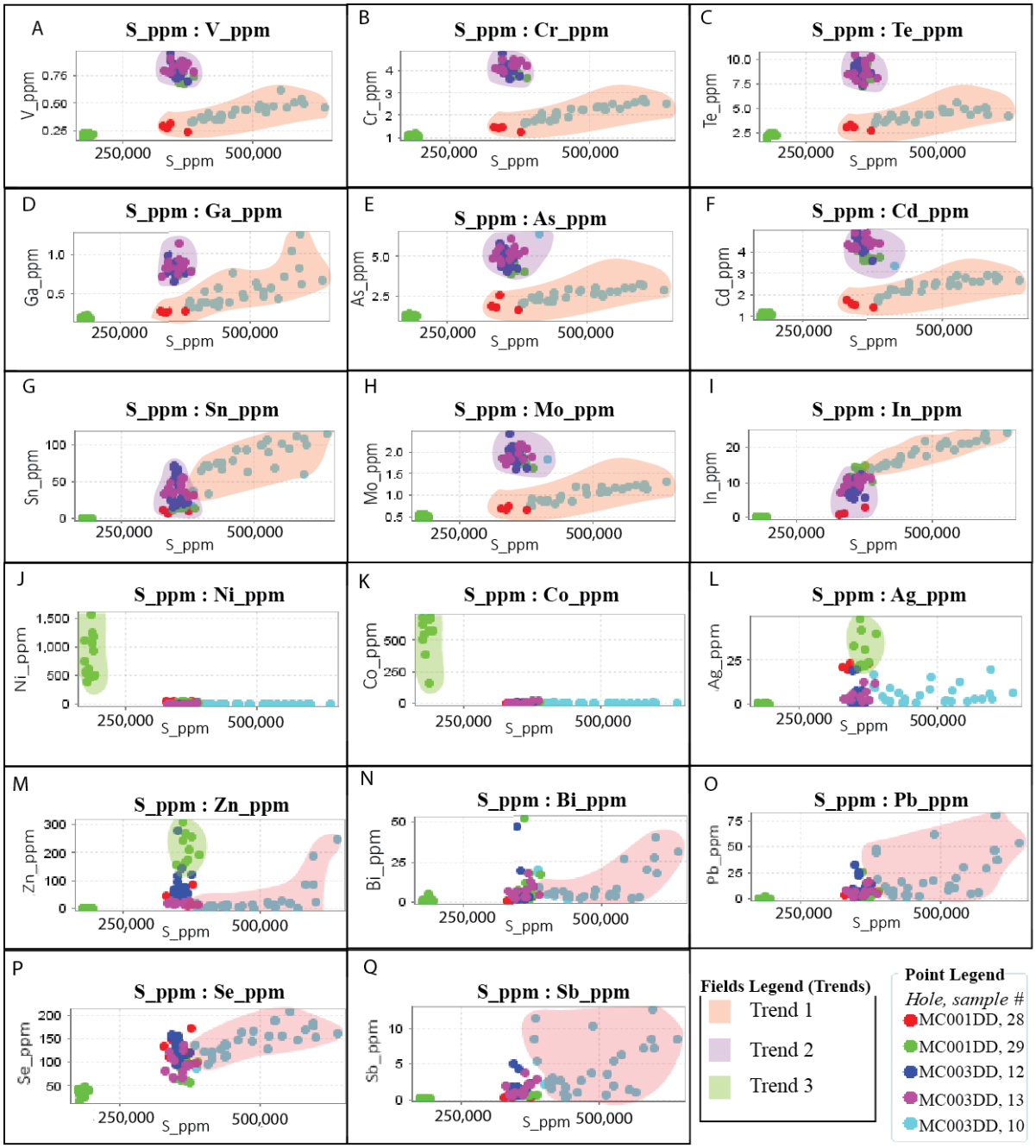

Figure 15: Graphs depicting trace element concetration in chalcopyrite: A) V v S; B) Cr v S; C) Te v S; D) Ga v S; E) As v S; F) Cd v S; G) Sn v S; H) Mo v S; I) In v S; J) Ni v S; K) Co v S; L) Ag v S; M) Zn v S; N) Bi v S; O) Pb v S; P) Se v S; Q) Sb v S. Light blue, purple and dark blue points (MC003DD, 10; MC003DD, 13; MC003DD, 12) represent chalcopyrites in the main dolomite-hosted minealised zone. Red and green points (MC001DD, 28; MC001DD, 29) represent chalcopyrite outsid eof the mineralised zone. Trends that are evident within the sulphides are highlighted. The fields highlight the trends eveident with in the chalcopyrite trace geochemistry.

DISCUSSION

Host Rocks

Previous to this study there has been inconclusive evidence as to the host unit of the Mount Cuthbert deposit. Marlow (1977) advocates an Argylla Formation host due to the presence of metasedimentary units within the mine area; however Rypkema (1986) suggested that locally the Leichhardt Volcanics could contain significant proportions of metasediments.

	Leichhardt Volcanics	Argylla Formation
Min Age	1852 ± 32	1761 ± 4
Max Age	1860 ± 3	1778 ± 3
Description	Felsitic quartz-feldspar porphyry, ignimbrite; minor basalt, andesite, agglomerate, bedded tuff, arenite, sericitic schist, phyllite	Porphyritic rhyolitic to dacitic tuff, andesite, quartz feldspar porphyry, quartzite, schist, gneiss; minor siltstone, arkose, conglomerate and metabasalt
Dominant rock types	Porphyry with 10-20% quartz, k-feldspar and plagioclase phenocrysts in a fine grained groundmass comprised of quartz +/- microcline +/- biotite	Pink to pink-grey porphyritic rhyolite with lesser non-porphyritic rhyolite, porphyritic rhyodacite, dacite and andesite
Shear zone characterisitcs	Gneissic metadacite, recrystallized rhyolite, psammitic schist and biotite schist	Sericite and talc schist, and phyllonite containing muscovite, chlorite, sillimanite, talc, biotite and quartz
Accessory minerals	Muscovite, opaques, apatite, sphene and zircon	Zircon, apatite, sphene, allanite, and fluorite
Other characteristics	-	Often strongly magnetic
References	Wilson, 1978; Blake et al., 1981; Blake 1987	Carter et al., 1961; Wilson, 1978; Blake, 1987

Table 4: Summary of Leichhardt Volcanic and Argylla Formation characteristics

This study identifies units that closely match with those identified as constituents of the Leichhardt Volcanics (identified in Table 4) and the associated Kalkadoon Batholith. Fine grained quartz-feldspar porphyritic felsic volcanics and biotite schists petrographically match descriptions of the Leichhardt Volcanics (Wilson, 1978). Further evidence is provided by the lack of accessory minerals commonly found in Argylla Formation volcanics (i.e. Fluorite) as well as a shear zone assemblage better represented by the Leichhardt Volcanics.

The Kalkadoon Batholith is known to frequently intrude the Leichhardt Volcanics. It is comprised of coarse grained granite and dominant granodiorite lithologies. Kalkadoon Granodiorite is frequently porphyritic and is comprised of microcline and perthitic k-feldspar, sericitised plagioclase and feldspar and ilmenite hosting biotite (Wyborn and Page, 1983).

These features are analogous to those described by the granodiorite and porphyritic granodiorite present in the Mount Cuthbert mine area (i.e. microcline - Figure 6, c; sericitised feldspar - Figure 9, b; ilmenite hosting biotite - Figure 18, b).

In addition to petrographic observations, *pers. comm.* Christie et al. (2015) conducted age dating on a selection of Mount Cuthbert intrusions. The porphyritic granodiorite was dated at 1883 ± 11 Ma, the granite dated to 1876 ± 13 Ma and coarse granodiorite dated to 1863 ± 16 Ma. These fall within the previously dated time frame for the Leichhardt Volcanics and Kalkadoon Batholith (Table 4).

Interpretation of Alteration Envelopes

The main constituents of the proximal alteration envelope (Figure 13) include chalcopyrite + pyrite + quartz + dolomite + chlorite alteration. This zone also displays an enrichment in the trace element concentrations of Au, Co, Ni, Se, Sb, Te and Ag compared to the surrounding area.

The main constituents of the intermediate alteration envelope (Figure 12) include quartz-carbonate veining with minor sulphide (chalcopyrite-pyrite-pyrrhotite) concentrations that increase in abundance towards the main copper zone. Potassic alteration (biotite, magnetite, red-rock), chlorite alteration and sporadic albite alteration are also present. This zone also displays enrichment in the trace element concentrations of Co, Ni, Sb, Se and Te.

It is difficult to determine the most distant alteration envelope due to the spacing of the drill holes however, assuming a fractal nature of the geology, small scale features both support the interpretation of the proximal and intermediate alteration envelope, and suggest that the distal alteration envelope may be comprised of albite alteration (see Figure 16, a, b).

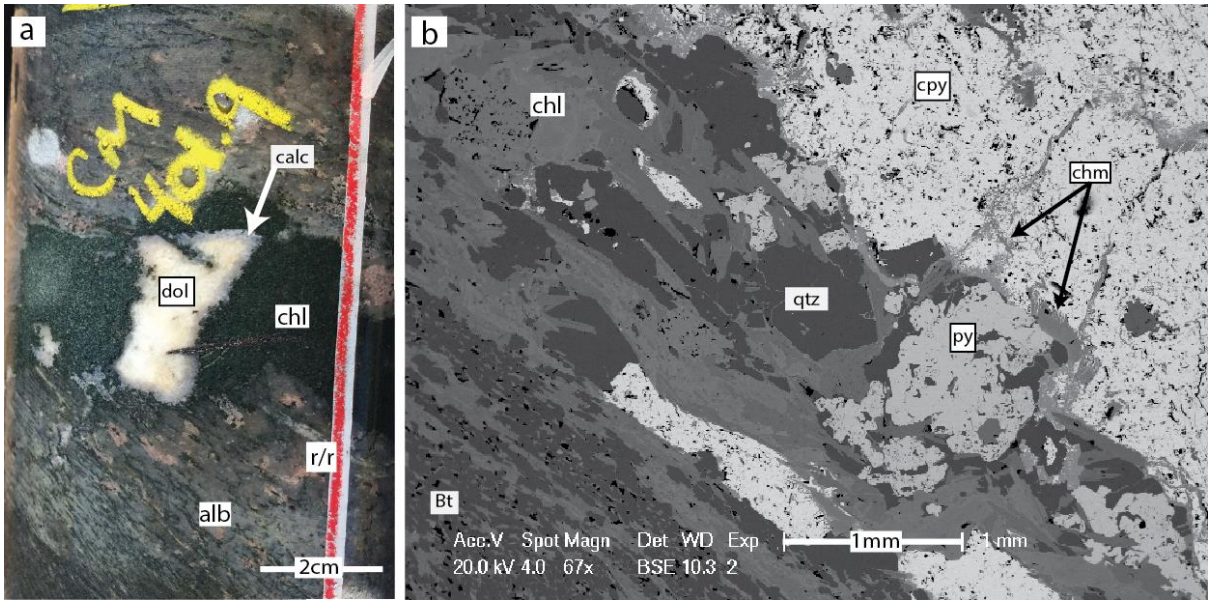

Figure 16: A) hand scale example of zonation from MC001DD, in which dolomite (dol) surrounded by a thin rim of calcite (calc) on the outer edge. The dolomite/calcite lies within a vein of intensely altered chlorite (chl). Alteration of the host rock surrounding the chlorite vein grades into low intensity red-rock and albite alteration. Assuming a fractal nature in the alteration at Mt Cuthbert, this is indicative of dolomite/calcite + chlorite proximal alteration, with a + red/rock (r/r) intermediate envelope, and with albite (alb) as the most distal alteration envelope (i.e. carbonate -> chlorite -> potassic alteration -> albite alteration); B) SEM image in which the alteration of the host rock surrounding chalcopyrite (cpy) grades from chamosite (chm), chlorite, pyrite (py) and quartz to more distant biotite This may represent a micro-scale example of chlorite and Fe enrichment closer to sulphides and more distant K-enrichment. (i.e. Cu-Fe-S enriched -> quartz-chlorite -> potassic alteration).

Paragenesis

Paragenesis of the major stages of alteration and mineralisation within the Mount Cuthbert mine area can be described by the following paragenetic sequence (Figure 17):

1. Albite ± quartz
2. Siderite, quartz, biotite, ilmenite, pyrite, calcite, dolomite, k-feldspar, albite, sericite, magnetite
3. Pyrite, pyrrhotite, chalcopyrite
4. Chlorite, chamosite (?), late pyrite
5. Chalcocite, hematite, k-feldspar, albite, quartz, apatite

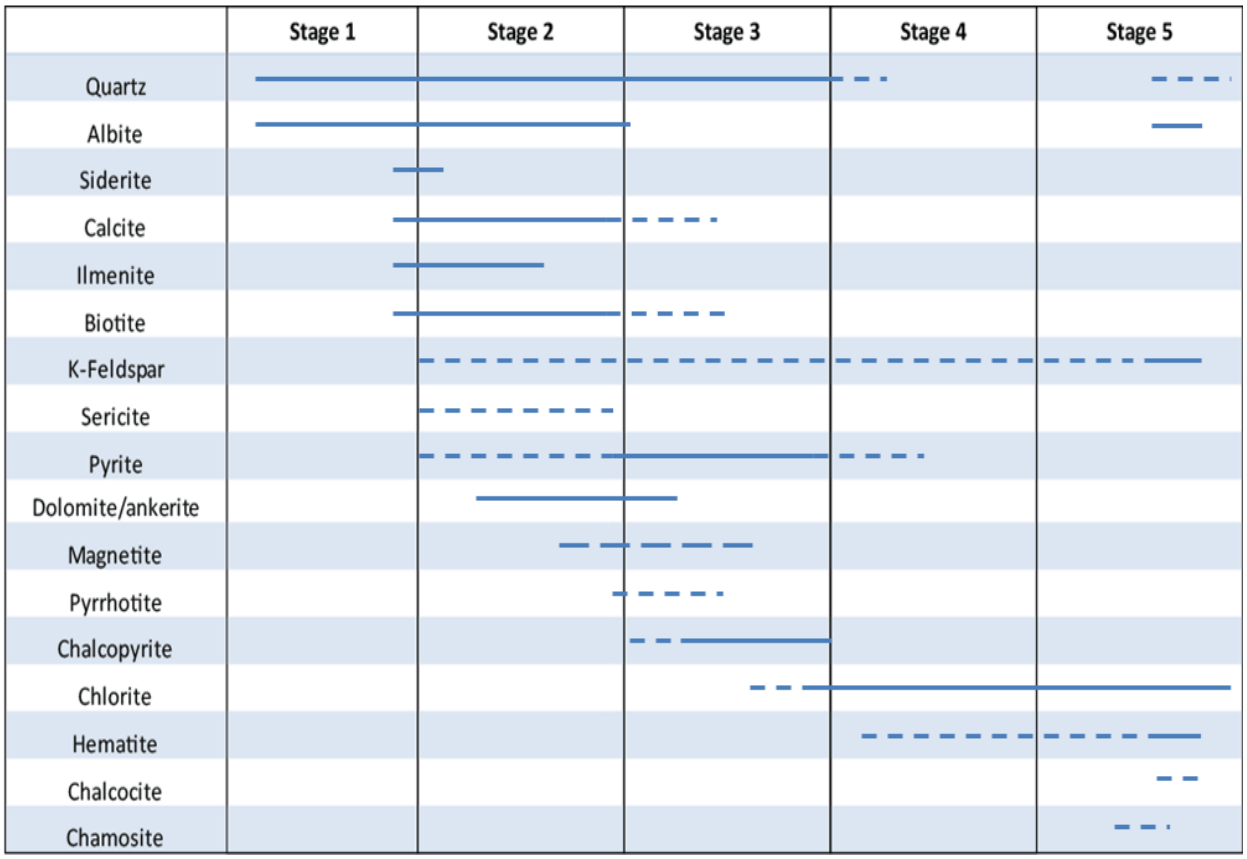

Figure 17: Image depicting mineral growth and stages of alteration

STAGE 1

Albite + quartz

Petrology and SEM work indicate that albite is the earliest alteration style in the Mount Cuthbert mine area. It forms both prior to quartz (Figure 18, b) and concurrently (Figure 18, a; d). In areas with strong fabric albite is deformed indicating that it was emplaced prior to deformation (Figure 18, b). Albite clearly occurs prior to biotite and chlorite as suggested by their deflection around albite crystals (Figure 18, b; c; d), although the presence of K-enriched outer edges in albite suggest K-enrichment began during the final stages of albite growth.

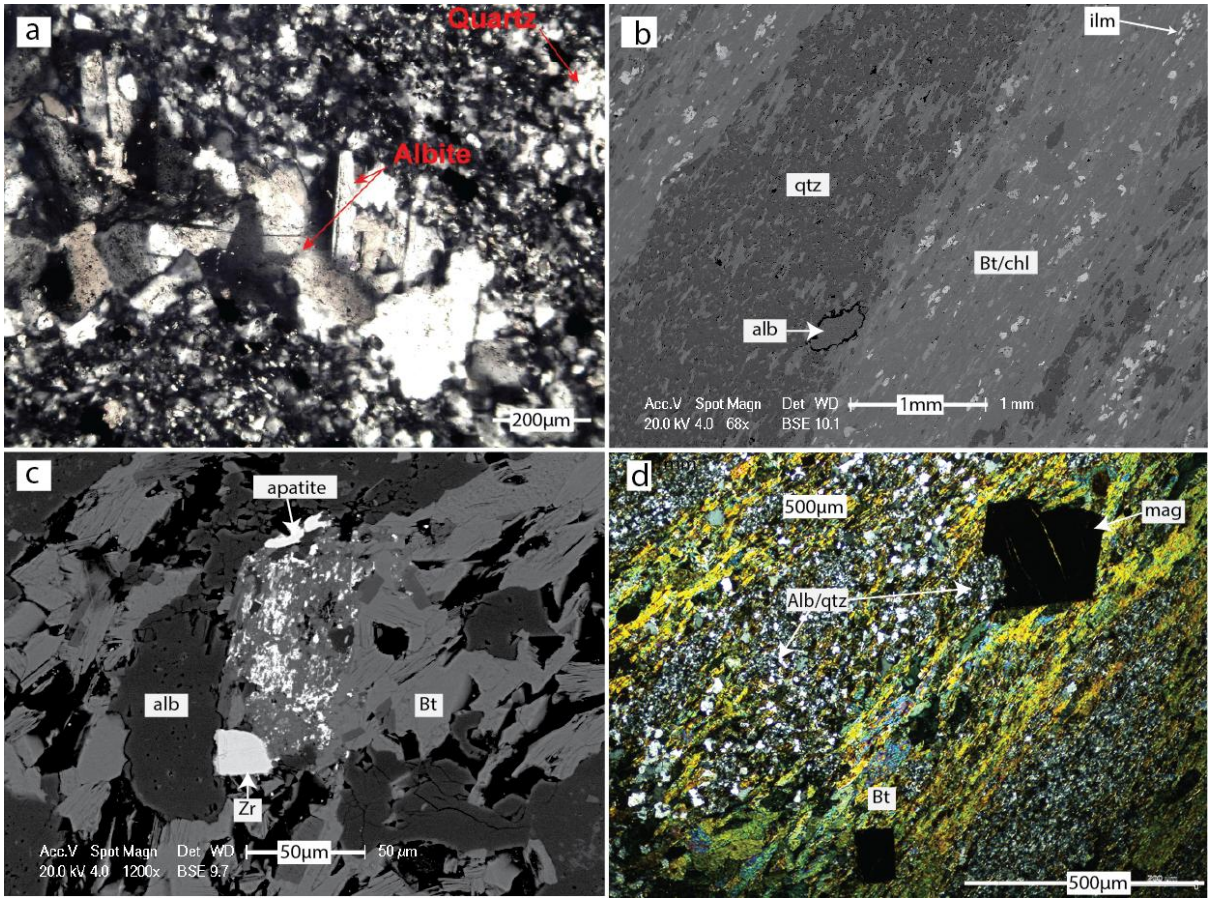

Figure 18: A) early albite + quartz veining and fine grained alteration from hole MC001DD (see Figure 9 from Appendix 1); B) an SEM image from hole MC003B depicting foliated quartz and bi/chl banding clearly deflected around deformed albite (alb); C) an SEM image from hole MC001DD that shows albite, apatite and zircon (Zr) in biotite, the edges of albite show a lightening of colour that represent K-enrichment within the structure; D) from MC001DD shows biotite and magnetite growing around albite/quartz aggregates The magnetite crystal displays a thin elongate (sub-vertical) biotite inclusion within its structure.

STAGE 2

2A: Siderite

2B: Quartz, biotite (±apatite ± REEs), ilmenite, early pyrite (±minor early chalcopyrite), calcite, dolomite.

2C: Magnetite

The second paragenetic stage of alteration refers to a series of minerals that grow more or less contemporaneously, and is associated with the greatest stage of deformation.

Stage 2A

Siderite is present as inclusions in quartz crystals (Figure 19, d) and as elongate crystals that have been overprinted by dolomite and chalcopyrite (Figure 19, c). These overprinting events are indicative of siderite growth prior to quartz and dolomite.

Stage 2B

Biotite alteration is abundant during this stage of alteration and occurs frequently with quartz. They occur together in veins (Figure 19, g) and as fine grained matrix. The strong grain contacts and frequent occurrence with one another suggests a contemporaneous growth history. An example of biotite alteration crosscutting albite and silica alteration is provided by Figure 8, f. This is believed to represent the overprinting of stage 1 albite-quartz alteration by stage 2 biotite.

An important constituent of biotite alteration is minor-moderate amounts of ilmenite (Figure 18, b; Figure 18, f) and apatite (Figure 18, c) in the biotite matrix. Ilmenite crystals clearly display elongation and a common orientation while apatite is commonly found elongated parallel to biotite. The deformation of ilmenite and apatite is interpreted as growth simultaneous to biotite during fabric development.

Quartz is accompanied regularly by biotite and calcite in veins and within the host rock matrix. Calcite typically illustrates a classic infill texture within quartz (Figure 19, b) and is observed to intrude between pre-existing quartz grains (Figure 19, d). There are also rarer examples of biotite/chlorite-quartz foliation diverted around coarse calcite crystals (i.e. the top part of Figure 19, a). These textures have been interpreted as representing minor calcite growth prior to fabric development, followed by the main phase of calcite growth during and after quartz growth.

Dolomite is another carbonate that grew during this alteration stage. Dolomite veins display strong fabric as well as occasional biotite alteration at their edges (Figure 19, h). Such

evidence suggests dolomite grew simultaneously to fabric development at a time similar to quartz-biotite formation.

Due to the similarity in timing, the variation in carbonate alteration (i.e. calcite, dolomite, ankerite and siderite) is interpreted as the product of a Ca-Mg-Fe rich fluid, in which the dominance of one carbonate is a function of local variations in the Mg^{2+}, Ca^{2+} and Fe^{2+} content of the fluid.

Early pyrite is also apparent in several samples, as evidenced by deformed pyrite (Figure 11, g) and pyrite that has grown along the boundary of the pre-foliation calcite grains (Figure 19, a), suggesting pre-deformation growth of pyrite.

Sericite alteration occurs most commonly within the core of feldspar and plagioclase crystals. The timing of its growth is unclear however Taylor (Appendix A) suggests it is likely to be an early alteration product due to its propensity to grow at high temperatures (Taylor and Pollard, 2006).

Stage 2C

Magnetite is present most commonly within the biotite matrix. Magnetite crystals display a lack of deformation despite their presence in the strongly foliated biotite. In one instance a biotite inclusion is visible within the magnetite structure (Figure 18, d). The lack of deformation in the magnetite crystals and biotites presence as an inclusion in magnetite suggests a late to post-biotite paragenesis of magnetite.

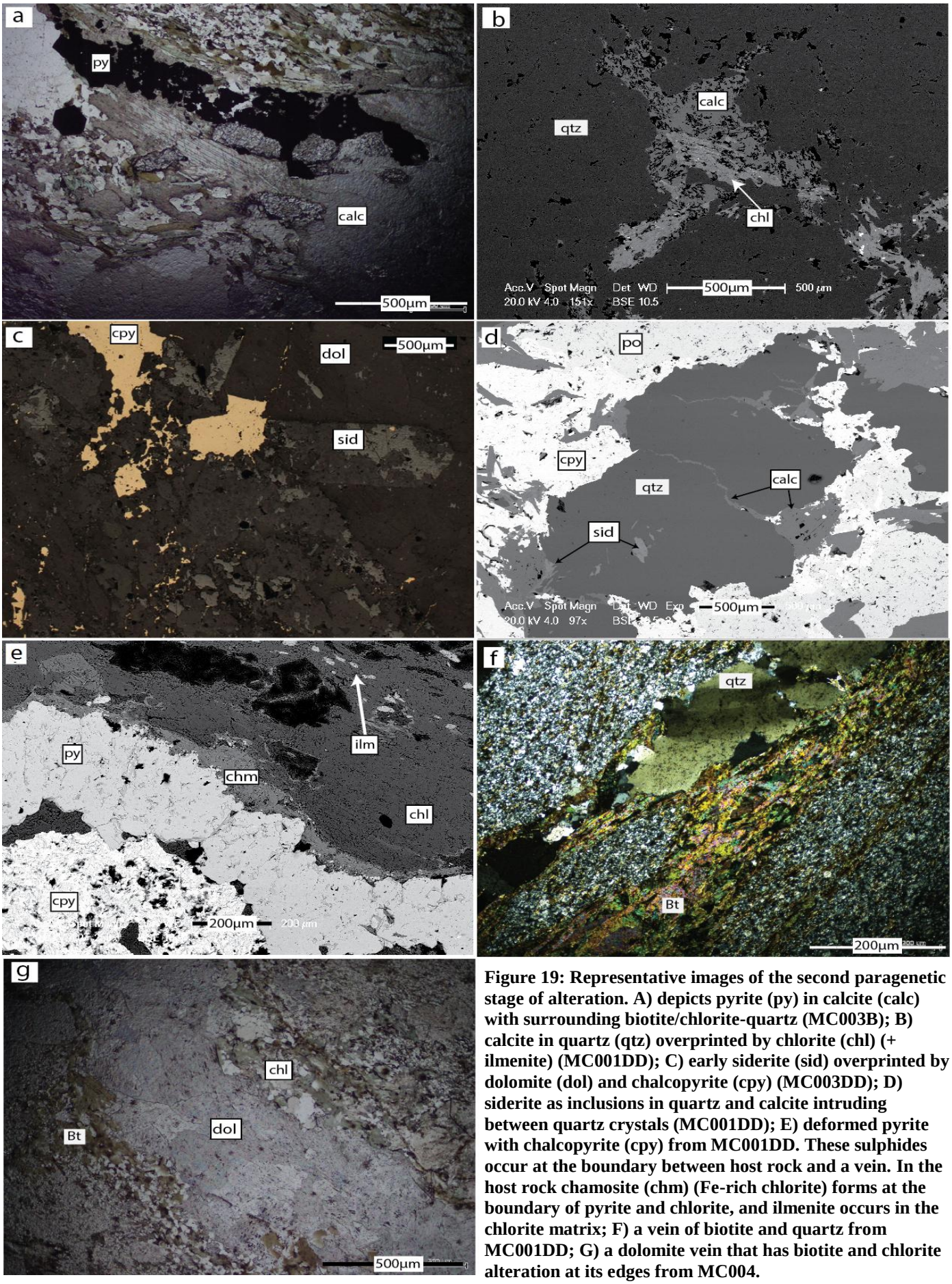

Figure 19: Representative images of the second paragenetic stage of alteration. A) depicts pyrite (py) in calcite (calc) with surrounding biotite/chlorite-quartz (MC003B); B) calcite in quartz (qtz) overprinted by chlorite (chl) (+ ilmenite) (MC001DD); C) early siderite (sid) overprinted by dolomite (dol) and chalcopyrite (cpy) (MC003DD); D) siderite as inclusions in quartz and calcite intruding between quartz crystals (MC001DD); E) deformed pyrite with chalcopyrite (cpy) from MC001DD. These sulphides occur at the boundary between host rock and a vein. In the host rock chamosite (chm) (Fe-rich chlorite) forms at the boundary of pyrite and chlorite, and ilmenite occurs in the chlorite matrix; F) a vein of biotite and quartz from MC001DD; G) a dolomite vein that has biotite and chlorite alteration at its edges from MC004.

STAGE 3

Main sulphide phase: quartz-carbonate +pyrite, pyrrhotite, chalcopyrite ±chlorite

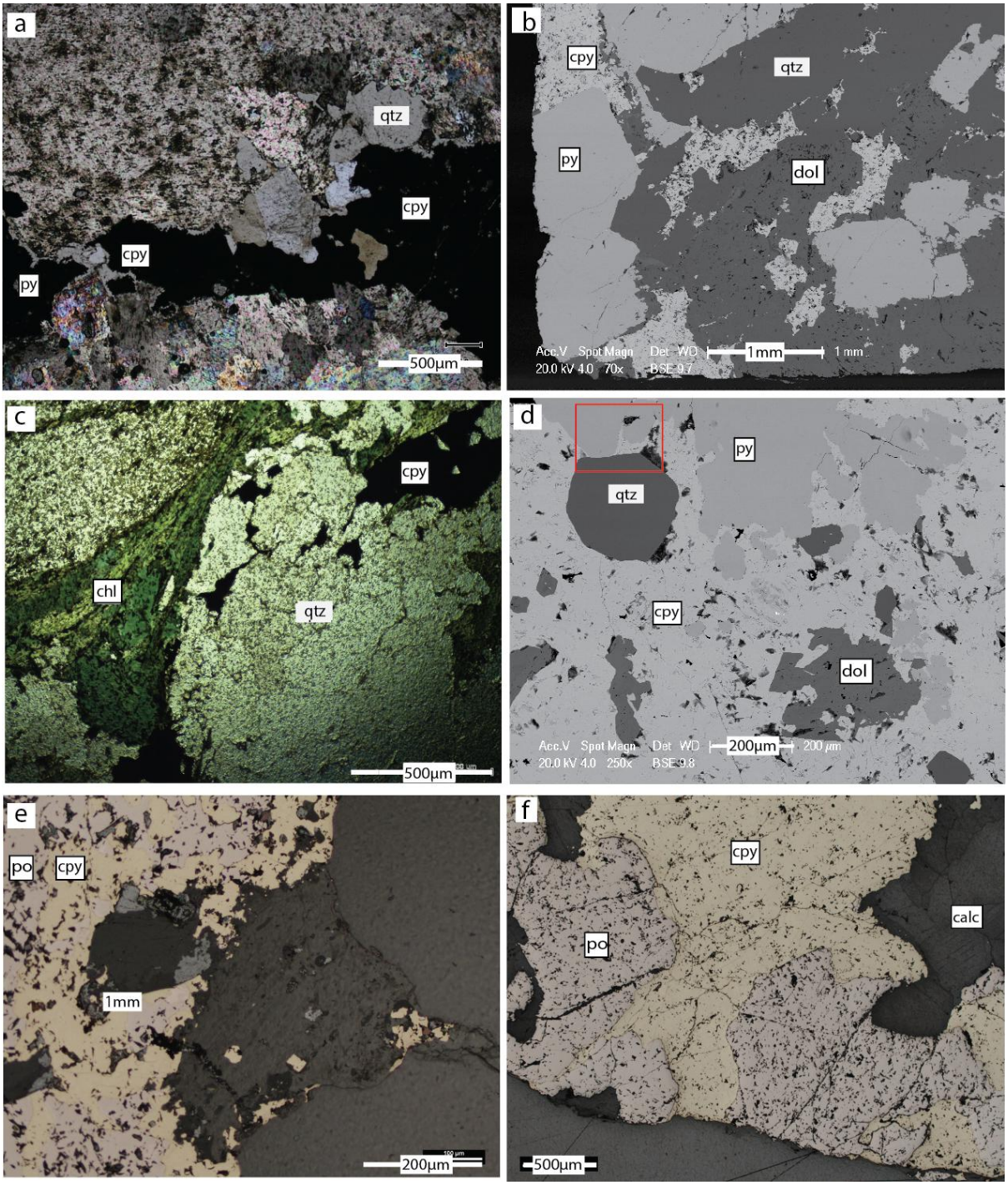

Figure 20: A) chalcopyrite and quartz infill in dolomite (MC003DD); B) euhedral pyrite, porous dolomite, porous, anhedral chalcopyrite and quartz from MC003DD; C) quartz vein with chalcopyrite growth at quartz grain boundaries. Chlorite alteration occurs at the edge of the quartz vein; D) strong grain contact between quartz and pyrite, and dolomite in a sea of chalcopyrite, the red box highlights the grain contact between quartz and pyrite, and the triangular infill shape of chalcopyrite, indicating post pyrite/quartz genesis of chalcopyrite (MC003DD); E) intergrown symplectic pyrrhotite and chalcopyrite; E) chalcopyrite infill between pyrrhotite crystals – evidence of some pre-chalcopyrite growth of pyrrhotite.

The main sulphide phase refers to the development of chalcopyrite ±pyrite ±pyrrhotite assemblages that occur in association with quartz, carbonate and chlorite. These assemblages clearly cross cut dolomite packages (Figure 10, a) as well as the other host rocks of the mine area, indicating they are a post stage 2 assemblage. The paragenetic sequence of sulphide growth is described by early pyrite, followed by pyrrhotite, followed by chalcopyrite.

The early formation of pyrite + quartz is evident by coarse euhedral pyrite crystals that display strong grain contacts with quartz (Figure 20, b), pyrite's presence as inclusions in chalcopyrite (Figure 19, b), and the deposition of chalcopyrite as infill around pyrite (Figure 10, e). Pyrrhotite displays evidence of forming prior to chalcopyrite in areas where chalcopyrite growth has occurred around pre-existing pyrrhotite crystals (Figure 20, f).

It is necessary to note that the growth of one sulphide is not exclusive, and there were periods in which these sulphides grow simultaneously. Such an inference is supported by the intergrown symplectic nature shared by chalcopyrite and pyrrhotite (Figure 20, e), and the strong grain boundaries shared by chalcopyrite-pyrite (Figure 20, b). In addition to the sulphides, calcite grew during early stage 3 alteration, quartz grew throughout stage 3 (Figure 20, a, b, c, d), and chlorite (Figure 20, c) is associated with late stage 3 alteration. Minor red-rock and albitisation occur in association with sulphide-quartz-carbonate veins suggests a minor Na-K component to this stage of alteration.

STAGE 4

Chlorite ± chamosite(?) ± minor late pyrite

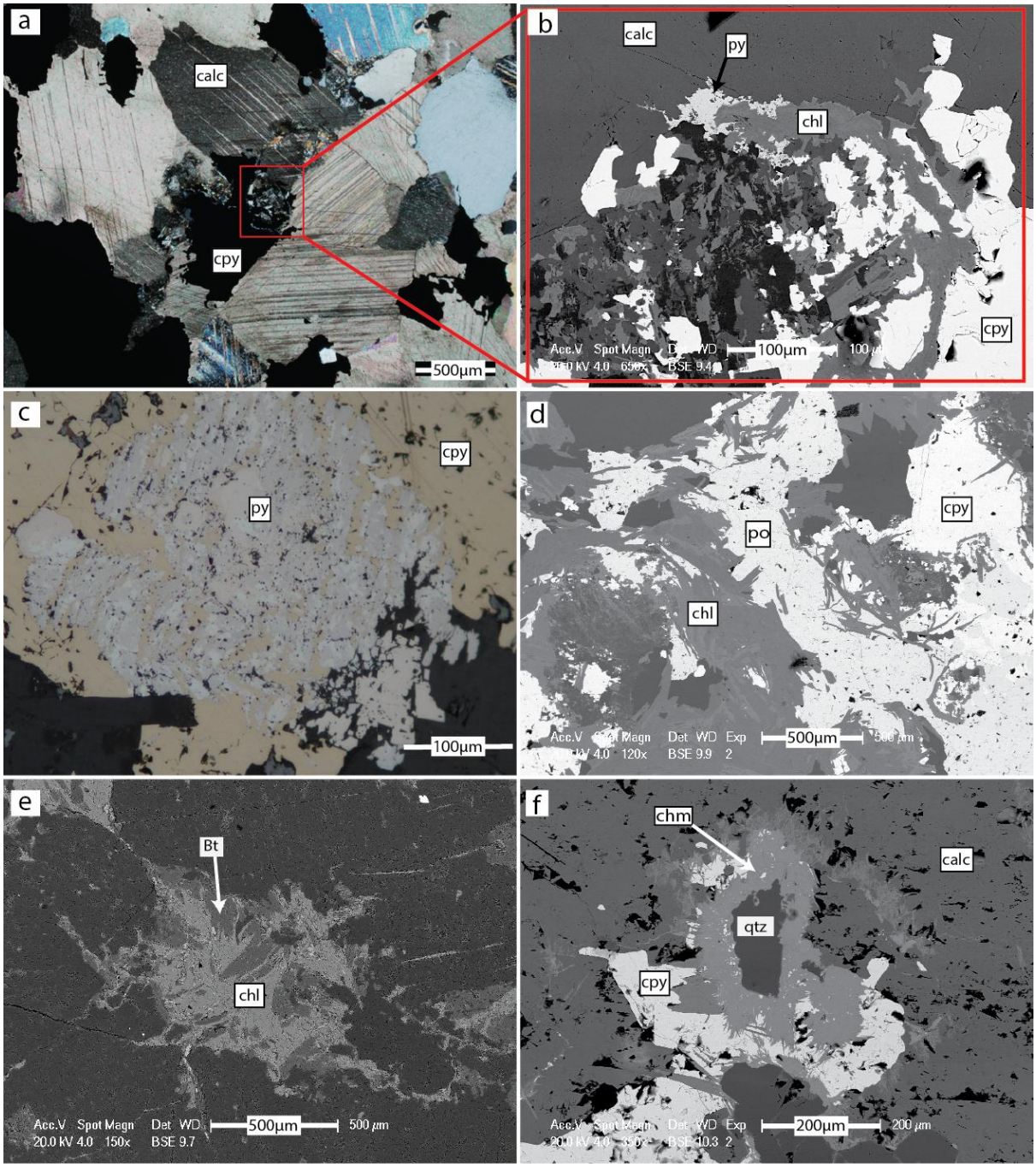

Figure 21: A, B) cross polarised light and SEM image of late chlorite + pyrite growth off chalcopyrite from MC001DD; C) from MC003DD, shows late pyrite (marcasite?) overprinting chalcopyrite; D) late stage chlorite overprinting sulphides (MC001DD); E) late stage chlorite overprinting biotite (MC003B); F) fibrous chamosite growing off quartz and over chalcopyrite (MC001DD).

Stage 4 of the alteration paragenesis occurs after the main stage of sulphide deposition as evidenced by the widespread overprinting of sulphides (Figure 21, d) (and biotite, Figure 21,

e) by chlorite. Minor, subhedral pyrite occurs in association with stage 4 chlorite (Figure. 21 a, b) and is occasionally present as marcasite (Figure 21, c). This study has tentatively identified chamosite, the Fe-rich chlorite end member present as a replacement of chlorite that occurs occasionally in association with Fe-sulphides and quartz (Figure 21, f). This is also depicted in Figure 19 e, where chlorite grades into chamosite before approaching pyrite.

STAGE 5

Supergene alteration (chalcocite, hematite, quartz, chlorite, red-rock and albite alteration [k-feldspar, quartz, albite, apatite])

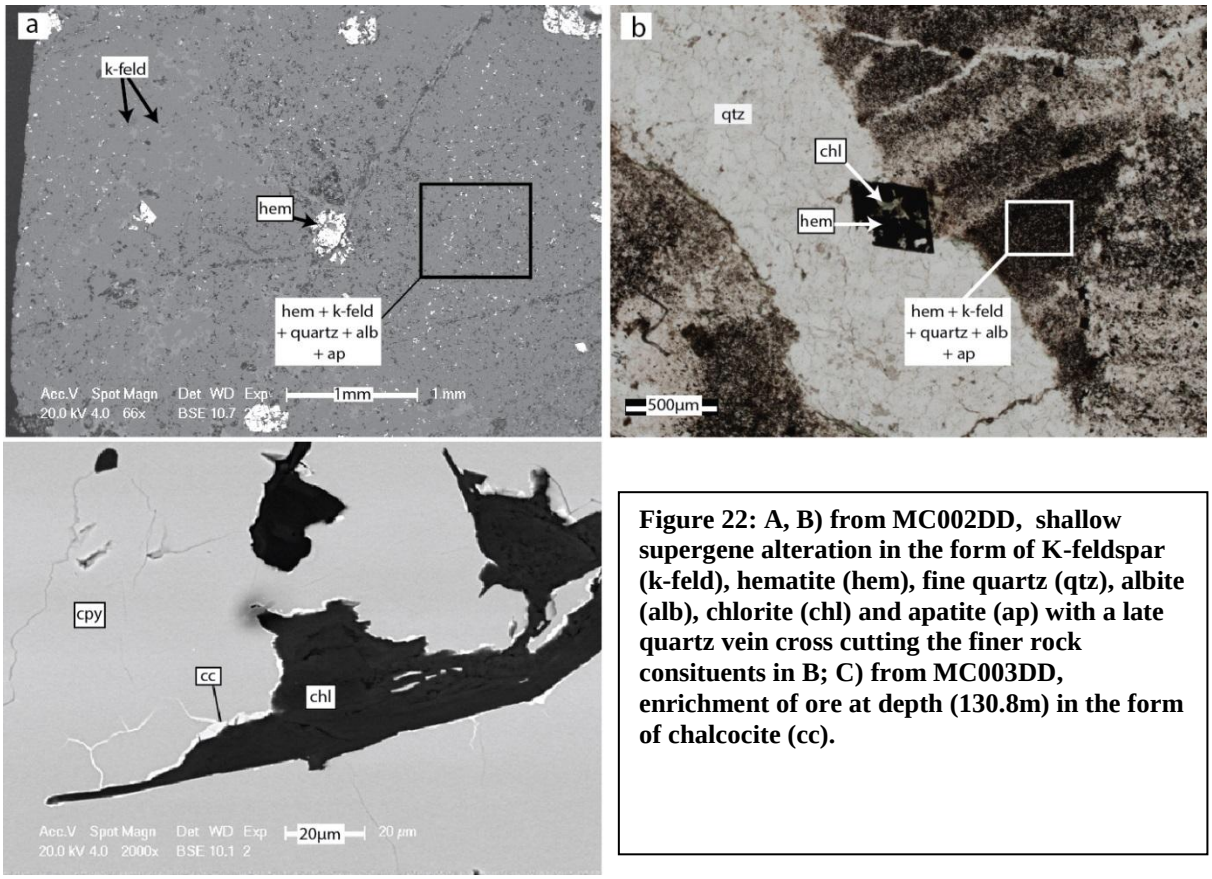

Figure 22: A, B) from MC002DD, shallow supergene alteration in the form of K-feldspar (k-feld), hematite (hem), fine quartz (qtz), albite (alb), chlorite (chl) and apatite (ap) with a late quartz vein cross cutting the finer rock consituents in B; C) from MC003DD, enrichment of ore at depth (130.8m) in the form of chalcocite (cc).

The final stage of alteration involves supergene enrichment of chalcopyrite to chalcocite within the main mineralised area hosted by silica-dolomite (Figure 22, c), and the replacement of magnetite by hematite in conjunction with red-rock and albitisation, which occurs above the mineralised silica-dolomite zone closer to the surface. Oxidising conditions

are indicated by the oxidation of magnetite to hematite (Figure 22, a, b). A late quartz vein + hematite also crosscuts this alteration (Figure 22, b).

Sulphide Geochemistry in Relation to Ore Genesis

The presence of differring trends in the trace geochemistry of pyrite support the paragenetic evidence suggesting that there were several phases of pyrite growth (i.e. Figure 14; main phase pyrite represented by the pink and green fields with the differences in geochemistry due to their presence within and outside of the silica-dolomite zone, early pyrite represented by the blue field).

However, the trends within the chalcopyrite trace geochemistry cannot be explained simply by differing phases of growth or by differences between chalcopyrites in the main mineralised zone and those outside of this zone. The differences in chalcopyrite trace geochemistry trends are most likely a product of textural differences between the chalcopyrite crystals. For example, chalcopyrite crystals from trend 1 display a continuous surface with minor or no inclusions, chalcopyrites from trend 2 display a dirty surface with abundant inclusions, and chalcopyrites from trend 3 occur exclusively with pyrrhotite. One explanation may be that the presence of inclusions may alter the geochemistry of the chalcopyrite either due to a reaction between the chalcopyrite and the inclusions mineral, or from the presence of the inclusion within the ablation radius during laser ablation. Similarly, the intermingled nature of chalcopyrite and pyrrhotite as well as the contemporaneous time of growth may have resulted in an exchange of trace elements. Due to the inconclusive nature of the chalcopyrite trace geochemistry their has been no conclusions drawn in regards to the genesis of chalcopyrite growth from the trae geochemistry.

Depositional Mechanisms and Environment

The vesicular-like texture of dolomite and occasionally quartz (Figure 20, b) suggests a permeability of rock that allowed fluid flow through (and consequently metal interaction with) carbonaceous rocks in a reducing environment. The product of this was the deposition of metals as a result of pH changes from interaction of these circulating fluids with wall rock, in particularly by inducing redox changes within the fluids due to the carbonaceous nature of the rock (Hutton et al., 2012). Pyrite specifically shows textural evidenced of partially replacing earlier carbonates suggesting that precipitation occurred due to the reduction of fluids by reaction with reduced carbon released from carbonaceous rocks (Beardsmore 1992). The low Au:Cu ratio and presence of pyrrhotite, magnetite and wüstite further support the inference of a highly reducing environment (Figure 23).

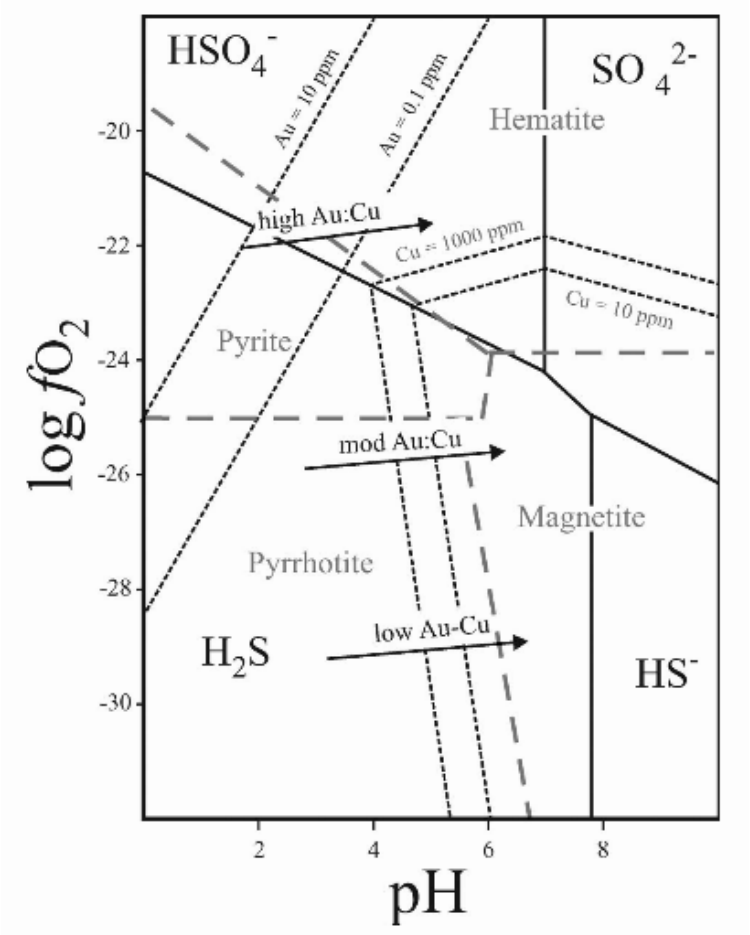

Figure 23: pH vs log fO_2 diagram outlining the stability relations between minerals in the Fe – S – O system at 450°C and 200 MPa. The solubility relationships of Cu and Au in saline, high-temperature solutions show how the Au:Cu ratio tends to lower values with decreasing fO2. From Mark et al. (2006).

Comparison and Classification

The Mt Cuthbert deposit is a shear hosted copper deposit with ore mineralogy typified by a chalcopyrite-pyrite-pyrrhotite assemblages. The main ore body is concentrated as a chalcopyrite + pyrite + quartz breccia matrix and veining in a ~65m thick silica dolomite body. Ore is also present, although less abundant, as chalcopyrite + pyrite and minor chalcopyrite + pyrrhotite in the surrounding biotite/chlorite-quartz schists and felsic volcanics. Here ore minerals are disseminated through the host rock, emplaced along foliation and present in quartz, calcite and dolomite veins that intrude the rock.

The paragenetic alteration sequence is described by early sodic alteration (albite + quartz), followed by K-Fe-Ca alteration (siderite + calcite + dolomite+ quartz + biotite ± magnetite ± apatite) during the main deformation period, followed shortly after by the main ore phase comprised of chalcopyrite + quartz ±pyrite ±pyrrhotite ± calcite ±chlorite. Finally widespread chloritisation and Ca-K alteration (k-feldspar, albite) followed by oxidation and localised enrichment of chalcopyrite to chalcocite occurred. This alteration paragenesis closely resembles that of regional alteration in the EFB (Oliver, 1995, Rubenach 2005, Laukamp et al., 2011,).

Although there is no absolute age dating on Mt Cuthbert mineralisation, this study has identified mineralisation that is more closely aligned with the retrograde mineral assemblage (i.e. chlorite) and is therefore a post peak metamorphism deposit. Previous workers (Foster and Rubenach 2006, Rubenach 2008) have identified peak metamorphism within the KLB to be concurrent with the regional D2 (ca. 1590 Ma; Murphy et al. (2011)) event during the Isan Orogeny. This would suggest a timing for mineralisation that is related to late stage/post orogenic events of the EFB, such as the intrusion of the Williams and Naraku Batholiths at ca. 1555-1485 Ma (Hutton et al. 2012).

Hutton et al. (2012) used the mineral systems approach designed by Barnicoat (2008) to conduct a generalised classification on deposits in the Mt Isa Inlier. Their work identified 2 mineral systems for the deposition of Cu ± Au ± Fe mineralisation:

1. Structurally-controlled epigenetic IOCGs – Eastern Fold Belt and Kalkadoon-Ewen Provinces
    a. Ironstone hosted deposits (i.e. Osborne, Starra) formed from c. 1600-1565 Ma
    b. Breccia and shear hosted deposits (i.e. Mt Elliot, Ernest Henry, Lady Ella, Mt Dore) that formed post-peak metamorphism, and synchronously with emplacement of the Williams and Naraku Batholiths
2. Structurally-controlled epigenetic Cu ± Au mineralising systems in metasediments – Western Fold Belt Province

Table 5 compares the geological features of a variety of mineral deposits within the Mount Isa Inlier. The Mount Cuthbert deposit most closely aligns with other shear zone and fracture controlled deposits (i.e. style 1b from Hutton et al. (2012)), and specifically it shares the greatest number of similarities with other low tonnage, high grade deposits in the KLB (i.e. Mighty Atom, Orphan) including similarities in host rock, size, metamorphic grade and alteration styles.

The clear link between the alteration paragenesis of the Mount Cuthbert deposit with that of regional alteration in the Eastern Succession, as well as the apparent timing of mineralisation that is analogous to that in the EFB, suggests a clear link between Mount Cuthbert and other breccia and shear hosted deposits of the EFB.

The similarity of the Mt Cuthbert deposit to others located in the KLB, may also suggest that KLB deposits are related to other post Isan Orogeny shear zone and fracture hosted vein deposits of the Eastern Succession. Their comparatively small size and tonnage to those deposits of the EFB is most likely a product of the tectonic setting of the KLB. Bierlein et al.

(2011) indicate that the long-lived, thick, uplifted basement of the KLB is less likely to favour the generation of major IOCG deposits based on the IOCG association to partial melting of hydrated (during subduction) subcontinental lithospheric mantle (SCLM), and subsequent epigenetic emplacement of subalkaline to alkaline granites (Groves et al. 2010). Their work suggests this process would be hindered by the thickening, uplift and underplating experienced by the KLB post 1800 Ma, and therefore limits the preservation potential for large IOCGs in the KLB.

An exploration model for KLB deposits is therefore best defined by NW-NE trending shear zones or faults that host carbonaceous rocks from the Argylla Formation or Leichhardt Volcanics, and which display metamorphism to amphibolite or greenschist facies with an alteration assemblage consisting of quartz, biotite, chlorite and minor magnetite, with sporadic albite (Table 3). An alteration envelope based on the Mount Cuthbert deposit is described by distal albite alteration that grades into extensively biotite and chlorite altered rock, with minor magnetism and abundant quartz-carbonate veining that increase in abundance towards a mineralised carbonate-quartz core.

Deposit, Location	Age (Ma)	Host Rocks	Main Alteration Types	Primary Ore	Secondary Ore	Gangue	Relationship to Host	Spatial/Temporal Relation to Intrusions	Style	References
Mt Cuthbert, KLB	-	silica altered dolomite, quartz-biotite-chlorite schist	silica dolomite, chlorite, biotite, albite, k-feld	chalcopyrite, pyrite, pyrrhotite	chalcocite, malachite, cuprite, azurite	dolomite, quartz	discordant	yes	shear zone and fracture controlled vein deposit	Rypkema, 1986; Jones, 1990; Williams, 1998; Marlow, 1977
Orphan, KLB	-	hornblende schist, felsic porphyritic volcanics	silicification, carbonate	chalcopyrite, bornite, pyrite	chalcocite, malachite, azurite, cuprite	quartz, siderite	discordant	yes	shear zone and fracture controlled vein deposit	Carter et al., 1661; Brooks, 1977; Blake, 1987
Mighty Atom, KLB	-	metasilstone, biotite schist, chlorite schist, metadacite	silcification, carbonate	chalcopyrite	chalcocite, malachite, azurite	quartz, calcite	discordant	yes	shear zone and fracture controlled vein deposit	Krosh and Sawers, 1974; Derrick and Wilson, 1982
Ernest Henry, EFB	1510	Metamorphosed volcanics (dacite, andesite, diorite)	Early regional Na-Ca + K-Fe (biotite-magnetite). Later K-feldspar alteration + mineralisation	chalcopyrite, pyrite, gold	sphalerite, arsenopyrite, molybdenite, coffinite	magnetite, calcite, quartz, feldspar, biotite, chlorite and hematite, with minor barite, fluorite and siderite	discordant	yes	shear zone and fracture controlled vein deposit	Mark et al. 2000, 2006; Williams et al. 2005
Osborne, EFB	1595	Metasedimentary rocks and metamorphosed mafic rocks	Magnetite, quartz, apatite, ironstone	chalcopyrite, cobaltian pyrite, pyrrhotite	bornite	magnetite, hematite, quartz, calcite, apatite, siderite, tourmaline	stratiform, discordant	yes but mineralisation predates nearby granites	Ironstone hosted stratiform deposit	Adshead, 1995; Adshead et al. 1998 (1); Gauthier et al. 2001; Fisher and Kendrick, 2008 (2)
Eloise, EFB	1536-1512	metaarkose, quartz-biotite schist and amphibolite	Early pervasive albite, overprinted by hornblende-biotite-quartz, followed by mineralisation	chalcopyrite, pyyrhotite, pyrite	gold, sphalerite, galena	hornblende, biotite, quartz, magnetite	discordant, concordant	yes	shear zone and fracture controlled vein deposit	Baker, 1998; Baker and Laing, 1998; Baker et al. 2001
Mt Elliot, EFB	1515	carbonaceous slate, metadolerite	silicification, albitisation, Ca-Mg-Na skarn alteration	chalcopyrito, pyrite, pyrrhotite	malachite, cuprite, tenorite, azurite, chrysocolla, native copper	calcite, magnetite, diopside, scapolite, gypsum, apatite, sphene, prehnite, hornblende	discordant	yes	shear zone and fracture controlled vein deposit	Duncan et al., 2011
Starra, EFB	1502 (1568)	BIF, quartz-feldspar-magnetite schist, chloritic schist	Magnetite + hematite ironstone lenses in intensely deformed albite-biotite-chlorite-magnetite-hematite-altered host rocks	chalcopyrite, bornite, pyrite, native gold, scheelite	covellite, chalcocite, malachite, native copper	magnetite, quartz, chalcedony, apatite, tourmaline, actinolite, siderite, chlorite, hematite, albite, scapolite, calcite	stratiform	yes	Ironstone hosted stratiform deposit	Davidson et al. 1989; Rotherham et al., 1998; Williams et al. 2001; Duncan et al., 2009
Mount Dore, EFB	-	carbonaceous slates, quartz-mica schists	k-feldspar, quartz, tourmaline, dolomite, calcite	pyrite, chalcopyrite, sphalerite, galena	chalcocite, malachite, azurite, torenite	quartz	discordant	yes	breccia hosted deposit in metasediments	Nisbet, 1980
Lady Clayre, EFB	-	Limestone, quartzite, carbonaceous schist and siltstone	(i) Early albitisation; (ii) biotite- and scapolite-rich Na – Cl – K – Fe – Ca – Mg metasomatism; (iii) albite–K-feldspar-rich veining; and (iv) Cu – Au mineralisation associated with carbonate veins and muscovite	chalcopyrite, pyrrhotite, pyrite	malachite, chalcocite, cuprite	quartz	concordant	yes	shear zone and fracture controlled vein deposit	Habermann, 1999
Mt Isa, WFB	1372 +/- 41	dolomitic pyritic carbonaceous shale, dolomitic pyritic carbonaceous siltstone	silica-dolomite, talc	chalcopyrite, pyrite, pyrrhotite, cobaltite, arsenopyrite, marcasite, galena, sphalerite	Chalcocite, chrysocolla, cuprite, malachite, native copper, tenorite	dolomite, quartz, talc, k-feldspar, graphite	stratbound, discordant	no	breccia hosted deposit in metasediments	Wilde, 2011
Mammoth, WFB	-	sandstone, siltstone, quartzite, stromatolitic chert, dolomite	silicification, gossan dolomite, sericite, chlorite, k-feldspar	chalcopyrite, pyrite, chalcocite, chalcocite, malachite bornite, digenite, covellite	chalcocite, malachite	quartz, calcite, chlorite, dolomite	stratbound, discordant	no	breccia hosted deposit in metasediments	Van Dijk, 1991
Mount Oxide, WFB	-	carbonacoous dolomitic shale, carbonaceous dolomitic siltstone	silica-dolomite, chlorite	chalcopyrite, pyrite	chalcocite, covellite, malachite, azurite, atacamite, brochantite, tenorite, cuprite, bornite	quartz, dolomite, chlorite, hematite, kaolinite	discordant, stratiform	no	breccia hosted deposit in metasediments	Van Dijk, 1991; Hutton and Wilson, 1984
Mount Kelly, WFB	-	dolomitic carbonaceous siltstone, chert, carbonaceous siliceous shale	silica-dolomite	chalcopyrite, pyrite	malachite, azurite	quartz, dolomite, chlorite	discordant	no	breccia hosted deposit in metasediments	Van Dijk, 1991
Mount Dore, EFB	-	carbonaceous slates, quartz-mica schists	k-feldspar, quartz, tourmaline, dolomite, calcite	pyrite, chalcopyrite, sphalerite, galena	chalcocite, malachite, azurite, torenite	quartz	discordant	yes	breccia hosted deposit in metasediments	Nisbet, 1980
Lady Clayre, EFB	-	Limestone, quartzite, carbonaceous schist and siltstone	(i) Early albitisation; (ii) biotite- and scapolite-rich Na – Cl – K – Fe – Ca – Mg metasomatism; (iii) albite–K-feldspar-rich veining; and (iv) Cu – Au mineralisation associated with carbonate veins and muscovite	chalcopyrite, pyrrhotite, pyrite	malachite, chalcocite, cuprite	quartz	concordant	yes	shear zone and fracture controlled vein deposit	Habermann, 1999

Table 5: Comparison of the geological features of a selection of deposits hosted by the Kalkadoon-Leichhardt Belt (KLB), Eastern Fold Belt (EFB) and Western Fold Belt (WFB)

CONCLUSIONS

1. Host rocks are comprised predominantly of biotite-chlorite-quartz schists, felsic volcanic units and porphyritic granodiorite analogous to the Leichhardt Volcanics and associated Kalkadoon Batholith
2. Alteration envelopes are described by:
    - Proximal (<50m): chalcopyrite, pyrite, quartz, dolomite and chlorite
    - Intermediate (50-500m): quartz-carbonate veining with minor sulphide (chalcopyrite-pyrite-pyrrhotite), in addition to extensive biotite and chlorite alteration and minor magnetite alteration
    - Distal (>500m): albite dominant
3. The paragenetic alteration sequence is characterised by 5 alteration stages:
    - Stage 1) sodic alteration (albite + quartz);
    - Stage 2) K-Fe-Ca alteration (siderite + calcite + dolomite + quartz + pyrite + biotite ± magnetite ± ilmenite ± apatite);
    - Stage 3) mineralisation (chalcopyrite + quartz ± pyrite ± pyrrhotite ± calcite ± chlorite);
    - Stage 4) major chloritisation;
    - Stage 5) minor supergene enrichment to chalcocite.
4. The trace geochemistry of the main chalcopyrite ± pyrite ore phase reveals elevated Ni, Zn, Cd and Hg in pyrite and elevated Sn, Pb, Se, V, Cr, Te, Ga, As, Cd, Mo, Ga, Bi and Sb in chalcopyrite. Differing elemental trends within the ore minerals supports paragenetic evidence suggesting several phases of sulphide growth.

5. Mount Cuthbert alteration, ore genesis and timing of mineralisation suggest a link to the metasomatic and tectonic events responsible for mineralisation in the EFB. Mount Cuthbert shows the greatest similarities to other KLB-hosted deposits (Mighty Atom, Orphan). This suggests that KLB-hosted deposits are uniquely their own style despite the association to EFB copper deposits.
6. An exploration model for KLB hosted deposits may be described by:
    - NW-NE trending shear zones or faults
    - Carbonaceous host rocks from Argylla Formation or Leichhardt Volcanics
    - Intense chloritisation and biotisation
    - Magnetic anomaly (may be subtle)
    - Rocks metamorphosed to greenschist or amphibolite facies
    - Shear zones that show alteration grading from albite alteration to potassic dominant alteration (i.e. biotite, red-rock) with retrograde chlorite alteration to a mineralised carbonate-quartz core.

ACKNOWLEDGMENTS

Foremost I would like to thank Bruce Godsmark for the opportunity this year has presented. The resources you invested throughout the year, including both your own personal time and the funding for the project were greatly appreciated. I can only hope that you will continue to support young geologists as you have me, the experience was truly invaluable. Secondly, I would like to thank Richard Lilly for the selflessness you have shown in helping me throughout the year. The project would not have been possible without your expertise, but more than that, your friendship and support meant a lot to me. I wish you continued success at Adelaide Uni and beyond. To Karin Barovich I want to thank for your positivity, your encouragement and your enthusiasm throughout the year. Please stay healthy, the Mawson building wouldn't feel right without your sunny presence to fill it. To Martin Hand thank you for your insight and intellect, the discussions we had were crucial in aiding my understanding of the project. My most sincere thanks to the Malaco geologists, specifically Lachlan Cole for your brilliant work with the down hole plots and Matt Thomas for your friendliness and advice during my time at Mount Cuthbert. An enormous thank you to Katie Howard, for your assistance and incredible organisation skills, to Ben Wade and the Adelaide Microscopy team for your patience, to Ioan Sanislav for your guidance during the core logging, and to Ross Christie for your conversation, your company and your sense of humour all of which I enjoyed immensely. Finally, thanks to my all my rippaz, you made the year worth it.

REFERENCES

BEARDSMORE T. J. 1992 Petrogenesis of Mount Dore-style breccia-hosted copper±gold mineralization in the Kuridala-Selwyn region of northwestern Queensland. James Cook University.

BETTS P. G., GILES D., MARK G., LISTER G. S., GOLEBY B. R. & AILLÈRES L. 2006. Synthesis of the proterozoic evolution of the Mt Isa Inlier. *Australian Journal of Earth Sciences* **53**, no. 1, pp. 187-211.

BIERLEIN F. P., MAAS R. & WOODHEAD J. 2011. Pre-1.8 Ga tectono-magmatic evolution of the Kalkadoon–Leichhardt Belt: implications for the crustal architecture and metallogeny of the Mount Isa Inlier, northwest Queensland, Australia. *Australian Journal of Earth Sciences* **58**, no. 8, pp. 887-915.

BLAKE D. H. 1987 Geology of the Mount Isa inlier and environs, Queensland and Northern Territory. Australian Govt. Pub. Service.

BLAKE D. H., STEWART A. J., SWOBODA R. & JEFFERY N. 1992 Geology of the Mount Isa-Cloncurry Transect. Australian Geological Survey Organisation, Department of Primary Industries and Energy.

BOCTOR N., BELL P., MAO H. & KULLERUD G. 1982. Petrology and shock metamorphism of Pampa del Infierno chondrite. *Geochimica et Cosmochimica Acta* **46**, no. 10, pp. 1903-1911.

BROOKS J. H. 1977. Small-scale copper mining in the Mt Isa and Cloncurry mining fields, 1976. *Queensland Government Mining Journal* **78**, pp. 446 - 462.

CARTER E. K., BROOKS J. H. & WALKER K. R. 1961 The Precambrian mineral belt of north-western Queensland. Bureau of Mineral Resources, Geology and Geophysics.

DERRICK G. & WILSON I. 1982. Geology of the Alsace 1: 100 000 sheet area (6858). *Bureau of Mineral Resources Record* **6**.

DUNCAN R. J., STEIN H. J., EVANS K. A., HITZMAN M. W., NELSON E. P. & KIRWIN D. J. 2011. A New Geochronological Framework for Mineralization and Alteration in the Selwyn-Mount Dore Corridor, Eastern Fold Belt, Mount Isa Inlier, Australia: Genetic Implications for Iron Oxide Copper-Gold Deposits. *Economic Geology* **106**, no. 2, pp. 169-192.

FORD A. & BLENKINSOP T. G. 2008. Evaluating geological complexity and complexity gradients as controls on copper mineralisation, Mt Isa Inlier. *Australian Journal of Earth Sciences* **55**, no. 1, pp. 13-23.

FOSTER D. R. & AUSTIN J. R. 2008. The 1800–1610Ma stratigraphic and magmatic history of the Eastern Succession, Mount Isa Inlier, and correlations with adjacent Paleoproterozoic terranes. *Precambrian Research* **163**, no. 1, pp. 7-30.

FOSTER D. R. W. & RUBENACH M. J. 2006. Isograd pattern and regional low-pressure, high-temperature metamorphism of pelitic, mafic and calc-silicate rocks along an east – west section through the Mt Isa Inlier. *Australian Journal of Earth Sciences* **53**, no. 1, pp. 167-186.

GROVES D. I., BIERLEIN F. P., MEINERT L. D. & HITZMAN M. W. 2010. Iron Oxide Copper-Gold (IOCG) Deposits through Earth History: Implications for Origin, Lithospheric Setting, and Distinction from Other Epigenetic Iron Oxide Deposits. *Economic Geology* **105**, no. 3, pp. 641-654.

HUTTON L. J., DENARO T. J., DHNARAM C. & DERRICK G. M. 2012. Mineral Systems in the Mount Isa Inlier. *Episodes* **35**, no. 1, pp. 120-130.

KROSCH N. J. & SAWERS J. 1974 Copper Mining in the Cloncurry and Mount Isa Mining Fields, 1971. Queensland Department of Mines.

LAUKAMP C., CUDAHY T., CLEVERLEY J. S., OLIVER N. H. & HEWSON R. 2011. Airborne hyperspectral imaging of hydrothermal alteration zones in granitoids of the Eastern Fold Belt, Mount

Isa Inlier, Australia. *Geochemistry: Exploration, Environment, Analysis* **11**, no. 1, pp. 3-24.

MARK G., OLIVER N. & CAREW M. 2006. Insights into the genesis and diversity of epigenetic Cu–Au mineralisation in the Cloncurry district, Mt Isa Inlier, northwest Queensland. *Australian Journal of Earth Sciences* **53**, no. 1, pp. 109-124.

MURPHY F. C., HUTTON L. J., WALSHE J. L., CLEVERLEY J. S., KENDRICK M. A., MCLELLAN J., RUBENACH M. J., OLIVER N. H. S., GESSNER K., BIERLEIN F. P., JUPP B., AILLÈRES L., LAUKAMP C., ROY I. G., MILLER J. M., KEYS D. & NORTJE G. S. 2011. Mineral system analysis of the Mt Isa–McArthur River region, Northern Australia. *Australian Journal of Earth Sciences* **58**, no. 8, pp. 849-873.

OLIVER N. 1995. Hydrothermal history of the Mary Kathleen Fold Belt, Mt Isa Block, Queensland. *Australian Journal of Earth Sciences* **42**, no. 3, pp. 267-279.

PAGE R. & BELL T. 1986. Isotopic and structural responses of granite to successive deformation and metamorphism. *The Journal of Geology*, pp. 365-379.

RAYMOND G. 1992. Mount Isa Inlier and environs mineral deposit database. *AGSO Record* **66**, p. 27.

RUBENACH M. 2008 Tectonothermal and Metasomatic evolution of the Mount Isa Inlier. Mineral system analysis of the Mount Isa–McArthur region, Northern Australia, Project I7: Predictive Mineral Discovery Report, 57 pp.

RUBENACH M. J. 2005. Relative timing of albitization and chlorine enrichment in biotite in Proterozoic schists, Snake Creek Anticline, Mount Isa Inlier, northeastern Australia. *The Canadian Mineralogist* **43**, no. 1, pp. 349-366.

RUDNICK R. & GAO S. 2003. Composition of the continental crust. *Treatise on geochemistry* **3**, pp. 1-64.

VAN DIJK P. M. 1991. Regional syndeformational copper mineralization in the western Mount Isa Block, Australia. *Economic Geology* **86**, no. 2, pp. 278-301.

WARING C., HEINRICH C. & WALL V. 1998. Proterozoic metamorphic copper deposits. *AGSO Journal of Australian Geology and Geophysics* **17**, pp. 239-246.

WILLIAMS P. J. 1998. Metalliferous economic geology of the Mt Isa Eastern Succession, Queensland. *Australian Journal of Earth Sciences* **45**, no. 3, pp. 329-341.

WYBORN L. 1998. Younger ca 1500 Ma granites of the Williams and Naraku Batholiths, Cloncurry district, eastern Mt Isa Inlier: Geochemistry, origin, metallogenic significance and exploration indicators. *Australian Journal of Earth Sciences* **45**, no. 3, pp. 397-411.

APPENDIX A

Petrology and overview comments concerning 9 samples from Mt Cuthbert, Cloncurry region, Queensland Australia.

Dr R. G. Taylor
BSc (Hons), D.I.C., PhD, M.A.I.G.
July 2015

c/o 15 Burns Street, Invermay, Launceston, Tasmania, 7248
Email – roger-taylor@bigpond.com
Tel. – 61 3832655622
Mobile - 0417621275

1. INTRODUCTION.

This report was commissioned by Malaco Leichardt Pty Ltd at the recommendation of Dr Richard Lilly (Department of Earth Sciences, University of Adelaide). The samples were accompanied by some field notes with a brief to provide petrological description and overview comment. Petrological details are provided in Appendix I (Figures 1-19).

2. HOST ROCKS.

Several problems were encountered concerning host rock identification.

1) Dolomite (Figures 14, 16, and 18).

The coarse grained carbonate±quartz in the MC003 samples is difficult to interpret from a small slab. It is presumed that the field name dolomite has been given from logging experience and thus is a more suitable name than carbonate veining?

2) Biotite – schist ±chlorite alteration (MC001 DD24-335.0),

(NB -Identified as chlorite schist in field notes-Figure 3).

3) Metavolcanics (Figures 8, 10, 12, and 13).

The fine grained dark samples tentively identified in the field notes as metavolcanics cover a wide range of different rocks and none are standard volcanics.

At the microscope level, the fine grain size and alteration has also caused identification problems. Tentative interpretations are discussed below:

1. Quartzite (or part of quartz veining). MC001 DD9-256.0 (Figure 2).
2. Fine grained crowded “granite” porphyry – MC001 DD 41-94.4 (Figures 9-10), (some confusion with biotite distribution and deformation).
3. Layered fine grained altered metasediments?/ volcaniclastics? (Figure 12-13). MC002 DD 3-29.1. The alternating darker and finer folded layers are possibly more in keeping with metasediment??
4. Fine grained mildly foliated feldspar/haematite rocks (Figures 8-9). MC001 57-422.0 (possibly ash originally??).

(NB. The writer is not an expert on altered fine grained volcanic/volcanoclastic rocks and further opinion via specialist expertise may provide further insight if considered vital to the project).

3. HYDROTHERMAL STAGES.

Despite the small sample range, hydrothermal stages are well represented and include:-
Early. Albite (±quartz).
Biotite.
Carbonate – quartz.
Sulphide dominant (chalcopyrite, pyrite, pyrrhotite, marcasite, chlorite, ?epidote).
Quartz.
? Unidentified minor stage(see below).
Late. Chalcocite (secondary enrichment).

Their detailed mineralogy is discussed below in the paragenetic section, with examples presented in the Appendix.

4. PARAGENESIS.

The suite of samples is small, and as such may not contain all the stages represented at the prospect. However, some 6-7 stages of structure disruption and fluid introduction are recognized here (see above) and Table 1 (p3).

1. Albite-quartz (vein/alteration), (Figures 8, 9, 12, 13).

This occurs in two of the samples (MC001 DD37-42.2, MC002 DD3-29.1) as narrow network veinlets. The stage is early in the evolution, and visible as faint pink (albitic) alteration weakly developed in the adjacent wall rocks.

2. Biotite (veins), (Figures 1-2).

Biotite veins occur in one sample (MC001 DD9 2-56).

3. Carbonate – quartz (veins), (Figures 4, 5).

These are well represented (Table 1) occurring at mm to low centimetre scales. They are often refractured and overprinted by sulphides.

4. Sulphides (Figures 5, 6, 16, 17).

This mineralising stage occurs in 8 of the 9 samples and is mostly infill vein style with some indications of replacement of pre-existing carbonate. Chalcopyrite and pyrite predominate, but two samples contain pyrrhotite/chalcopyrite with no pyrite. Minor marcasite is recorded and chlorite (infill) is abundant in places. Chloritic alteration of host rocks is linked to the infill stage (MC001 009-56). Brittle fracture predominates

5. Quartz (veins), (Figures 12-13)

A minor stage with narrow infill veinlets.

6. Unknown mineral (minor), (cracks).

A late stage unidentified brown acicular mineral occurs in sample MC001 DD24-255. It has a wispy crackle control and replaces carbonate.

7. Chalcocite (replacement).

Supergene alteration (minor) – (MC003 DD 10-59.5).

5. COMMENTS/DISCUSSION.

The general sequence (albite, biotite, carbonate, sulphide, and quartz) could be interpreted as a progressive down temperature paragenesis from a single source, but considerable more field and laboratory data would be required to support this. Albitic alteration is abundant in the Cloncurry region and not always linked to sulphide occurrence. Similarly the minor late quartz could be much later than the sulphide. The sulphide assemblage is of interest with both pyrite-chalcopyrites, pyrite-pyrrhotite occurring as separate assemblages.

This could be regarded as a zonation effect and **merits detailed logging** to establish distribution. A similar situation occurs at Eloise (Baker, 1998), where the paragenesis is similar.
I albite, II biotite/hornblende/quartz, III chalcopyrite/magnetite, pyrrhotite pyrite, actinolite, chlorite, quartz/calcite.

(NB. Stage III seems incorrect see below).

Sample	Albite±quartz	Biotite	Carbonate±quartz	Sulphide	Chalcopyrite Pyrite Marcasite Chlorite	Quartz	Unknown mineral	Chalcocite (supergene)
MC001 DD37-422	✓	-	✓	✓ Cpy Pyrr + epidote?	-	-	-	-
MC001 DD29 385.6	-	-	✓	✓ Cpy Pyrr	-	-	-	-
MC001 DD 24-335	-	-	✓	✓ Cpy Py	-	-	✓	-
MC001 DD 9-256	-	✓	-	✓ Cpy Py	-	-	-	-
MC001 DD 41-94.4	-	-	✓	✓ Cpy Py	-	-	-	-
MC002 DD 3-29.1	✓ +chlorite?		-	✓ Cpy Py	-	✓	-	-
MC002 DD 13-90.7	-		-	✓ Cpy Py Marc	-	✓	-	-
MC003 DD 12-83.8	-		-	✓ Cpy Py Marc	-	-	-	-
MC003 DD 10-59.5	-		-	✓ Cpy Py	-	-	-	✓

Key (cpy – chalcopyrite, py – pyrite, pyrr – pyrrhotite, marc – marcasite).

Table 1: Distribution of stages

"The lodes occupy a narrow portion of a zoned mineralised system that is at least 2km in length. Magnetite pyrite rich mineralization occurs in the south, with chalcopyrite-pyrrhotite rich mineralisation in the central lode zone and pyrrhotite rich mineralization in the north".(Baker 1988).

The zonation is interpreted as zoned from north to south, with the pyrrhotite sector representing a distal situation. The reasons for the zonation can only be interpreted, possibly temperature variation or a change in sulphur chemistry resulting in pyrrhotite v pyrite. It is worth noting that the paragenesis looks a little odd in that magnetite/actinolite usually precede sulphides in the Cloncurry region (overprinting suspected). There are also temperature problems with magnetite usually being much higher temperature than chlorite. The coexistence of chlorite with actinolite is also anomalous.
In terms of classification the deposit is clearly similar to many others in the Cloncurry district and can be embraced in the IOCG category. The gold values are currently a little low, but assays of up to 0.35pp are recorded (R. Lilly – pers com).

REFERENCE.

Baker, T., 1998. Alteration, mineralisation and fluid flow evolution at the Eloise Cu-Au deposit, Cloncurry district, Northwest Queensland, Australia. Econ. Geol., v93, pp1213-1236.

APPENDIX 1, PART B

Petrological descriptions.
MC001 DD 9-256.00m.
MC001 DD 24-335.00m.
MC001 DD 29-385.60m.
MC001 DD 37-42.20m.
MC001 DD 21-94.40m.
MC002 DD 3-29.10m.
MC003 DD 10-59.50m.
MC003 DD 12-83.80m.
MC003 DD 13-90.70m.

Specimen MC001DD9-256.

Hand specimen.
Pyrite crystals ,1-2mm scale spread over a zone some 2cm long and 0.5-1.0cm wide, set within a zone of pale green fine grained ?chlorite. These are overprint broken grey quartz. A dark zone occurs in several places overprinting the quartz and dying out on approaching the chlorite alteration. (Biotite in thin section).

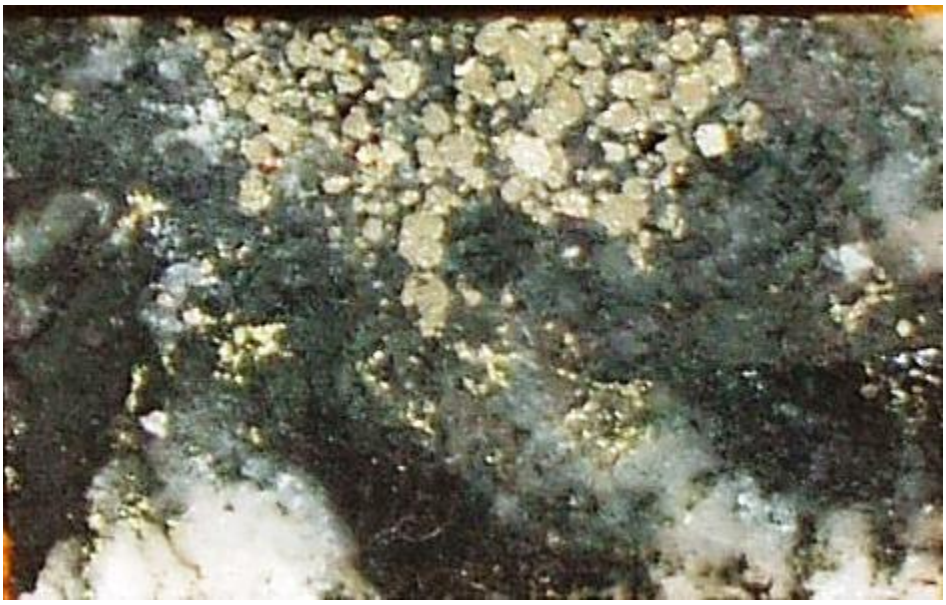

Figure 1: MC001DD 9-256.00m. Quartz rich host rock (quartzite?) overprinted by dark-biotite veins (lower half). Pyrite (yellow) and chlorite (pale green). Early biotite (dark) is altered to chlorite at the boundary zone (Mid photograph) Slab. Width of frame (WOF) – 3.6cm.

Petrology.

The host quartz dominant material is composed of coarse (400 micron) and fine (100 micron) mosaic style quartz grains. From the small amount of material available, these could be ex-quartz vein or quartzitic materials. The field description of metavolcanics suggests the latter.

Biotite veins.

Biotite veins/stringers cut the quartz rich host rocks. The grains/flakes are 100-500 microns in size with both brown and green variations. The biotite becomes chloritized approaching the sulphide zone.

Sulphide stage

Pyrite, chalcopyrite, chlorite±carbonate. Pyrite and chlorite predominate. The pyrite occurs as crystals (infill) at the 100micron to 2.0mm range. Minor chalcopyrite occurs in association (replacing carbonate?) with carbonate. (Spider infill veins (discontinuous) and replacive blebs). The chlorite occurs as infill and alteration of pre-existing biotite.

Paragenesis.

Early. 1. Biotite (veins-infill).
2. Carbonate, pyrite, chalcopyrite chlorite (chlorite infill and alteration of biotite). Chalcopyrite occurs as infill and also as carbonate replacive.

Comments.

Major chlorite component.

:

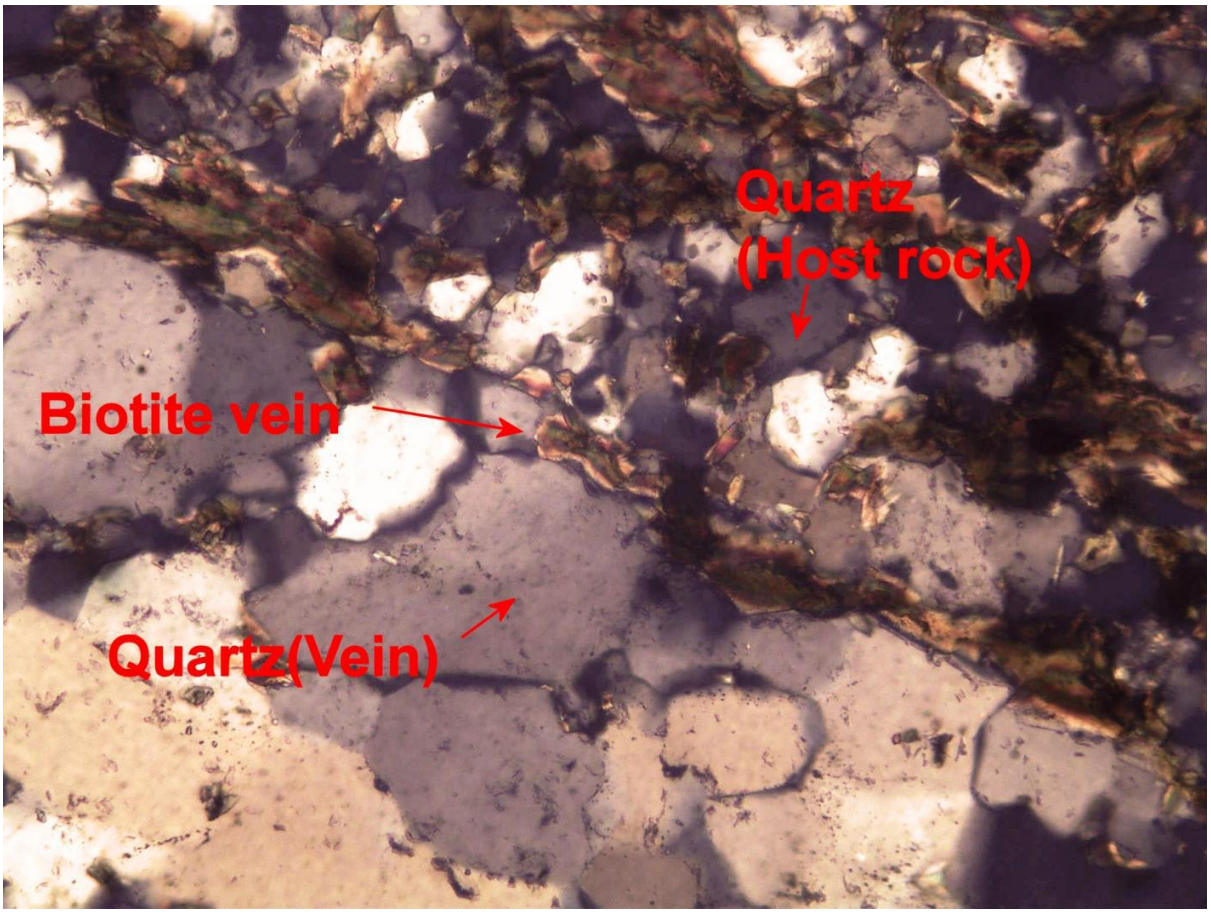

Figure 2: MC001DD 9-256.00m. Biotite veins overprinting quartz dominant host rocks. Ordinary light (OL). WOF c820 microns.

Specimen MC001 DD 24-335.

Hand specimen.

A centimetre scale vein composed of carbonate, quartz±chalcopyrite and pyrite occurring as infill within a dark schistose rock. Minor sulphides are speckled within the foliated host rock.

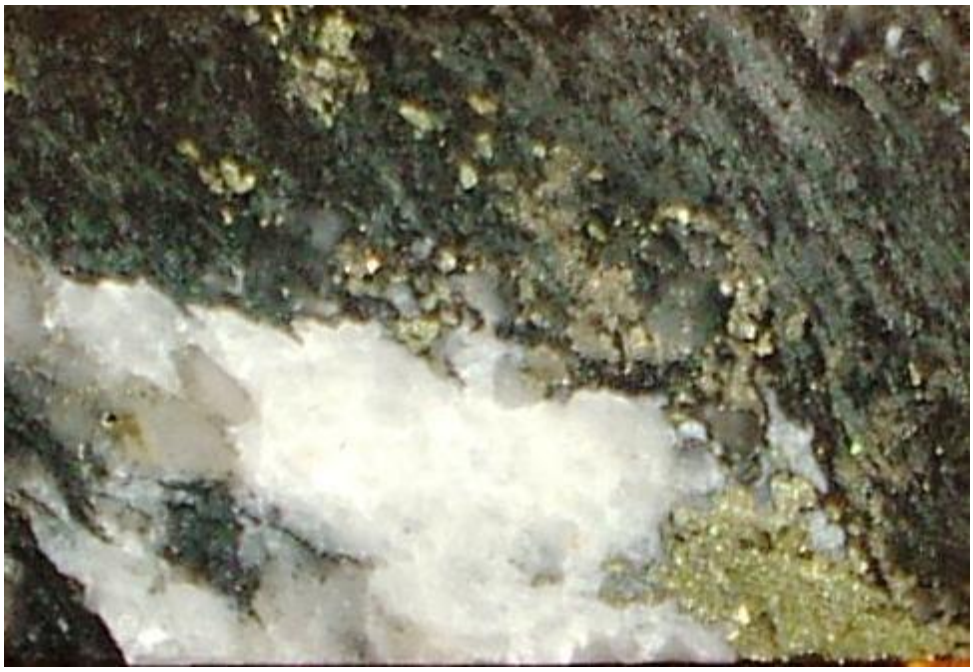

Figure 3: MC001DD 24-335m. Chloritised (pale green-top right) biotite-quartz schist (dark). Carbonate (white) and quartz (grey) vein, cut by pyrite/chalcopyrite (yellow). Slab WOF 3.6cm.

Petrology

Host rock.
The host rock is well foliated quartz-biotite schist. The proportions of quartz (50-70 micron) and biotite (100 x 20 microns) vary considerably. The biotite is part altered to chlorite.

Vein.
The vein is composed of quartz (500 micron – 3.0mm) crystal infill and carbonate 2-3.0mm), overprinted by sulphides (chalcopyrite, pyrite).

The chalcopyrite also occurs as stringers and lenses along the foliation of the host rock . Carbonate (infill) patches also runs parallel to the fabric. The pyrite (200-300 micron) is subcrystalline. Total sulphide is around 3-5% with pyrite/chalcopyrite in equal proportions. Minor chlorite is present. A late overprint of finely acicular brown needle-like mineral occurs along carbonate boundaries. The mineral replaces carbonate and remains unidentified. It associated with green chlorite in places. Some replacement of carbonate by chalcopyrite is suspected?.

Paragenesis.
1. Quartz – carbonate (infill).
2. Pyrite, chalcopyrite, chlorite (mostly infill, some chalcopyrite replaces carbonate.
3. Unidentified late acicular mineral.

Comments.

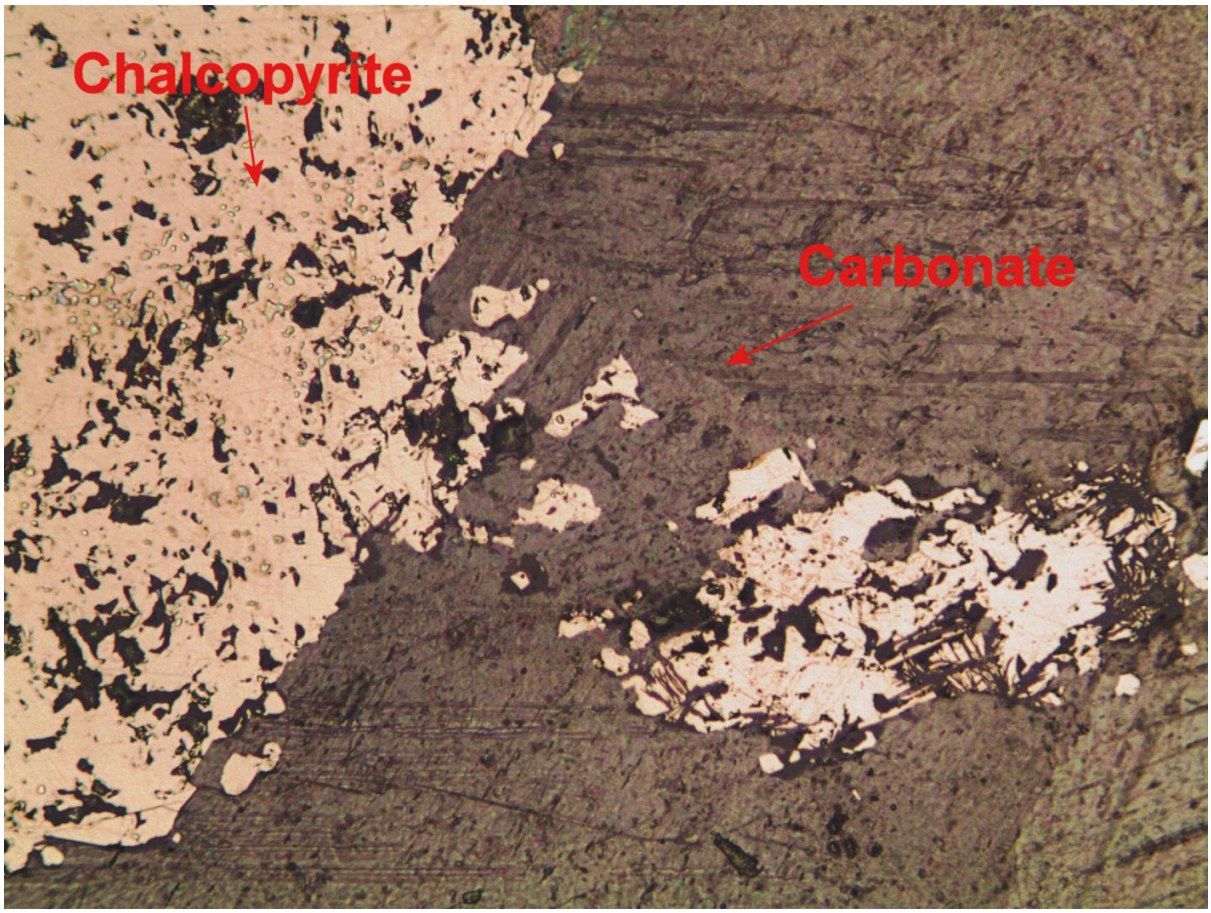

Figure 4: MC001DD 24-335.00m. Chalcopyrite in carbonate host. Replacement suspected at the boundary zones? Reflected light (RL). WOF c820 microns.

MC001 DD 29-385.6.

Hand specimen.

White carbonate vein with grey quartz, overprinted by chlorite (green) and wispy elongate discontinuous stringers and blebs of chalcopyrite and pyrrhotite.

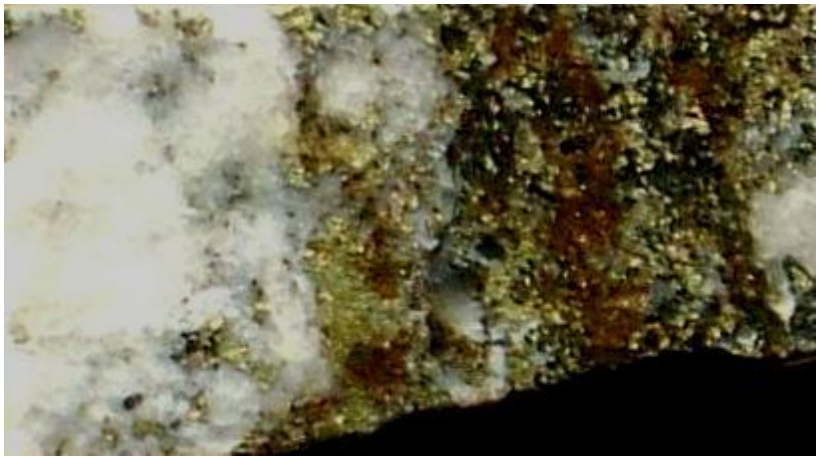

Figure 5: MC001DD 29-385.6m. Carbonate-quartz vein (white/grey) overprinted by chalcopyrite (yellow) and pyrrhotite (brown). Slab WOF 3.6cm.

Petrology.
The carbonate vein is visible towards one end of the slide, and consists of some 95% coarse grained carbonate (5.0mm scale) and 5% quartz. The latter occurs in granular clusters and discrete grains (100-400 microns). One patch (2.0mm) consists of quartz and highly sericitised feldspar. The feldspar is untwinned and distinction with K-spar is uncertain. It is suspected as a wall rock fragment – possibly an albitic vein?

The carbonate material is overprinted at one end by sulphide/chlorite dominant materials. The sulphides/chlorite form a vague anastmosing network with millimetre scale grains. Chlorite crystals are common (infill style) and associate with a pale orange/brown pleochroic, highly anisotropic mineral tentatively identified as an epidote? Some sulphide replacement of prexisting carbonate is suspected.

Paragenesis.
Early. 1. Carbonate, quartz infill vein.
Late. 2. Chalcopyrite, pyrrhotite, chlorite± ? epidote (early sericitisation of feldspar in? fragments).

Comment.
The epidote identification is tentative.

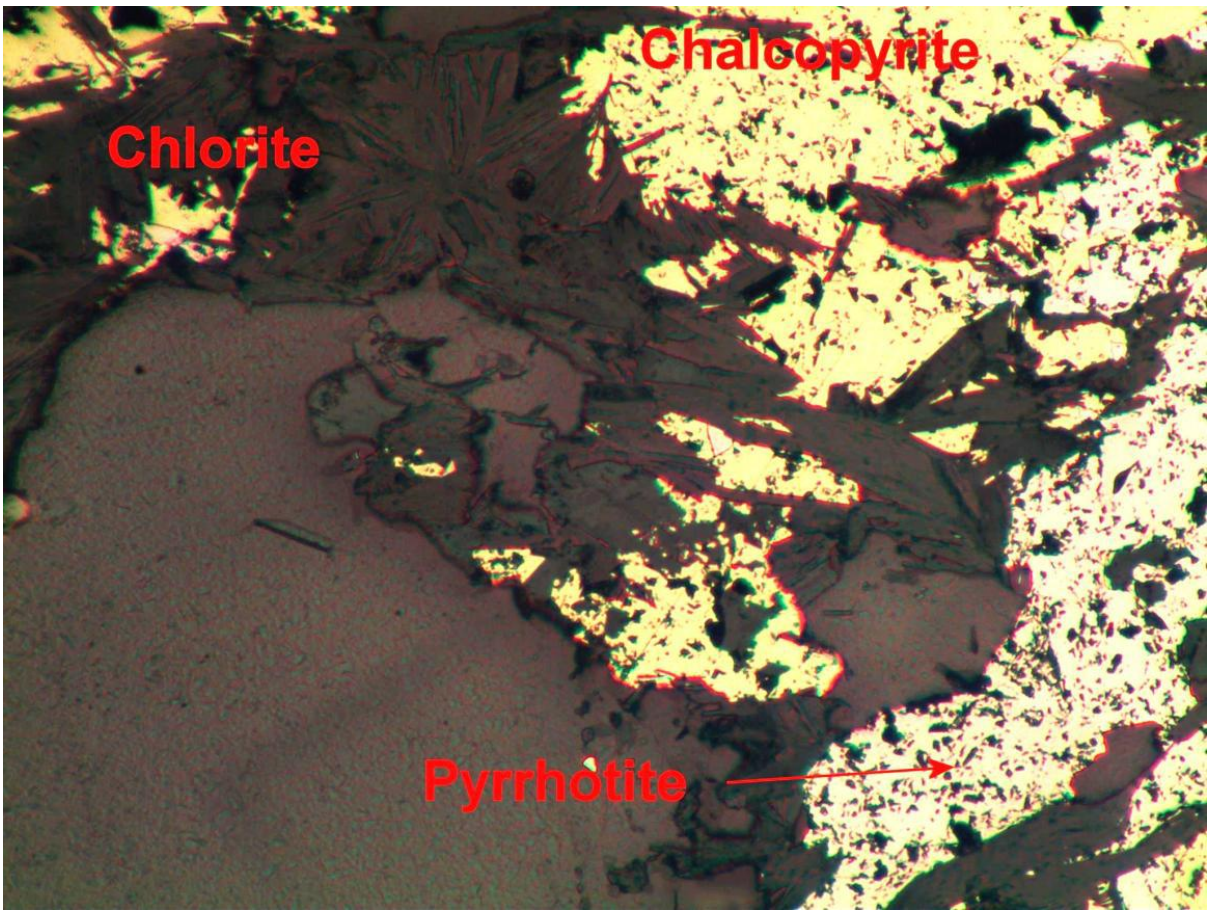

Figure 6: MC001DD 29-385.6m. Carbonate-quartz vein (white/grey) overprinted by chalcopyrite (yellow) and pyrrhotite (brown). Slab WOF 3.6cm.

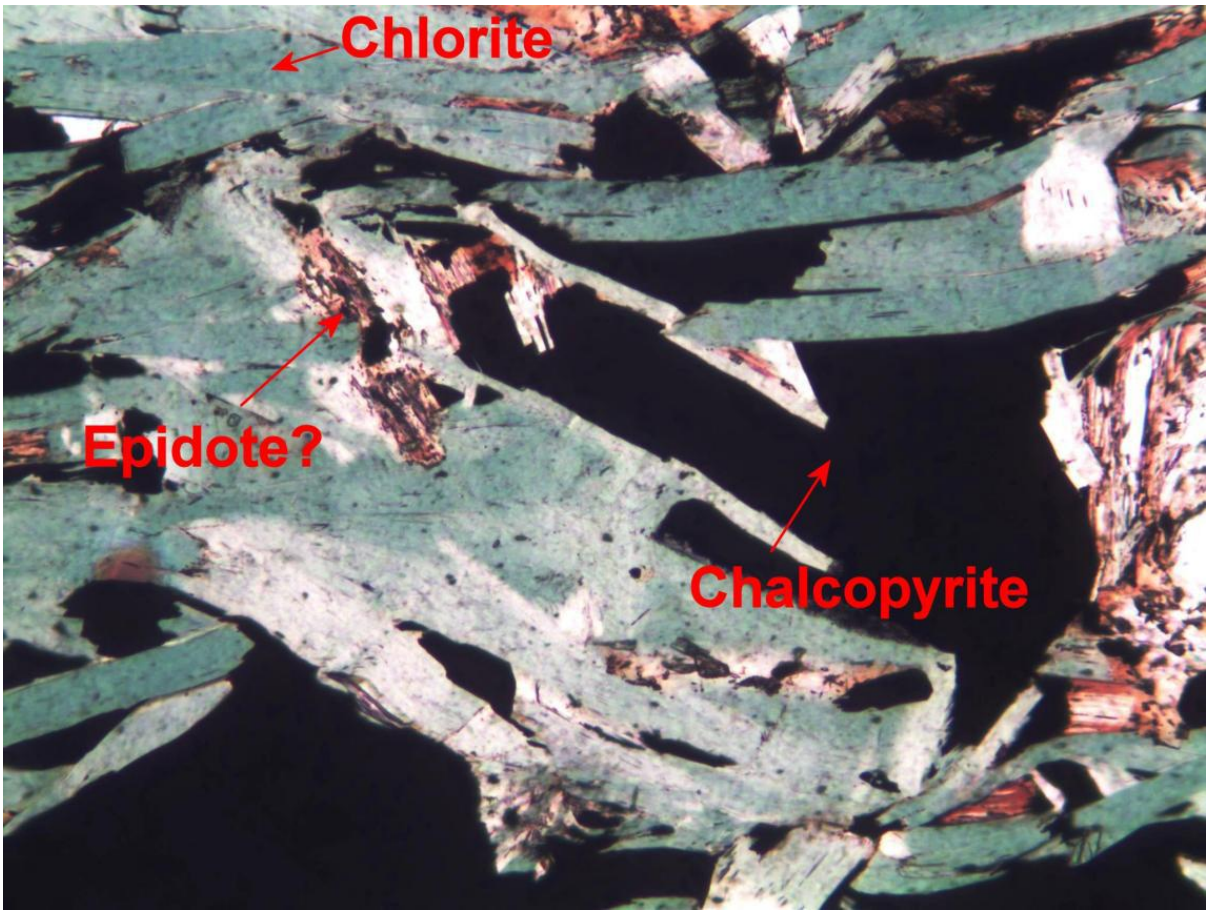

Figure 7: MC001DD 29-385.60m. Chalcopyrite, pyrrhotite, chlorite stage. RL. WOF c820 microns.

Specimen MC001 DD 37-42.20.

Hand specimen.
The specimen is a fine grained dark host rock, cracked and overprinted by a network of white carbonate infill. The fragmented host has broken into 2-5mm rounded fragments. In isolated areas the fine host is tinged pale pink (albitic alteration?). Trace amounts of fine grained chalcopyrite (wispy) overprint the carbonate and host rock.

Figure 8: MC001DD 37-422.00m. Early albite (pale pink) in fine grained host rock brecciated and overprinted by carbonate network veining (white) and late wispy chalcopyrite (yellow). Slab. WOF 3.6m.

Petrology.

Host rock.

The fragments are 2-5m in general scale, rounded/smooth edged with a jigsaw fit. The grain size of 5-20 micron is at the limit of resolution, but is composed of vague elongated felted textured material (weakly foliated). In rare instances multiple twins are visible (plagioclase – albite suspected). Also present are 2-3% opaque grains, these are roughly equant and although identified as haematite, were probably magnetite originally. Minor sericite (1-2 microns) and carbonate? (1-2 micron) are also present.

Veins/alteration.

Carbonate.

1. The carbonate network veining (0.5-1.0mm widths) occupies some 20-40% of the area, with grains at the 250 micron to 1.0mm scale.
2. Albite-quartz. These are cut by the carbonate and composed of variable amounts of carbonate and multiply twinned plagioclase (5-50 microns). Symmetrical multiple twin angles of around 9o and white anisotropy suggest albite.
3. Sulphide. Sulphides occupy some 2-3% of the slide with chalcopyrite predominating over pyrrhotite. They occur as discontinuous veinlets, and irregularly shaped blebs. Infill predominates with minor carbonate replacement.

Paragenesis.

1. Albite±quartz, veining and alteration.
2. Carbonate veins.
3. Pyrite, pyrrhotite – discontinuous crack style veins, minor alteration.

Comments.
The identification of the host rock is difficult with the original fine grain size and albitisation providing problems. However, the fine grained plagioclase dominance suggests a possible volcanic ash style provenance?? The field identification is metavolcanic.

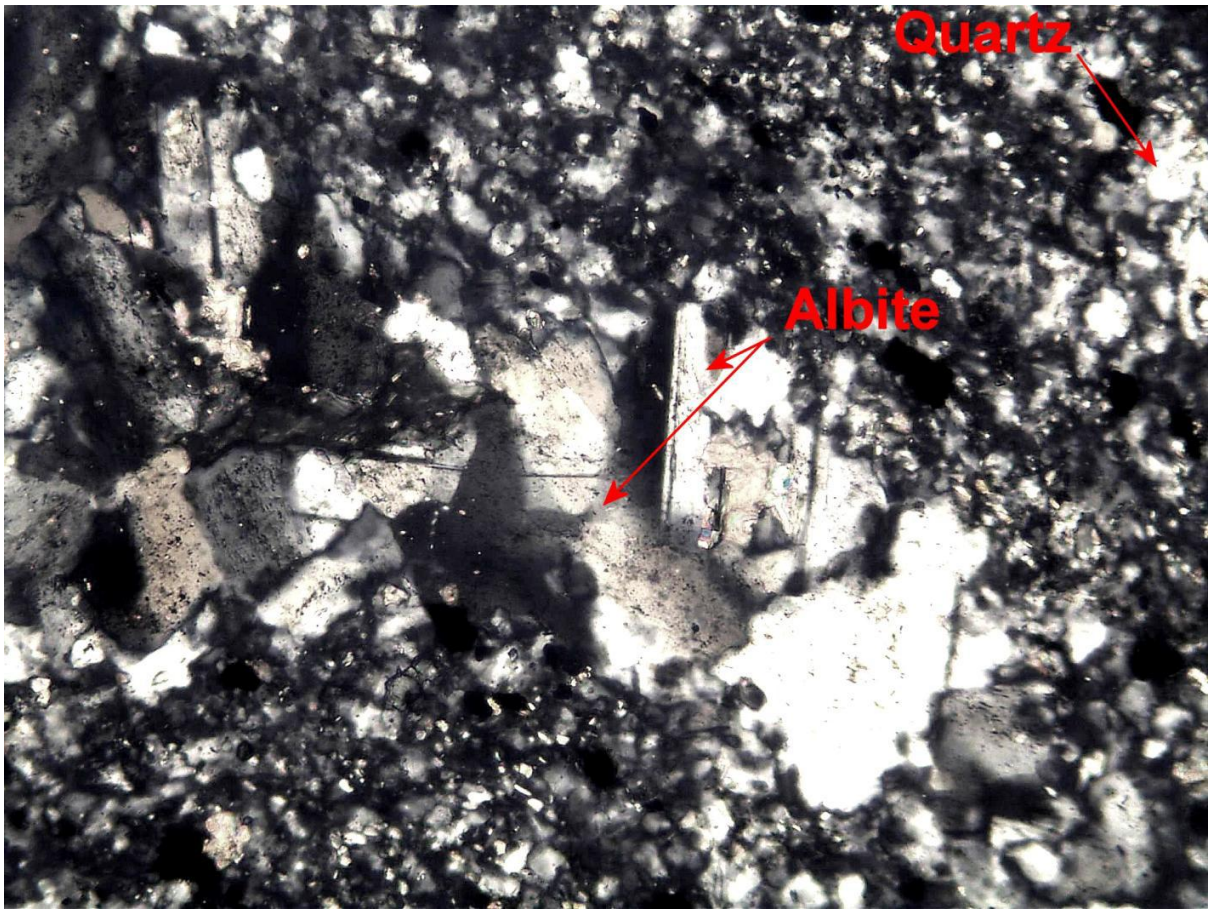

Figure 9: MC001DD 385.00m. Chalcopyrite, chlorite infill. OL. WOF 820m.

MC001 DD 41-94.40m.

Hand specimen.
Irregularly bordered, pyrrhotite/chalcopyrite vein overprinting a pinkish tinged quartz vein.
The dark host rocks are of different texture on either side.
1. Well foliated with grey elongate phenocrysts (feldspar) (1.0mm) and some whiter (quartz?) set in a fine dark matrix.
2. Similar to the above, but with no obvious foliation. Grey phenocrysts of feldspar are visible, but smaller than those above. The phenocrysts (c20%) are set in a fine grained dark matrix.

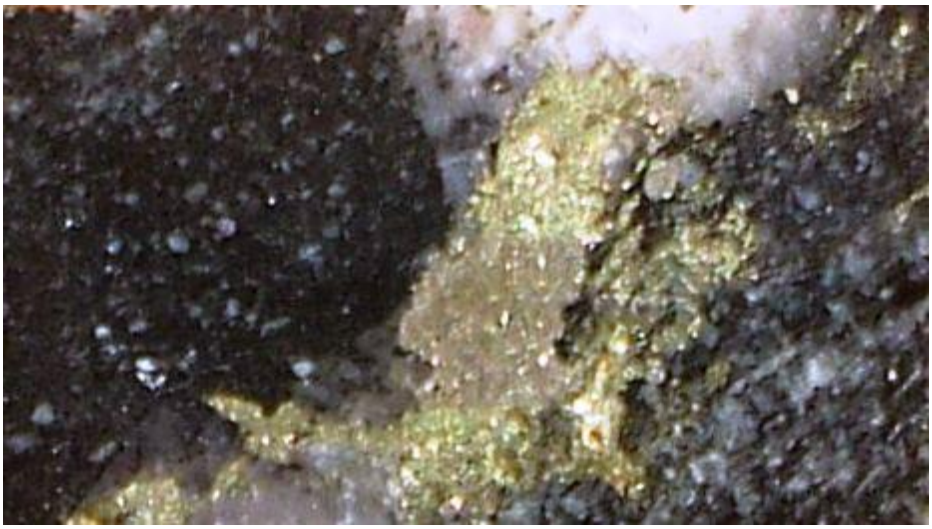

Figure 10: MC001DD 37-422.00m. Early albite (pale pink) in fine grained host rock brecciated and overprinted by carbonate network veining (white) and late wispy chalcopyrite (yellow). Slab. WOF 3.6m.

Petrology.

1. Foliated area. This sector exhibits a good foliation via elongate wispy brown biotite grains, and localised biotite meshworks. Biotite occupies some 5-10% of the slide, but is distributed irregularly. In places it is 2-5% but goes up to 40-50% in an anastosing meshwork. The biotite is brown and flakes are around the 200 micron scale. The rock consists of phenocrysts (some 50%) of quartz (0.5-1.0m). The quartz phenocrysts are 40-50% of the crowded porphyry and the proportion of K-spar v albite are difficult to estimate (say 10-15% K-spar), (35-40 albite).

The matrix between the phenocrysts is at the 100-200 micron scale and is mosaic textured. Quartz grains predominate (60%) and proportions of K-spar v albite are difficult to estimate (say 40% albite, 20% K-spar). Lensoid patches of fine quartz/albite are present and similarly these are elongate patches (5-10%) of carbonate (±trace fine grained epidote?).

Sericitic alteration of the feldspars is present and more strongly developed in the K-feldspar. With the variable texture overall mineral proportions are difficult across but are in the region of:

Quartz – 30-40%
Albite – 35-40%
K-feldspar – 10-15%
Biotite – 5-10%

2. This region is similar to the above with slightly finer phenocrysts size (500 microns). The foliation is very weakly defined by low biotite content at one end and the rock is essentially plutonic igneous texture (crowded porphyry). However, approaching the vein biotite becomes more concentrated (up to 505). Minor muscovite is present.

Veins – sulphide-quartz.

The quartz (50-900 microns) is mosaic textured and is overprinted by the sulphides. The sulphides (chalcopyrite, pyrite) occur is infill within broken quartz (brecciated). Pyrite is an early product with one good crystal (5.0mm) forming and overgrown by chalcopyrite. Minor trace chlorite is present.

Paragenesis.
1. Quartz vein (infill).
2. Chalcopyrite, pyrite (infill) ±chlorite).

The timing of the sericitic alteration is unclear (early?).

Comments.
The felsic igneous host rocks are essentially crowded quartz-feldspar-biotite 'granitic' porphyry. The biotite variation is not understood,(but is not biotite alteration).

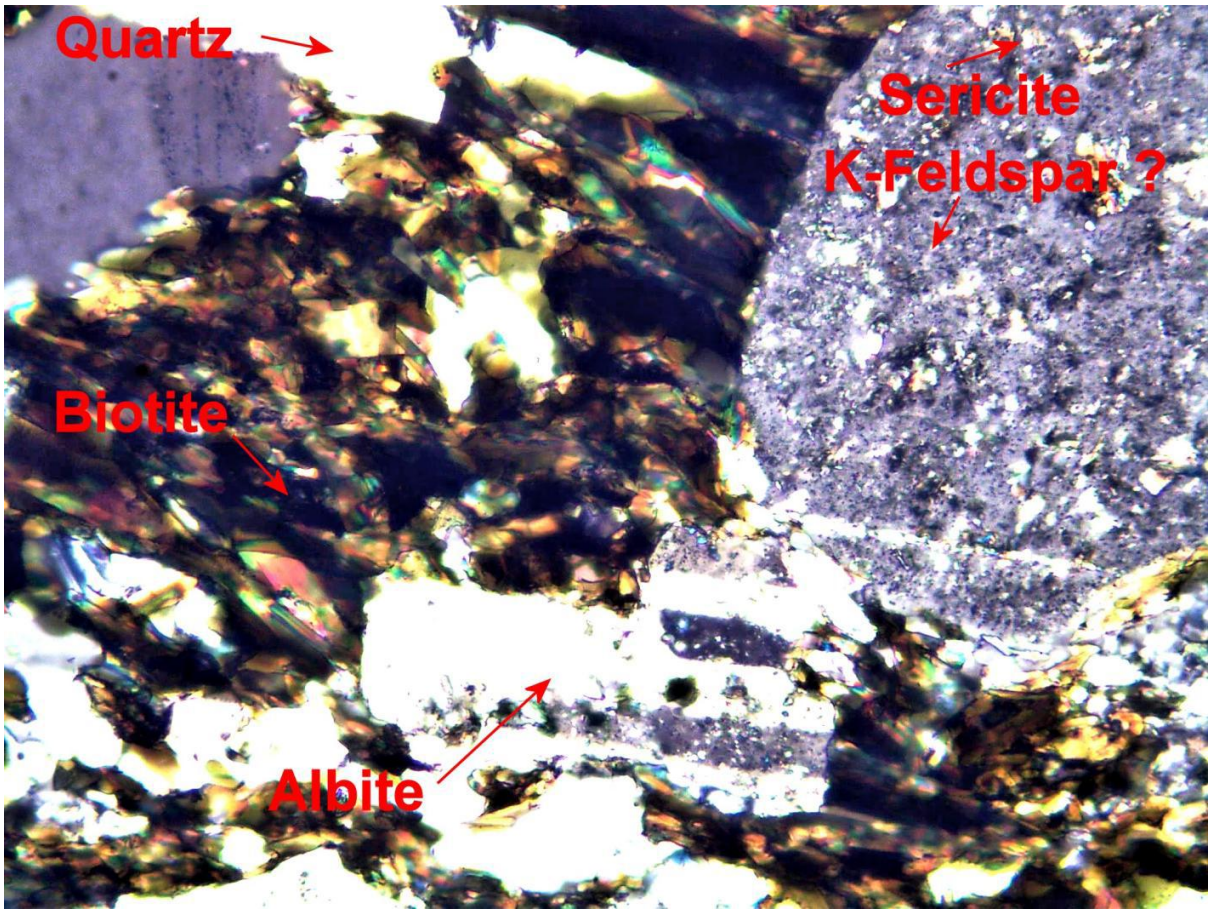

Figure 11: MC001DD 37-422.00m. Albite (infill) vein, crossed nicols (CN). WOF c820 microns.

Specimen MC002 DD 3-29.10m.

Hand specimen.
The rock is a breccia with 0.5-1.0 centimetre size fragments of finely layered dark 'sediments', contained within a network of 1-2mm wide pink tinged infill veining. The layered materials consist of 1-2mm scale bands of dark and slightly paler colours, and some fragments contain folded layers.

The paler bands are slightly coarser than the darker layers and many are tinged with pale pink colouration. The pink tinge is irregularly distributed and often occurs along the layer boundaries. Alteration is suspected (?albite). A few later 1-2mm grey glassy quartz veins cut the above.

Figure 12: MC002DD 3-29.00m. Fine grained folded bedded volcanics/metasediments??, brecciated and network veined by quartz-albite veining . Minor albitisation of host rocks (pinking) and late quartz (grey). Slab. WOF 3.6cm.

Petrology.

Host rocks.
The fine grain size of the layered materials (5-50 microns) hinders mineral identification. The coarser layers (30-50 micron) contain a few grains identifiable as plagioclase with multiple twinning. However, the majority of the grains are not twinned (both the twinned and untwinned grains are suspected as albite, and constitute some 90% of the rock. Opaque (5-10%) at 1-10 microns are similarly difficult to identify, a few larger ones are clearly haematite. Traces of quartz and apatite are tentatively identified.

The finer layers are at the limits of microscope resolution (5-10 micron scale) and characterised by intense development of fine (5 micron) opaques. The opaque content is 50-60% and tentatively identified as haematite. The remaining 40-50% is below microscopic definition. An occasional quartz grain (50 microns) is present.

Network veining.
The network of pink veins is composed of 1-2mm scale infill of 50-200 micron scale albite±chlorite. A few large (50-250 micron scale) opaques are haematite. Some of the shapes are vaguely magnetite shaped (often broken?) and these larger grains also occur within the layered materials.

Quartz veins.
2-3 quartz veins (1-2mm wide) cut across the above.

Paragenesis.
Early. Albite±chlorite infill (and alteration of host rock).

Late. Quartz veining.

Comments.
The field notes suggest that the samples come from materials suspected as volcanics. The fine layering and compositional variation is compatible with either a fine grained volcaniclastic or sedimentary origin. The major haematite content of the darker layers is difficult to interpret (altered volcanic??).

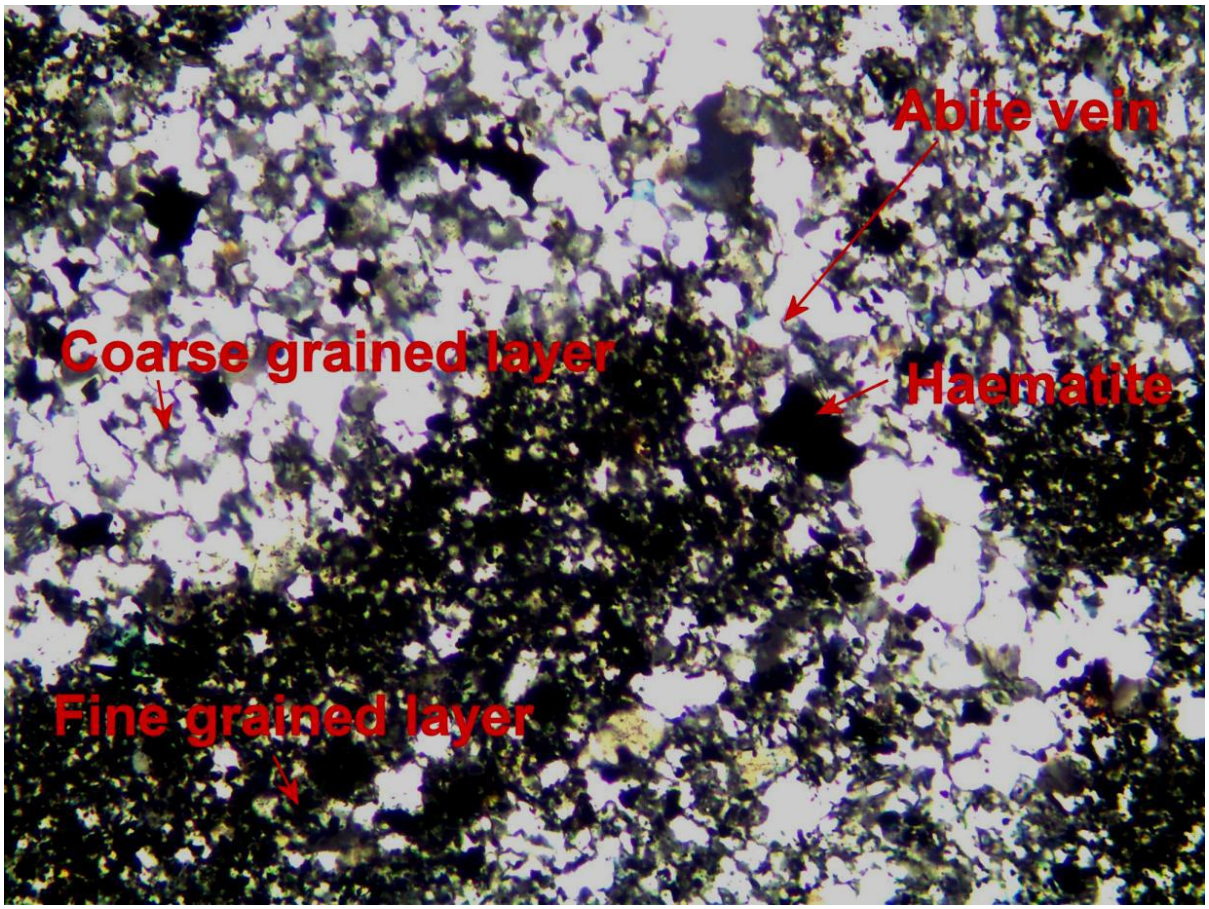

Figure 13: MC002DD 3-29.00. Albite vein, cutting fine grained host rocks (finer, dark) and coarser (lighter). Identification of host rocks unclear (volcaniclastic?/ metasediment?. CN. WOF 820m.

Specimen MC003 DD 10-59.50m.

Hand specimen.
Breccia. The host material is carbonate (white/vein infill) containing fine elongate pink/pale orange spikey materials (1.0-5.0mm scale) which has been brecciated/fractured and overprinted by chalcopyrite (c50% of the sample). The host carbonate becomes darker when surrounded by chalcopyrite (recrystallization effect) and some replacement of carbonate by chalcopyrite is also suspected. Fragment size is around 1-5mm.

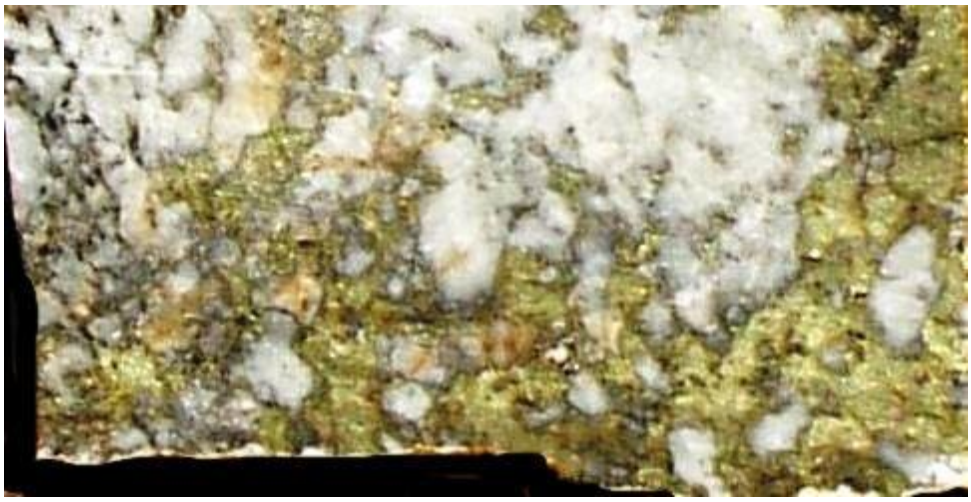

Figure 14: MC003DD 10-59.50m. Dolomite (white) broken and overprinted by chalcopyrite/pyrite (yellow). Slab. WOF 3.6cm.

Petrology.

The slide is composed of around –

40% - chalcopyrite
1% - pyrite
2% - quartz
2% - chlorite
55% - carbonate

Carbonate.
The carbonate is vein infill style with two major styles.
1. Elongate – spindles/spikes of fine grained carbonate. The fine carbonate seems to replace large 1-5mm scale crystals. These are the orange crystal shapes noted in the hand specimen.
2. Coarse interlocking mosaic vein style infill (1.0mm – 100 micron). Some recrystallization suspected in finer patches, mottled extinction, seems to part replace the finer materials of 1) above.

Chalcopyrite±chlorite±pyrite.
This combination occurs predominately as infill in a network around the fragments. Chalcopyrite (c90% predominates and may also replace some carbonate at infill edges. Small amounts (1-5%) of pyrite occur mostly within the chalcopyrite in sub crystalline formats (100 micron), suggesting it precedes chalcopyrite paragenetically. Chlorite occurs as crystal flakes (100-200 micron) – 2-5%. Trace chalcocite is also present (supergene).

Paragenesis.
Early. 1. Elongate crystals – needles/spindles of ?carbonate (now replaced by fine grained 5-10 micron new carbonate). Carbonate – coarse, mosaic style – clear.
3. Chalcopyrite, pyrite, chlorite (infill).
4. Minor – trace chalcocite – supergene enrichment.

Comments.

The early pink tinged crystals are interpreted as ex-carbonate spikes (possibly with Mn content?). Some 90 minutes of searching for gold within the chalcopyrite yielded no occurrences).

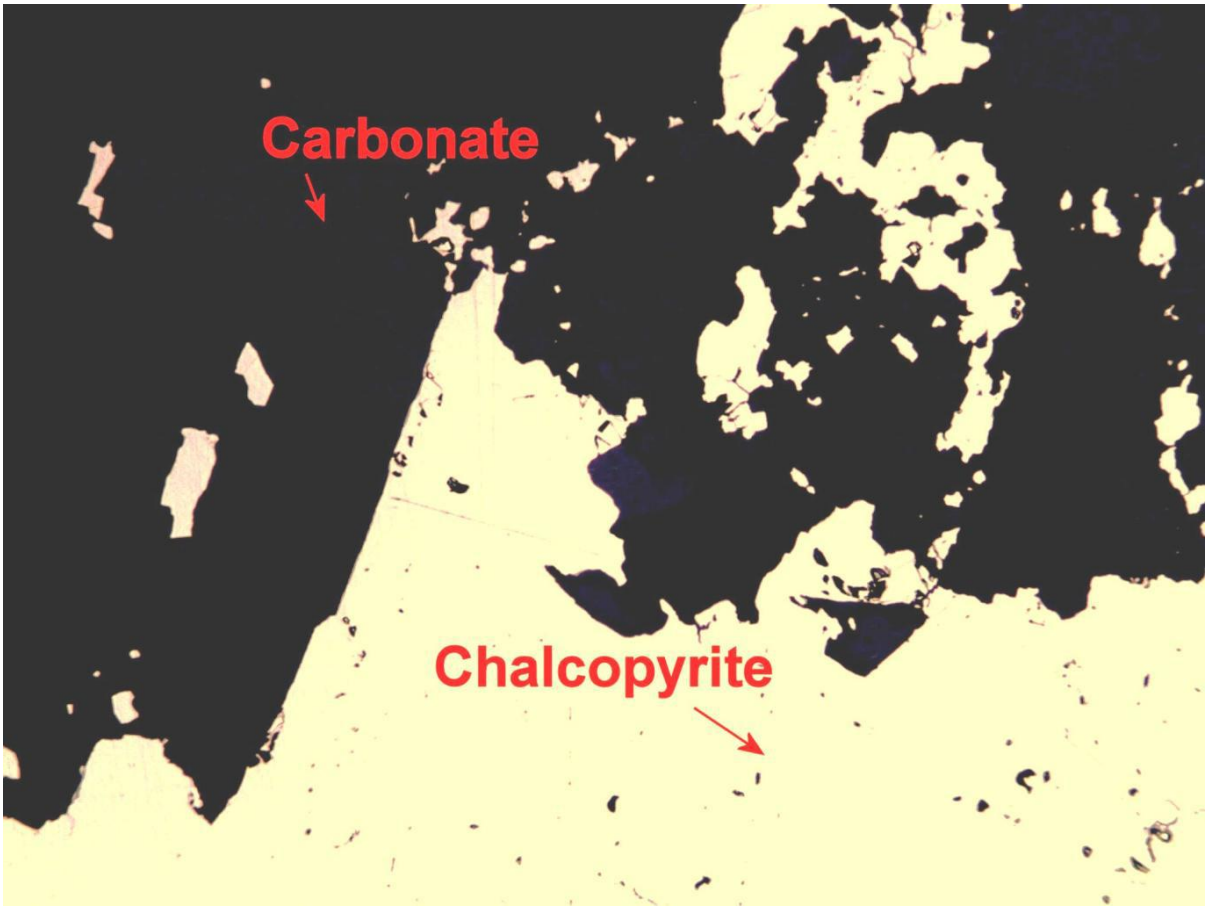

Figure 15: MC003DD 10-59.50m. Chalcopyrite with possible replacement of carbonate. RL. WOF c820 micron.

Specimen MC003 DD 12-83.80m.

Hand specimen.

Breccia. Fragments of coarse carbonate±quartz crystals (white/grey) at 2-5mm scales, with infill of chalcopyrite/pyrite. The total sulphide is c70% with chalcopyrite predominating (70%). Minor dark chlorite. Darker materials near sulphide may represent recrystallization of host carbonate. Some replacement of carbonate suspected.

Figure 16: MC003DD 12-83.80m. Dolomite, broken and overprinted by chalcopyrite-pyrite (yellow). Pyrite-slightly less yellow , (top left). Slab 3.60cm.

Petrology.
Similar to MC003 DD 10-59.5.

The host rock is coarse granular carbonate±quartz. The carbonate is irregularly mosaic bordered (50-200 micron) and the quartz is coarser (200 micron – 2.0mm). It looks like vein material?, but the sample is too small to be certain (could be coarse carbonate rock?) – need sample context. The carbonate/quartz content is around 90 and 80% respectively. The sulphides (some 60% of the slide) are predominately infill chalcopyrite with 20-30% pyrite. The pyrite is pre chalcopyrite with subcrystalline formats (rounded), (50 micron to 2.5mm). Some spongy 'pyrite' styles normally at the fringes of the larger crystals are suspected marcasite (slightly anisotropic).
Chlorite occurs (5%) as crystals/crystal clumps associated with the sulphides.

Paragenesis.
Early. 1. Carbonate/quartz (host rock or vein?).
Late. 2. Chalcopyrite, pyrite, marcasite, chlorite.

Comments.
The sample is too small to judge whether the carbonate is from a vein or a coarser host rock. No field data provided.

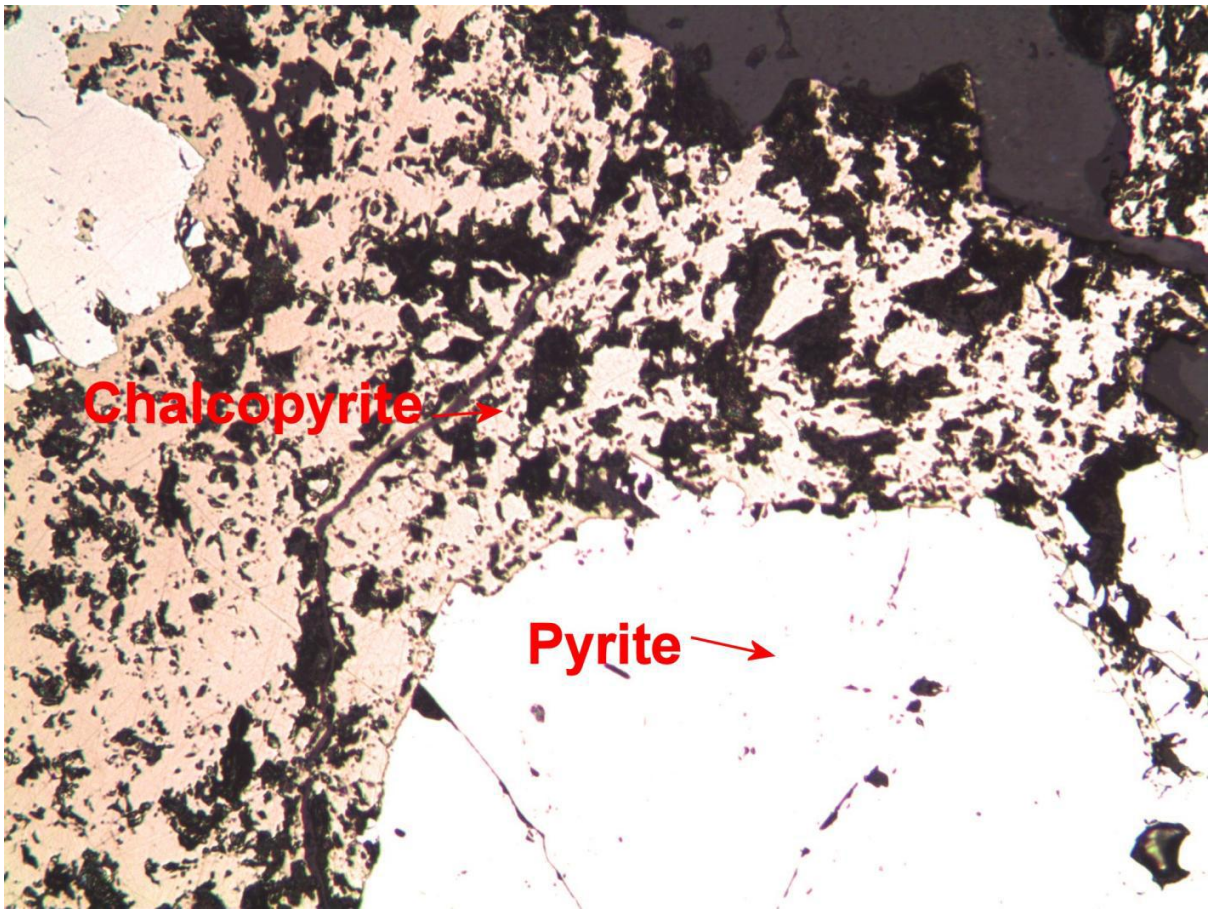

Figure 17: MC003DD 12-83.80m. Chalcopyrite/pyrite. Pyrite has good crystal shape, crystallising slightly pre-chalcopyrite. RL. WOF c820 microns.

Specimen MC003 DD 13-90.70m.

Hand specimen.
Coarse grained, white/grey carbonate±quartz (grey). Broken and cut by discontinuous crack style infill veins of chalcopyrite, pyrite and chlorite. Sulphides occupy some 2.5% of the slab and chalcopyrite predominates (90-95% of sulphide).

Petrology.
Coarse grained mosaic style carbonate (100 microns to 500 micron) – some of the finer sizes might be a recrystallization effect. Minor quartz (c5.0%) ranging from 100-500 microns.
The sulphides occur in minor amounts (2-5%) as discontinuous crack style veinlets and irregular blebs with a general infill style and include chalcopyrite±pyrite (50-100 micron crystals), chlorite and traces of ?marcasite. Some replacement of carbonate is possible at border contacts. Quartz is less prone to replacement. A late quartz vein of 20 micron width is present.

Paragenesis.
The sample was collected as representative of dolomite host rock.
Early – chalcpyrite±pyrite, marcasite?, chlorite.
Late – quartz vein.
Comments.

Similar to MC003 DD 12-83.8, MC003 DD 10-59.5.

Figure 18: MC003DD 13-90.70m. Chalcopyrite, cutting/brecciated carbonate. Mostly infill (fragments fit back together). RL. WOF x10.

APPENDIX B

Appendix B consists of summary images from Scanning Electron Microscope (SEM) work.

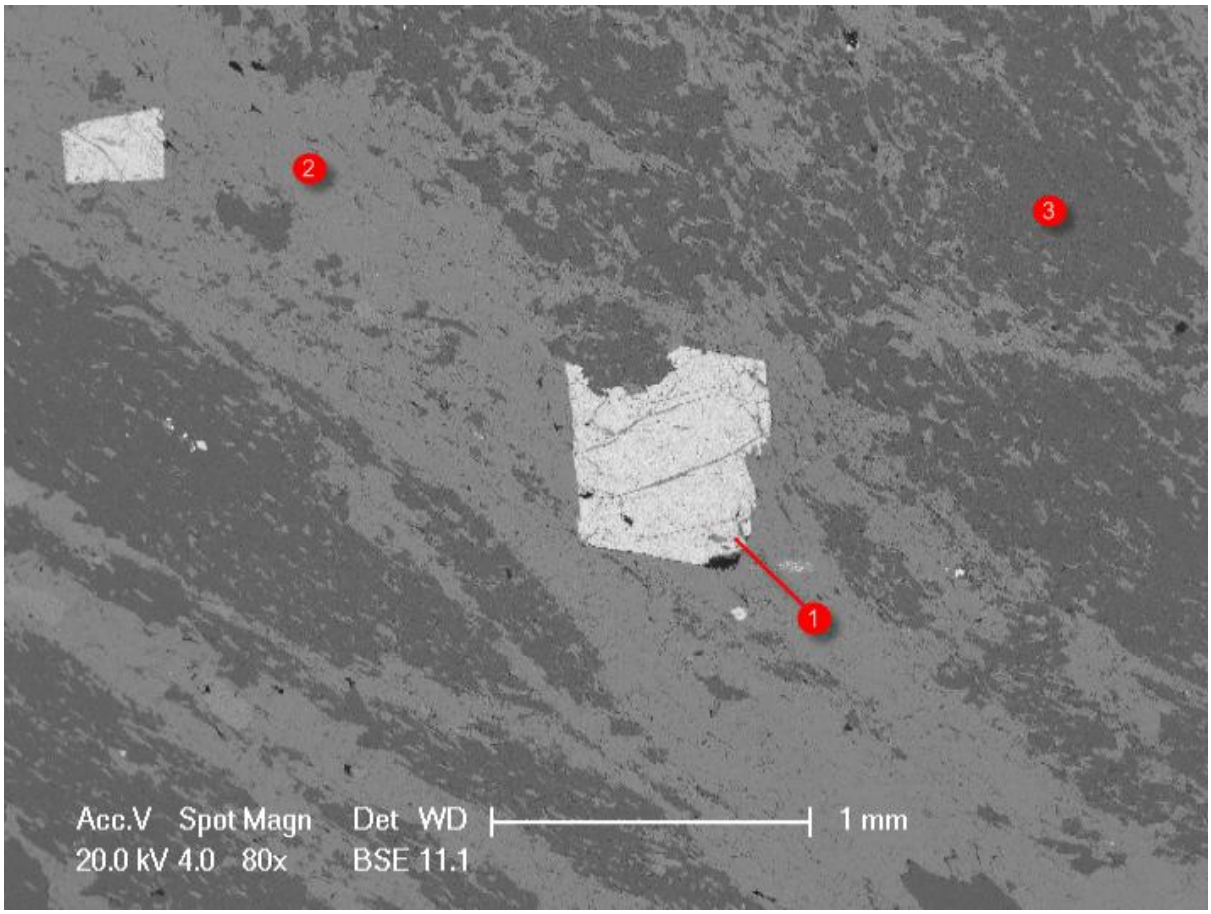

Figure 19: Euhedral Fe-mineral (1) in biotite (2) and albite (3). From hole MC001DD, sample #10

Interp.

- Fe≈O, therefore *Wüstite ($Fe^{2+}O$)??*
- *Or is this ferrous carbonate?*
- *Fe-mineral euhedral/subhedral (early)*
- *Fe-mineral restrained by albite (i.e. cannot grow into space as albite is there)*
- Fe-mineral late as bt and alb show no deflection around fe-mineral and there is no evidence of Fe-mineral deformation despite strong fabric of surrounding minerals
- Paragen: albite+bt>fe-mineral

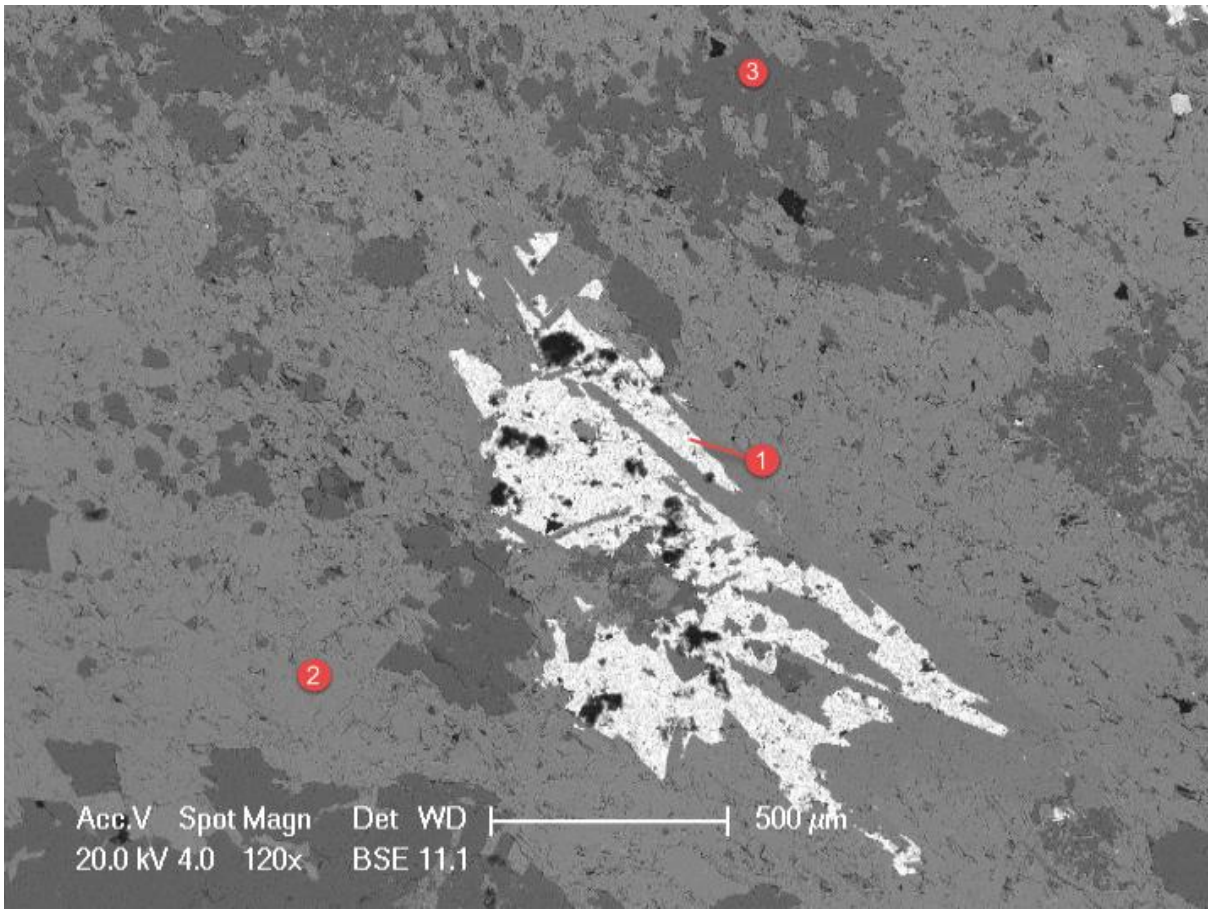

Figure 20: Chalcopyrite (1) in biotite (2) and quartz (3). From hole MC001DD, sample #10

Interp.

- Mottled, anhedral texture with biotite and quartz inclusions within suggest that the chalcopyrite is late stage
- Quartz in biotite and biotite in quartz so simultaneous?
- Cpy being constrained by biotite, cpy clearly late.
- Qtz+bt in cpy
- Paragen: quartz+bt>cpy

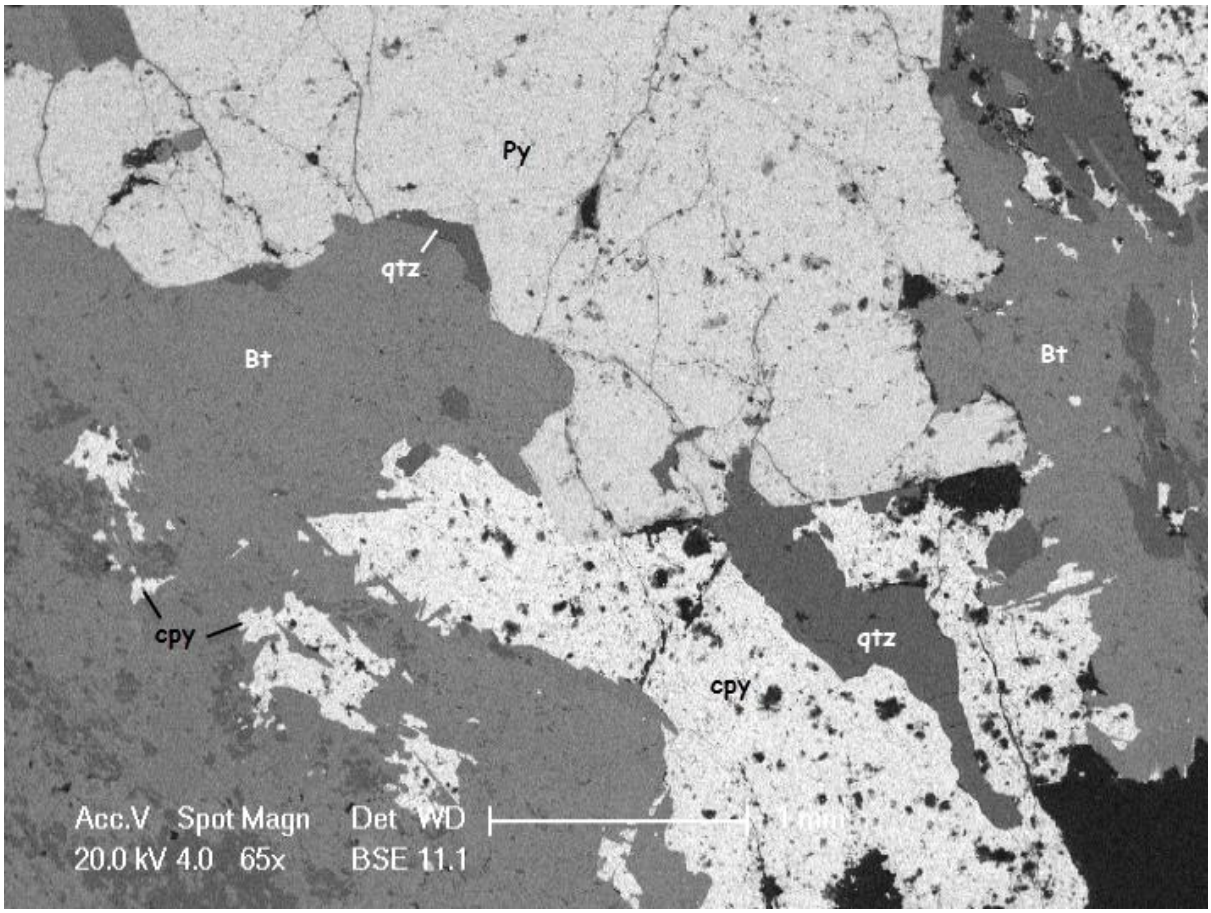

Figure 21: Subhedral pyrite (Py) and anhedral chalcopyrite (cpy) in quartz (qtz) and biotite (Bt). From hole MC001DD, sample #10

Interp.

- Py largest crystal size, other minerals appear to have grown around it
- Cpy grown around quartz
- Unsure of how bt fits in
- Ambiguous
- Paragen: py+qtz> (+bt?)> cpy

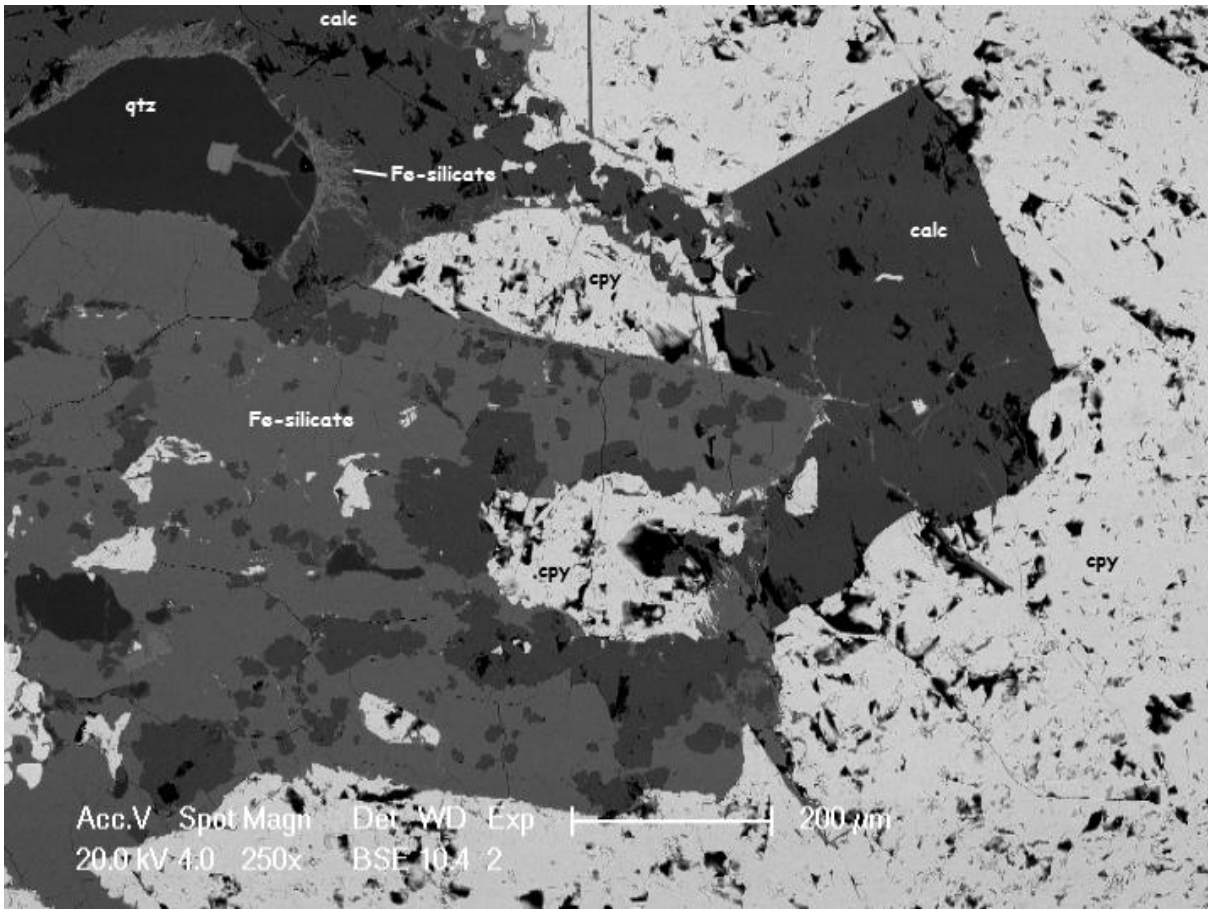

Figure 22: An Iron rich aluminosilicate (Fe-silicate) with calcite (calc), quartz (qtz) and coarse chalcopyrite (cpy). From hole MC001DD, sample #24

Interp.

- The only thing I can say with some certainty is that the Fe-silicate appears to have grown after quartz, calcite and cpy. AS evidenced by the fact that it has abundant inclusions of these minerals within it, as if it has grown around them. Also the late stage strands that overprint calcite.
- Fe-mineral matches with FeSiO3?

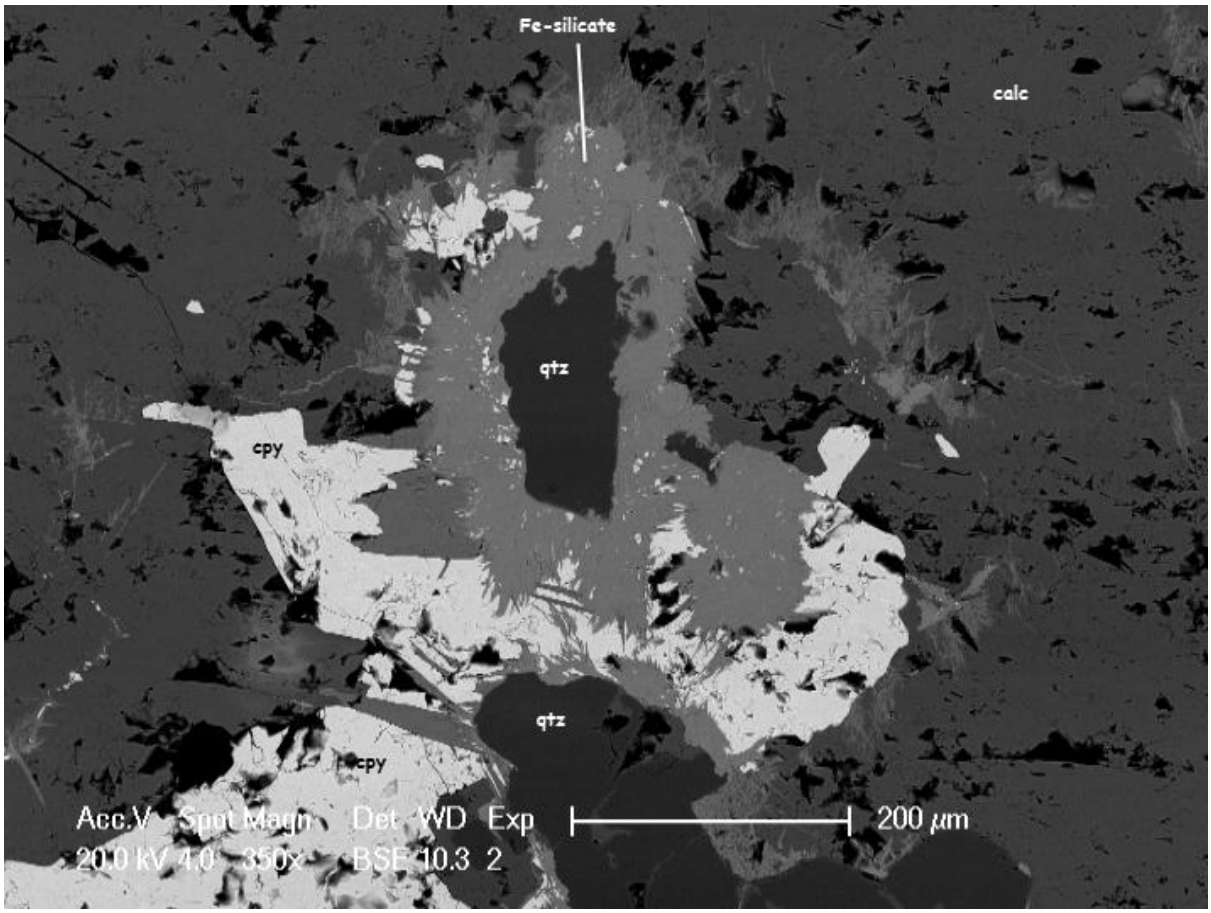

Figure 23: Quartz grain with abundant late stage Fe-silicate mineral as a halo that extends into calcite and chalcopyrite. From hole MC001DD, sample #24.

Interp.

- Radial pattern of Fe-silicate around quartz
- There is also Fe-silicate growing of quartz grain at the bottom of the image and linking to the Fe-silicate growing off the central quartz.
- Fair to say that there is some sort of reaction between Fe-rich minerals and quartz occurring late stage.

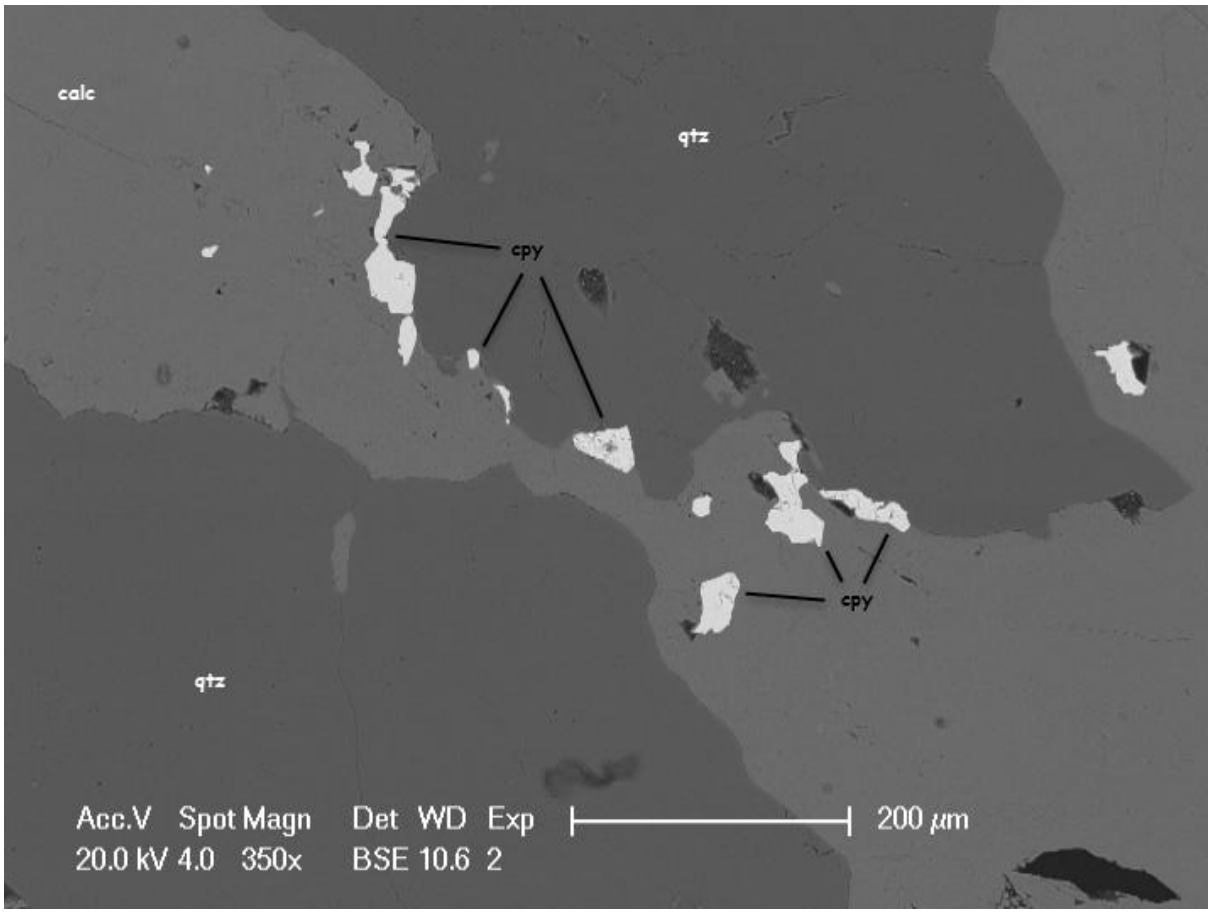

Figure 24: Chalcopyrite grains forming at the boundary between quartz and calcite. From hole MC001DD, sample #29

Interp.

- Cpy infill texture, very small grain size
- Along edge of calc/qtz
- Calc in qtz and cpy in calc
- Paragen: cpy>calc>qtz?

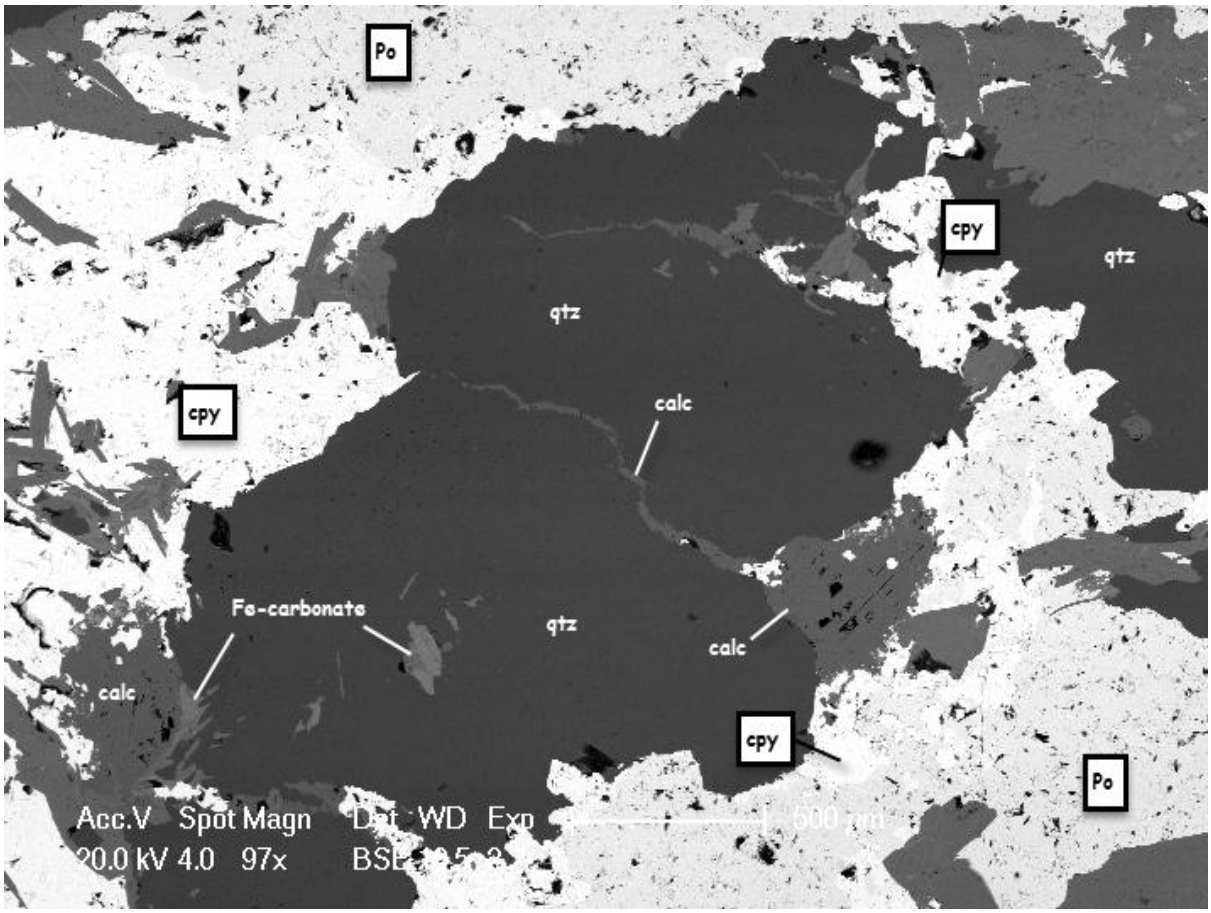

Figure 25: Calcite with chalcopyrite forming microveins through quartz. Fe-carbonate (siderite?) forming at the boundary of calcite. Also note the chalcopyrite forming at the edge of pyrrhotite. From hole MC001DD, sample #29

Interp.

- Calc in intruding between quartz crystals
- Fe-carbonate in quartz
- Paragen: fe-carbonate>qtz>calc>sulphides

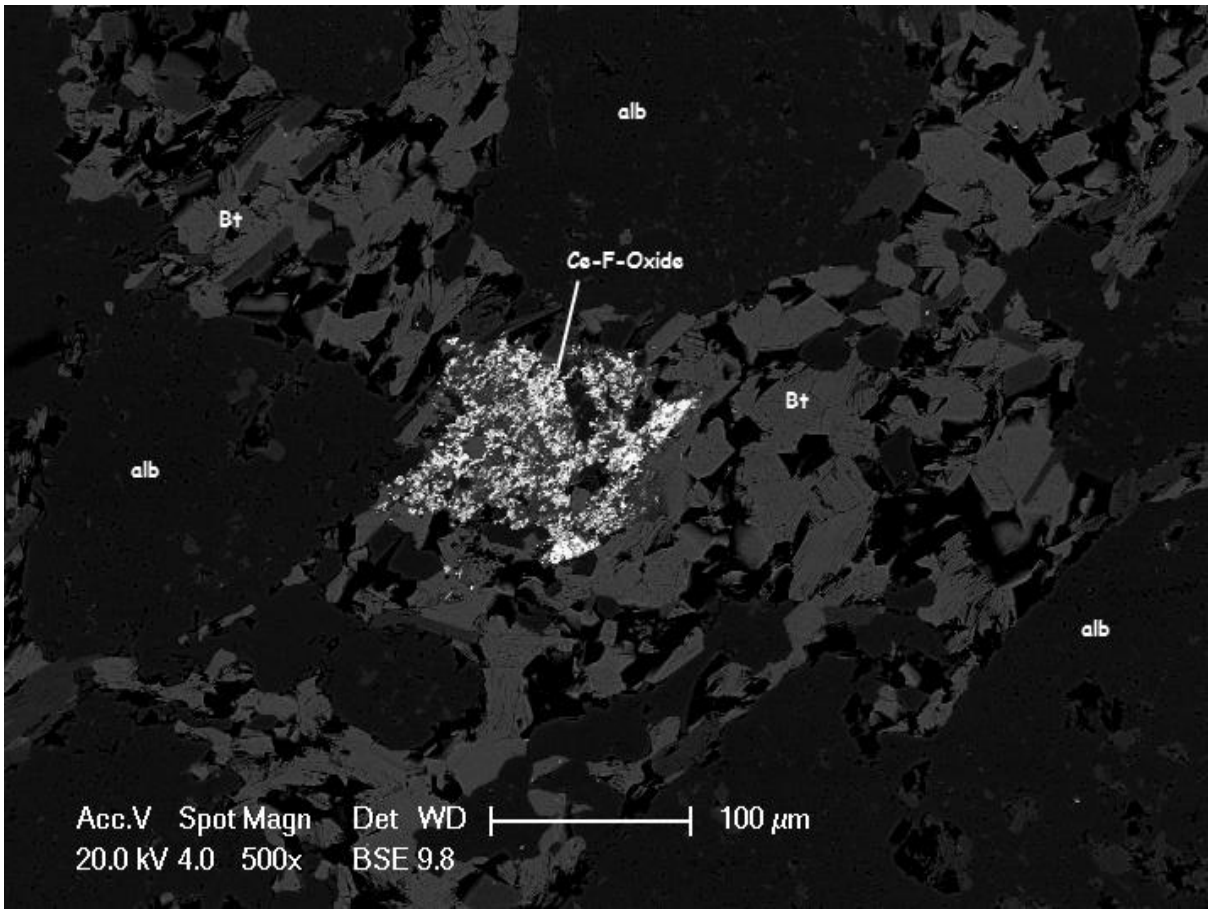

Figure 26: REE enriched mineral in biotite and albite (alb). From hole MC001DD, sample #41

Interp.

- Alb>bt

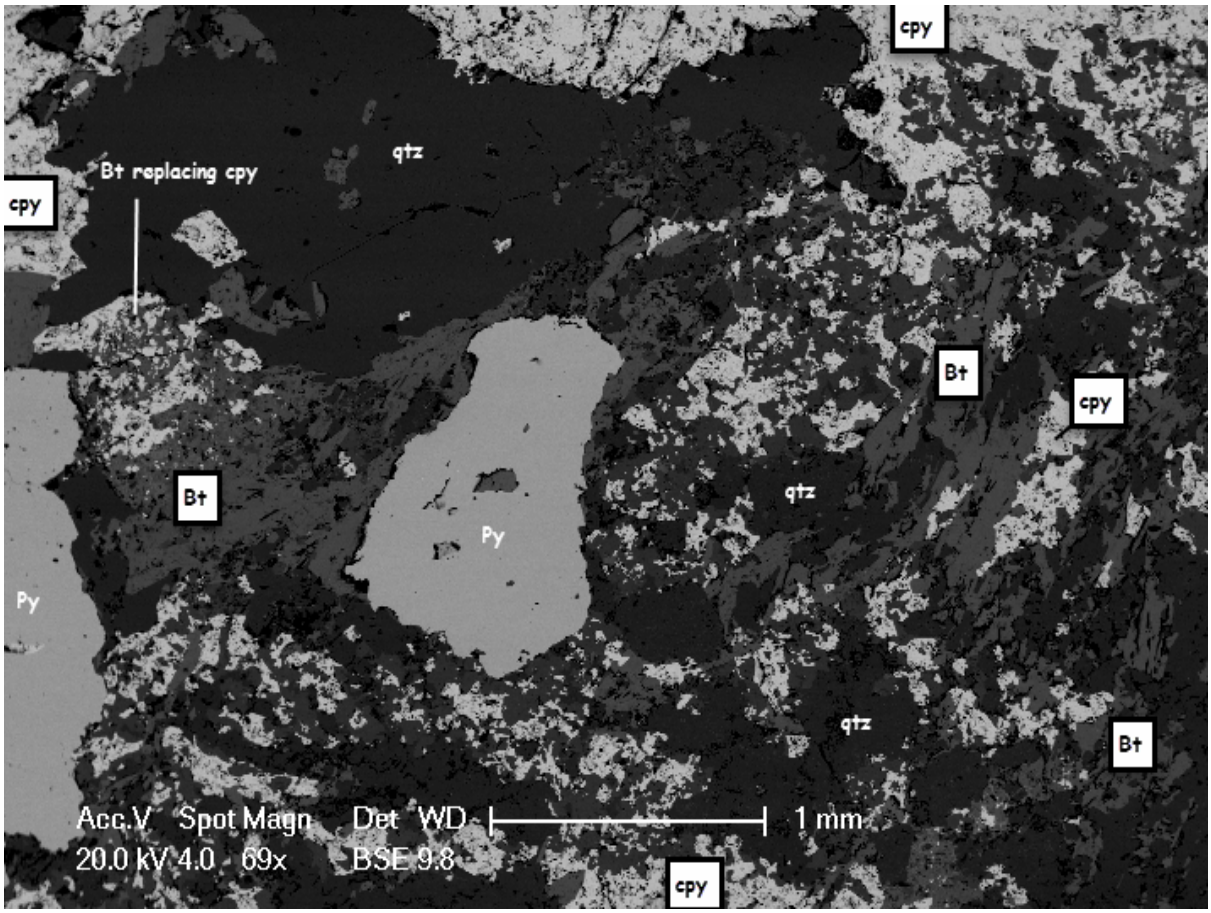

Figure 27: subhedral pyrite, anhedral chalcopyrite with biotite and quartz. From hole MC001DD, sample #41

Interp.

- Bt has weak fabric whereas cpy doesn't really seem to have any fabric. So cpy must be overprinting bt after strain

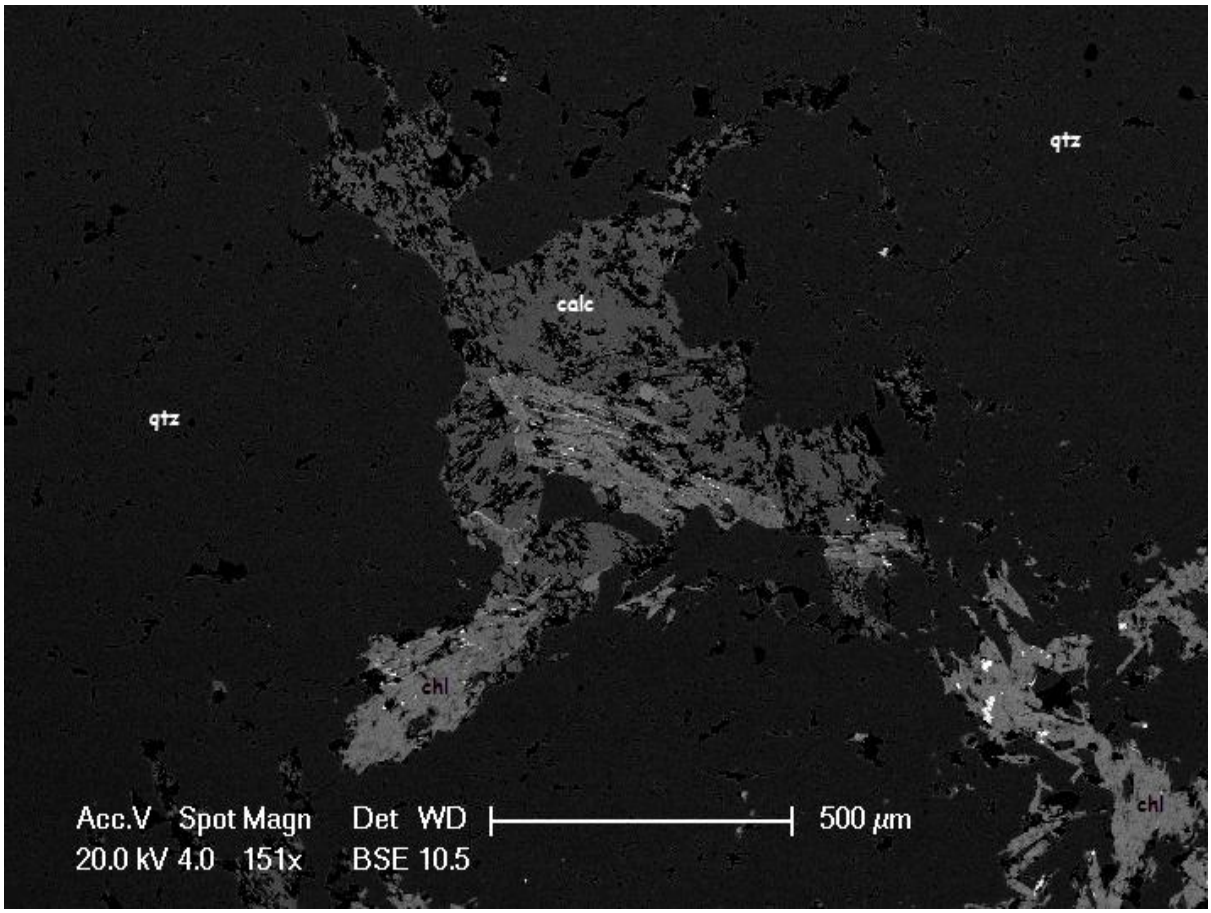

Figure 28: Lower magnification of fig. 100. Bright white spots are ilmenite, coming with chlorite in calcite and quartz. From hole MC001DD, sample #9

Interp.

- Calcite has infill texture in qtz and appears to be overprinted by chl + ilm
- Paragen: quartz>calcite>chlorite+ilmenite
-

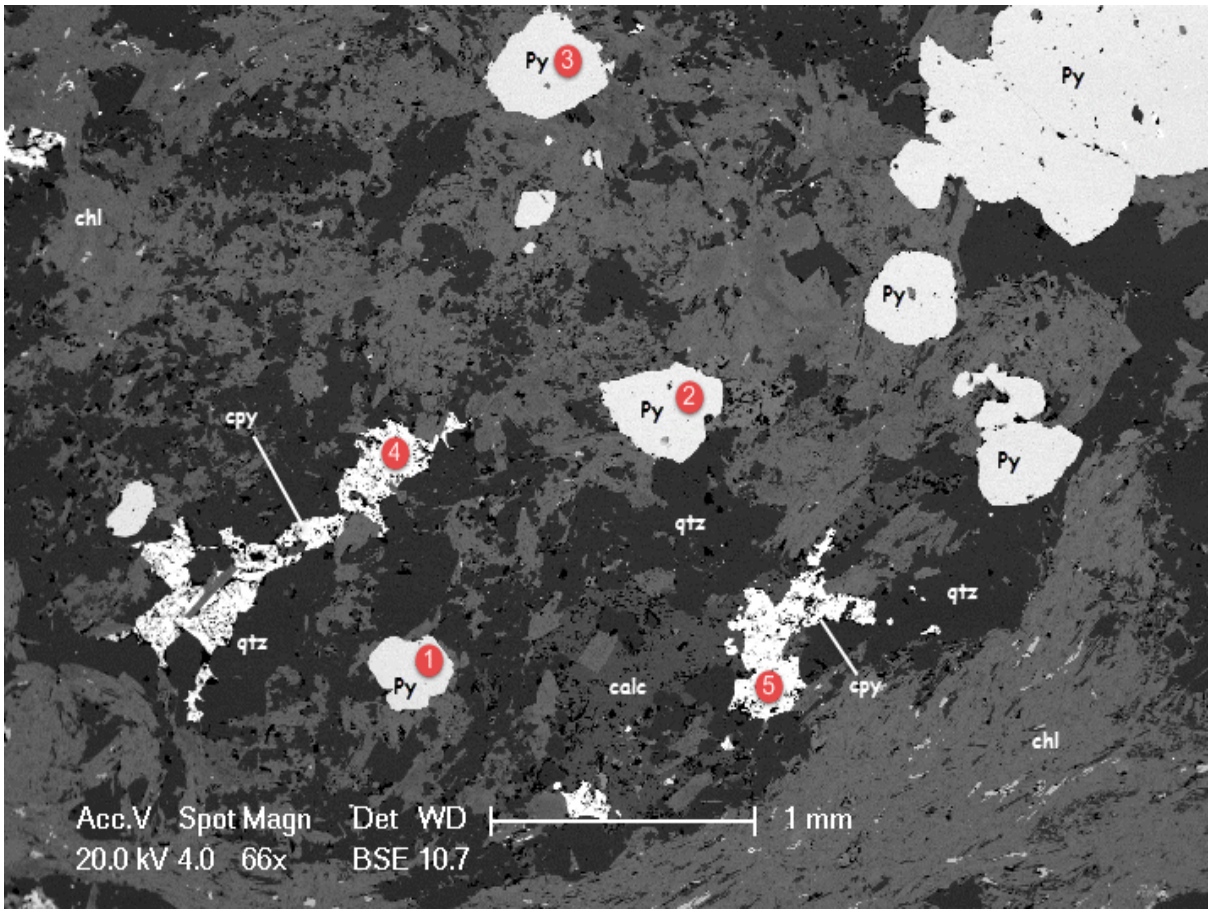

Figure 29: Early fine grained, euhedral pyrite and late chalcopyrite with quartz, chlorite and calcite. 1 represents the analysis shown in fig. 108, 2 represents the analysis shown in fig. 109, 3 represents the analysis shown in fig. 110 and fig. 111, 4 represents the analysis shown in fig. 112, 5 represents the analysis shown in fig. 113. From hole MC001DD, sample #9.

Interp.

- Difficult to tell
- Subhedral pyrite may suggests they had space to grow, hence early.
- However foliation not deflected around py crystals and py crystals hardly deformed despite strong foliation of chl, may suggest late growth
- Cpy has an anhedral infill texture in quartz, as does calcite
- Calc grows with cpy?
- Paragen: qtz+py>cpy+calc>chl
- OR qtz>cpy + calc> py + chl
- Bit unsure about this one

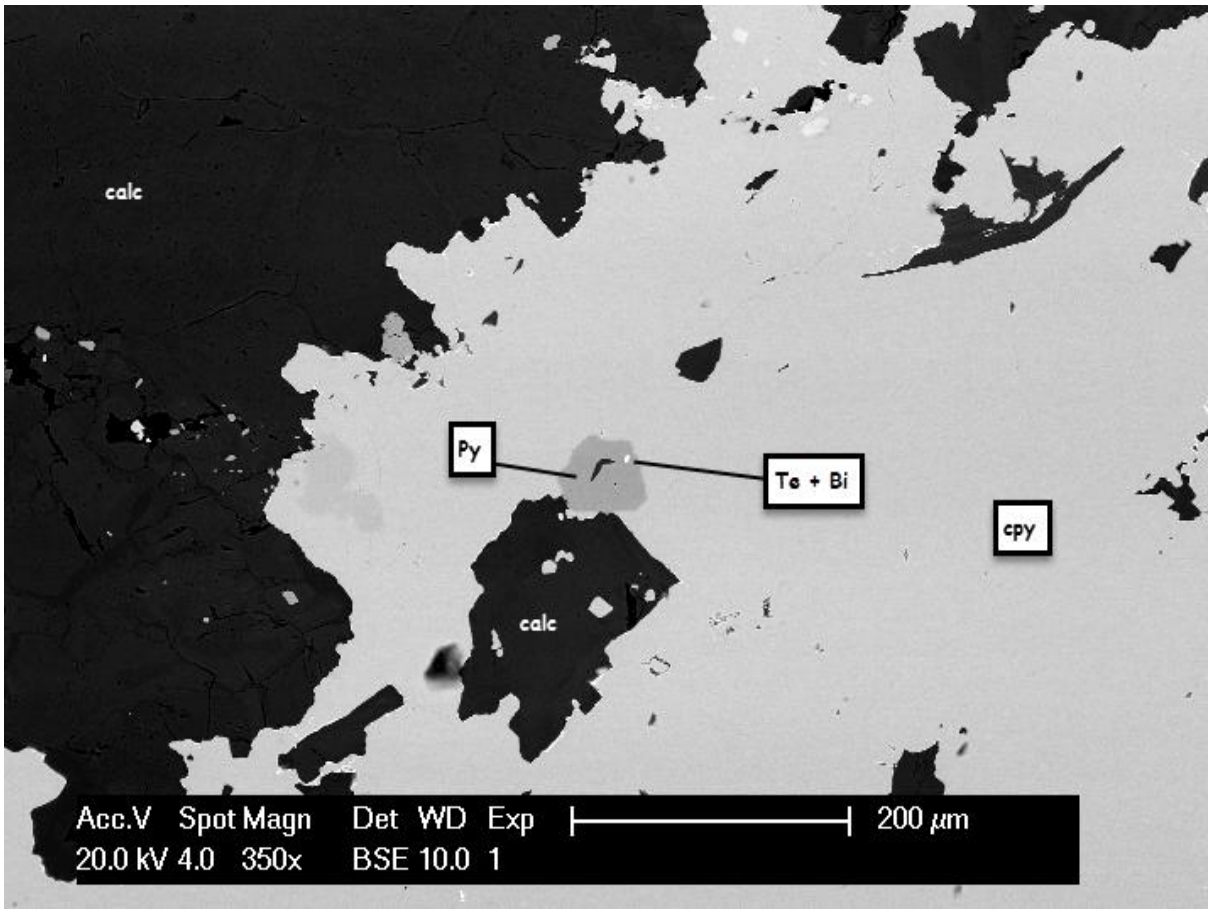

Figure 30: Tellurium and Bismuth inclusion at boundary between chalcopyrite and pyrite. From hole MC003DD, sample #10

Interp.

- Calc and py in cpy
- Calc in py
- Calc>py>cpy

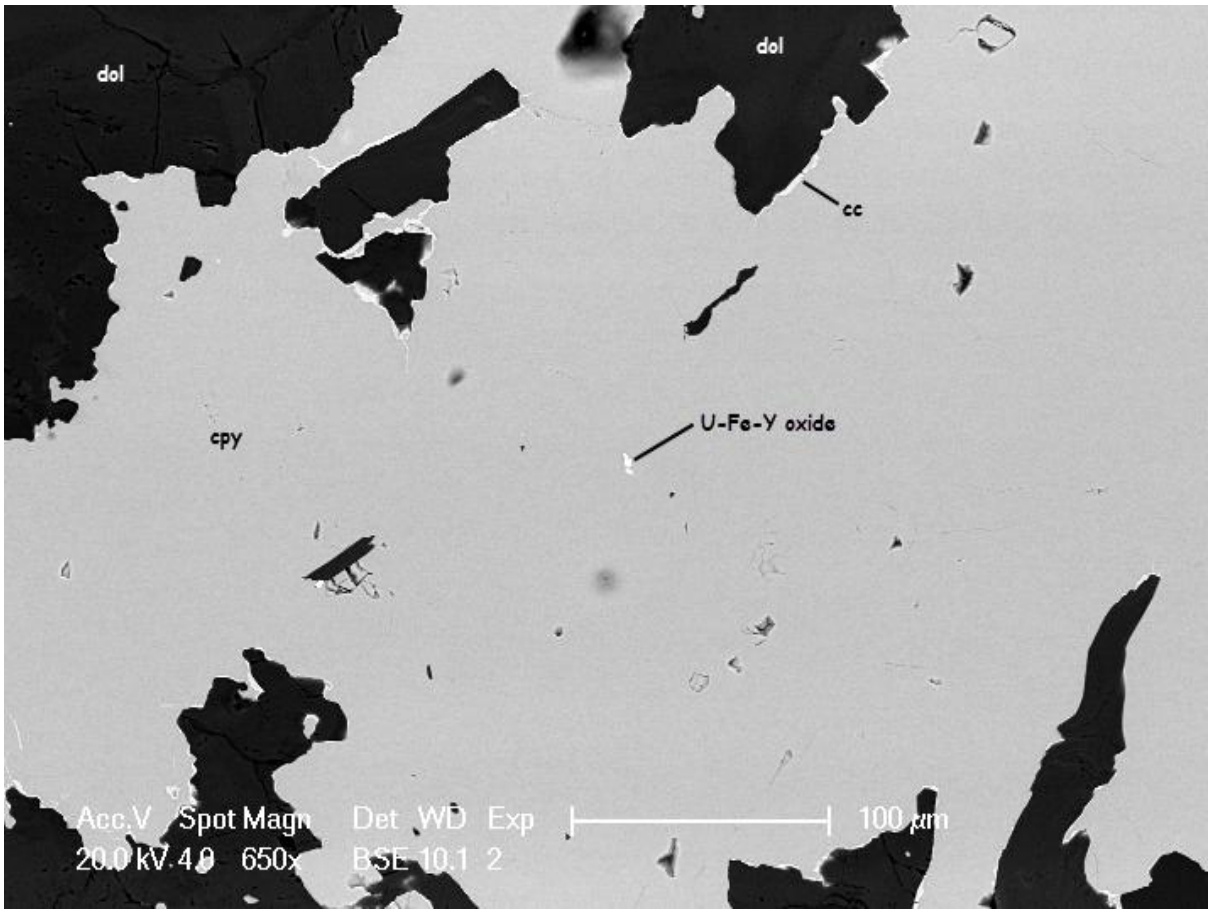

Figure 31: U-Fe-Y oxide in chalcopyrite with chalcocite edges. From MC003DD, sample #10

Interp.

- Dol in cpy
- Dol>cpy>cc

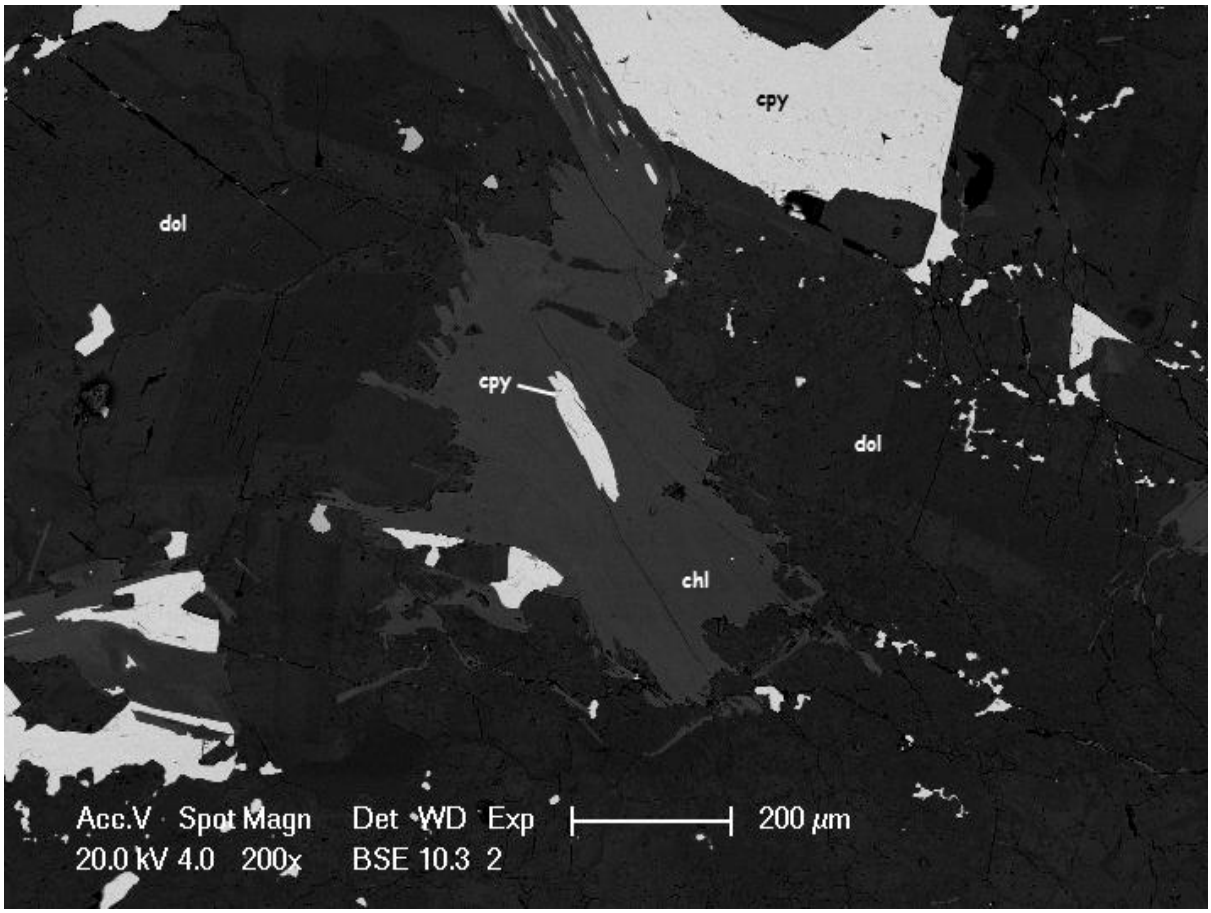

Figure 32: chalcopyrite in chlorite in dolomite; From hole MC003DD, sample #10

Interp.

- Cpy and chl have infill texture
- Cpy in chl
- Paragen: dol>cpy>chl

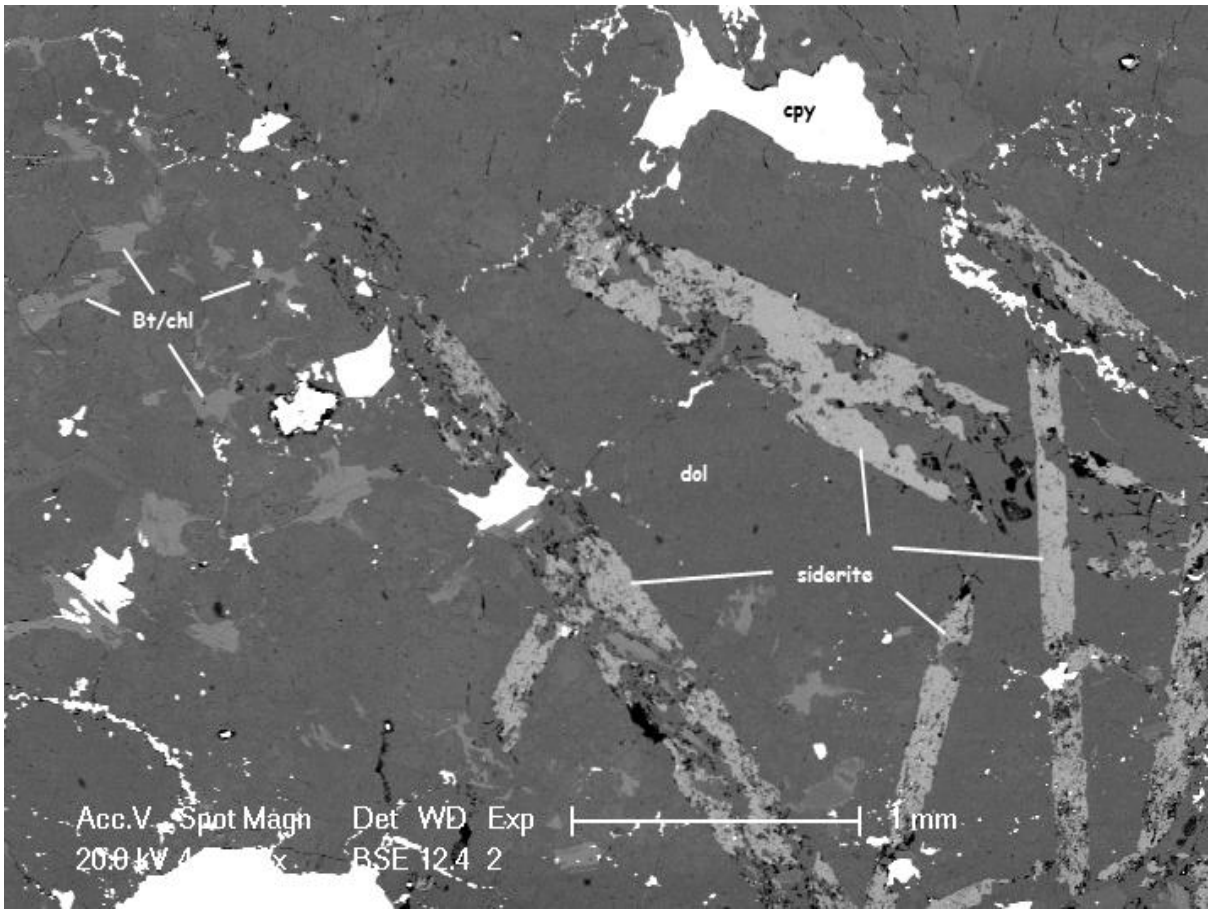

Figure 33: Siderite(?) in dolomite with chlorite and minor biotite/chlorite. From hole MC003DD, sample #10

Interp.

- Is siderite growing in euhedral shape that is being replaced?
- Or are the areas where there is an anhedral shape a sign that it was growing after dolomite or at least simultaneously
- Cpy and bt/chl later
- I reckon it's early but also has random orientation as if retrograde?
- Paragen: side>dol>cpy+bt/chl

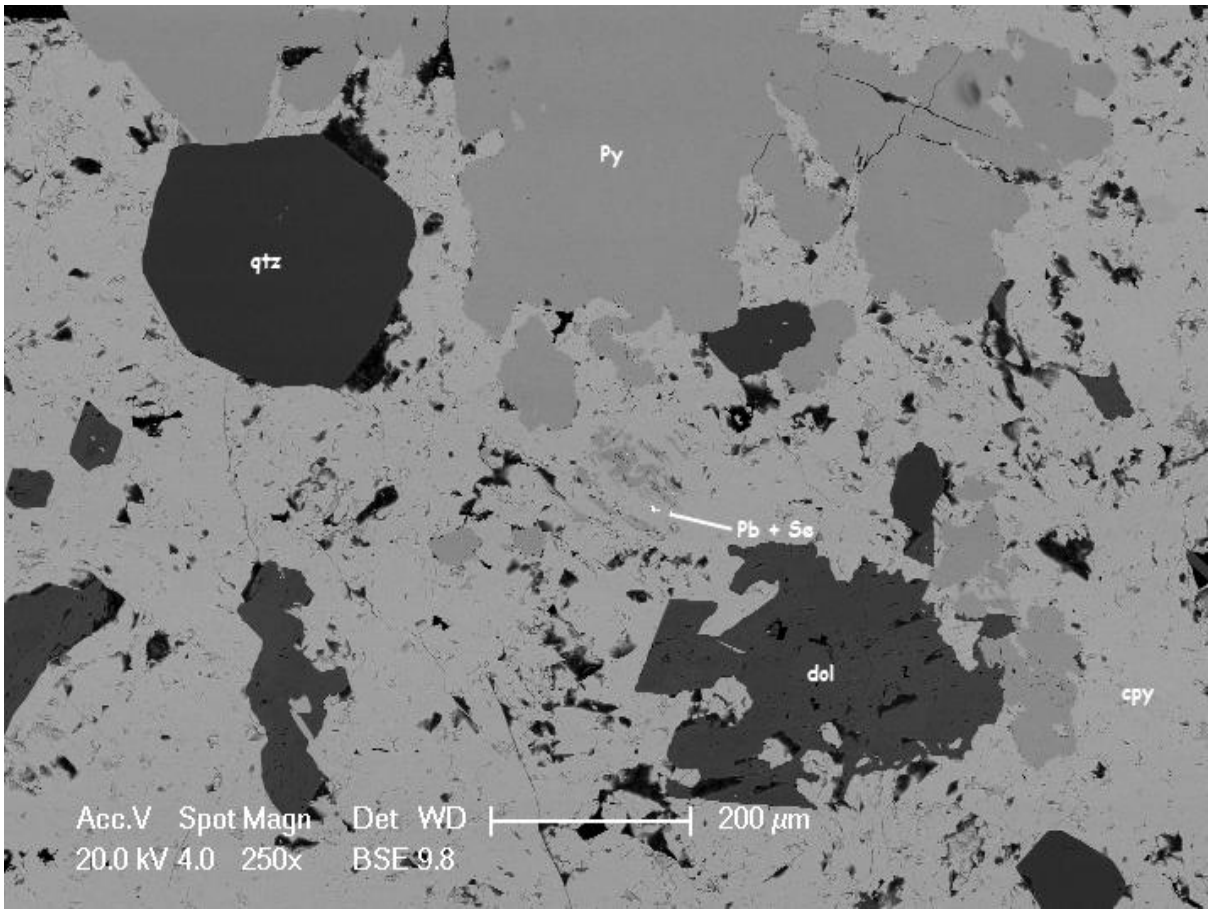

Figure 34: Lower magnification on same area as in fig. 231. From MC003DD, sample #12

Interp.

- Py + qtz grew early – look at grain contact of qtz and cpy in top left corner
- Cpy looks like it has infill texture trying to squeeze into that grain contact
- Py inclusion in cpy
- Also dol and cpy have inclusions in each other
- Cpy and dol grew late

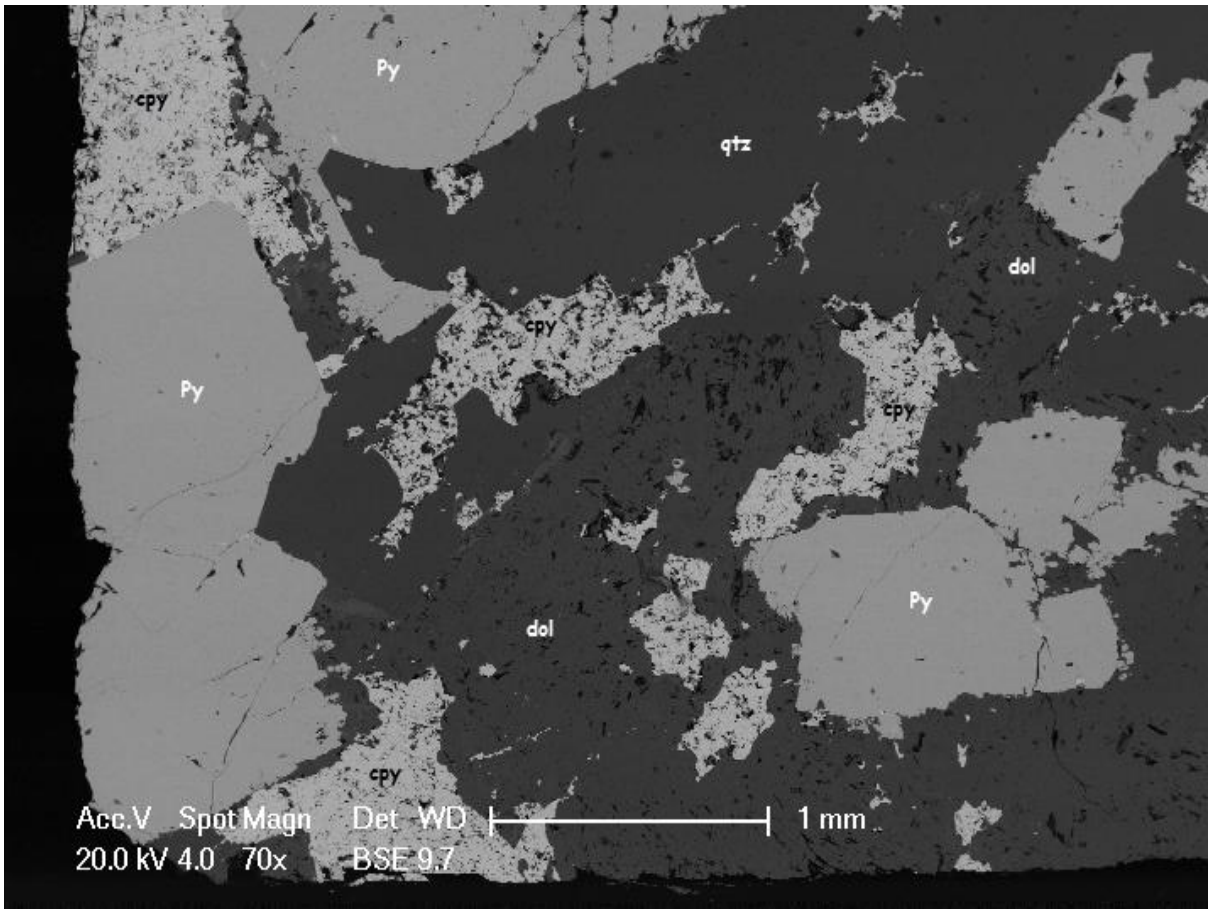

Figure 35: Euhedral pyrite crystals with quartz and mottled chalcopyrite and dolomite

Interp.

- Pyrite crystal shape looks like first to form
- Dolomite has subtle crystal shape growing off pyrite (i.e. top right)
- Chalcopyrite infill texture
- Paragen: Py>dol>quartz> cpy
- There is a dissolution process needed to allow fluid flow of sulphides so that they are precipitated. It's possible dol and cpy have same texture due to this dissolution processes preferentially using dolomite to allow flow of sulphide fluid

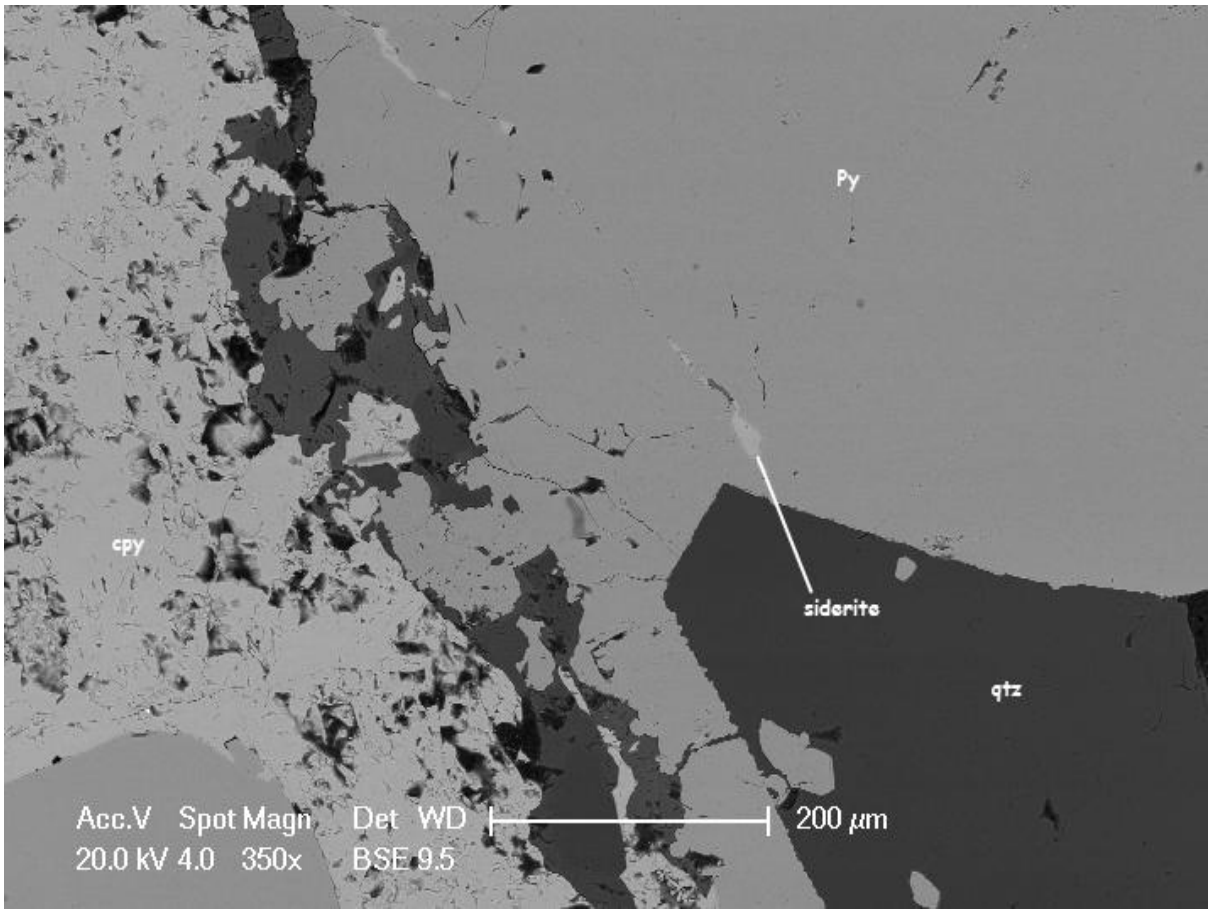

Figure 36: Chalcopyrite and pyrite with a siderite in micro-fractures. From Mc003DD, sample #12

Interp.

- Siderite forming microfractures hence after py?

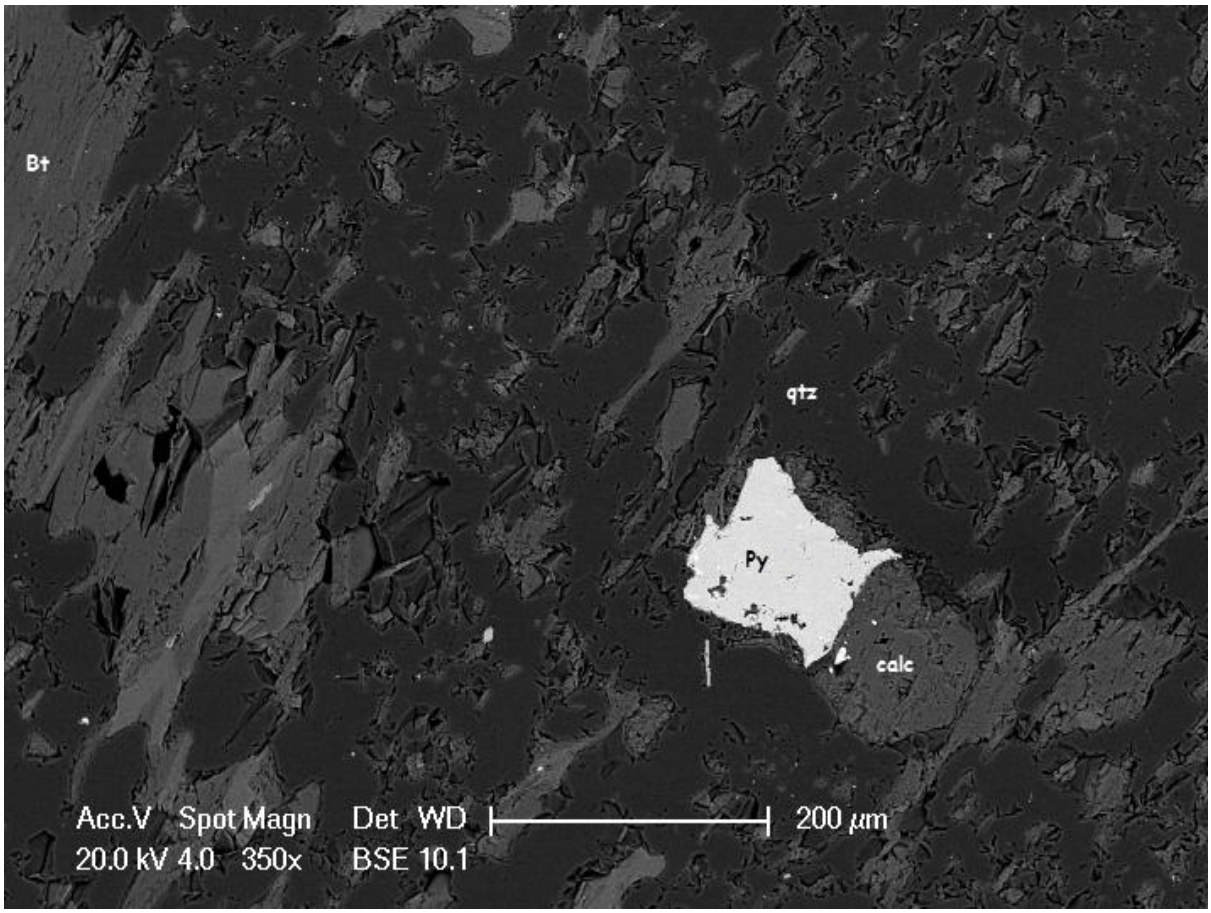

Figure 37: Calcite growing around pyrite? In a quartz background with minor biotite. From hole MC003B, sample #2

Interp.

- Calcite growing around py
- Paragen: Pyrite before calcite?
- Could use this as example of dissolution relationship between carbonates and sulphides

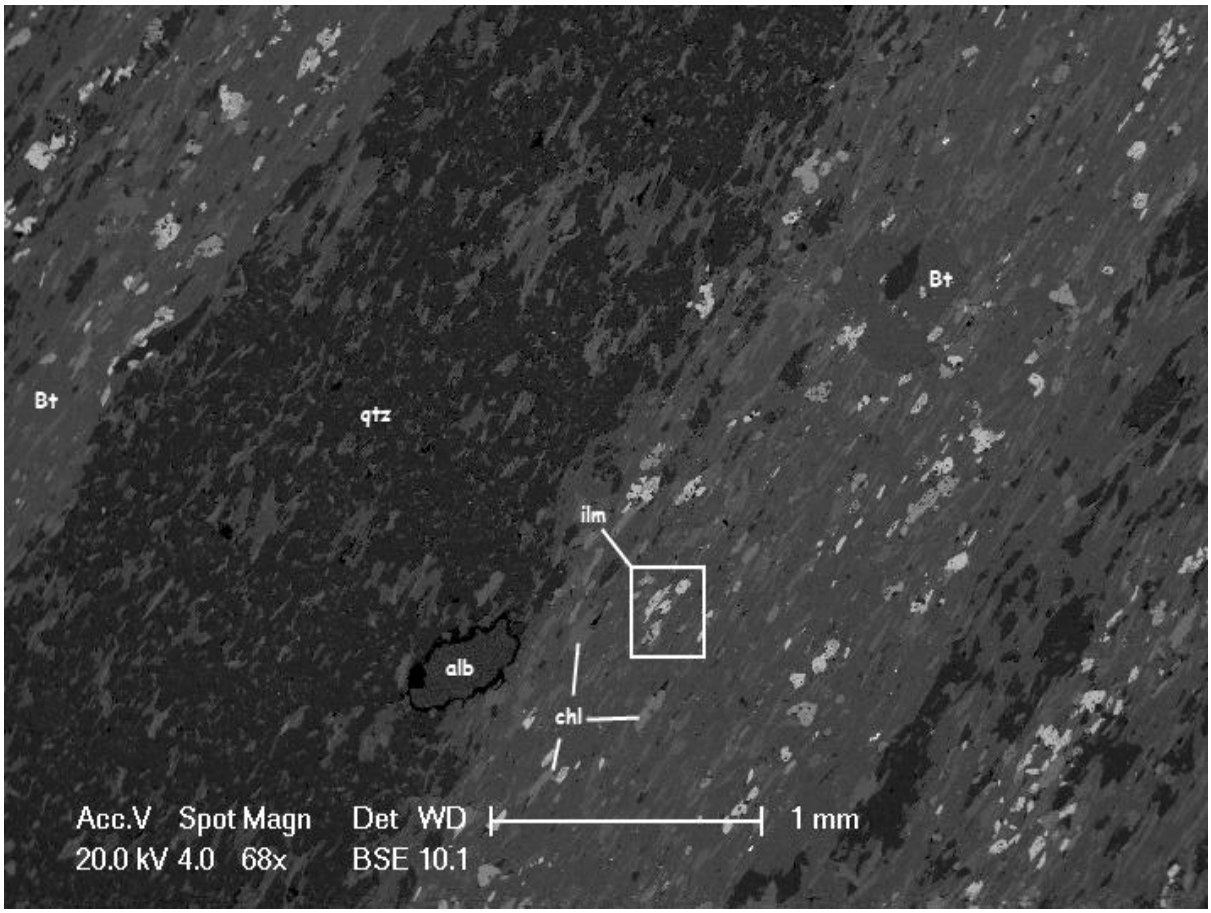

Figure 38: Biotite with chlorite and ilmenite alternating with quartz rich layers. Albite present at the border between the 2 layers. From MC003B, sample #2

Interp.

- Quartz-Chl+-bt+-ilmenite schist
- Confinement of ilmenite to chlorite layer
- Albite is early? Large crystal size, quartz/chl moving around it and it looks like it's being replaced around the edges
- Qtz being overprinted by bt, etc
- Paragen: alb>qtz>bt+ilm+chl
- Has similar shape to albite in fig. 43 which is clearly early in a low strain zone. This is a much higher strain zone and hence albite is defomed, yet still early – might see undulose extinction in microscopy which would suggest grain has undergrone high strain and hence is early to support this

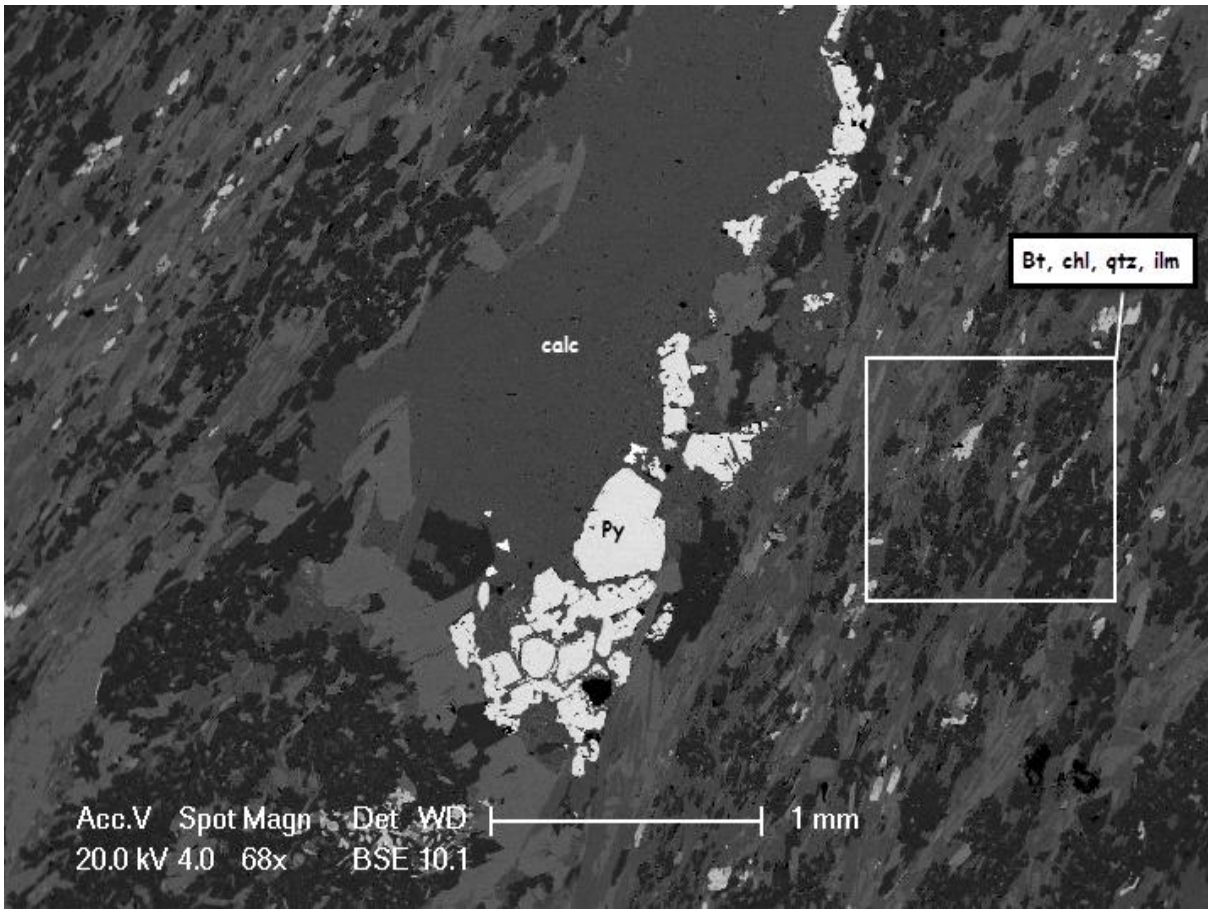

Figure 39: Pyrite growing at the edge of calcite in biotite, chlorite, ilmenite - quartz schist. From hole MC003B, sample #2

Interp.

- early calcite? Qtz, chl, bt growing around it.
- Although the pyrite has certainly grown along the edge of this calcite crystal, hard to tell what order though
- Sulphide shows evidence of deformation, early py

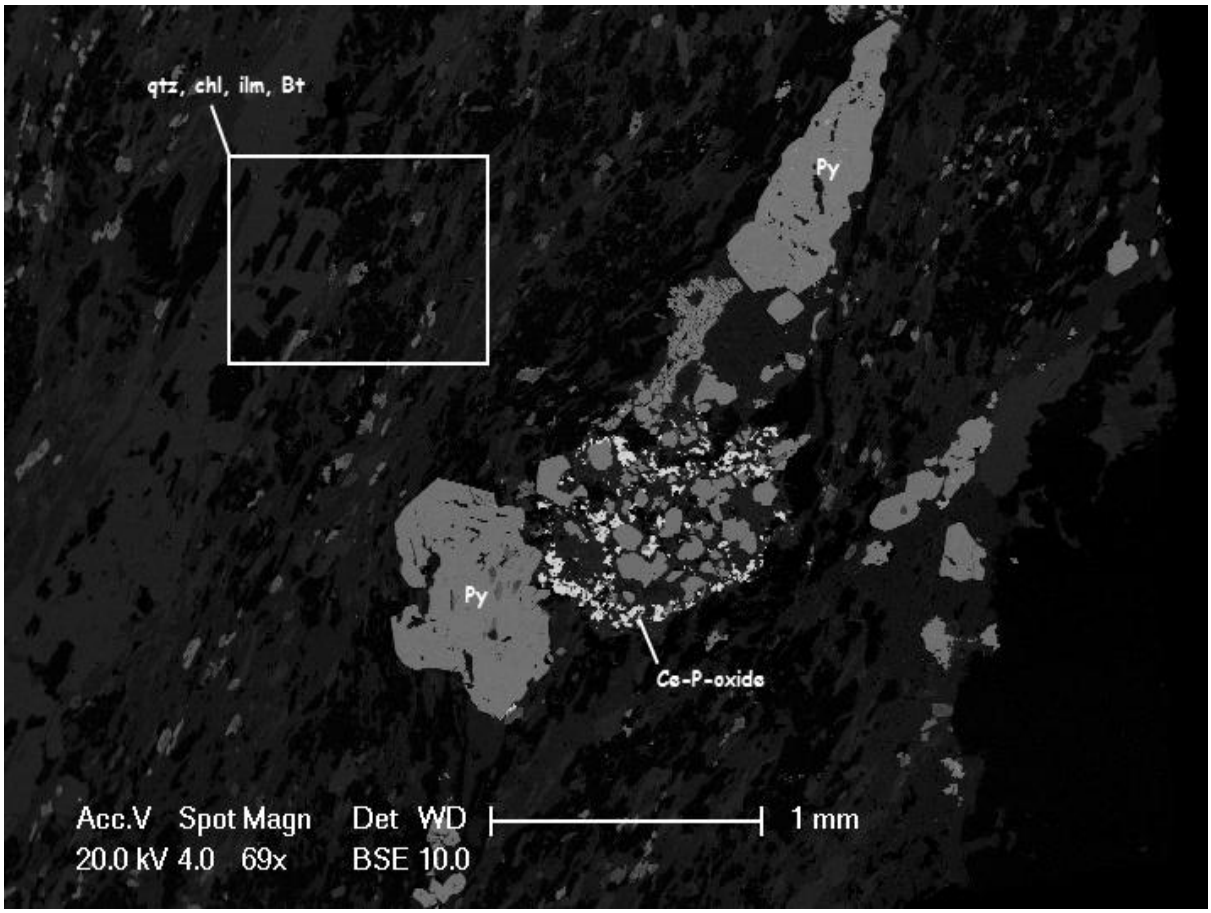

Figure 40: Large py crystal in quartz and chlorite. Ce-P-Oxide (white) replacing/being replaced? From MC003B, sample #2

Interp.

- This is an early pyrite crystal that has been sheared (i.e. dragged downwards in this image) and brecciated and probably has recrystallised. Replacing/infill minerals are chlorite and apatite-ce and quartz
- Early py, highly deformed, could date mineralisation with monazite

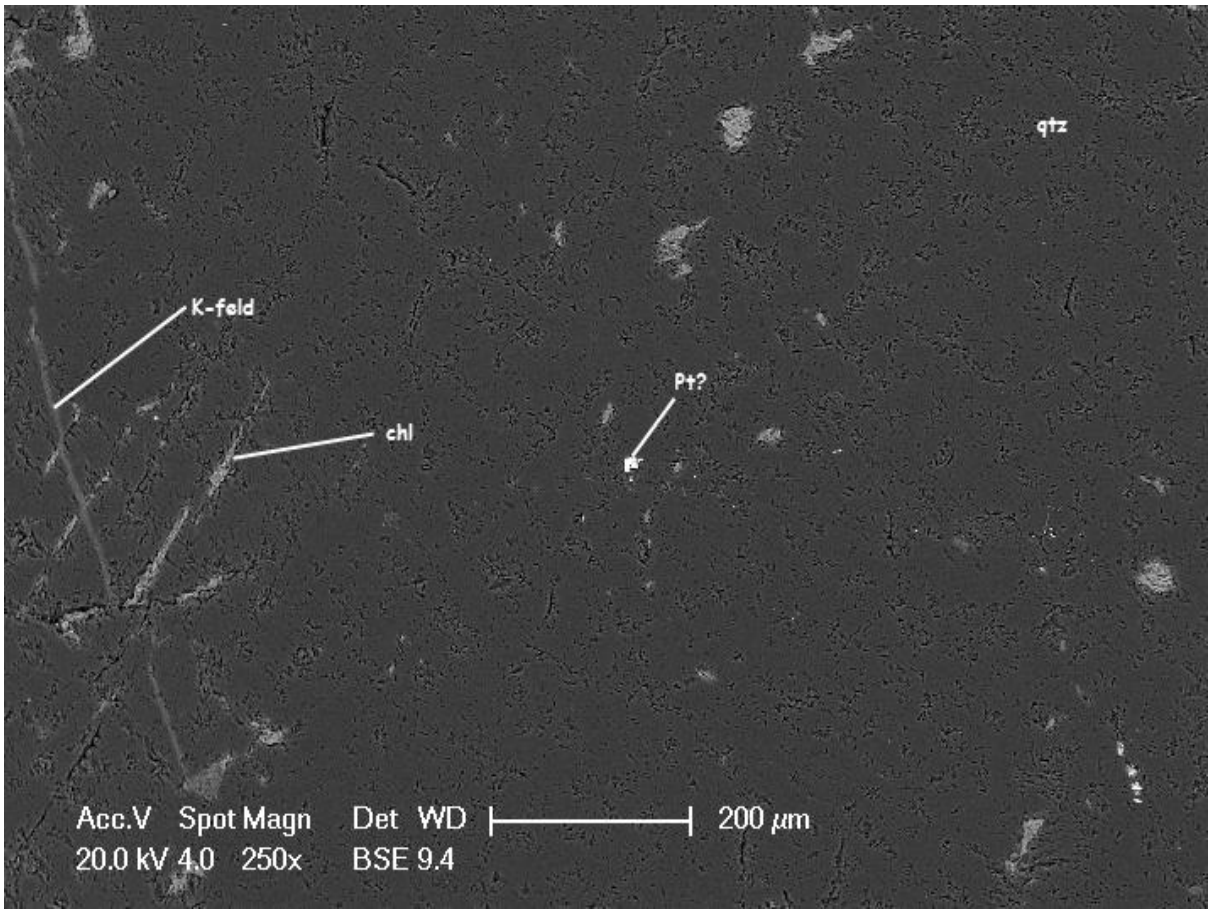

Figure 41: some sort of platinum silicate in quartz. In the left of the picture are a set of conjugate veins, veins moving to the top left of the image are k-feldspar and veins moving to top right are chlorite

Interp.

- Chl vein displaces k-feld
- Chlorite after K-feld

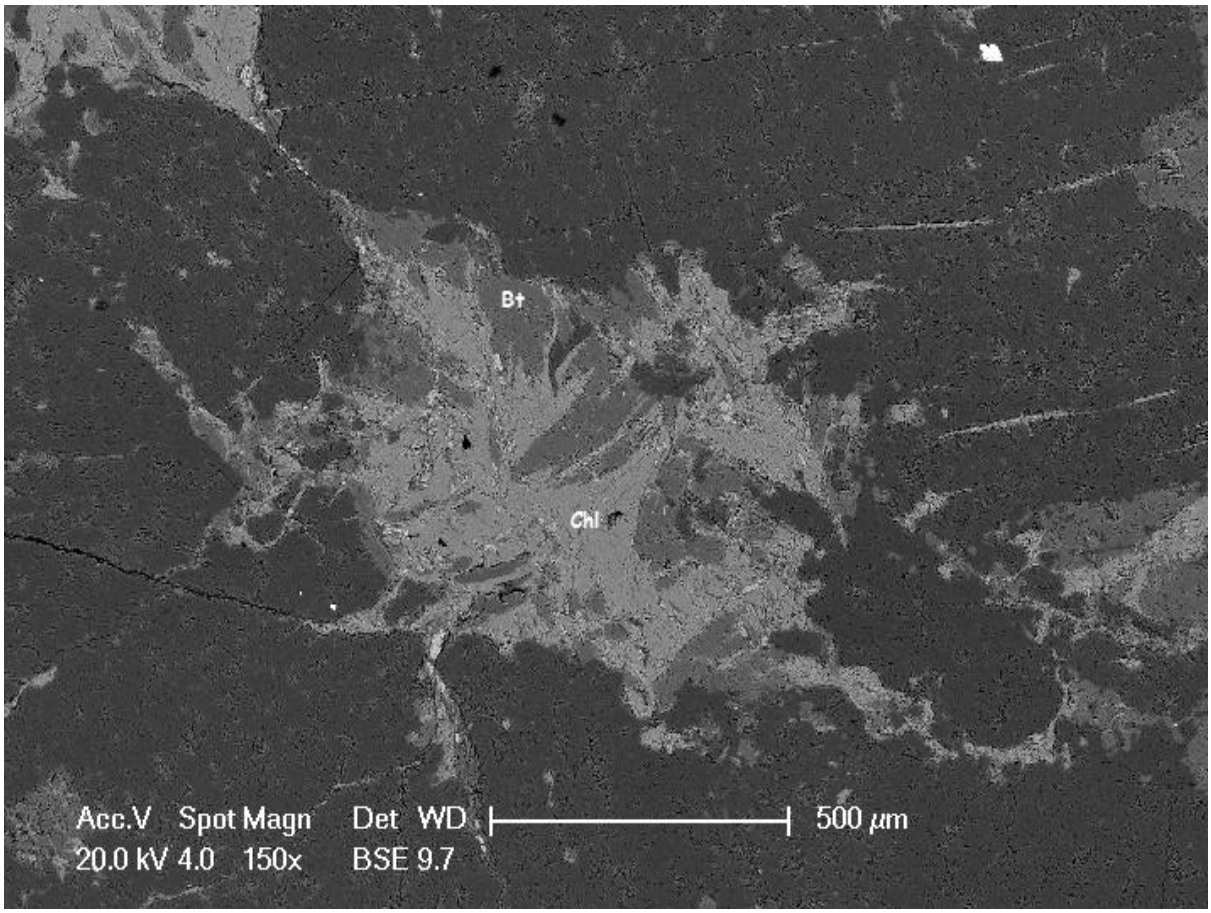

Figure 42: Chlorite replacing biotite. From MC003B, sample #5

Interp.

- Chlorite pseudomorphing biotite, evidence of chl as alteration product

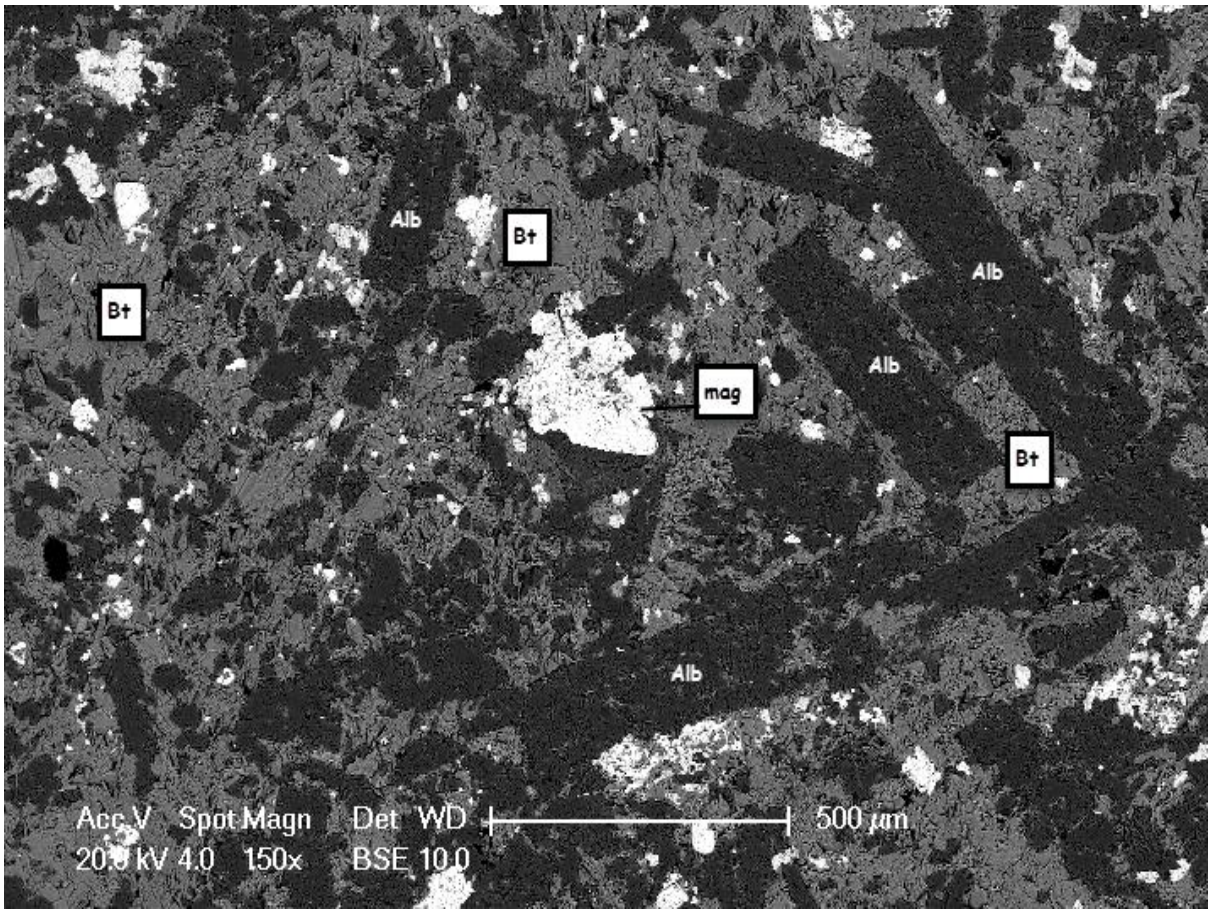

Figure 43: An example of magnetite in biotite with euhedral, elongated albite crystals. From hole MTC12, sample 1

Interp.

- Early alb

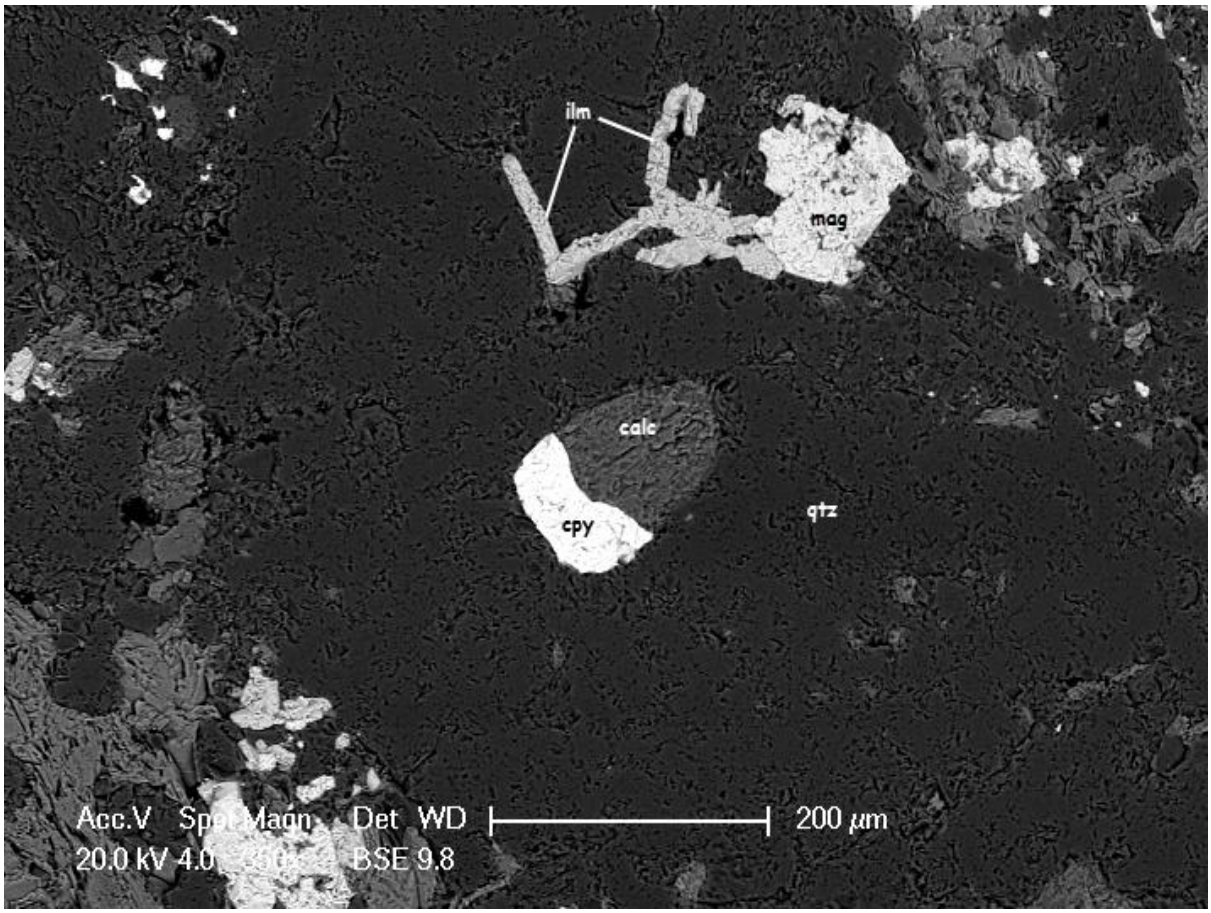

Figure 44 Chaclopyrite pseudomorphing? Growing with? calcite in surrounding quartz. Magnetite present with strands of Ti-Fe-Oxide extending of the bottom left corner. From hole MTC12, sample 1

Interp.

- Probably an example of ilmenite growing off magnetite and is thus later??
- Another example of dissolution process with cpy and calcite

APPENDIX C

ORE GEOCHEMISTRY

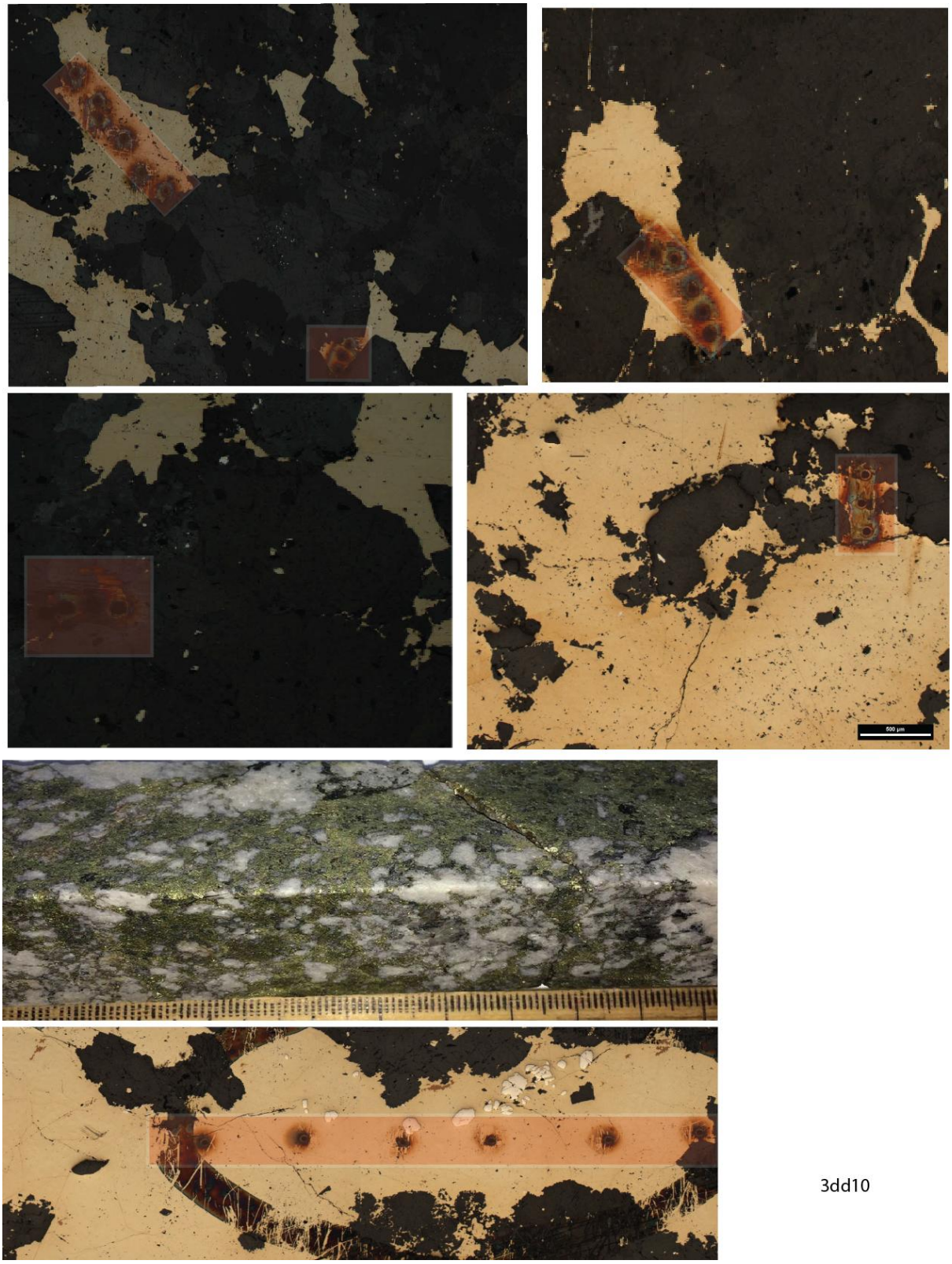

Figure 45: examples of laser ablation sites from 'trend 1' in chalcopyrite (MC003DD, sample #10)

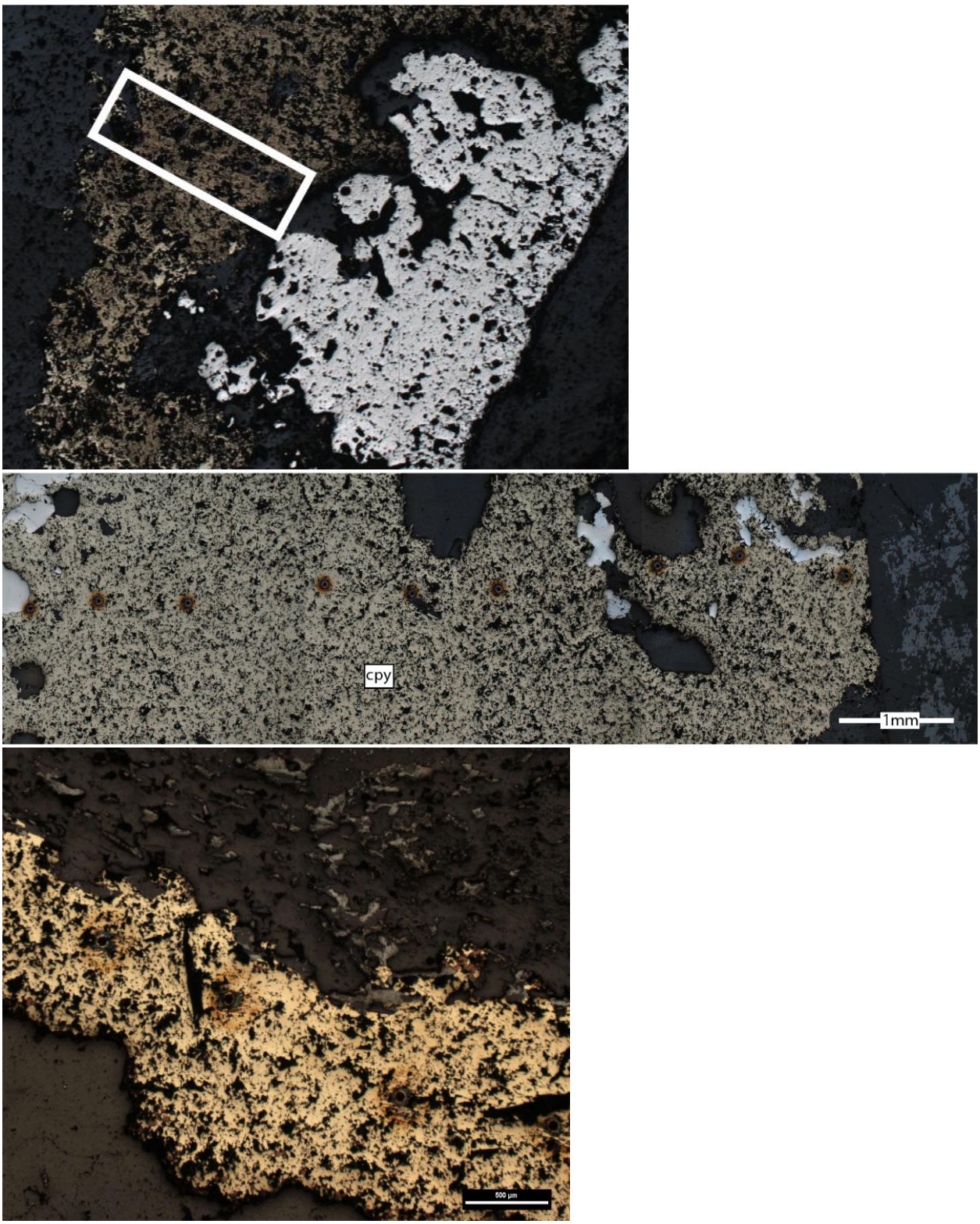

Figure 46: Example of laser alblation sites from 'trend 2' in chalcopyrite

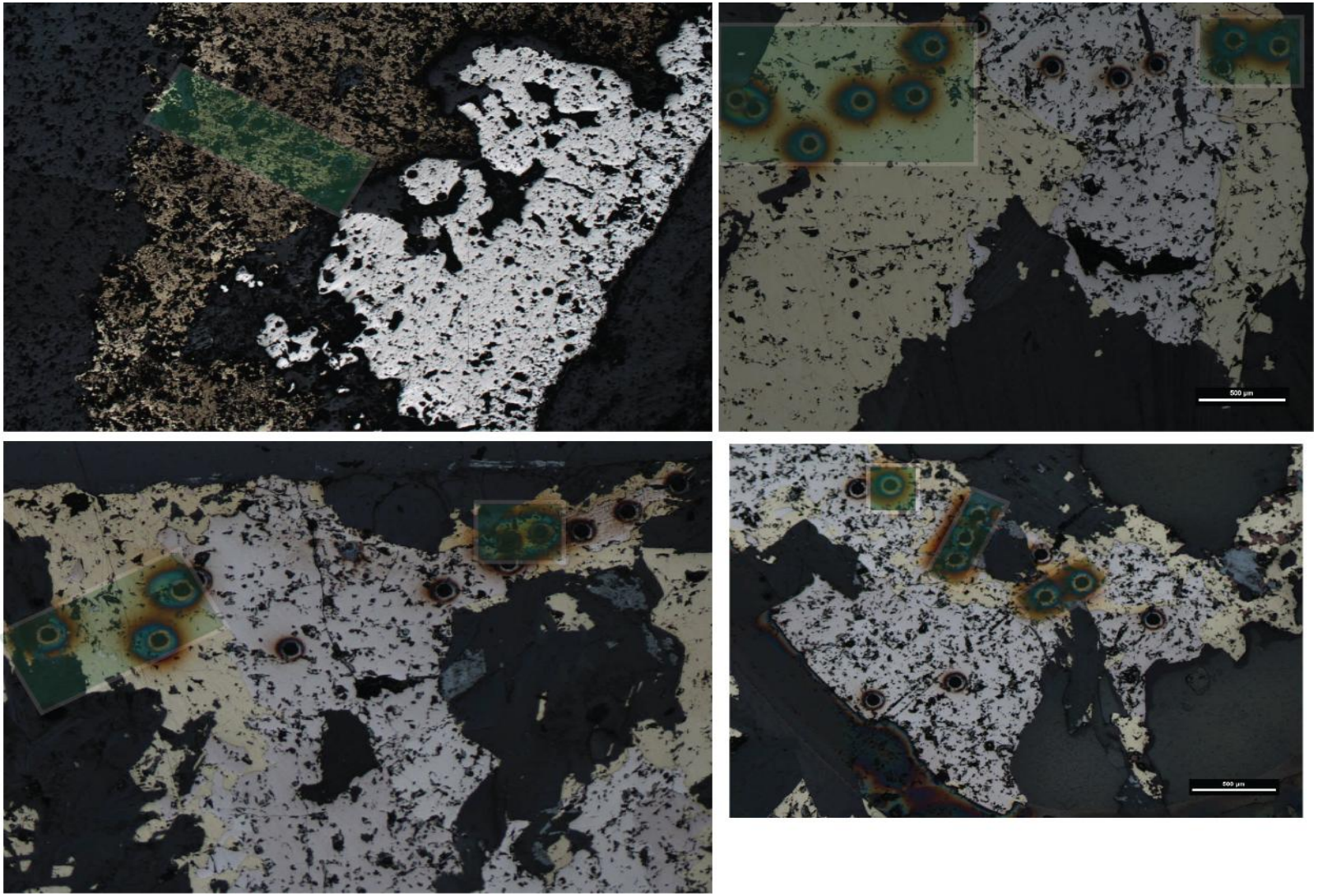

Figure 47: examples of laser ablation sites from 'trend 3' in chalcopyrite

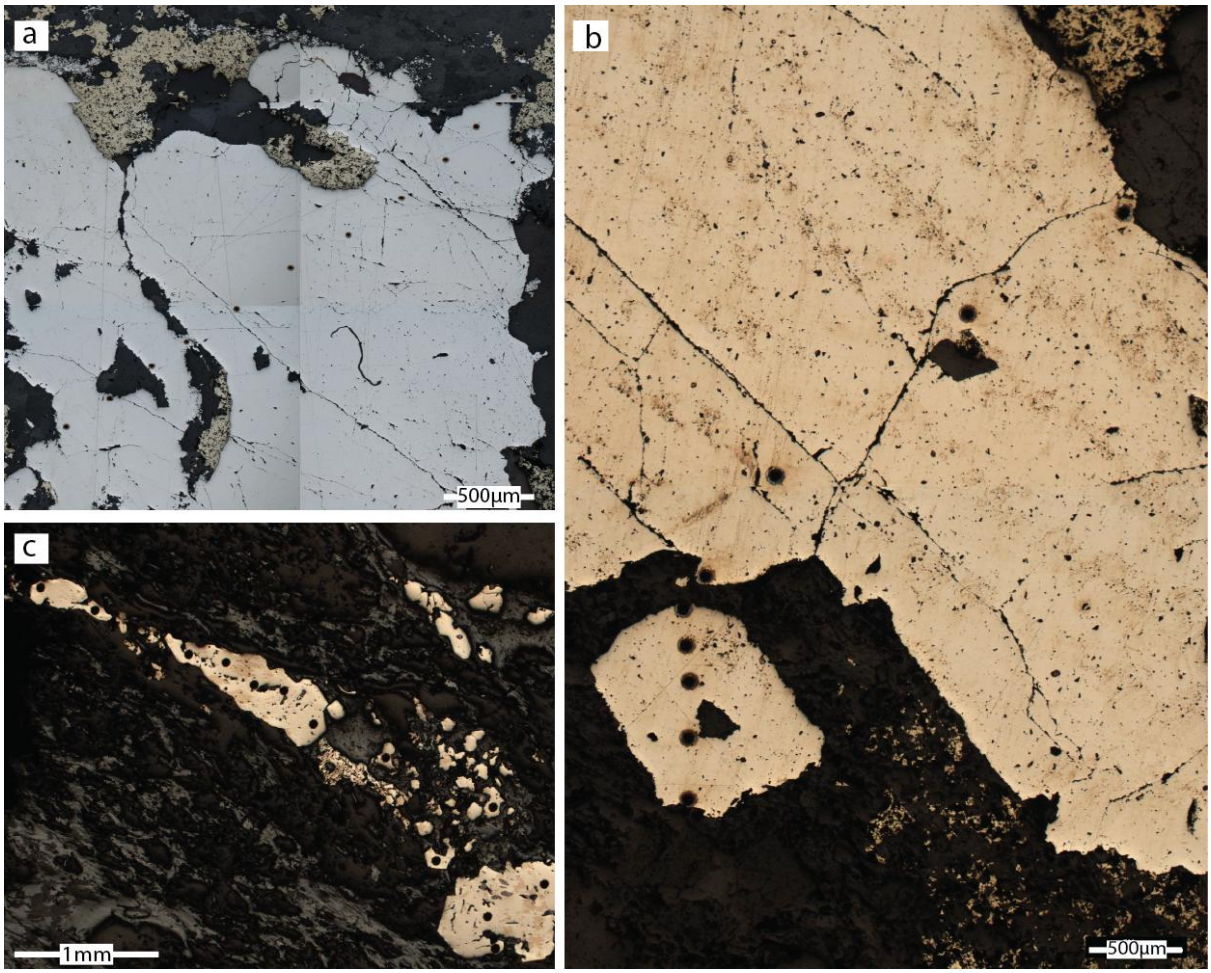

Figure 48: example of pyrite from trend 1 (a and b) and trend 2 (c) (hole MC001DD, sample #28)

Table 2: Trace element geochemistry obtained from the LA-ICPMS.

Hole	Sample	Sulph	Sulph. Type2	Loc.	Na 23	S 33	V 51	Cr 52	Mn 55	Fe 57	Co 59	Ni 60	Cu 65	Zn 66	Ga 69	As 75	Se 82	Mo 95	Ag 107	Cd 111	In 115	Sn 118	Sb 121	Te 125	Ba 137	W 184	Ir 193	Au 197	Hg 202	Tl 205	Pb 208	Bi 209
MC003DD	10	cpy	main	edge	5.68	596422.81	0.51	2.72	2.53	236535.67	3.61	2.31	542258.75	86.57	1.24	3.27	175.91	1.26	19.85	2.61	23.88	108.02	12.62	5.01	13.63	0.45	0.16	0.39	0.3	0.157	80.52	39.64
MC003DD	10	cpy	main	centre	3.96	595057.06	0.54	2.69	4.19	236535.67	1.28	2.31	529158.88	186.87	0.81	3.29	181.57	1.16	5.94	2.86	22.79	59.57	8.39	5.14	13.75	0.52	0.126	0.47	0.26	0.18	46.28	26.89
MC003DD	10	cpy	main	centre	6.45	638558.13	0.46	2.53	2.4	236535.67	0.48	1.98	534451.75	248.34	0.66	2.9	160.9	1.31	6.29	2.63	24.21	114.52	8.4	4.26	11.76	0.45	0.116	0.42	0.22	0.15	54.06	30.32
MC003DD	10	cpy	main	centre	3.81	580605.88	0.5	2.55	2.39	236535.69	0.97	2.26	502480.91	86.82	1.02	3.05	167.67	1.24	2.96	2.86	21.72	111.3	7.2	4.95	11.38	0.46	0.133	0.42	0.21	0.155	28.95	19.12
MC003DD	10	cpy	main	centre	3.87	599834.19	0.49	2.57	2.44	236535.67	1.75	2.06	506245.13	23.32	0.61	3.17	152.84	1.13	2.8	2.72	22.15	100.43	7.23	4.4	11.07	0.45	0.149	0.44	0.21	0.161	36.83	17.24
MC003DD	10	cpy	main	centre	3.71	540734.31	0.47	2.51	2.31	236535.67	1.11	2.12	474914.63	27.53	0.56	2.8	155.73	1.17	12.9	2.72	19.25	68.71	6.24	5.61	11.06	0.43	0.13	0.42	0.2	0.149	30.24	26.37
MC003DD	10	cpy	main	edge	3.71	566957.81	0.46	2.47	2.31	236535.66	0.45	2.2	463952.84	2.89	0.7	3.02	146.01	1.21	2.79	2.58	21.21	95.14	1.02	4.36	11.47	0.43	0.128	0.39	0.19	0.146	6.11	2.05
MC003DD	10	cpy	main	edge	3.46	554580.56	0.62	2.32	2.16	236535.67	0.4	1.82	470127.72	20.07	0.42	2.77	206.49	1.13	1.49	2.57	21.12	100.87	1.31	5.04	10.78	0.39	0.132	0.35	0.22	0.145	4.61	1.68
MC003DD	10	cpy	main	centre	3.4	527169.13	0.42	2.24	2.11	236535.69	0.42	1.74	435091.16	4.64	0.45	2.47	188.76	1.08	7.64	2.41	21.14	89.58	5.48	4.66	9.84	0.38	0.12	0.38	0.169	0.132	19.68	7.08
MC003DD	10	cpy	main	centre	3.48	487069.69	0.44	2.27	2.16	236535.69	0.44	2.11	438009.19	12.28	0.48	2.79	142.82	1.16	8.36	2.4	21.78	92.73	3.67	4.39	9.3	0.38	0.117	0.38	0.18	0.155	17.37	2.94
MC003DD	10	cpy	main	centre	3.64	515772.94	0.48	2.39	2.22	236535.67	0.47	2.02	434988.97	15.53	0.58	3.04	155.04	1.19	2.08	2.6	20.86	99.88	3.59	4.59	9.24	0.43	0.118	0.41	0.186	0.151	12.93	4.3
MC003DD	10	cpy	main	centre	4.06	525675.38	0.46	2.39	2.27	236535.67	0.44	2.04	446686.56	14.89	0.51	2.63	188.63	1.08	1.61	2.82	21.76	106.77	2.03	4.69	9.9	0.45	0.129	0.32	0.179	0.138	10.01	2.93
MC003DD	10	cpy	main	edge	3.49	513296.22	0.45	2.33	3.67	236535.66	0.42	2.09	421892.88	20.95	0.62	2.61	128.21	1.07	1.34	2.38	20.07	99.24	0.66	4.99	9.28	0.39	0.129	0.34	0.177	0.125	8.39	2.79
MC003DD	10	cpy	main	edge	3.44	467480.59	0.44	2.29	2.15	236535.67	0.43	2.14	400332.78	9	0.75	2.91	163.9	1.19	5.1	2.47	19.45	92.87	2.69	4.43	9	0.36	0.101	0.33	0.177	0.138	14.9	2.66
MC003DD	10	cpy	main	edge	3.47	488001.56	0.44	2.26	2.21	236535.67	1.06	2.05	398222.16	2.1	0.43	2.86	165.26	1.04	15.31	2.52	17.52	62.65	10.33	4.33	9.2	0.38	0.111	0.31	0.164	0.14	61.67	7.03
MC003DD	10	cpy	main	edge	3.19	414870.94	0.41	2.07	4453	236535.67	12.57	7.37	317208.22	2.18	0.37	6.4	111.83	1.82	8.98	3.28	15.16	33.6	3.01	4.31	9.57	0.36	0.106	0.32	0.22	0.116	2.74	6.19
MC003DD	10	cpy	main	edge	50.87	461341.69	0.39	1.91	3.25	236535.69	0.36	1.71	368959.03	7.2	0.38	2.37	145.99	0.85	0.94	2.11	17.84	78.73	0.95	3.7	7.39	0.33	0.104	0.3	0.18	0.104	1.86	1.33
MC003DD	10	cpy	main	edge	25.43	440785.41	0.38	1.99	1.98	236535.67	0.38	1.9	365572.66	7.73	0.39	2.7	112.87	0.97	1.53	2.25	17.64	75.73	0.52	4.05	7.4	0.35	0.107	0.38	0.178	0.13	3.47	1.66
MC003DD	10	cpy	main	edge	8.39	438353.72	0.35	1.81	1.78	236535.66	1.34	1.58	358933.06	3.23	0.33	2.14	138.69	0.91	0.77	2.08	16.58	75.23	0.39	3.89	7.26	0.32	0.095	0.29	0.154	0.121	1.43	0.7
MC003DD	10	cpy	main	edge	57.42	440345.69	0.39	2.11	1.97	236535.66	0.37	1.85	356100.56	13.98	0.56	2.42	136.01	0.96	2.6	2.52	16.63	67.13	1.69	4.37	27.66	0.35	0.11	0.35	0.169	0.127	10.51	3.52
MC003DD	10	cpy	main	centre	3	437233.28	0.37	1.93	1.81	236535.66	0.35	1.78	342060.19	12.2	0.37	2.17	112.58	0.94	0.93	2.11	15.05	72.89	0.92	3.93	7.28	0.36	0.092	0.32	0.156	0.115	3.04	1.66
MC003DD	10	cpy	main	centre	5.46	406476.53	0.35	1.85	1.74	236535.66	0.36	1.62	334803.72	11.48	0.37	2.26	95.78	0.86	1.87	2.19	14.87	71.94	2.52	3.89	5.78	0.34	0.096	0.32	0.147	0.109	7.24	4.72
MC003DD	10	cpy	main	centre	2.8	414610.5	0.38	1.81	1.78	236535.66	0.49	2.23	319476.16	9.38	0.38	2.25	122.86	0.85	1.19	2.18	14.94	69.59	2.5	4.23	7.12	0.34	0.09	0.27	0.143	0.109	6.31	3.72
MC003DD	10	cpy	main	centre	2.91	414377.44	0.37	1.85	1.75	236535.67	0.57	1.66	343395.56	6.56	0.52	2.58	105.9	0.9	1.48	2.15	15.38	71.05	1.54	4.39	7.3	0.31	0.104	0.27	0.138	0.105	7.82	2.75
MC003DD	10	cpy	main	edge	39.42	429639.59	0.35	1.77	2.93	236535.67	0.5	1.59	327591.63	7.61	0.36	2.14	126.84	0.81	5.98	2.08	15.38	74.44	2.69	3.74	6.37	0.32	0.106	0.32	0.137	0.091	16.7	5.97
MC003DD	10	cpy	main	edge	2.79	401239.44	0.37	1.76	1.69	236535.67	0.39	1.76	324007.34	2.96	0.31	2.37	120.9	0.9	4.02	1.91	14.04	65.33	2.17	3.61	6.03	0.3	0.093	0.26	0.135	0.093	11.49	3.35
MC003DD	10	cpy	main	edge	2.63	384477.63	0.33	1.7	2.31	236535.66	0.31	1.53	309000.13	17.53	0.39	2.04	136.73	0.75	16.67	1.67	13.93	36.77	11.4	3.77	5.39	0.31	0.086	0.26	0.124	0.134	48.18	19.7

MC003DD	10	cpy	main	edge	2.7	386555.06	0.34	1.72	1.65	236535.67	0.31	1.65	303611.22	4.16	0.32	2.09	87.99	0.91	9.08	1.83	13.66	35.92	5.36	4.1	5.81	0.29	0.093	0.24	0.125	0.099	18.77	8.54
MC003DD	10	cpy	main	edge	2.6	383734.19	0.33	1.64	1.56	236535.69	0.44	1.55	295771.66	3.58	0.33	2.05	97.7	0.77	10.67	1.72	13.89	17.15	8.53	3.5	5.64	0.27	0.076	0.23	0.125	0.59	44.85	17.39
MC003DD	12	cpy	main	edge	529.3	185377.625	0.77	3.95	3.62	236535.72	0.83	3.53	241868.92	71.15	0.77	4.19	137.64	1.72	2.09	4.14	5.01	45.97	1.55	9.66	20.84	0.61	0.202	0.6	0.14	0.216	6.22	5.16
MC003DD	12	cpy	main	edge	538.61	192119.61	0.72	4.03	3.66	236535.72	0.83	3.27	244027.67	114.08	0.78	4.36	138.37	1.73	1.95	3.67	5.26	22.18	2.38	9.42	39.84	0.71	0.172	0.61	0.135	0.214	13.1	8.8
MC003DD	12	cpy	main	edge	19.9	170735.345	0.7	3.74	8.75	236535.72	3.73	3.03	246260.88	40.04	0.74	4.01	128.38	1.73	16.75	3.87	6.79	13.61	4.36	8.03	75.14	0.57	0.19	0.58	0.123	1.09	27.99	40.84
MC003DD	12	cpy	main	edge	20.94	176404.64	0.75	3.9	3.5	236535.72	0.85	3.5	243807.77	37	0.64	4.47	130.37	1.89	19.06	4.09	6.82	18.4	4.33	8.25	17.92	0.64	0.21	0.61	0.124	0.21	25.59	18.28
MC003DD	12	cpy	main	edge	22.16	179840.875	0.75	4.02	3.75	236535.7	0.86	3.06	251760.36	75.55	0.83	4.25	152.54	2	7.7	4.27	7.79	26.64	1.39	8.74	17.52	0.67	0.215	0.58	0.127	0.226	10.54	6.39
MC003DD	12	cpy	main	centre	22.52	173641.42	0.78	4.08	3.73	236535.72	0.92	3.61	247881.53	119.49	0.78	4.81	162.08	2.11	1.02	4.15	9.56	66.28	0.59	9	20.28	0.75	0.215	0.71	0.125	0.213	2.2	1.12
MC003DD	12	cpy	main	centre	22.74	173295.265	0.76	4.08	3.87	236535.73	0.88	3.5	250114.08	282.25	0.79	4.79	110.48	1.91	0.74	4.81	8.89	69.52	0.65	8.65	18.35	0.73	0.208	0.69	0.128	0.205	3.43	1.57
MC003DD	12	cpy	main	edge	22.29	173418.78	0.71	3.99	3.7	236535.72	0.89	3.28	245088.38	46.06	0.82	4.94	180.52	1.83	7.02	4.72	7.72	21.02	1.72	7.99	17.88	0.65	0.187	0.56	0.125	0.2	21.39	3.8
MC003DD	12	cpy	main	edge	22.56	177946.985	0.75	3.94	3.78	236535.7	0.88	3.35	242960.58	50.1	0.82	4.69	128.99	1.74	0.76	4.42	7.81	56.48	0.68	8.11	17.31	0.67	0.201	0.54	0.12	0.18	2.61	0.77
MC003DD	12	cpy	main	edge	31.86	172690.28	0.95	4.5	4.89	236535.75	0.96	3.99	244396.06	57.22	0.96	5.88	185.09	2.25	3.58	5.35	7.47	33.14	1.66	7.54	18.88	0.89	0.27	0.68	0.145	0.34	8.94	1.72
MC003DD	12	cpy	main	centre	28.25	171749.94	0.88	3.89	4.2	236535.75	1.66	4.02	247658.17	66.49	0.74	5.01	174.49	1.87	0.86	5.12	6.7	24.92	0.75	7.67	14.25	0.71	0.2	0.59	0.132	0.22	5.19	1.29
MC003DD	12	cpy	main	edge	27.28	173799.61	0.84	3.81	4.2	236535.75	0.87	3.84	254984.25	49.79	0.79	5.15	134.22	1.62	3.48	4.8	5.98	22.8	1.01	7.58	15.72	0.75	0.2	0.63	0.128	0.22	5.06	1
MC003DD	12	cpy	main	centre	27.25	179806.83	0.78	3.73	4.11	236535.75	0.91	3.54	247141.92	73.23	0.69	4.89	96.33	1.84	0.72	4.46	10.35	39.85	0.69	5.96	13.47	0.66	0.213	0.57	0.119	0.209	4.25	1.25
MC003DD	12	cpy	main	edge	29.17	175474.89	0.81	3.88	7.88	236535.75	1.03	3.9	246654.48	84.04	0.79	5.45	117.86	1.89	0.77	4.95	11.1	57.52	0.74	7.83	13.73	0.72	0.23	0.63	0.124	0.23	3.07	1.04
MC003DD	12	cpy	main	centre	29.63	173888.28	0.8	3.98	4.43	236535.75	1.12	4.2	248322.8	102.64	0.86	5.22	152.9	1.91	1.08	5.16	10.52	52.87	0.78	7.93	14.32	0.68	0.24	0.63	0.129	0.24	5.51	1.21
MC003DD	12	cpy	main	centre	28.14	178226.595	0.74	3.78	6.38	236535.75	1.58	4	246375.98	159.08	0.84	4.83	149.19	1.56	0.65	4.79	11.97	64.06	0.65	6.78	13.41	0.61	0.205	0.61	0.117	0.22	3.07	1.18
MC003DD	12	cpy	main	centre	29.05	182406.94	0.85	3.85	4.24	236535.75	0.93	3.7	248293.28	63.03	0.76	4.79	108.97	1.64	0.72	4.71	12.64	20.03	1.5	6.75	12.95	0.64	0.195	0.64	0.121	0.228	8.94	1.82
MC003DD	12	cpy	main	edge	28.52	181030.94	0.75	3.68	4.03	236535.73	0.91	3.84	239767.14	78.11	0.77	4.82	134.9	1.61	1.2	4.59	8.23	23.23	0.79	6.92	14.47	0.63	0.185	0.58	0.119	0.23	5.9	1.42
MC003DD	12	py	late	edge	34.46	395570.16	0.205	1.03	2.49	361838.31	1918.35	836.63	28.28	2.19	0.19	4.29	23.88	0.47	0.61	1.13	0.048	0.42	40.81	2.13	6.54	0.167	0.056	0.35	0.033	0.058	219.72	7.69
MC003DD	12	py	main	edge	5.9	398614.16	0.178	0.94	0.89	361838.31	5969.93	67.33	486.69	1.93	0.188	100.29	30.69	0.44	0.154	0.96	0.044	0.41	0.16	2.34	5.55	0.146	0.051	0.158	0.03	0.045	0.089	1.18
MC003DD	12	py	main	centre	6.07	411882.41	0.201	0.97	0.97	361838.31	8658.25	98.59	1.03	2.09	0.185	81.23	38.43	0.42	0.145	1.05	0.046	0.39	0.162	2.05	5.8	0.149	0.048	0.159	0.031	0.048	0.098	0.049
MC003DD	12	py	main	centre	5.98	418232.34	0.18	0.95	0.94	361838.34	7876.51	239.28	1.27	1.64	0.173	77.08	47.54	0.44	0.18	0.85	0.043	1.73	3.24	2.18	6.2	0.155	0.044	0.136	0.03	0.047	11.82	6.39
MC003DD	12	py	main	centre	5.86	410117.47	0.182	0.96	0.9	361838.31	8545.42	93.5	1.38	1.6	0.184	75.45	31.17	0.44	0.147	0.96	0.041	0.41	0.155	1.9	5.32	0.179	0.047	0.145	0.028	0.049	0.093	0.056
MC003DD	12	py	main	centre	5.54	425651.38	0.171	0.89	0.86	361838.34	10178.18	112.56	0.99	2.05	0.191	82.86	25.05	0.44	0.16	0.97	0.045	0.38	0.148	1.86	5.44	0.164	0.04	0.136	0.028	0.052	0.141	0.16
MC003DD	12	py	main	centre	5.32	401414.44	0.165	0.84	0.82	361838.31	7890.19	87.24	1.11	1.9	0.177	74.33	53.13	0.4	0.122	0.89	0.042	0.35	0.134	1.92	4.82	0.149	0.043	0.13	0.031	0.045	0.076	0.046
MC003DD	12	py	main	centre	5.94	418114.06	0.19	0.95	0.94	361838.34	9501.23	167.41	36.59	1.69	0.181	92	26.83	0.42	3.55	0.96	0.042	0.51	5.97	2.07	4.95	0.154	0.05	0.153	0.033	0.48	18.86	25.74
MC003DD	12	py	main	edge	5.88	388735.91	0.188	0.92	1.06	361838.34	0.196	0.84	1.89	1.9	0.182	1.27	13.3	0.44	0.138	1.05	0.045	0.37	0.318	2	5.13	0.142	0.037	0.156	0.032	0.049	3.78	0.317
MC003DD	12	py	main	edge	11.43	406917.75	0.178	0.87	0.89	361838.31	8334.87	132.41	4.24	1.55	0.159	85.07	35.24	0.38	0.66	0.88	0.042	0.36	7.16	1.92	5.26	0.156	0.053	0.211	0.029	0.054	20.08	14.23

MC003DD	12	py	main	edge	5.96	423112.28	0.189	0.94	0.96	361838.31	3988.67	53.16	1.11	1.58	0.176	148.7	24.27	0.44	0.163	0.97	0.044	0.37	0.145	1.87	5.4	0.16	0.04	0.16	0.031	0.055	0.089	0.051
MC003DD	12	py	main	edge	5.5	415634.53	0.153	0.85	0.9	361838.34	9085.2	102.2	0.9	1.59	0.173	76.68	27.8	0.42	0.146	0.92	0.037	0.37	0.156	1.64	5.48	0.133	0.043	0.141	0.027	0.047	0.081	0.048
MC003DD	12	py	main	edge	5.19	428776.16	0.159	0.8	0.81	361838.31	1131.74	821.3	40.63	1.69	0.162	1.02	62.26	0.38	3.6	0.79	0.034	0.31	0.239	1.79	5.25	3.03	0.043	0.121	0.029	0.046	1.24	1.64
MC003DD	12	py	main	centre	4.67	408804.34	0.149	0.7	0.92	361838.31	2382.06	3536.25	45.87	1.53	0.146	0.94	182.4	1.82	3.41	0.69	0.031	0.29	2.16	1.56	4.4	25.77	0.033	0.111	0.023	0.78	2.19	0.299
MC003DD	12	py	main	centre	5.2	417791.09	0.167	0.78	0.82	361838.34	1144.73	2332.66	10.13	1.76	0.154	0.92	161.22	0.35	0.12	0.76	0.036	3.2	12.66	1.54	4.78	2.44	0.034	0.116	0.025	0.062	0.225	0.258
MC003DD	12	py	main	centre	4.52	401396.03	0.135	0.67	0.71	361838.34	1774.68	2705.77	23.77	1.21	0.148	0.81	137.39	1.96	0.59	0.74	0.028	0.28	0.78	1.54	4.29	24.42	0.032	0.122	0.022	0.62	0.79	0.16
MC003DD	12	py	main	centre	4.85	409703.78	0.141	0.74	0.74	361838.31	2444.95	4651.54	122.33	1.37	0.135	1	170.1	0.96	3.94	0.77	0.032	0.29	6.2	1.59	4.78	17.59	0.035	0.106	0.022	2.64	4.42	0.489
MC003DD	12	py	main	centre	4.68	386469.81	0.144	0.84	0.74	361838.31	463.87	1394.58	27.16	1.27	0.143	0.86	10.46	0.33	0.268	0.76	0.04	0.75	10.18	1.51	4.43	1.62	0.034	0.105	0.022	0.04	0.069	0.039
MC003DD	12	py	main	centre	5.13	425545.59	0.142	0.73	0.75	361838.34	2270.34	4245.44	314.43	1.32	0.15	0.89	132.36	0.84	19.57	0.69	0.037	2.08	41.58	1.79	4.13	9.64	0.038	0.1	0.021	0.43	14.64	0.073
MC003DD	12	py	main	edge	22.13	428098.53	0.216	1.06	8.54	361838.31	2826.9	1180.64	20.53	1.86	0.195	1.17	15.61	0.47	0.77	1.04	0.043	0.44	7.02	2.41	7.06	0.132	0.051	0.149	0.032	0.057	256.83	0.54
MC003DD	13	cpy	main	centre	33.97	183868.155	0.79	3.65	4.26	236535.73	0.9	4.15	242513.05	8.91	0.76	5.11	97.25	1.84	12.55	5.34	10.01	53.44	3.61	6.34	13.54	0.63	0.186	0.58	0.146	0.23	15.23	16.82
MC003DD	13	cpy	main	centre	35.78	180985.89	0.87	3.83	4.43	236535.75	1.03	4.1	238054.7	24.83	1.04	5.24	125.41	1.82	1.21	5.75	11.17	53.37	0.77	6.85	13.77	0.7	0.209	0.6	0.147	0.21	2.88	2.04
MC003DD	13	cpy	main	centre	37.24	172875.875	0.92	3.91	4.46	236535.73	0.98	4.45	240990.02	19.42	0.86	5.71	118.1	1.64	4.72	5.96	12.17	46.74	0.76	6.02	13.01	0.75	0.224	0.63	0.146	0.25	3.71	3.97
MC003DD	13	cpy	main	centre	35.61	180334.33	0.85	3.6	4.31	236535.75	0.95	4.55	242152.2	28.96	0.76	5.29	66.39	1.79	2.93	5.4	13.01	46.52	1.08	5.76	13.87	0.75	0.206	0.56	0.141	0.215	4.91	6.48
MC003DD	13	cpy	main	centre	74.13	188511.94	0.86	3.77	4.32	236535.77	18.34	4.25	232953.48	17.39	0.82	5.2	93.23	1.73	2.45	5.28	13.06	28.82	1.93	6.93	13.89	0.64	0.21	0.57	0.141	0.23	7.41	8.46
MC003DD	13	cpy	main	edge	76.17	165059.86	0.79	3.47	4.64	236535.78	0.75	3.86	233896	17.33	0.67	4.94	71.07	1.54	3	5.25	8.15	31.62	1.81	5.71	12.27	0.53	0.212	0.55	0.133	0.206	7.85	6.67
MC003DD	13	cpy	main	centre	36.75	180690.065	0.83	3.63	4.29	236535.77	0.85	4.23	237780.88	16.43	0.85	6.11	131.45	1.73	2.42	5.42	10.51	44.7	1.36	6.36	10.97	0.55	0.212	0.55	0.134	0.25	7.46	6.45
MC003DD	13	cpy	main	edge	35.69	193460.72	0.78	3.52	5.14	236535.77	20.02	9.63	238271.16	15.13	0.73	5.34	97.98	1.55	11.57	5.27	12.65	29.92	2.54	5.31	11.34	0.65	0.221	0.54	0.127	0.21	4.69	3.58
MC003DD	13	cpy	main	centre	35.69	169403.485	0.78	3.43	4.05	236535.78	0.73	4.02	246827.94	30.36	0.75	4.9	69.84	1.49	2.53	5.25	13.19	34.96	0.58	6.89	11.78	0.63	0.184	0.53	0.126	0.208	1.35	1.27
MC003DD	13	cpy	main	centre	36.67	177762.125	0.8	3.46	4.07	236535.77	0.82	4.2	238661.02	33.14	0.77	5.47	124.52	1.45	3.4	5.31	10.45	40.96	0.68	5.63	11.76	0.64	0.205	0.51	0.129	0.23	6.62	4.77
MC003DD	13	cpy	main	edge	36.87	186144.095	0.83	3.57	4.16	236535.77	0.94	4.18	242203.39	34.59	0.75	5.67	91.13	1.5	6.95	5.28	12.26	34.27	1.98	5.49	12.66	0.57	0.181	0.58	0.13	0.23	16.49	11.82
MC003DD	13	cpy	main	centre	35.66	174248.345	0.84	3.28	9.05	236535.77	0.81	4.2	241288.55	24.44	0.75	4.62	101.02	1.5	5.99	5.23	11.19	32.38	0.98	5.09	11.93	0.84	0.194	0.57	0.12	0.23	6.4	5.49
MC003DD	13	cpy	main	centre	37.36	178878.455	0.85	3.55	4.19	236535.78	0.88	4.42	245047.69	15.18	0.68	4.93	77.84	1.61	4.4	6.12	11.38	37.04	0.65	4.83	12.49	0.61	0.212	0.6	0.125	0.24	1.68	2.35
MC001DD	28	cpy	vein/HR boundary	vein	1.98	376040	0.24	1.26	1.21	236535.66	0.39	35.03	296264.72	86.25	0.26	1.6	172.26	0.65	23	1.38	2.69	10.07	0.25	2.77	4.23	0.22	0.065	0.19	0.125	0.082	8.23	2.77
MC001DD	28	cpy	vein/HR boundary	centre	2.26	342477.09	0.31	1.46	1.36	236535.67	0.74	37.42	305935	40.59	0.26	2.52	147.12	0.75	23.41	1.52	7.45	10.21	0.38	3.09	4.94	0.27	0.074	0.21	0.127	0.075	9.11	1.59
MC001DD	28	cpy	vein/HR boundary	centre	2.34	328301	0.29	1.49	1.35	236535.66	0.3	35.36	264853.88	43.72	0.29	1.89	132.05	0.7	20.7	1.74	0.81	11.9	0.28	3.1	4.85	0.27	0.076	0.23	0.123	0.075	3.4	0.55
MC001DD	28	cpy	vein/HR boundary	edge	5.5	336531.53	0.27	1.43	1.98	236535.66	0.91	29.49	273241.97	27.31	0.27	1.82	110.82	0.67	19.81	1.58	0.95	6.89	0.59	3.38	4.6	0.28	0.072	0.22	0.119	0.079	4.83	0.7
MC001DD	28	py	vein/HR boundary	edge	0.25	156967.34	0.031	0.159	0.146	361838.16	15.22	901.81	2.98	0.143	0.032	93.26	71.22	0.076	0.028	0.165	0.0074	0.063	0.028	0.88	0.47	0.032	0.0082	0.026	0.0129	0.0092	0.177	0.05
MC001DD	28	py	vein/HR	edge	0.82	145204.8	0.029	0.148	9.98	361838.13	104.1	835.94	45.02	0.46	0.029	11.91	66.66	0.067	0.053	0.151	0.0068	0.075	0.146	0.4	0.46	0.029	0.0071	0.023	0.0118	0.008	4.41	0.68

MC001DD	28	py	boundary vein/HR boundary	edge	0.48	155857.39	0.03	30.154	0.153	361838.16	16.78	230.85	0.3	0.143	0.03	3.71	35.98	0.078	0.024	0.167	0.0078	0.066	0.192	0.29	0.46	0.025	0.0093	0.023	0.0116	0.0088	1.97	0.112
MC001DD	28	py	vein/HR boundary	centre	0.52	139857.44	0.03	20.147	2.6	361838.13	18.43	281.39	0.31	0.125	0.032	5.7	16.89	0.071	0.031	0.173	0.0062	0.061	0.51	0.36	0.43	0.025	0.008	0.02	0.0108	0.0086	7.89	0.75
MC001DD	28	py	vein/HR boundary	centre	0.24	141568.66	0.03	0.15	0.146	361838.13	14.03	296.28	0.252	0.124	0.027	15.74	19.34	0.077	0.025	0.21	0.0075	0.058	0.053	1.1	0.41	0.031	0.0072	0.0216	0.0113	0.0092	0.282	0.102
MC001DD	28	py	vein/HR boundary	edge	0.7	139745.45	0.03	10.152	3.82	361838.16	122.43	197.64	0.71	0.129	0.028	8.84	53.28	0.069	0.161	0.18	0.0068	0.296	0.46	0.43	0.42	0.027	0.0083	0.023	0.0127	0.0128	5.65	1.75
MC001DD	29	cpy	main	edge	8.79	117293.86	0.42	3.46	1.71	155999.95	1.06	11.95	169631.19	113.32	0.55	2.84	60.88	1.68	12.99	1.86	7.27	9.94	0.43	13.89	28.19	0.62	0.133	0.44	0.089	0.126	0.22	0.55
MC001DD	29	cpy	main	centre	13.61	174911.64	0.65	5.2	2.57	236535.69	1.45	19.72	256086.52	207.37	0.84	4.15	95.81	2.67	19.08	2.99	11.07	16.95	0.73	22.84	43.18	0.76	0.23	0.59	0.126	0.208	0.63	1.08
MC001DD	29	cpy	main	centre	13.25	182395.61	0.66	4.98	2.47	236535.69	1.26	19.47	253496.75	218.51	0.8	3.84	88.46	2.29	21.42	2.91	11.46	18.36	0.7	19.75	42.02	0.83	0.205	0.67	0.117	0.193	1.45	3.73
MC001DD	29	cpy	main	centre	13.29	176118.375	0.66	4.78	2.41	236535.69	1.75	22.12	263589.41	227.61	0.77	3.59	85.64	2.25	20.21	3	11.02	17.29	0.73	19.51	37.53	0.75	0.199	0.72	0.117	0.196	1.37	3.33
MC001DD	29	cpy	main	edge	13.88	174565.155	0.74	5.02	3.1	236535.7	3.32	30.44	259878.94	264.27	0.84	4.6	133.89	2.57	19.66	3.06	11.31	16.27	0.63	19.57	33.73	0.79	0.197	0.65	0.122	0.198	1.77	3.59
MC001DD	29	cpy	main	edge	19.58	173937.83	0.77	4.44	5.19	236535.72	4.49	15.83	249768.31	151.71	0.85	4.97	78.47	2.09	31.72	3.83	10.68	10.91	0.73	9.79	36.87	0.7	0.225	0.68	0.127	0.23	2.84	6.53
MC001DD	29	cpy	main	edge	18.9	178745.455	3.95	4.25	18.21	236535.72	19.53	72.6	234860.78	137.78	1.61	4.8	161.24	2.02	45.1	3.53	8.77	12.47	0.68	9.1	20.15	0.74	0.222	0.62	0.124	1.33	25.21	52.71
MC001DD	29	cpy	main	edge	5.37	92267.275	0.21	1.2	0.97	236535.73	680.64	566.2	82.1	2.11	0.22	1.32	54.7	0.52	0.175	0.99	0.044	0.43	0.184	2.39	4.98	0.191	0.053	0.177	0.034	0.068	0.1	0.777
MC001DD	29	cpy	main	edge	19.9	181712.83	0.77	4.21	6.64	236535.7	2.08	21.77	247561.66	169.7	0.8	4.75	130.01	1.96	29.72	4.15	12.11	14.34	0.72	10.88	19.06	0.72	0.205	0.76	0.118	0.203	4.45	16.96
MC001DD	29	cpy	main	edge	20.8	175790.815	0.82	4.26	3.86	236535.72	13.69	32.63	243189.88	165.27	0.75	4.97	134.88	2.08	40.07	3.87	7.5	13.53	0.66	10.27	20.13	0.68	0.215	0.6	0.153	0.22	4.54	10.83
MC001DD	29	cpy	main	edge	22.34	177137.97	9.1	4.12	54.44	236535.72	27.44	101.52	226865.17	175.19	4.69	4.2	124.4	1.8	35.58	3.8	9.28	13.57	0.82	9.6	30.36	0.78	0.216	0.59	0.21	0.24	10.52	25.42
MC001DD	29	po	main	edge	11.36	384231.81	0.4	2.18	2.47	484498	1564.31	845.56	423.13	5.9	0.42	2.52	94.45	1.09	0.35	1.96	0.1	0.98	0.4	4.24	10.9	0.36	0.12	0.35	0.079	0.124	0.201	0.507
MC001DD	29	po	main	centre	11.91	392431.81	0.47	2.29	1.47	484498	1546.22	974.27	4.69	4.68	0.39	2.41	78.72	1.04	0.38	2	0.101	1	0.38	4.72	11.8	0.4	0.122	0.33	0.082	0.139	0.33	2.18
MC001DD	29	po	main	centre	11.69	366545.25	0.42	2.21	1.41	484498.03	1534.05	1074.07	2.59	3.64	0.44	2.64	79.93	1.16	0.35	2.29	0.1	0.93	0.39	4.66	12.84	0.39	0.112	0.37	0.078	0.127	0.22	0.69
MC001DD	29	po	main	edge	11.94	405882.44	0.41	2.27	1.48	484498	1572.71	948.68	8.35	13.57	0.4	2.66	74.81	1.03	0.53	2.38	0.106	0.94	0.36	4.71	23.37	0.42	0.129	0.32	0.078	0.114	1.52	22.79
MC001DD	29	cpy	main	edge	14.73	179637.78	0.71	5.01	2.68	236535.7	1.52	35.45	259225.56	201.28	0.79	4.06	89.83	2.36	12.61	3.16	16.44	21.83	0.74	17.45	36.5	0.87	0.241	0.68	0.117	0.212	0.36	0.68
MC001DD	29	po	main	edge	41.9	719324.94	1.47	7.87	5.1	484498	3.01	81.01	506365.91	484.72	1.44	8.49	127.04	3.66	27.91	7.57	39.87	44.78	1.42	16.36	40.8	1.51	0.47	1.24	0.28	0.46	0.75	1.45
MC001DD	29	cpy	main	edge	15.43	174248.315	0.75	5.26	2.65	236535.7	1.45	35.19	257092.69	292.81	0.88	4.58	125.76	2.52	14.58	3.62	16.87	23.52	0.71	18.12	39.02	0.88	0.22	0.68	0.119	0.218	1.31	2.04
MC001DD	29	po	main	edge	45.37	731204.75	1.6	8.63	5.26	484498	2.82	82.33	526292.94	689.53	1.68	9.94	174.52	4.1	32.78	8.99	42.81	50.01	1.42	18.03	46.43	1.59	0.45	1.29	0.29	0.49	2.85	4.37
MC001DD	29	cpy	main	edge	15.63	175527.845	0.73	4.77	2.94	236535.69	2.95	25.58	254423.75	353.38	0.78	4.08	158.49	2.26	15.74	3.46	13.74	19.23	0.76	14.08	27.31	0.74	0.228	0.65	0.129	0.194	1	2.59
MC001DD	29	po	main	edge	41.97	713801.25	1.47	7.77	5.57	484498	5.97	59.03	519451.81	843.03	1.43	8.37	204.98	3.66	35.35	7.92	33.28	39.61	1.45	15.9	37.68	1.31	0.44	1.19	0.3	0.41	2.09	5.21
MC001DD	29	cpy	main	centre	17.14	176646.75	0.85	5.09	3.28	236535.69	2.21	26.77	257722.47	281.23	0.85	4.47	126.6	2.36	13.22	3.58	11.7	17.8	0.76	14.99	31.53	0.85	0.23	0.76	0.136	0.22	0.44	1.04
MC001DD	29	po	main	centre	48.24	739150.75	1.82	8.78	6.54	484498.03	4.33	61.38	532037.56	644.25	1.65	9.65	185.65	4.06	29.4	8.59	28.71	37.8	1.54	18.14	46.73	1.59	0.47	1.47	0.33	0.49	0.95	2.23
MC001DD	29	cpy	main	centre	40.58	176907.015	0.8	4.86	3.74	236535.69	1.97	25.19	256209.66	288.35	0.84	4.76	106.18	2.33	13.98	3.7	10.55	17.15	0.72	15.06	31.89	0.73	0.25	0.63	0.129	0.225	0.39	0.83

MC001DD	29	po	main	centre	113.65	740027.19	1.69	8.43	7.48	484498.03	3.86	57.65	529358.63	658.73	1.63	10.27	156.52	4.03	31.03	8.84	25.81	36.43	1.45	18.55	48.21	1.36	0.51	1.21	0.31	0.5	0.85	1.77
MC001DD	29	cpy	main	centre	17.84	180460.97	0.85	5.19	3.38	236535.7	1.05	30.27	257786.47	320.2	0.93	4.64	94.43	2.49	14.05	4.41	11.26	19.36	0.82	15.3	31.58	0.9	0.23	0.74	0.129	0.21	0.67	1.27
MC001DD	29	po	main	centre	49.75	754676.94	1.81	9.03	6.76	484498.03	2.06	69.12	533063.63	729.42	1.81	10	139.95	4.33	31.15	10.49	27.46	41.11	1.66	19.18	48.68	1.68	0.47	1.43	0.31	0.47	1.45	2.72
MC001DD	29	cpy	main	edge	16.84	181966.89	0.7	4.86	3.14	236535.69	1.83	29.58	256047.95	204.23	0.8	4.41	84.26	2.45	13.9	3.55	10.41	18.2	0.72	14.12	27.09	0.79	0.2	0.74	0.123	0.209	0.37	0.42
MC001DD	29	po	main	edge	46.73	760755.88	1.5	8.51	6.28	484498	3.59	67.42	529912.88	463.93	1.55	9.48	125.52	4.27	30.79	8.44	25.29	38.65	1.45	18	42.58	1.49	0.4	1.44	0.29	0.46	0.8	0.91
MC001DD	29	cpy	main	edge	30.22	174649.295	0.79	4.69	4.03	236535.7	0.94	28.28	257729.78	214.87	0.81	4.05	85.06	2.45	13.33	3.45	10.03	18.49	0.72	11.87	27.4	0.83	0.217	0.73	0.126	0.201	0.42	0.66
MC001DD	29	po	main	edge	83.46	729952.75	1.69	8.25	8.07	484498	1.84	64.31	533841	486.72	1.58	8.7	127.37	4.3	29.49	8.15	24.29	39.26	1.45	15.39	43.88	1.55	0.44	1.41	0.3	0.44	0.91	1.4
MC001DD	29	cpy	main	centre	21.81	186205.485	0.72	4.84	3.28	236535.7	2.57	14.04	252619.81	165.62	0.86	4.55	158.51	2.29	16.65	3.95	13.78	15.31	0.69	13.45	24.36	0.8	0.22	0.7	0.129	0.25	2.46	4.61
MC001DD	29	po	main	centre	59.11	777355.63	1.53	8.67	6.58	484498	5.07	31.67	525012.88	370.93	1.68	9.75	242.25	4.1	36.67	9.2	32.91	32.5	1.42	18.61	41.97	1.52	0.44	1.37	0.3	0.54	5.27	9.82
MC001DD	29	cpy	main	edge	16.85	178579.53	0.7	4.39	6.03	236535.7	110.89	422.28	233576.97	161.47	0.75	4.45	108.43	2.34	20.26	3.63	13.02	14.52	0.64	11.9	22.2	0.7	0.176	0.66	0.117	0.36	13.47	34.58
MC001DD	29	po	main	edge	43.44	735232.06	1.42	7.56	14.63	484498	88.17	115.38	507639.75	379.97	1.41	9.11	184.43	4.02	46.32	8.07	31	34.32	1.28	15.99	37.22	1.28	0.34	1.24	0.26	0.74	26.74	72.37
MC001DD	29	cpy	main	edge	18.18	177066.89	0.73	4.34	3.49	236535.7	4.64	46.32	246921.8	166.82	0.75	4.29	79.92	2.13	18.86	3.55	4.66	11.63	0.7	9.8	22.29	0.73	0.21	0.65	0.13	0.218	16.11	41.38
MC001DD	29	po	main	edge	47.12	727189.25	1.55	8.11	7.06	484498.03	7.27	100.41	515617	360.3	1.48	9.15	127.61	4	40.32	8	10.84	23.91	1.43	15.47	44.65	1.42	0.42	1.31	0.3	0.47	34.08	88.12
MC001DD	29	cpy	main	centre	18.82	187448.315	0.8	4.51	3.61	236535.72	3.39	38.67	247324.53	168.78	0.8	4.66	132.45	2.15	16.07	3.66	6.11	18.98	0.66	11.35	22.41	0.71	0.23	0.67	0.137	0.211	0.7	1.79
MC001DD	29	po	main	centre	49.53	787381.94	1.72	8.65	7.46	484498	6.57	85.4	512335.03	366.75	1.64	10.13	196.31	4.14	34.6	8.39	14.12	40.37	1.39	18.54	46.55	1.41	0.48	1.37	0.32	0.46	1.47	3.46
MC001DD	29	cpy	main	edge	19.64	179783.235	0.82	4.64	3.7	236535.72	1.05	29.64	250204.78	133.21	0.91	4.56	91.02	2.25	19.42	4.47	8.99	10.09	0.67	10.58	21.89	0.8	0.232	0.71	0.135	0.22	2.14	5.99
MC001DD	29	po	main	edge	50.36	748158.13	1.73	8.75	7.5	484498	2.08	65.3	524795.25	288.93	1.82	9.69	146.7	4.26	42.23	9.99	20.65	21.39	1.38	17.16	45.24	1.57	0.47	1.44	0.31	0.47	4.55	12.71
MC001DD	29	po	main	edge	13.22	367943.34	0.43	2.28	2	484498.03	1413.63	2421.55	2.49	4.47	0.43	2.66	65.52	1.05	0.49	2.37	0.102	0.97	0.4	5.02	13.38	0.37	0.097	0.32	0.074	0.12	0.43	3.69
MC001DD	29	po	main	centre	12.85	381157.25	0.44	2.18	1.91	484498	1464.76	2125.8	2.4	4.46	0.4	2.35	102.71	1.01	0.39	2.32	0.097	0.93	0.36	4.67	12.1	0.4	0.111	0.35	0.071	0.112	0.21	0.98
MC001DD	29	po	main	edge	48.01	731316.13	1.68	8.3	7.37	484498.06	4.85	57.51	537156.69	358.57	1.56	9.78	186.86	4	59.74	8.9	12.8	35.63	1.33	17.87	48.22	1.38	0.4	1.3	0.26	0.47	1.44	1.86
MC001DD	29	po	main	edge	12.12	346090.16	0.38	2.02	4.94	484498.06	1297.76	1072.57	3.5	3.37	0.4	2.34	81.52	0.96	0.33	2.05	0.1	0.85	0.33	4.33	12.31	0.34	0.108	0.33	0.064	0.104	0.217	0.222
MC001DD	29	po	main	edge	13.49	437449.88	0.49	2.31	2.1	484498	331.73	2679.73	7595.96	12.58	0.45	2.56	79.4	1.11	2.13	2.58	0.56	1.1	0.44	4.73	12.63	0.42	0.132	0.38	0.07	0.129	2.26	7.49
MC001DD	37	py	early	edge	0.63	449249.5	0.082	0.38	0.73	361838.31	38.98	0.6	0.291	0.36	0.073	59.96	64.2	0.17	0.059	0.42	0.0184	0.137	0.159	0.74	1.36	0.056	0.0187	0.05	0.0177	0.0211	2.36	1.123
MC001DD	37	py	early	edge	0.66	474171.41	0.078	0.38	2.47	361838.31	62.35	1.4	0.81	0.94	0.078	61	69.31	0.153	0.057	0.55	0.0178	0.142	1.019	0.67	2.75	0.068	0.02	0.057	0.0174	0.067	10.34	3.24
MC001DD	37	py	early	edge	5.92	502192.63	0.173	0.4	32.21	361838.31	363.43	6.95	33.53	0.41	0.852	179.89	72.55	0.182	0.259	0.45	1.172	0.222	3.12	0.68	404.46	0.088	0.0193	0.413	0.0193	0.116	28.42	14.45
MC001DD	37	py	early	edge	0.63	472161	0.071	0.38	0.51	361838.31	328.11	3.1	0.166	0.41	0.068	194.47	108.41	0.16	0.057	0.44	0.0191	0.143	0.064	0.72	1.33	0.062	0.0166	0.049	0.017	0.0222	0.243	0.322
MC001DD	41	py	main	edge	0.54	461186.75	0.072	0.36	0.39	361838.31	87.09	1704.45	1.92	0.44	0.061	3085.71	35.16	0.16	0.05	0.4	0.017	0.133	0.055	0.55	1.38	0.056	0.02	0.051	0.017	0.0181	0.028	0.101
MC001DD	41	py	main	edge	0.53	444739.84	0.069	0.35	0.55	361838.31	196.05	1279.42	0.178	0.38	0.062	4154	55.87	0.145	0.052	0.45	0.0155	0.126	0.061	0.67	1.18	0.052	0.0186	0.05	0.0166	0.0183	0.031	0.0165
MC001DD	41	py	main	centre	0.6	454685.91	0.068	0.37	0.45	361838.31	206.94	445.88	5.01	0.42	0.065	466.08	52.4	0.168	0.058	0.45	0.0157	0.137	0.054	0.62	1.19	0.059	0.0184	0.049	0.0168	0.0195	0.032	0.0216
MC001DD	41	py	main	centre	0.57	455091.72	0.066	0.38	0.59	361838.31	83.75	500.19	0.176	0.39	0.064	143.25	96.65	0.162	0.058	0.48	0.0181	0.135	0.058	0.72	1.33	0.06	0.0183	0.057	0.0169	0.0219	0.031	0.024

MC001DD	41	py	main	centre	0.59	481559.72	0.073	0.38	0.44	361838.31	53.21	199.46	0.189	0.39	0.064	477.4	81.86	0.15	0.055	0.44	0.018	0.137	0.063	0.7	1.42	0.063	0.0193	0.05	0.017	0.0187	0.032	0.0201
MC001DD	41	py	main	centre	0.59	447829.97	0.072	0.47	0.57	361838.31	91.41	774.23	0.155	0.37	0.055	270.75	100.43	0.172	0.058	0.44	0.0179	0.14	0.053	0.75	1.38	0.06	0.0193	0.05	0.0172	0.0209	0.033	0.0172
MC001DD	41	py	main	centre	0.64	490856.81	0.076	0.41	0.45	361838.31	130.09	1629.1	0.18	0.41	0.074	601.37	158.05	0.188	0.061	0.49	0.0152	0.147	0.063	0.78	1.4	0.063	0.0197	0.049	0.0172	0.0224	0.032	0.03
MC001DD	41	py	main	centre	0.6	472954.06	0.076	0.38	0.43	361838.34	72.03	499.06	0.164	0.77	0.068	510.89	109.67	0.158	0.054	0.5	0.0164	0.153	0.058	0.58	1.23	0.066	0.0206	0.058	0.0171	0.0182	0.034	0.0192
MC001DD	41	py	main	edge	0.61	450718.31	0.072	0.38	0.44	361838.31	90.06	547.69	0.259	0.61	0.068	1200.52	57.33	0.153	0.056	0.42	0.0188	0.14	0.059	0.77	1.51	0.057	0.0185	0.056	0.0168	0.0207	0.033	0.4
MC001DD	41	py	main	centre	0.65	461358.22	0.083	0.4	0.51	361838.34	52.18	183.29	0.314	0.44	0.075	127.32	68.66	0.194	0.059	0.48	0.0184	0.151	0.072	33.6	1.29	0.058	0.022	0.059	0.0175	0.023	0.033	57
MC001DD	41	py	main	edge	0.63	477788.56	0.076	0.39	0.47	361838.31	138.29	496.81	0.147	0.35	0.066	1632.9	49.36	0.149	0.066	0.43	0.016	0.138	0.06	0.72	1.35	0.062	0.0221	0.058	0.0178	0.0223	0.038	0.733
MC001DD	41	py	main	edge	0.63	469931.69	0.073	0.39	0.51	361838.34	2842.58	42.3	0.347	0.42	0.065	147.81	26.33	0.178	0.068	0.51	0.0185	0.133	0.071	0.7	1.26	0.067	0.0188	0.058	0.0179	0.0219	0.031	0.0197
MC001DD	41	py	main	centre	0.62	496997.91	0.074	0.37	0.9	361838.31	6748.45	48.56	0.175	0.36	0.065	209.69	57.95	0.158	0.054	0.46	0.0174	0.14	0.062	0.67	1.32	0.069	0.0206	0.051	0.0171	0.0215	0.036	0.0196
MC001DD	41	py	main	centre	0.6	453379.56	0.073	0.37	0.49	361838.31	8314.74	62.41	0.173	0.41	0.063	262.5	43.71	0.171	0.048	0.45	0.0182	0.132	0.061	0.65	1.19	0.056	0.0164	0.05	0.0173	0.0213	0.035	0.0171
MC001DD	41	py	main	edge	0.64	493934.34	0.083	0.38	0.53	361838.31	6923.3	80.82	0.144	0.39	0.071	229.25	29.42	0.154	0.064	0.51	0.0185	0.148	0.055	0.74	1.39	0.057	0.0194	0.059	0.0176	0.023	0.035	0.0203
MC001DD	41	py	main	edge	0.61	443674.66	0.072	0.36	0.55	361838.31	4893.13	25.36	0.189	0.41	0.077	258.27	27.94	0.168	0.054	0.45	0.0161	0.145	0.07	0.69	1.35	0.056	0.0201	0.05	0.0171	0.0202	0.031	0.0193
MC001DD	41	py	main	centre	0.65	500799.41	0.116	0.39	0.52	361838.34	13157.62	34.47	0.28	0.43	0.07	422.54	32.63	0.18	0.057	0.47	0.02	0.14	0.069	0.86	1.61	0.058	0.018	0.063	0.018	0.02	0.038	0.169
MC001DD	41	py	main	centre	0.57	439831.16	0.065	0.35	0.48	361838.31	14356.08	24.62	0.159	0.35	0.058	448.61	29.23	0.161	0.055	0.44	0.0164	0.126	0.051	0.63	1.26	0.056	0.0192	0.046	0.0153	0.0181	0.031	0.0191
MC001DD	41	py	main	edge	0.84	463102.53	0.073	0.35	0.48	361838.31	13455.58	21.36	0.148	0.33	0.058	528.41	24.75	0.134	0.049	0.44	0.0158	0.138	0.058	0.59	1.25	0.055	0.0173	0.051	0.016	0.0182	0.03	0.0213
MC001DD	41	py	main	edge	0.66	497957.19	0.093	0.39	0.53	361838.31	7383.34	111.62	0.172	0.36	0.065	220.76	30.27	0.182	0.061	0.44	0.0177	0.156	0.055	0.67	1.51	0.054	0.0192	0.063	0.017	0.022	0.037	0.073
MC001DD	41	py	main	edge	0.63	478145.25	0.076	0.38	1.1	361838.31	267.25	1788.58	0.259	0.8	0.064	4261.13	81.32	0.161	0.057	0.47	0.0181	0.133	0.064	0.63	1.46	0.063	0.0193	0.062	0.0212	0.0197	0.036	0.0184
MC001DD	41	py	main	centre	0.65	469863.72	0.079	0.38	0.54	361838.34	147.38	911.88	0.243	0.4	0.077	680.86	111.83	0.159	0.055	0.47	0.0198	0.147	0.065	0.7	1.32	0.062	0.0183	0.052	0.02	0.023	0.039	0.0198
MC001DD	41	py	main	centre	0.64	453954.5	0.076	0.39	0.53	361838.31	195.66	878.87	0.192	0.43	0.07	2550.09	67.1	0.168	0.058	0.46	0.0192	0.143	0.064	0.68	1.32	0.053	0.0175	0.048	0.0197	0.023	0.035	0.0189
MC001DD	41	py	main	centre	0.66	511733.16	0.078	0.38	0.54	361838.31	237.38	1426.13	0.349	0.41	0.072	3406.46	77.12	0.168	0.064	0.52	0.0195	0.147	0.067	0.73	1.4	0.069	0.0223	0.059	0.0188	0.0203	0.035	0.022
MC001DD	41	py	main	centre	34.9	449697.66	8.86	6.32	6.61	361838.31	153.74	593.74	0.201	0.96	14.91	629.53	43.86	0.201	0.063	0.59	0.037	1.23	0.157	5.57	7753.03	0.125	0.02	0.067	0.0216	0.04	0.111	25.89
MC001DD	41	py	main	centre	0.74	474479.66	0.09	0.43	0.58	361838.31	119.75	424.39	0.207	0.46	0.083	347.23	84.4	0.196	0.069	0.54	0.0212	0.175	0.069	0.77	9.2	0.072	0.0211	0.056	0.021	0.025	0.04	0.111
MC001DD	41	py	main	edge	0.66	462646.97	0.087	0.39	0.54	361838.31	197.6	1139.84	1.37	0.54	0.071	1919.91	74.51	0.151	0.064	0.57	0.0189	0.145	0.063	0.79	1.41	0.06	0.0189	0.059	0.0185	0.022	0.034	0.062
MC003B	2	py	early	edge	9.12	468773.5	0.077	0.38	3.85	361838.31	42.22	1383.56	643.33	0.46	0.075	2.2	244.83	0.163	0.055	0.48	0.0186	0.301	0.113	0.74	14.73	0.058	0.0214	0.057	0.022	0.036	2.62	3.79
MC003B	2	py	early	edge	7.82	459276.81	0.065	0.35	0.98	361838.31	6162.35	624.84	138.09	0.42	0.065	1.06	225.9	0.138	0.058	0.42	0.0153	0.23	0.405	0.54	1.32	0.062	0.0168	0.087	0.019	0.0216	0.94	10.79
MC003B	2	py	early	edge	2.01	450898.34	0.962	0.38	50.57	361838.31	36.28	999.61	14.18	0.45	0.066	174.03	212.13	0.159	0.06	0.49	0.019	0.14	0.49	0.72	2.63	0.527	0.02	0.054	0.02	0.02	1.79	6.92
MC003B	2	py	early	centre	0.62	457198.75	0.074	0.36	0.9	361838.31	99.42	1122.22	0.367	0.4	0.07	193.42	186.42	0.165	0.053	0.4	0.0174	0.142	0.053	0.76	1.46	0.059	0.0208	0.056	0.0184	0.024	0.03	0.31
MC003B	2	py	early	edge	0.97	465483.31	0.092	0.36	0.52	361838.31	77.2	385.93	122.69	0.47	0.061	128.82	129.76	0.164	0.142	0.5	0.0163	0.135	1.84	2.58	1.98	0.06	0.0176	0.092	0.0184	0.091	111.71	21.34
MC003B	2	py	early	edge	0.65	486329.56	0.079	0.39	0.52	361838.34	90.08	979.76	0.37	0.4	0.066	63.94	246.3	0.163	0.051	0.46	0.0166	0.134	0.067	0.73	4.72	0.067	0.0199	0.056	0.0189	0.021	0.193	3.84
MC003B	2	py	early	edge	0.63	442862.25	0.074	0.37	1.02	361838.31	64.61	755.43	0.68	0.46	0.062	146.88	244.99	0.147	0.05	0.5	0.018	0.13	0.061	0.66	1.35	0.055	0.0185	0.051	0.0185	0.0207	0.03	0.12

MC003B	2	py	early	edge	0.69	498047.97	0.107	0.4	0.66	361838.34	69.23	813.84	950.03	1.49	0.072	36.84	165.98	0.165	1.32	0.49	0.072	0.396	0.505	1.74	4.13	0.066	0.0199	0.572	0.0197	0.023	2.12	15.92
MC003B	2	py	early	centre	0.65	471865.75	0.076	0.37	0.51	361838.31	52.17	1556.33	345.11	0.38	0.065	24.35	225.81	0.171	0.255	0.48	0.0176	0.136	0.101	0.73	1.17	0.061	0.0194	0.066	0.0182	0.0233	0.052	6.48
MC003B	2	py	early	centre	548.89	491999.69	0.105	0.42	1.23	361838.31	284.05	249.17	0.21	0.39	0.078	64.81	197.11	0.195	0.058	0.51	0.0195	0.149	0.068	0.74	10.78	0.066	0.023	0.059	0.0189	0.023	0.131	0.272
MC003B	2	py	early	edge	145.66	499399.94	0.093	0.4	0.94	361838.34	2885.97	73.69	0.183	0.44	0.073	181.74	109.32	0.176	0.057	0.5	0.0188	0.154	0.06	0.7	4.49	0.062	0.0194	0.063	0.0185	0.024	0.047	0.16
MC003B	2	py	early	unknown	0.95	507004.75	0.083	0.37	0.54	361838.31	17826.92	29.44	0.169	0.39	0.065	224.05	62.61	0.169	0.056	0.48	0.0155	0.141	0.057	0.81	1.47	0.06	0.02	0.047	0.0181	0.0216	0.118	0.419
MC003B	2	py	early	unknown	1210.78	498558.31	0.237	0.42	1.23	361838.31	33610.73	16.79	0.322	0.43	0.076	2291.93	33.63	0.177	0.062	0.5	0.0191	0.199	0.207	0.82	12.44	0.336	0.0183	0.064	0.0202	0.024	0.556	2.71
MC003B	2	py	early	unknown	0.65	498585.47	0.076	0.38	0.53	361838.31	18853.04	8.77	0.37	0.4	0.062	294.29	29.09	0.153	0.054	0.5	0.0196	0.148	0.062	0.71	1.36	0.067	0.0188	0.056	0.0169	0.02	0.035	0.052
MC003B	2	py	early	unknown	0.66	452486.56	0.08	0.37	0.53	361838.31	9732.84	10.97	0.403	0.82	0.066	57.21	23.52	0.167	0.06	0.48	0.0166	0.143	0.06	0.71	1.17	0.068	0.0178	0.051	0.0173	0.022	0.036	0.02
MC003B	2	py	early	unknown	0.67	478727.78	0.077	0.38	3.43	361838.31	10098.76	991.94	0.287	0.49	0.064	4.18	253.76	0.174	0.06	0.45	0.0188	1.56	0.985	0.67	1.48	0.071	0.02	0.057	0.023	0.0204	1.98	0.39
MC003B	2	py	early	unknown	0.67	460908.03	0.068	0.38	12.04	361838.34	10349.73	2714.03	172.32	0.46	0.068	1.5	235.64	0.159	0.056	0.5	0.0172	0.143	3.21	0.73	2.16	0.061	0.0178	0.054	0.0218	0.0199	7.34	1.72
MC003B	2	py	early	unknown	2.57	452025.13	0.088	0.39	79.23	361838.34	213.01	2956.79	99.25	1.14	0.069	12.22	216.54	0.19	0.389	0.51	0.019	0.344	15.23	2.96	5.35	0.077	0.024	0.07	0.021	0.054	45.77	26.38
MC003B	2	py	early	unknown	0.76	489930.91	0.161	0.39	176.37	361838.31	1257.68	3256.7	97.43	0.44	0.078	8.23	224.18	0.177	0.33	0.55	0.0174	0.254	8.85	2	7.71	0.061	0.018	0.057	0.021	0.024	45.49	16.83
MC003B	2	py	early	unknown	2.33	471497.78	0.11	0.38	0.58	361838.34	0.103	0.35	0.79	0.43	0.077	635.47	53.36	0.171	0.061	0.51	0.0182	0.153	0.699	0.79	3.46	0.074	0.0195	0.064	0.0197	0.021	1.4	0.018
MC003B	2	py	early	unknown	0.63	471116.97	0.069	0.35	18.5	361838.31	10.29	1730.53	1.73	0.53	0.064	1.67	101.86	0.181	0.056	0.4	0.0181	0.146	2.18	0.58	1.54	0.063	0.0197	0.049	0.0177	0.0231	3.52	1.38
MC003B	2	py	early	unknown	13.83	469596.59	0.404	0.38	59.78	361838.34	146.95	1687.76	1681.02	0.64	0.091	62.83	121.1	0.253	0.452	0.42	0.0186	0.139	22.06	0.73	17.75	0.058	0.022	0.107	0.0194	0.464	48.63	8.18
MC003B	2	py	early	unknown	1.28	460579.06	0.08	0.39	0.56	361838.31	0.258	0.35	0.88	0.42	0.076	918.16	83.3	0.194	0.056	0.48	0.0174	0.141	0.667	0.76	1.26	0.071	0.024	0.051	0.0193	0.06	0.85	0.022
MC003B	2	py	early	unknown	13.56	503658.81	0.122	0.46	314.5	361838.34	179.45	940.33	9.35	0.59	0.087	11.56	100.7	0.185	0.071	0.55	0.02	0.296	4.31	0.79	12.73	0.071	0.024	0.079	0.022	0.025	19.43	3.28
MC003B	2	py	early	unknown	0.69	474391.25	0.082	0.4	1.38	361838.31	8.81	1333.99	0.79	0.42	0.065	0.46	82.74	0.168	0.056	0.48	0.0188	0.153	1.191	0.78	1.52	0.065	0.0192	0.055	0.0185	0.021	2.75	1.81
MC003B	2	py	early	unknown	0.66	463947.97	0.073	0.37	0.54	361838.31	9.75	1596.62	32.64	0.58	0.064	0.52	121.18	0.162	0.064	0.44	0.0159	2.05	0.9	0.65	1.41	0.061	0.017	0.057	0.0179	0.023	3.5	1.43
MC003B	2	py	early	unknown	1.9	459483.81	0.073	0.37	0.97	361838.34	25.77	1559.82	69.67	0.41	0.064	0.76	96.68	0.163	0.171	0.42	0.0174	0.131	3.91	0.67	2.48	0.058	0.02	0.06	0.017	0.02	14.36	4.94
MC003B	2	py	early	unknown	0.67	475367	0.075	0.38	0.54	361838.31	53297.82	33.41	0.178	0.42	0.062	3.66	152.03	0.164	0.058	0.44	0.0172	0.143	0.063	2.51	1.34	0.059	0.0179	0.046	0.0173	0.023	0.033	0.021
MC003B	2	py	early	unknown	0.68	461605.09	0.081	0.39	0.92	361838.31	2.03	1165.19	0.205	0.42	0.071	0.49	105.51	0.183	0.057	0.47	0.0184	0.137	0.112	0.74	1.48	0.066	0.0194	0.063	0.0174	0.023	0.334	0.028
MC003B	2	py	early	unknown	0.63	477565.22	0.072	0.36	1.15	361838.31	24541.74	198.16	1.19	0.42	0.061	35.07	47.33	0.177	0.057	0.45	0.0162	0.136	0.529	0.64	1.44	0.056	0.0182	0.057	0.021	0.0182	0.805	0.246
MC003B	2	py	early	unknown	0.67	511104.59	0.074	0.38	0.52	361838.34	116061.26	9.7	0.49	0.4	0.068	29.22	172.43	0.192	0.055	0.43	0.0194	0.13	0.084	3.45	1.51	0.066	0.0195	0.056	0.022	0.023	0.031	2.68
MC003B	2	py	early	unknown	1.04	547264.19	0.087	0.39	1.42	361838.34	110863.34	17.13	1.89	0.46	0.068	9.46	157.24	0.3	0.058	0.51	0.0186	0.266	3.17	6.72	1.51	0.065	0.0187	0.066	0.021	0.021	5.19	2.89
MC003B	2	py	early	unknown	0.65	489912.53	0.077	0.36	0.98	361838.31	76371.47	8.37	0.157	0.4	0.073	6.13	103.45	0.156	0.053	0.43	0.0166	0.14	0.321	0.87	1.36	0.06	0.0185	0.056	0.0193	0.0167	0.367	0.218
MC003B	2	py	early	unknown	0.69	521556.31	0.082	0.38	0.55	361838.34	92251.14	9.71	0.294	0.44	0.069	8.74	200.24	0.187	0.065	0.43	0.0182	0.143	0.055	5.83	1.69	0.064	0.02	0.056	0.0199	0.021	0.033	0.0205
MC003B	2	py	early	unknown	0.72	557736.69	0.084	0.42	0.58	361838.34	101629.91	8.78	0.6	0.92	0.074	5.75	180.72	0.154	0.062	0.49	0.0177	0.147	0.07	2.43	1.61	0.061	0.018	0.064	0.0199	0.023	0.039	0.0199
MC003B	2	py	early	unknown	0.71	524923.94	0.083	0.39	0.57	361838.34	88728.19	5.72	0.232	0.41	0.074	16	181.21	0.187	0.06	0.57	0.0186	0.142	0.059	4.14	1.52	0.065	0.022	0.057	0.021	0.023	0.035	0.0201
MC003B	2	py	early	unknown	3.16	495841.22	0.215	0.42	11.85	361838.34	14877.1	471.32	2.88	0.88	0.077	122.93	74.37	0.22	0.058	0.6	0.0204	0.162	8.69	0.91	2.31	0.07	0.021	0.069	0.0205	0.051	34.9	2.63

APPENDIX D

Hole MC001DD, sample #1

Hand Sample

Meterage: 33.5m
Host lithology: Chl schist
Description: 1cm vein of cpy (1) with minor qtz (2)

Petrology

Mineral	Primary/Alt/Infill	Crystal size (µm)	Modal%	Characteristics
quartz	primary	50-3000	40	strong foliated
biotite	primary	50-100	20	strong foliation, most abundant adjacent to quartz
chlorite	alteration	50-100	20	strong foliation, most abundant distant to quartz
pyrite	infill	700	1	isolated cyrstals
chalcopyrite	infill	500	20	Occurs as intruded vein along foliation with minor quartz at the edges

Host rock

Host rock is a strongly foliated quartz-biotite-chlorite schist.

Sulphides

Intruded vein along foliation with quartz grains (5mm) at the edges

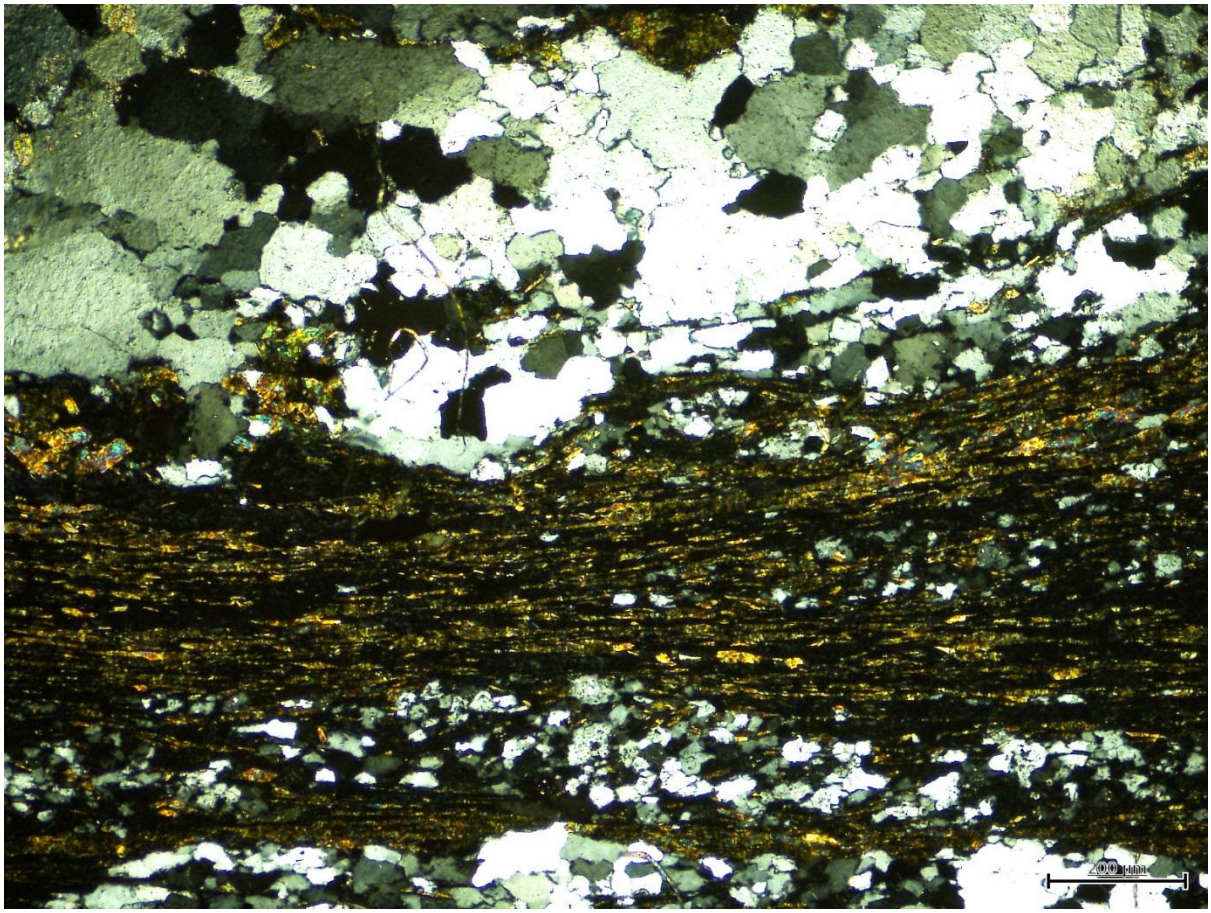

Figure 49: quartz-biotite-chlorite schist

Hole MC001DD, sample #3

Hand Sample:

Meterage: 122.2m
Host lithology: Chl schist? Chl altered volcanic? (lith 4)
Description: 15cm QCV with blocky actinolite or chlorite alteration (1) at the edges along with some speckled pyrite veins (2).

Figure 50: 15cm QCV with blocky actinolite or chlorite alteration (1) at the edges along with some speckled pyrite veins (2).

Petrology:

Mineral	Primary/Alt/Infill	Crystal size (µm)	Modal %	Characteristics
Actinolite?	alteration	2000	45	extremely large grains, radial cleavage, proximal to vein
Actinolite?	alteration	<100	15	fine grains, distant to vein
calcite	infill	500-3000	20	infill texture around actinolite
pyrite	infill	500-3000	20	individual crystals form pyrite aggregate

Host rock

Actinolite/chlorite crystals show 2 distinct textures. On the vein side of the pyrite (left side as seen in hand sample image) crystals are coarse (2mm) with a fan-like shape and with 1 radial cleavage (and hints of 2 cleavages (60/120) at the ends of crystals). On the host rock side of the pyrite (right in the hand sample image) the crystals are fine (<100µm) with cleavage development parallel to the long axis of the crystal, and the same hint of 2 cleavages. Both mineral sets display undulose extinction.

Pods of coarse grained calcite occur through the thin section; however they are concentrated on the vein side of the pyrite. The calcite displays in infill texture in relation to coarse actinolite growth.

Sulphides

Pyrite occurs as a mass of med-coarse euhedral/subhedral crystals adjacent to all 3 mineral constituents of the thin section (i.e. in contact with calcite, fine grained actinolite and coarse grained actinolite). Minor fine grained, euhedral pyrite is also disseminated through the coarse grained actinolite groundmass, suggesting the actinolite + pyrite are infill from the same fluid.

Veining hypothesis

In figure 1 the calcite vein showcases both a strong contact with actinolite alteration (left of image) and a less defined contact (middle of image), the rounded pods of calcite within the actinolite suggest that the calcite/quartz vein was not fully crystallised when actinolite growth occurred, and calcite has consequently been torn off from the vein and lodged in the alteration mineral. This is suggestive of a single fluid source of calcite, actinolite and pyrite.

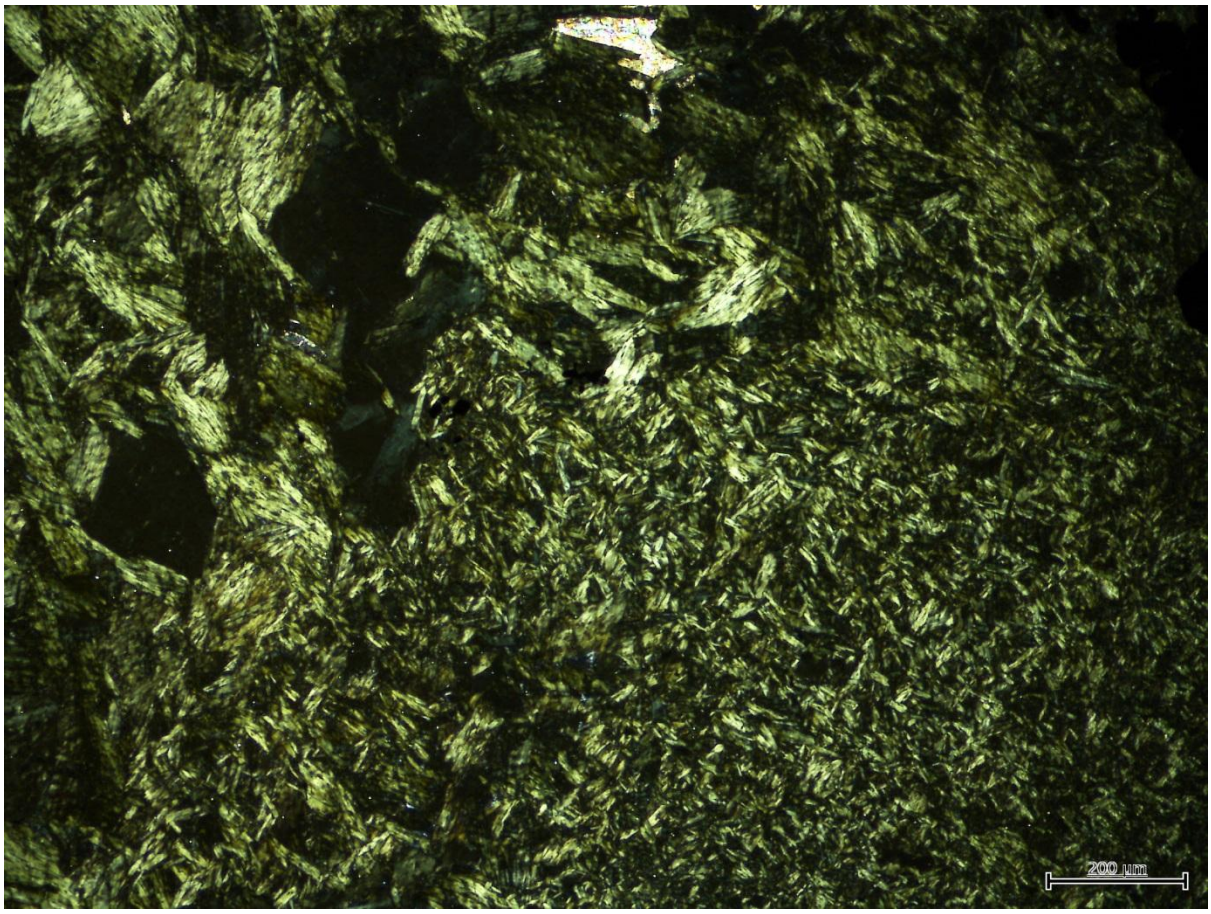

Figure 51: fine grained actinolite/chlorite alteration in XPL

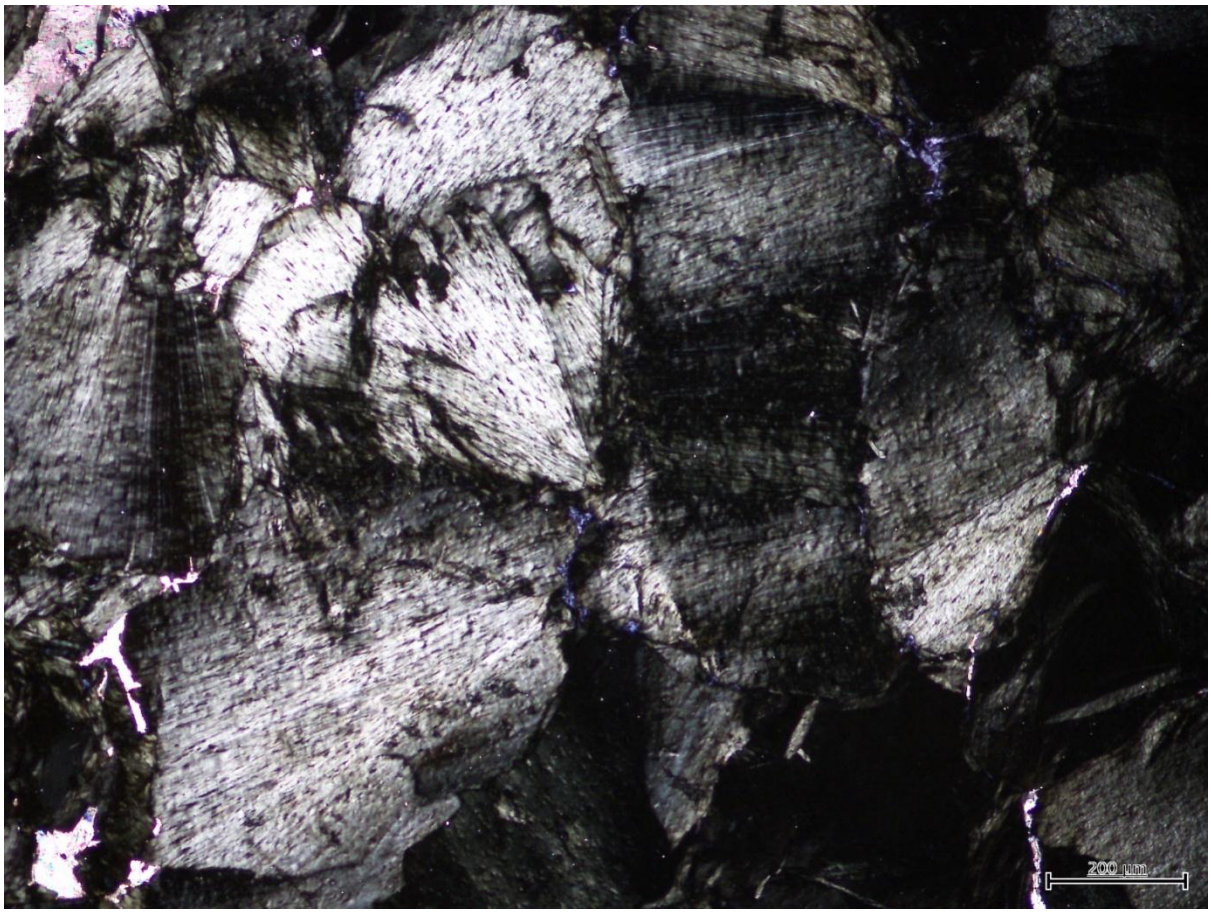

Figure 52: coarse grained actinolite/chlorite in XPL

MC001DD.10

Hand Sample

Meterage: 262m
Host lithology: Fine grained, light grey, felsic volcanic (Lith 2)
Description: Lead coloured mineral alteration in fractures (1) sometimes with calcite (2). Minerals in fractures (py=cpy) (3).

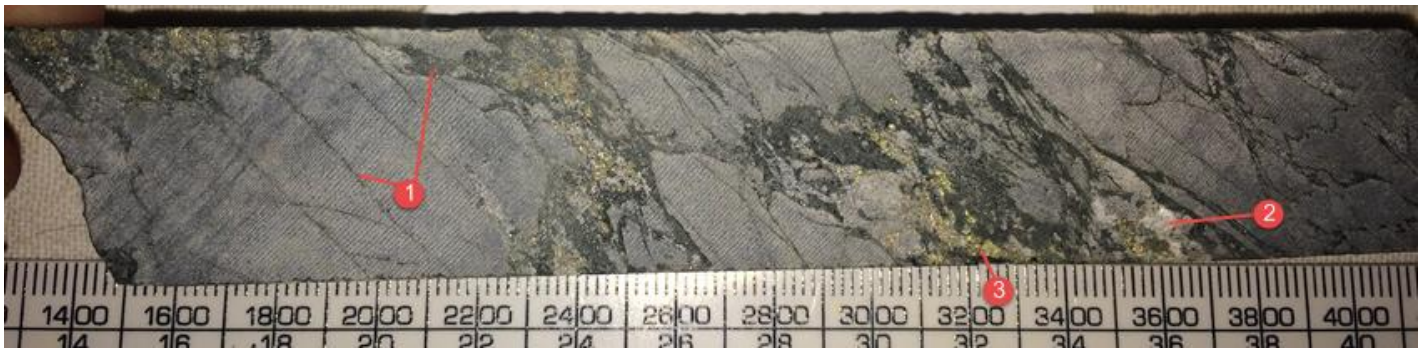

Petrology

Mineral	**Primary/ Alt/Infill**	**Crystal size (μm)**	**Modal %**	**Characteristics**
Biotite/ actionolite?	infill	50-200	20	green-brown pleochroism, 2nd order birefringence, parallel extinction, 1 cleavage, mottled appearance
quartz + plag + feldspar	primary	<50	50	occurs as fine groundmass taken to be ignimbrite
quartz	infill	500	10	occurs with actinolite in veins
magnetite	infill	200-400	1	euhedral but not deformed, moves around quartz, with infill and in host rock
pyrite	infill	500	5	occurs with infill
chalcopyrite	infill	100-300	5	occurs with infill
muscovite	infill	50-200	5	occurs with biotite
chlorite	alteration	100	1	rare alteration

Host rock

Host rock consist of an amalgamation of very fine minerals, quartz is the most distinguishable, compromising ~70% of the groundmass, rare feldspar, biotite and isotropic minerals (mag?) make up the remaining 30%.

Veining

Quartz + biotite veins cross cut the host rock with minor sulphides occurring at grain boundaries within these veins. Euhedral magnetite is also present within veins and occasionally within the host rock.

Sulphides

Occur within veins at grain boundaries, strong infill texture.

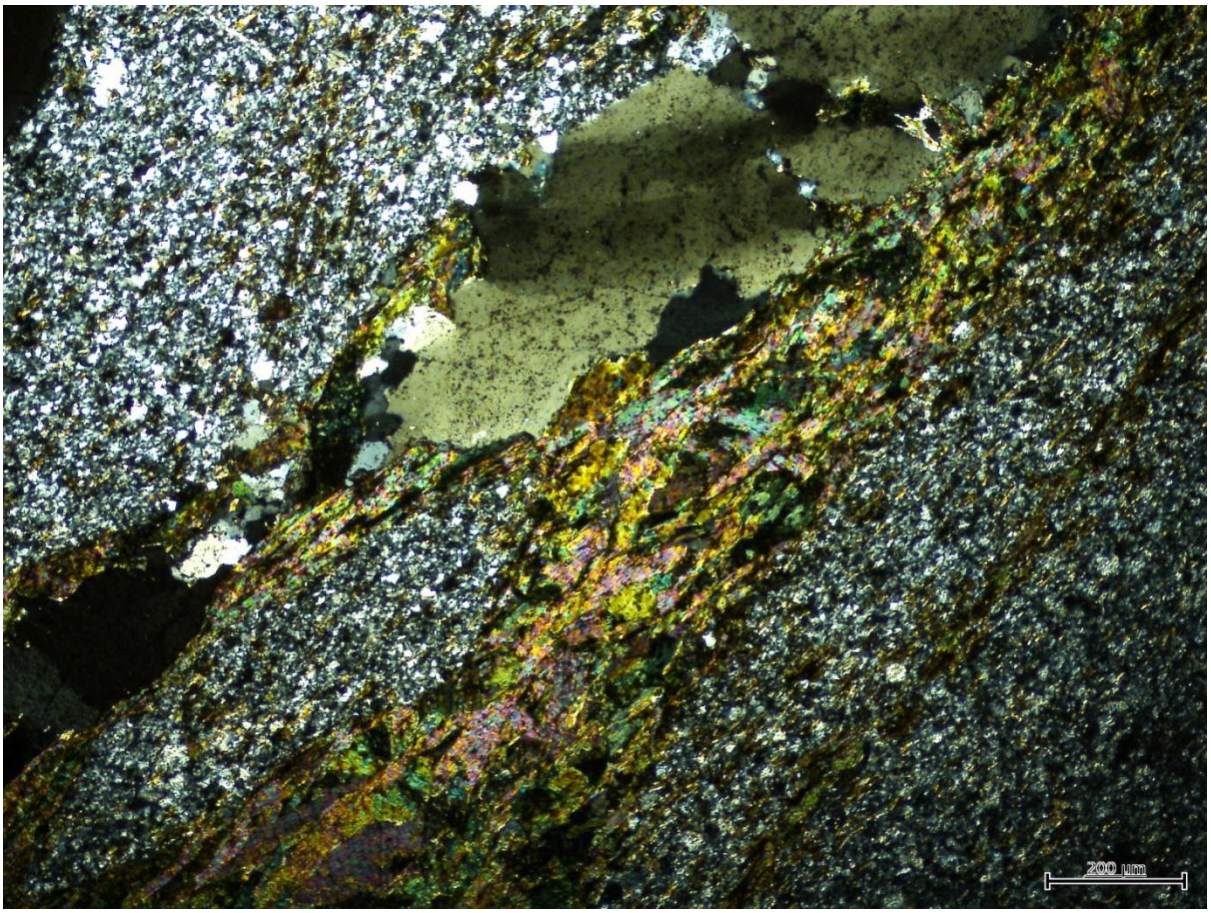

Figure 53: biotite and quartz vein cross cutting fine grained host rock.

Alteration

Chlorite alteration predominantly occurs adjacent to sulphides.

Hole MC001DD, sample #12

Hand Sample

Meterage: 273.4m
Host lithology: Fine grained, light grey, banded felsic volcanic (Lith 2)
Description: Very strong chl (and maybe diopside) alteration with strong foliation (1). Incorporated into foliation are QCVs (2) and sulphides (3)

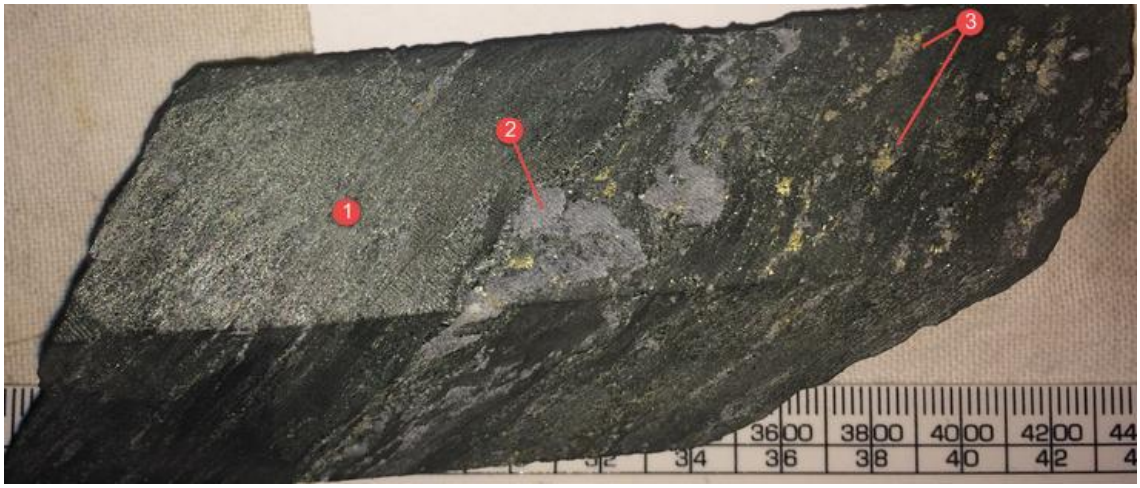

Petrology

Mineral	Primary/Alt/Infill	Crystal size (µm)	Modal%	Characteristics
quartz	infill	50-5000	40	range in sizes suggest silicification?
biotite	-	50-300	25	
chlorite	alteration	50-300	25	
chalcopyrite	infill	500-2000	5	in quartz
pyrite	infill	1000	5	in host rock

Host rock

Host rock consists of fine (50-300µm) strongly foliated green biotite crystals that are altered to chlorite more distant to quartz. It is a biotite-chlorite schist.

Veining and Sulphides

Quartz infill (veining) occurs as aggregates of quartz ranging from 50µm to 5000µm (5mm). Chalcopyrite (500-2000µm) is disseminated throughout quartz whereas minor pyrite crystals (1000µm) have grown in the host rock.

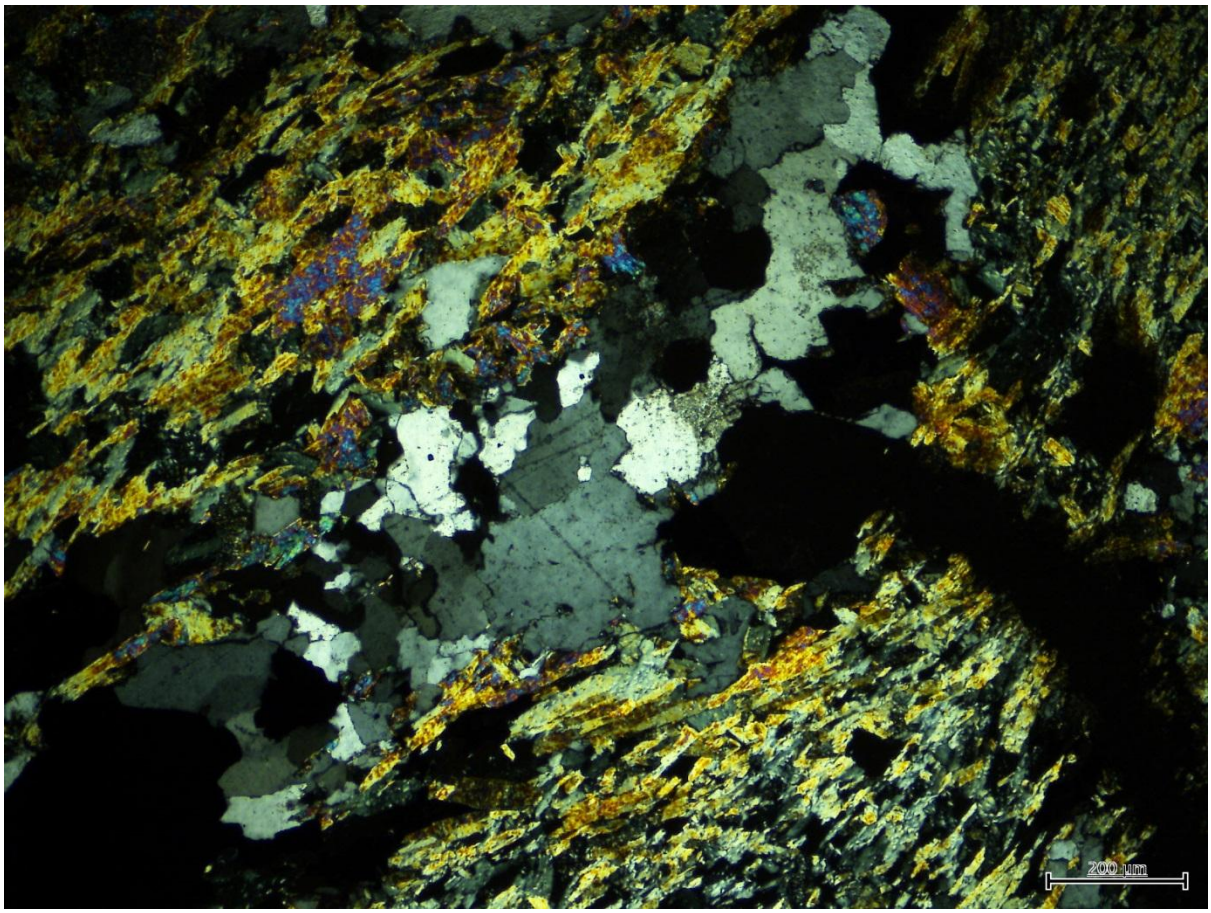

Figure 54: quartz veining with associated sulphides and surrounding strongly foliated biotite

Hole MC001DD, sample 28 - 365.5m

Hand Specimen

Figure 55: Mineralisation (py=cpy) at edge of calcite, in boundin neck? (1). Order: calcite(2)>cpy(3)>py(4)>chl (5)

Petrology

Mineral	Primary/Alt/Infill	Crystal size (µm)	Modal%	Characteristics
quartz	primary	100-500	25	colourless PPL, undulose extinction, 1st order birefringence
biotite	primary	100	1	strong foliation, brown-yellow in PPL, 2nd order birefringence, 1 cleavage
chlorite	primary	50	25	green in PPL and in XPL, elongated pencil shape
siderite	primary	250	1	Subhedral dirty crystals, high relief, 2nd order birefringence with faint pink, yellow and green colours
calcite	infill	500-1000	40	colourless PPL, occasional lamellar twinning, high birefringence
quartz	infill	200	1	colourless PPL, undulose extinction, 1st order birefringence
chalcopyrite	infill	500-1000	5	golden-yellow in RFL, infill texture, subhedral
pyrite	infill	500	5	silver/yellow in RFL, euhedral shape or subhedral where fractured
chlorite	alteration	<25	<1	acicular, green in PPL,
quartz	infill	25	<1	clear PPL, undulose extinction, 1st order birefringence

Host rock:

The thin section illustrates the relationship between the host rock, quartz veining and sulphides. The host rock is well represented in one half of the thin section as strongly foliated quartz-chlorite schist with minor biotite. The schist consists of quartz crystals of less than 100μm in diameter forming pod like aggregates in a sea of very fine chlorite (50μm). Biotite is present at only the furthest edges of the thin section (distant to the quartz vein). Late stage subhedral squares of siderite (?as suggested by RT) form as depicted in F9100012 and F9100013.

Figure 56: chlorite-quartz schist with late siderite in PPL.

Veining:

The other half of the thin section represents calcite (+/- quartz) veining greater than 2cm in width. It consists of course grained calcite (500μm-1mm) in size with ~5% fine grained quartz (<200μm in diameter) and minor chlorite alteration at grain boundaries. Alteration is subtle olive green in PPL and anisotropic in XPL, possibly due to glassy needle like crystal structure.

A late stage quartz micro-vein (<50*μm in width) follows foliation in the host rock, consisting of undeformed quartz crystals <25µm in diameter.*

Sulphides:

There is significant sulphide (chalcopyrite and pyrite) formation along the boundary between the calcite vein and the host rock, as well as contained within the calcite vein. At the host rock/vein

boundary, chalcopyrite forms consistently on the vein side and pyrite consistently on the host rock side. Chalcopyrite also forms within the vein, and has a classic infill texture.

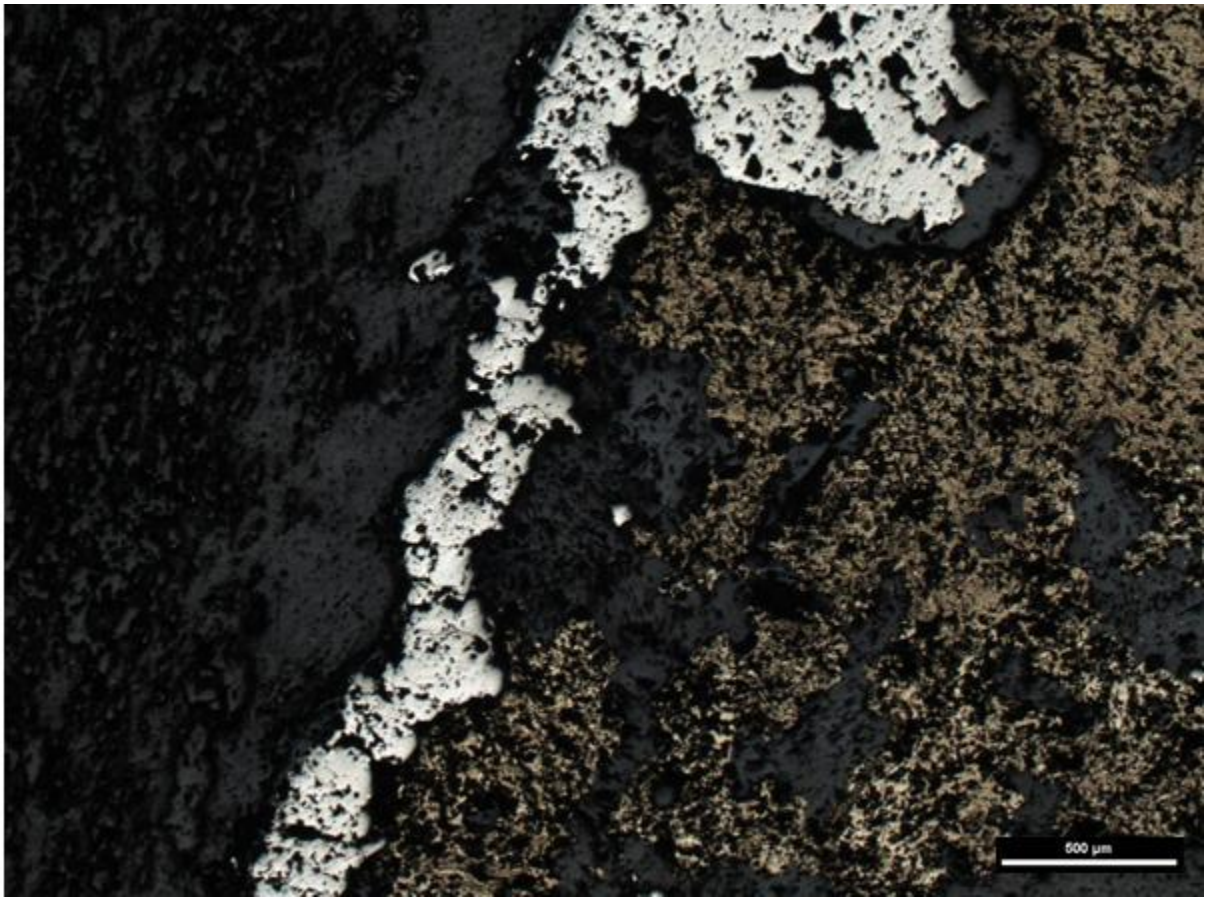

Comments:

Forming at the boundary between pyrite and the host rock (strongly chloritised) is an acicular brown/green mineral (in PPL) with low birefringence that is believed to be Fe-rich chlorite (Chamosite). It grows off pyrite into the chloritised host rock.

Paragenesis:

Host rock:

Quartz
Biotite
Chlorite
Siderite

Vein:
Calcite +/- quartz
Chalcopyrite
Pyrite

Hole MC001DD. Sample #31

Hand Sample

Meterage: 401.9m
Host lithology: Grey-purple fine felsic volcanic with abundant calcite stockwork fractures (lith 10)
Description: Dolomite core (1), with calcite rim (2), with chlorite/diopside outer rim (3), with biotite over growth (4) with sil+alb+hem alteration (5) surrounding this

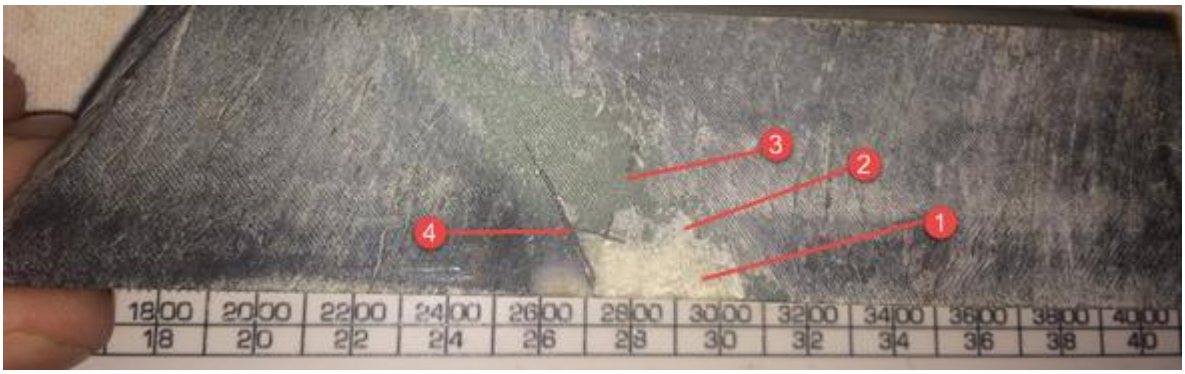

Petrology

Mineral	Primary/Alt/Infill	Crystal size (µm)	Modal%	Characteristics
quartz	primary	<50	70	fine groundmass
calcite	primary	2500	10	extremely overprinted
quartz	infill	100-200	5	abundant veins hosts sulphides
chlorite	alteration	100	7	abundant as veins
biotite	infill	100	3	
galena	infill	100-1000	5	comes with biotite/chlorite

Host rock:

Host rock consists predominantly of a fine grained, quartz rich matrix that is cross cut by moderate quartz and biotite/chlorite veins. Also present in the sample are calcite pods extremely overprinted by quartz, chlorite and an opaque mineral.

Veining

Veining consists of quartz +/- biotite veins and chlorite +/- biotite veins

Figure 57: Over printed calcite in a fine grained matrix of quartz with foliated chlorite

Paragenesis

Biotite
calcite
quartz
Biotite, galena, quartz
chlorite

Hole MC001DD, sample 38

Hand Specimen

Meterage: 148.6m
Host lithology: granite? Felsic igneous (lith 7)
Description: Sample has the appearance of a sheared igneous rock. It consists of quartz and k-feldspar pods with biotite between the cracks. Silica alteration has given a sheen to the sample and increased its hardness. Sulphides present shown an association with quartz.

Petrology

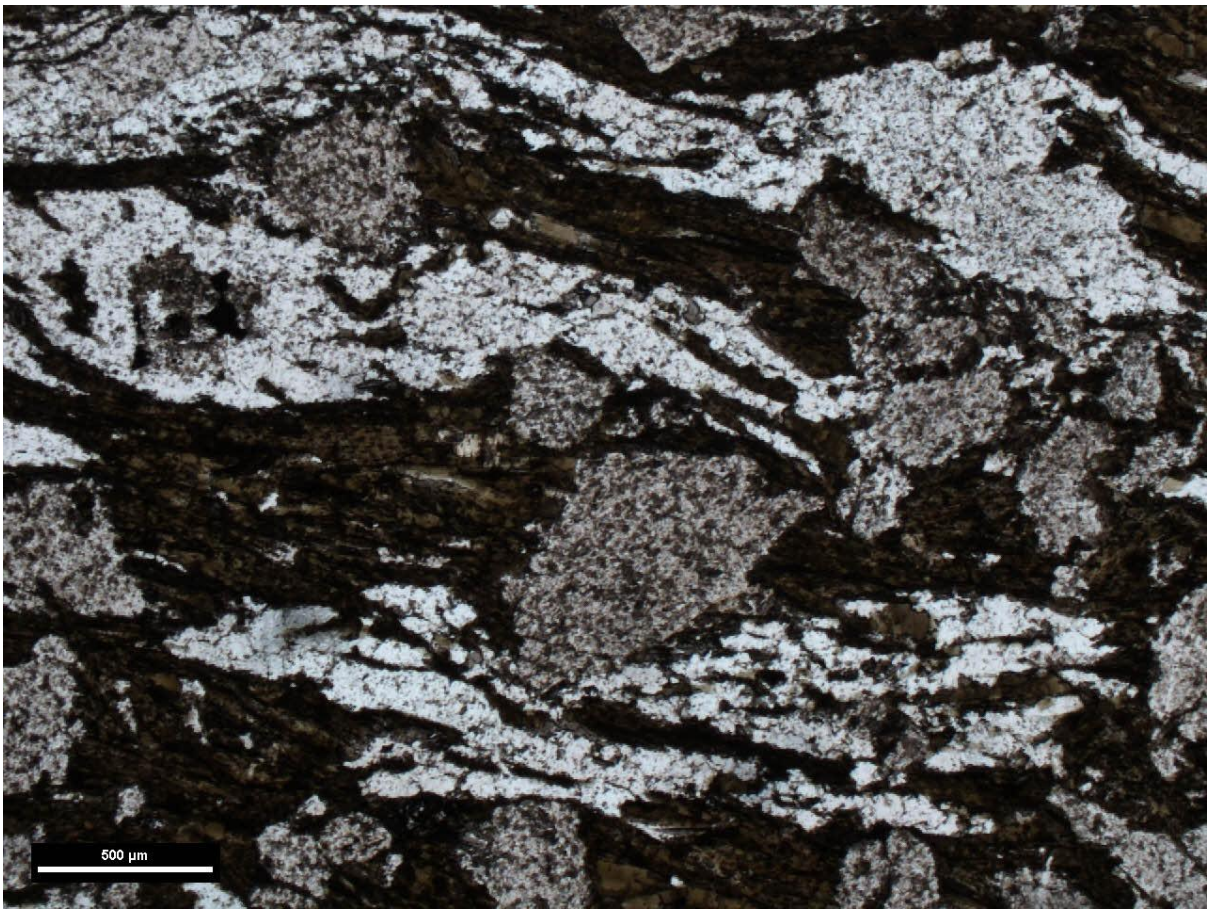

Minerals	Primary/Alt/ Infill	Crystal size (µm)	Modal %	Characteristics
k-feldspar	primary	500	15%	Clear with faint pink tinge in PPL, subhedral grain shape deformed, 1st order birefringence (grey), dirty, med-low relief, tartan and simple twinning in XPL
quartz	primary	500-700	20	colourless PPL, undulose extinction, 1st order birefringence, strongly deformed
quartz	infill	100	15	colourless PPL, undulose extinction, 1st order birefringence
biotite	Primary/infill	100	40	strong foliation, brown-yellow in PPL
chlorite	alteration	300-400	5%	green in PPL and in XPL, elongated pencil shape
Pyrite	infill in vein	1000	5%	silver/yellow in RFL, euhedral shape or subhedral where practured
Chalcopyrite	infill in vein	500	1%	golden-yellow, infill texture, subhedral

Host rock

Host rock is a strongly foliated biotite-quartz-potassium feldspar schist. Primary quartz, k-feldspar and biotite share strong grain boundaries. Secondary, fine grained (100µm) quartz growth is present through the matrix suggesting silicification of the sample. It is the secondary infill quartz that largely make up the deformed, elongated quartz aggregates as shown in fig. 2. Associated with this silicification and hosted by a potential quartz vein are the sulphides (py>cpy).

Veining and sulphides

Quartz vein consisting of fine-medium quartz grains 100-700μm in diameter. Sulphides, both pyrite and chalcopyrite, occur within the vein in association with chlorite alteration at grain boundaries. Sulphides appear to have grown along the boundaries of courser (>500 μm) quartz grains. Pyrite growth occurred before deformation as suggested by fracturing and deformation of structure, and chalcopyrite has a strong infill texture.

Paragenesis

K-feldspar + quartz (primary)
biotite + quartz (infill) + sulphides
Chlorite

Hole MC003DD, sample #4

Hand Sample

Meterage: 45.3m
Host lithology: Lith 4 – fine grained felsic volcanic
Description: light pink alteration (alb? Sil? Hem/feld?) (1) with black mineral growth (bi?) (2) and sulphides (cpy (3) + po?) disseminated throughout sample. Po potentially has association with black mineral (4)

Petrology

Minerals	Primary/ Alt/Infill	Crystal size (µm)	Modal%	Characteristics
k-feldspar	primary	300	10	colourless in PPL, tartan twinning, low relief
albite	primary	400	20	simple and carlsbad twinning, colourless PPL
quartz	primary	300	5	clear PPL, undulose extinction, 1st order birefringence
quartz	infill	<50	15	clear PPL, undulose extinction, 1st order birefringence
glassy matrix	infill	<10	25	brown in PPL, no pleochroism, very fine, glassy? Isotropic
muscovite or sillimanite	?	100	1	(1 cleavage plan, colourless PPL, high relief I think, low/mid 2nd order [vibrant blues] birefringence, parallel extinction
chalcopyrite	infill	300	2	occurs in quartz veins, glassy veins and in matrix
pyrite	infill	200	1	predominantly occurs in matrix
hematite	Infill/alteration?	200-400	10	associated with matrix
calcite	infill	200	1	occurs as vein
biotite	infill/alteration	50-200	10	occurs in veins and alteration

Host rock

The sample consist of abundant fine grained (~50µm) quartz that form proximal to microveins and occasionally as larger quartz aggregates (1cm) assumed to represent silcification. The sample has abundant albite crystals with lesser k-feldspar (as microcline). Muscovite (or perhaps sillimanite?) occurs as rare phenocrysts. The matrix consists of a fine grained glassy aggregate of minerals that are indistinguishable under optical microscopy, and fine grained quartz.

Veining and Sulphides

One example of micro-calcite veining is present within this sample, as well as several microquartz grains that crosscut the rock. Chalcopyrite is particularly abundant in and around the quartz veins. The fine grained glassy matrix is often seen as veining that crosscuts course crystals, under reflective light microscopy hematite is observed to be abundant within these veins and disseminated heavily throughout the matrix. Biotite alteration around these veins and crystals in the matrix are often present.

Infill and alteration

It is my hypothesis that a fluid influx has result in the fracturing and alteration of the host rock. This fluid would have been responsible for the presence of fine grained quartz (silicification), hematite, the sulphides, and the glassy matrix within the rock.

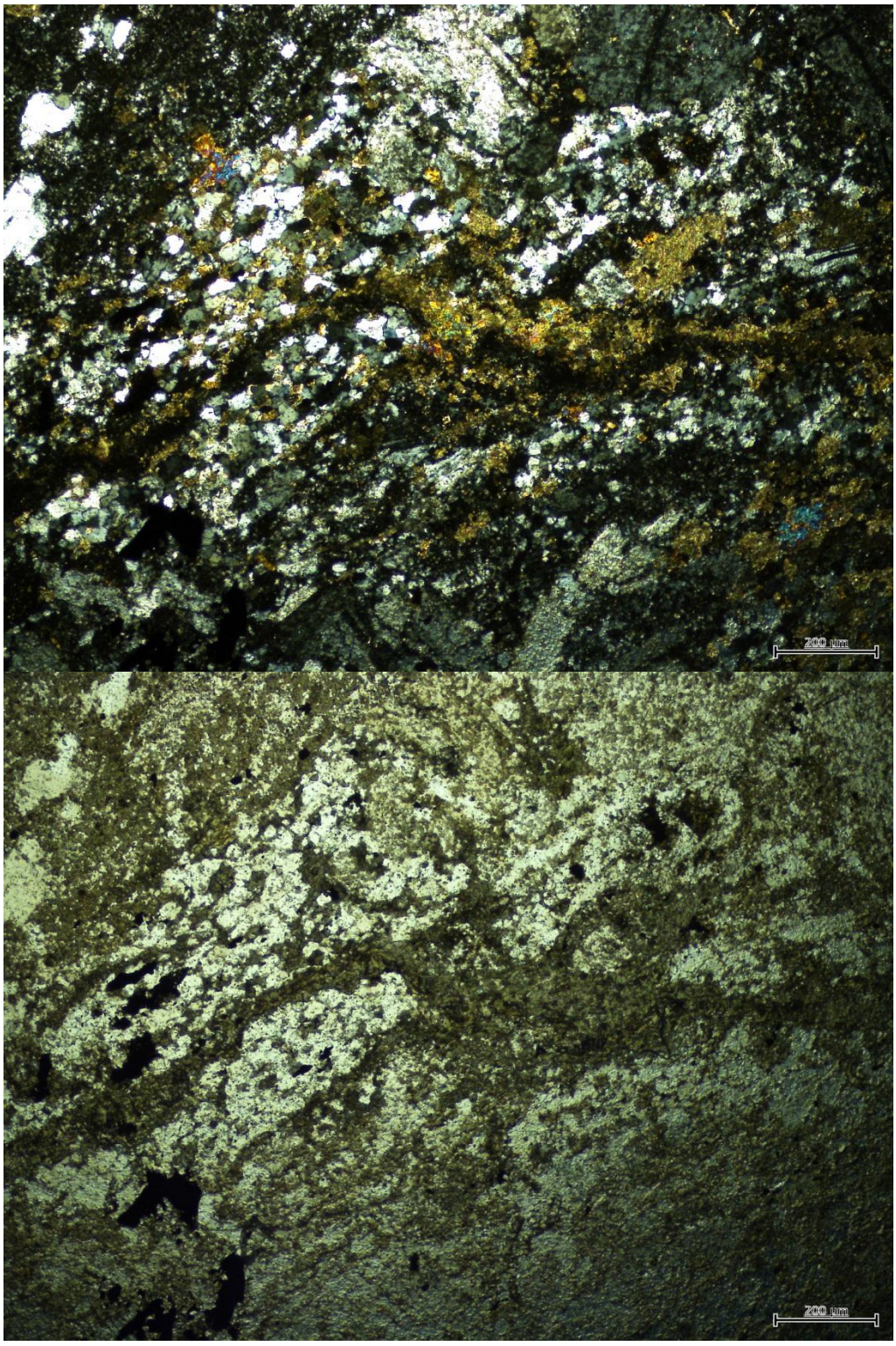

Figure 58: fine grained glassy matrix as veins and as matrix, isotropic in XPL (top). Biotite alteration around these veins can be seen due to the higher birefringence. In the PPL image (bottom) quartz aggregates and sulphides (isotropic) can be seen.

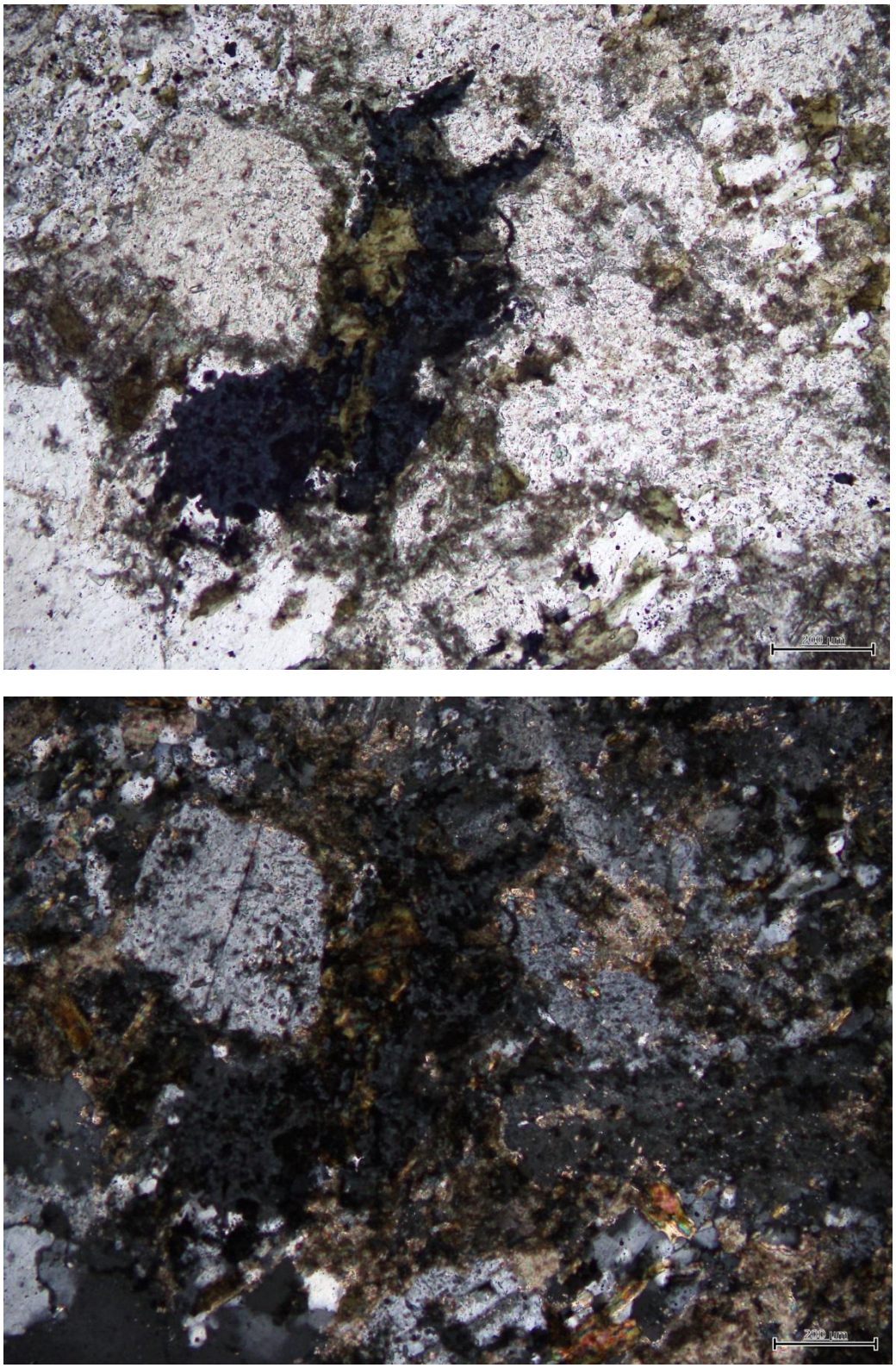

Figure 59: alteration matrix between feldspar and plagioclase. Alteration consists of hematite (blue [top]), biotite (green [top]) and fine grained quartz visible in the bottom image

Paragenesis

Primary k-feld, albite and quartz
matrix quartz, glassy minerals, biotite, hematite, sulphides
quartz and calcite veins

MC003DD, sample #14

Hand Specimen

Meterage: 98.8m
Host lithology: Dolomite
Description: Dolomite with cpy in neck of boundin?(1). Strong euhedral shape of dolomite and infill chalcopyrite shape. Sharp boundaries (2). Quartz is also visible in the neck of the boundin

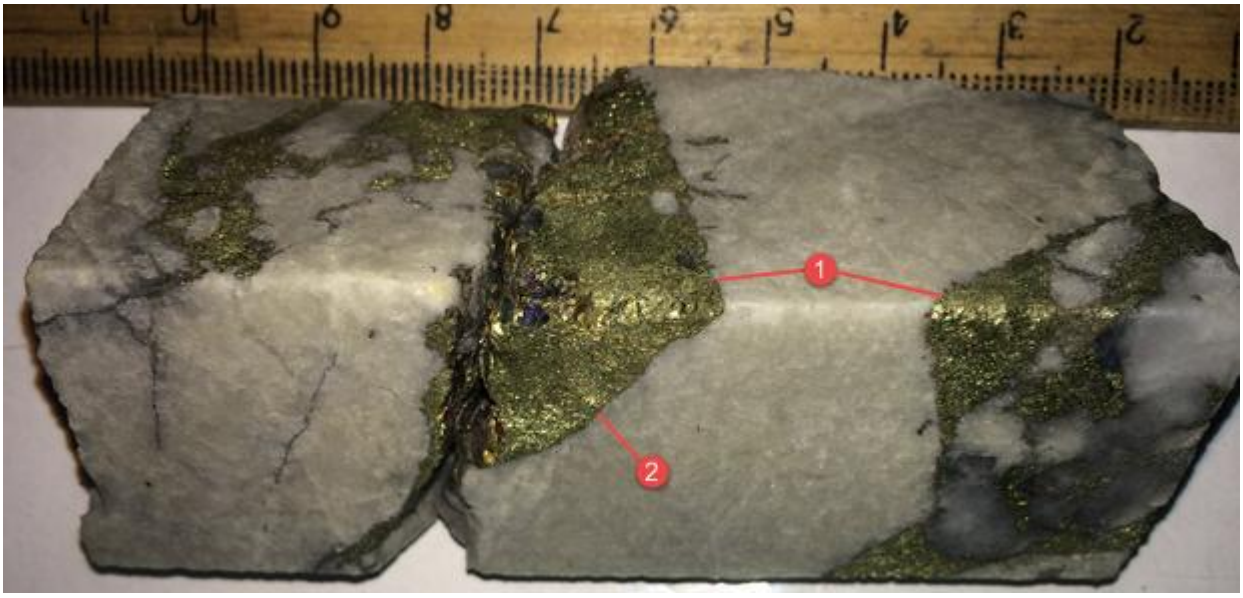

s

Petrology

Minerals	Primary/Alt/ Infill	Crystal size (µm)	Modal%	Characteristics
Dolomite	Infill	500-1500	80	clear in PPL, most crystals low 1st order birefringence and some (20%) 2nd order (might be ethanol?), undoluse extinction
scapolite	trace in vein	200	<1	high relief, clear in PPL, dark-grey brown in XPL, dirty, abundant inclusions, subhedral
quartz	infill	1000	10%	clear PPL, grey XPL, undulose extinction
Chalcopyrite	infill	500	10%	golden yellow in RFL, pockmarked, anhedral
Pyrite	trace	100	<1%	silver-yellow in RFL, euhedral
quartz	infill	50-100	<1	clear PPL, grey XPL, undulose extinction, associated with sulphides

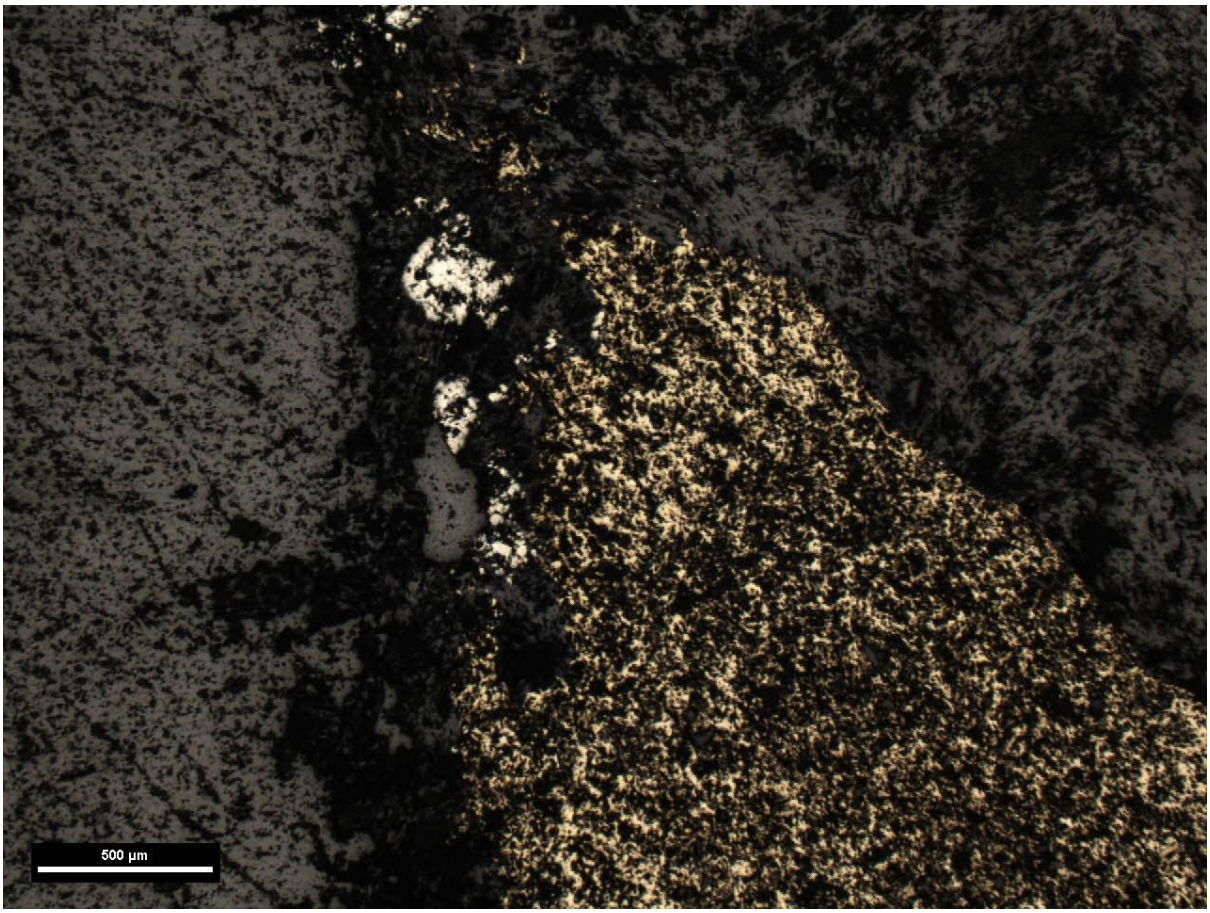

Petrology:

Thin section consists of dolomite vein with course quartz crystals possibly growing in the neck of a boudin. At the boundary between the quartz and dolomite chalcopyrite, minor pyrite and fine quartz crystals have intruded with clear infill textures. One case of early scapolites can be seen within the dolomite vein.

Paragenesis:

Scapolite
Dolomite + quartz
sulphides + quartz (infill)

Hole MC003DD, sample #17

Hand Sample

Meterage: 130.8m
Host lithology: Dolomite
Description: Sulphides and quartz (3) present in microfractures in dolomite. In some places a gold-coloured mineral seems to form at the outer edge of chalcopyrite

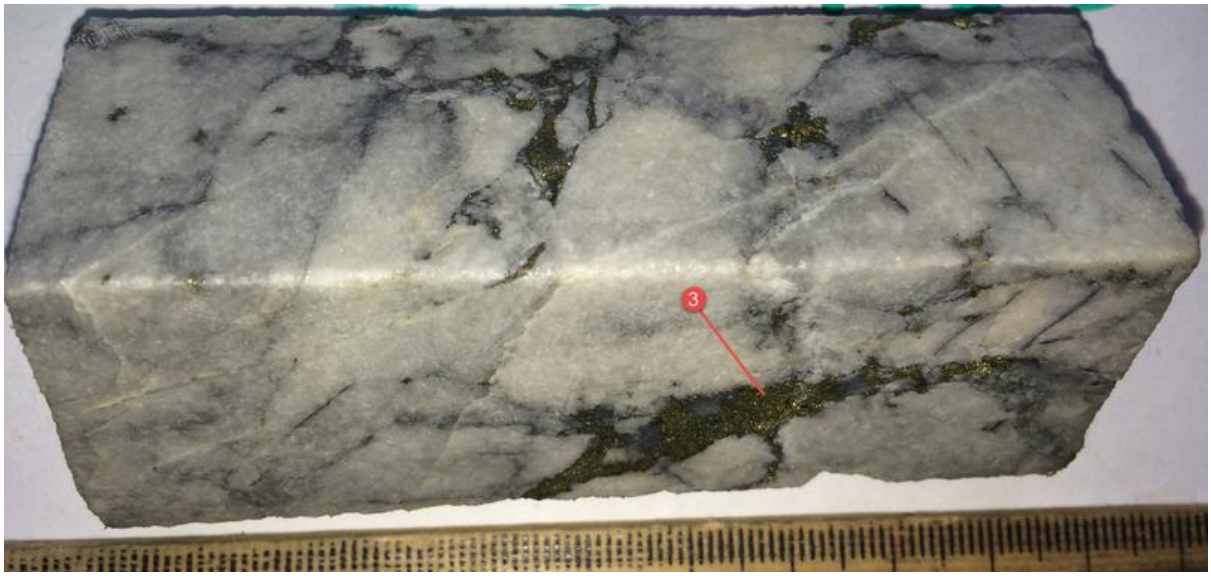

Petrology

Host Rock:

Host rock is dolomite (95%) with rare (<5%) quartz crystals.

Infill, alteration and sulphides

Mineral	Primary/ Alt/Infill	Crystal size (µm)	Modal%	Characteristics
dolomite	primary	700	83	clear in PPL, lamellar twinning in XPL, both parallel and inclined extinction
quartz	primary	500	1	clear PPL, undulose extinction, 1st order birefringence
quartz	infill	100-600	5	clear PPL, undulose extinction, 1st order birefringence, occurs with sulphides
chalcopyrite	infill	1000	10	golden-yellow in RFL, infill texture, subhedral
tremolite?	alteration	100	1	60/120 cleavage, elongate and fiberous crystals, birefringence low-mid 2nd order, occurs with sulphides
Muscovite?	alteration	100	1	colourless in PPL, 1 cleavage, parallel extinction, 3rd order birefringence

Sulphides are present in discontinuous vein-like features and between dolomite grain boundaries. Occurring with the sulphides are both course (1500µm) and fine (100-300µm) grained quartz. It is

common to see fine-grained quartz forming a layer between sulphides and dolomite. Minor, randomly orientated muscovite and the tentatively named tremolite (grunerite may be a better match? Due to fiberous nature) also form at the boundary of sulphide crystals, and occasionally overprint quartz and chalcopyrite.

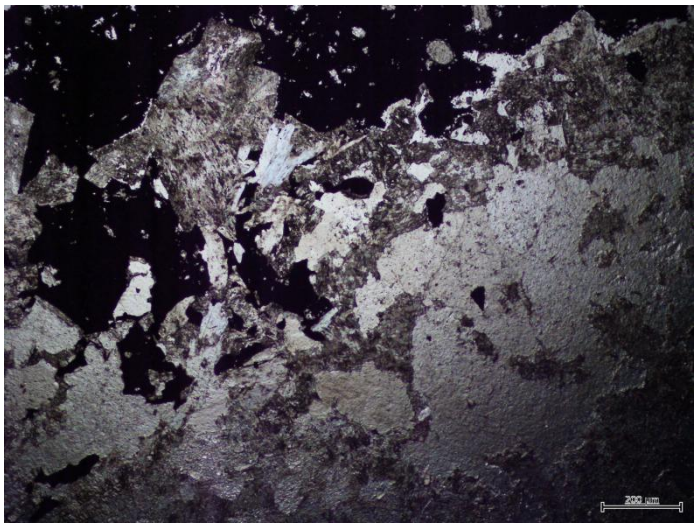

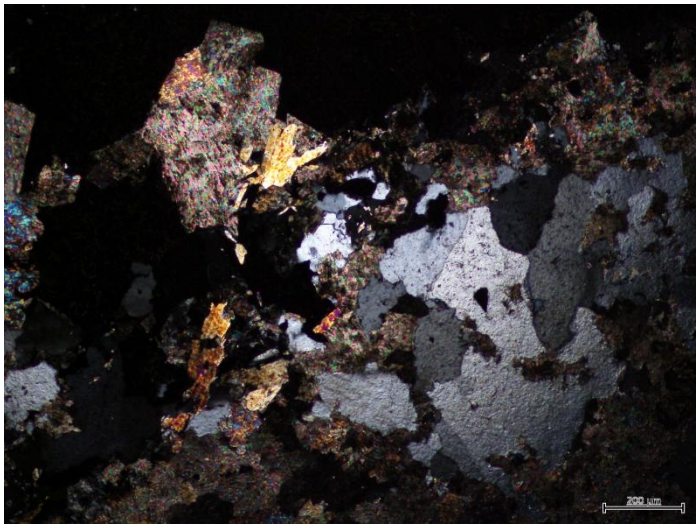

Paragenesis

Dolomite + rare primary quartz
quartz (infill) + sulphides +/- muscovite +/- tremolite

Hole MC001, sample #3

Hand Specimen

Meterage: 351.5m
Lithology: unsure
Description: Very fine, dark, soapy textured rock. Rare phenocrysts beige in colour. Rock appears foliated. Brown alteration –albitisation? Some chl alteration

Petrology

Mineral	Primary/Alt/Infill	Crystal size (µm)	Modal %	Characteristics
quartz	primary	500-1000	30	abundant phenocrysts
albite	primary	500	10	rare phenocrysts
groundmass	primary/alteration?	<50	58	quartz and other low birefringence crystals too fine to see
chlorite	infill	<50	1	microvein
biotite	infill	<50	1	microvein

Host rock

Quartz and albite phenocrysts reside in a fine grained matrix that consist of quartz +/- other minerals. This suggests the brown alteration called albitisation may actually be silicification.

Veining

Quartz vein with minor biotite

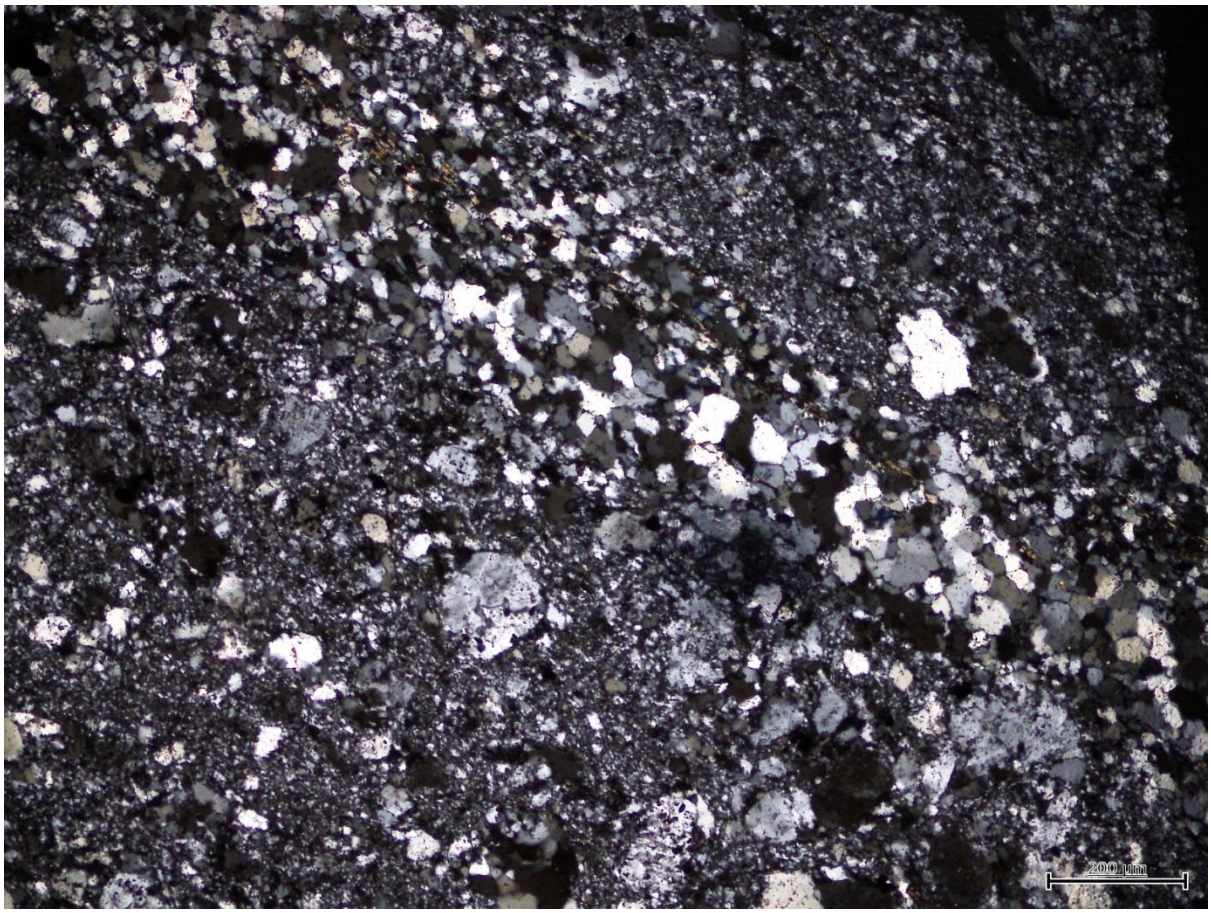

Figure 60: Quartz + minor biotite infill. Fine grained matrix with quartz and albite phenocrysts visible

Paragenesis

Quartz + albite
Quartz + biotite

Hole MC001, sample #4

Meterage: 49m

Lithology: igneous rock with grain size 1-3mm of black mineral bi often altered to green (chl?)(2), pink feldspar (may be hem/potassic altered plag) and qtz. Potential gabbro protolith.

Description: Qtz vein (5cm) cuts rock has hem/potassic alt (3) and diposide(?)(4) alt inside

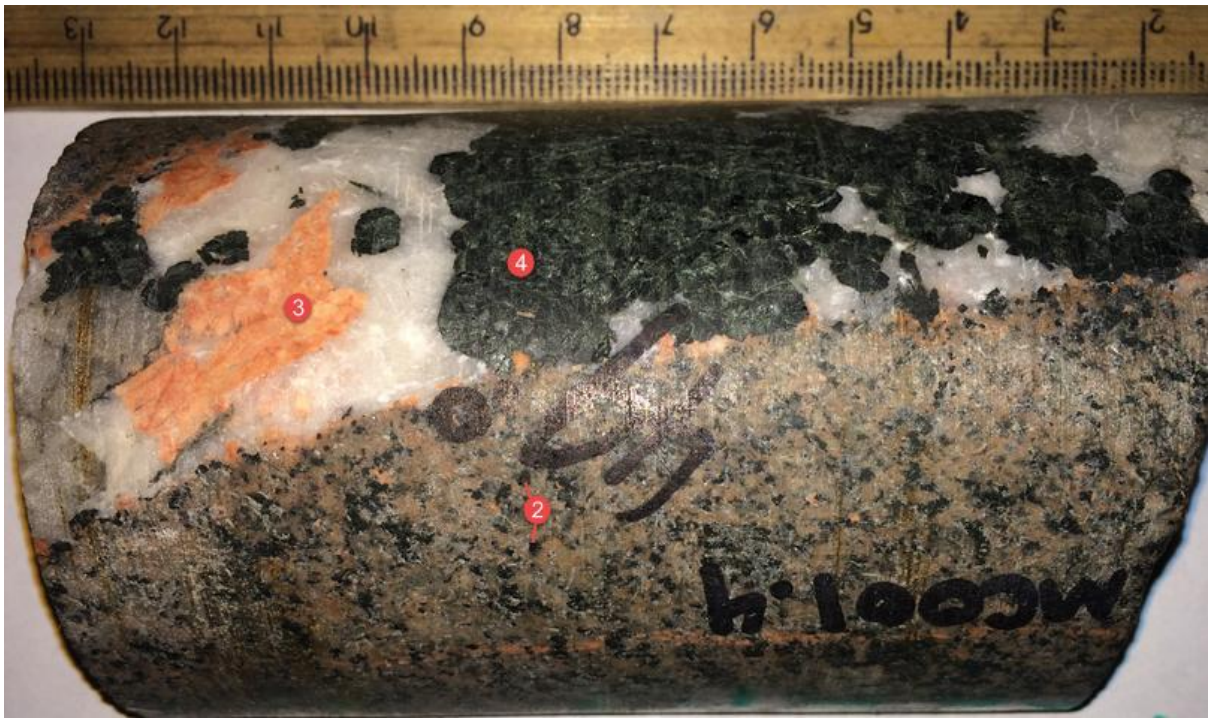

MC001.6

Hand Sample

Meterage: 404.1
Lithology: Unsure – chl schist? Heavily chl altered (1).
Description: Mineralised (py=cpy) qtz veining. Sulphides both coarse overprinting (2), strung out with chlorite (3) and as microcreccia matrix between grains

Petrology

Host rock

The host rock from this thin section is undefinable due to the infill within the sample.

Infill and Sulphides

There appears to be 2 stages of infill in this sample. The first phase is a quartz/dolomite +/- chalcopyrite phase that fills the majority of the sample. The relationship between the 3 minerals is evidenced by the inclusion of each mineral within the other without any fluid flow paths to suggest a later stage of infill. The second phase is a biotite (largely altered to chlorite) + fine grained quartz +/- pyrite.

Paragenesis

Quartz/dolomite +/- chalcopyrite
Biotite + fine grained quartz +/- pyrite
Chlorite

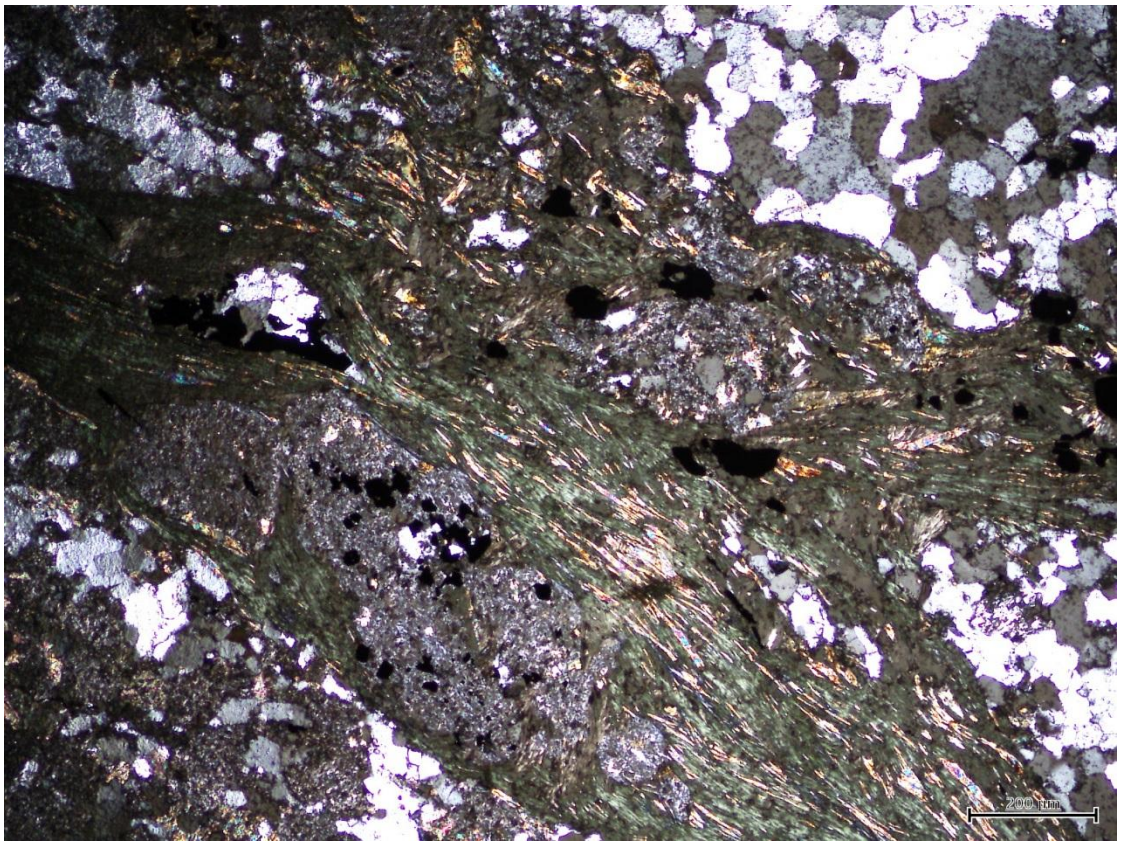

Figure 61: fine biotite/chlorite infill with pyrite (isotropic crystals) intruding into quartz/dolomite

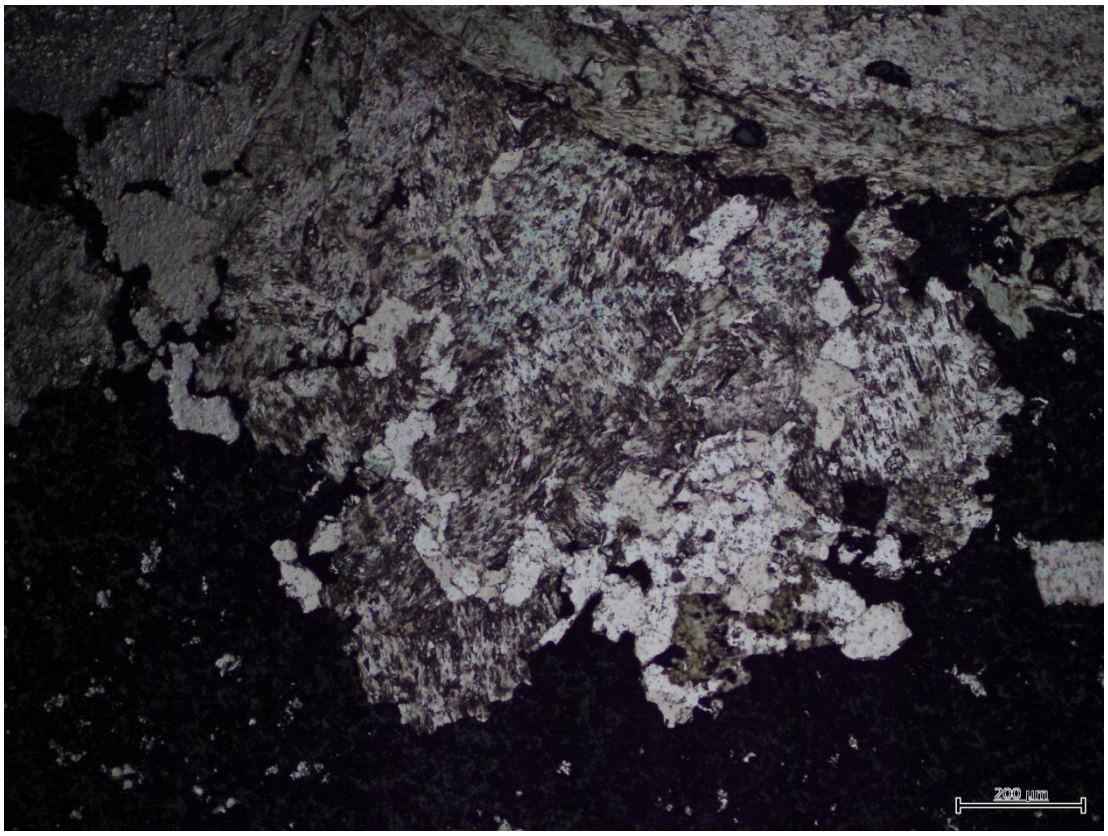

Figure 62: Central dolomite/quartz aggregate surrounded by chalcopyrite (black) with classic infill texture, chlorite vein intruding at the top with pyrite (black isolated crystals)

Hole MC001, sample #7

Meterage: 335.5

Lithology: Coarse feldspar (1) and qtz crystals (2), fine bi crystals (3), in a dark fine grained matrix (4)

Description: as above, some chl alteration

- Coarse quartz and potassium feldspar phenocrysts with minor plagioclase phenocrysts.
- 0.2-1cm in diameter
- Dark grey groundmass consisting of coarse biotite, fine grained, intergrown biotite and muscovite, and fine grained quartz.
- Phenocryst supported texture

Hole MC004, sample #2

Hand Sample

Meterage: 26m
Lithology: Felsic tuff, bi foliation
Description: strong foliation defined by elongated biotite grains (1), light grey groundmass with qtz grains, rest of groundmass too fine to see. Dolomite vein (2) with black mineral as rim (3)

Petrology

Mineral	Primary/Alt/Infill	Crystal size (µm)	Modal %	Characteristics
quartz	primary	500-2000	10	isolated angular phenocrysts
k-feld	primary	500-2000	10	isolated angular phenocrysts
plagioclase	primary	500-2000	10	isolated angular phenocrysts
matrix	primary	<10	40	very fine
biotite/chlorite	primary/infill/alt?	1000-3000	19	alteration around vein, in vein and primary biotite altered to chlorite
dolomite	infill	300-500	10	vein
calcite	infill	300	1	associated with quartz

Host rock

Angular phenocrysts of quartz, plagioclase and k-feldspar (500-2000µm) and clusters of biotite/chlorite (1000-3000µm) in an extremely fine matrix (<10µm) assumed to consist of quartz, plagioclase and k-feldspar. Minor calcite is associated with quartz phenocrysts.

Veining

A dolomite vein crosscuts the rock and has a chlorite/biotite alteration halo.

A Quartz +/- biotite microvein is also present within the sample.

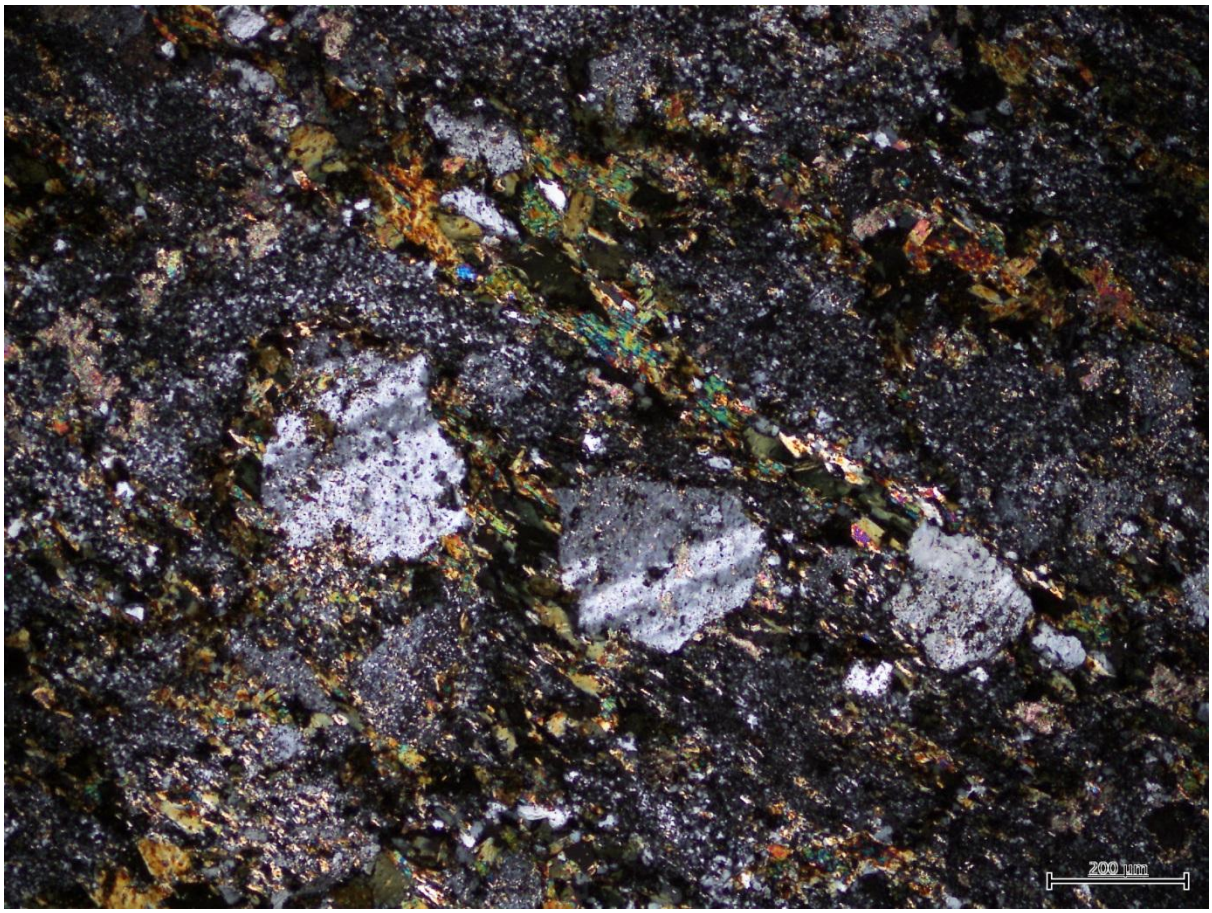

Figure 63: biotite/chlorite infill around plagioclase, fine grained matrix visible

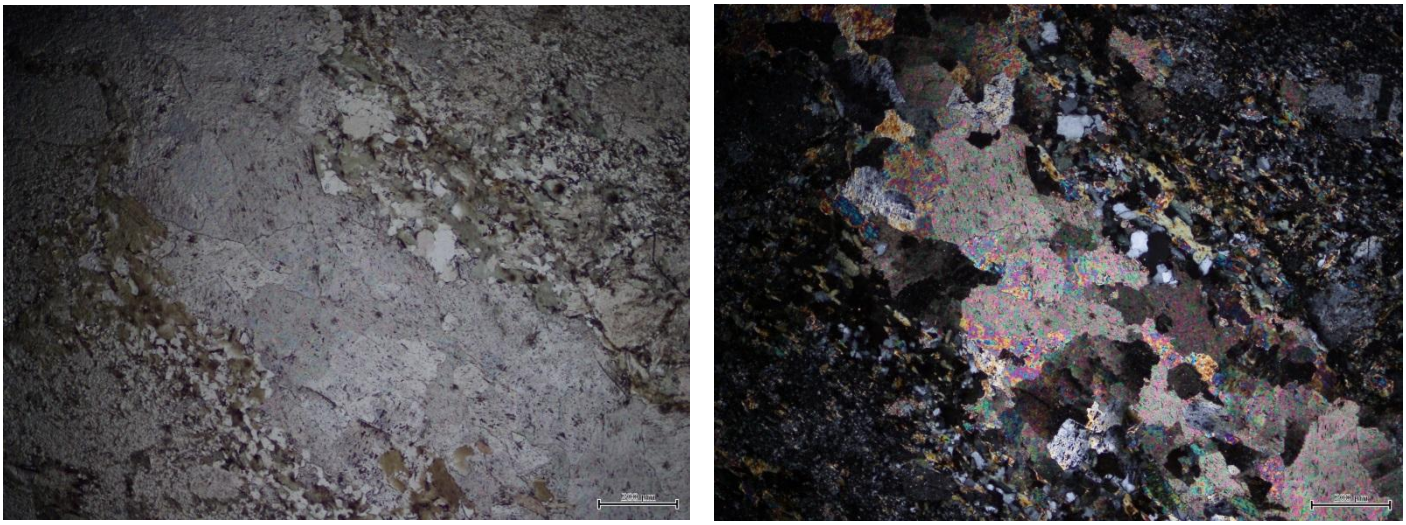

Figure 64: dolomite vein with biotite/chlorite alteration

Hole MC002A, sample #3

Hand Specimen

Meterage: 574.4m
Lithology: Granite or granodiorite feldspars>qtz>bi(chl?)
Description: no (or minimal) alteration

Petrology:

Mineral	Primary/Alt/Infill	Crystal size (µm)	Modal %	Characteristics
sericitised feldspar	alteration/primary	10000 (1cm)	25	sericitised
quartz	primary	10000 (1cm)	25	
plag	primary	5000 (5mm)	30	
biotite/chlorite	primary/alteration	300	15	between crystal boundaries and abundant at 3 point contacts
quartz	infill	50	5	between crystal boundaries

Host Rock

Coarse grained quartz, feldspar, plagioclase and biotite altered to chlorite. Granodiorite

Alteration and Infill

Biotite often altered to chlorite and quartz form small grains at the boundaries between grains. Sericitisation of feldspars has occurred extensively. This sample is distant to the main Cu orebody and may represent a distant alteration halo.

Paragenesis

Feldspar + quartz + plag + biotite
quartz + biotite + sericite?
chlorite?

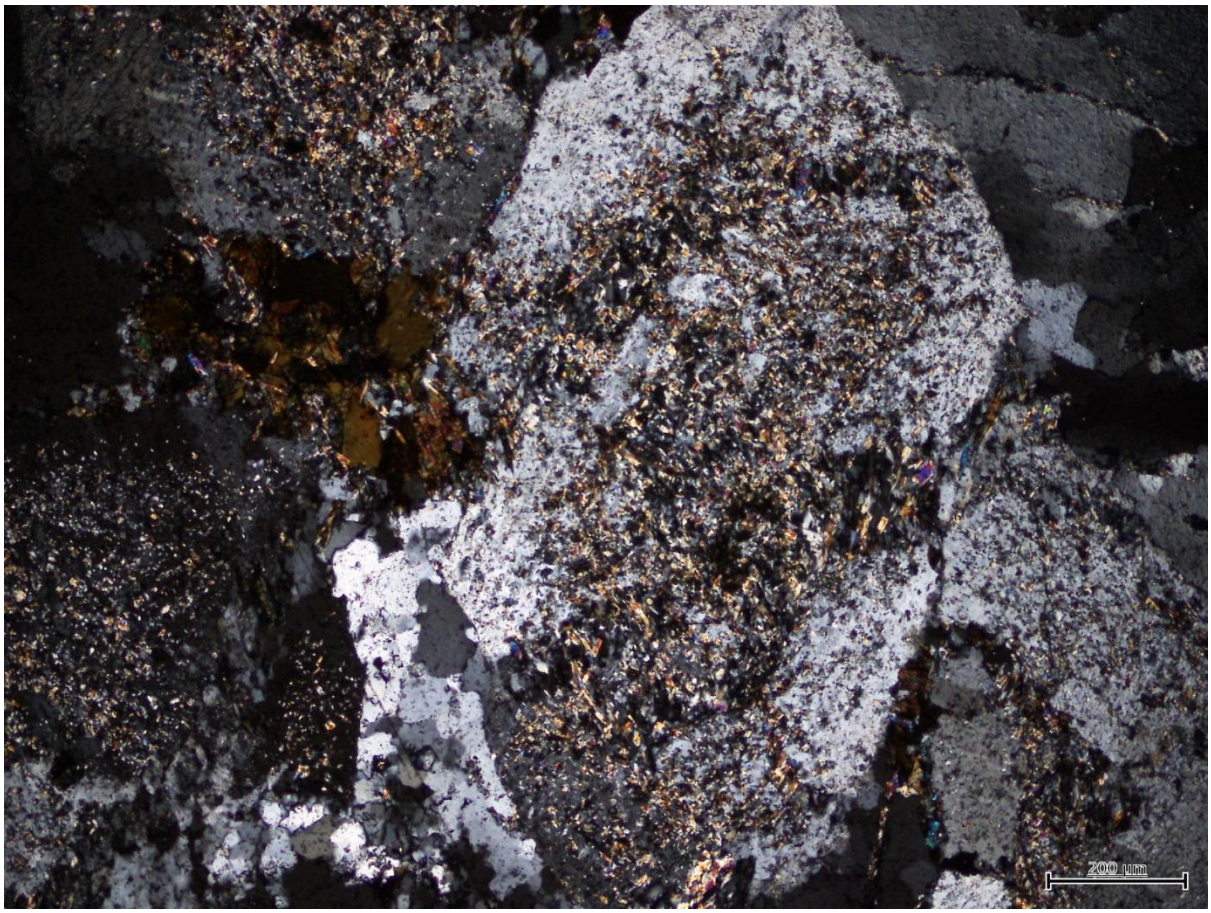

Figure 65: Sericitised feldspar , biotite and quartz

Hole MTC12, sample #1

Hand Sample

Meterage: 131.1m
Lithology: Fine grained, biotite rich, quartz with magnetite (check) showing common orientation (1). Fibrous randomly orientated white retrograde mineral growth present (2).
Description: As above

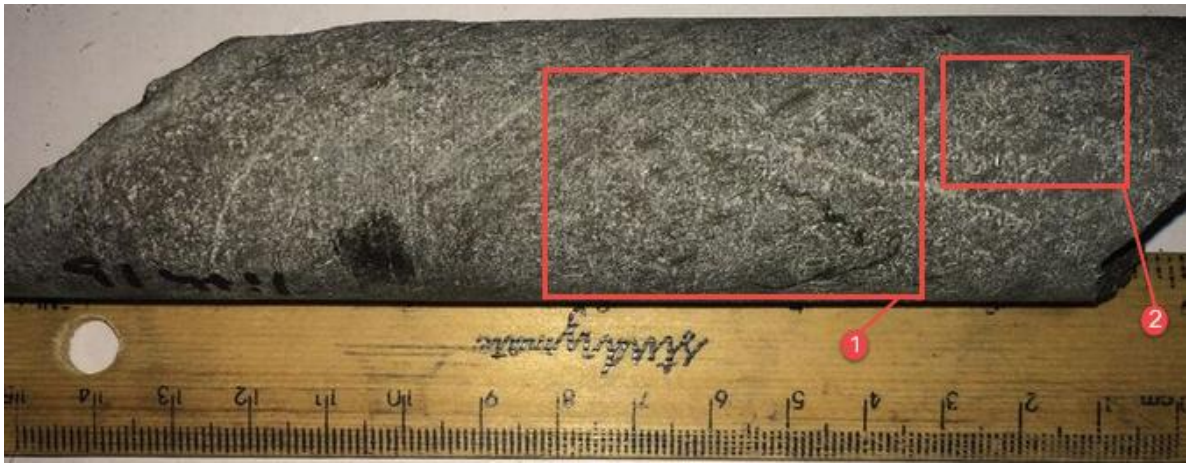

Petrology

Mineral	Primary/Alt/Infill	Crystal size (µm)	Modal%	Characteristics
albite	primary	300-2000	35	phenocrysts
biotite	infill	<100	30	groundmass
quartz	infill	1000	5	veining
quartz	primary	300	5	groundmass
magnetite	primary?	1000	20	phenocrysts
feldspar	primary	2000	5	rare phenocrysts
spinel	-	100	<1	very rare in groundmass
calcite	infill	1000	<1	with quartz in vein

Host rock

Host rock is dominated by elongate plagioclase phenocrysts (300-2000µm) with no common orientation, subhedral magnetite crystals, rare feldspar phenocrysts and a fine matrix (<100 µm) that consists mainly of biotite with lesser quartz, spinel, calcite and ilmenite.

Magnetite is abundant in the sample as subhedral crystals, their relationship to the rock – be it primary or infill – is unclear as they appear to force plagioclase crystals to grow around them in some cases, and have an apparent infill texture in others. Due to the high temperature of magnetite crystallisation and the igneous nature of the sample it seems more likely that it is a primary mineral.

A tentative name for this rock is Andesite.

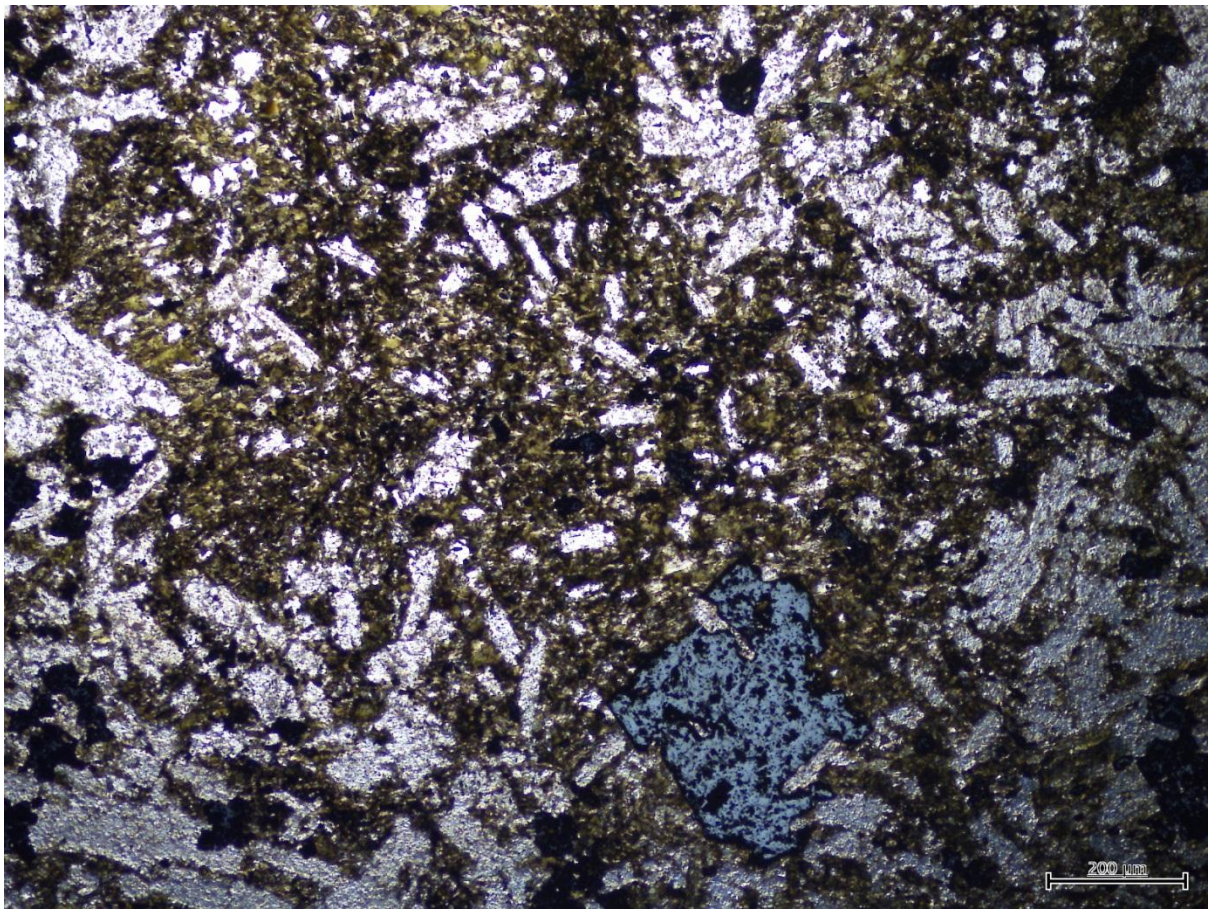

Figure 66: Elongate albite crystals dominate this rock, isotropic magnetite, late pyrite and the biotite groundmass are also visible in this image under plane polarised light with reflective light to illuminate the pyrite.

Veining

A quartz vein (2mm) with course (relative to the host rock) quartz and (rare) calcite crystals cross cuts the sample and hosts trace chalcopyrite.

Sulphides

One pyrite crystal (1mm) is visible in the host rock, it shows growth around earlier crystals hence suggesting late growth.

As mentioned above chalcopyrite occurs with quartz in a vein.

Paragenesis

Albite
biotite + quartz + magnetite(?) + spinel + feldspar + pyrite
quartz + calcite + chalcopyrite (vein)

MC003B.2 - 205.8-206m

Hand Specimen:

Description: Chl schist with deformed quartz and dolomite veins (1) following foliation. Quartz appears as inclusions in dolomite (2) which shows zonation into a darker boundary (5). Disseminated pyrite is visible in both the veins (3)and host rock (4).

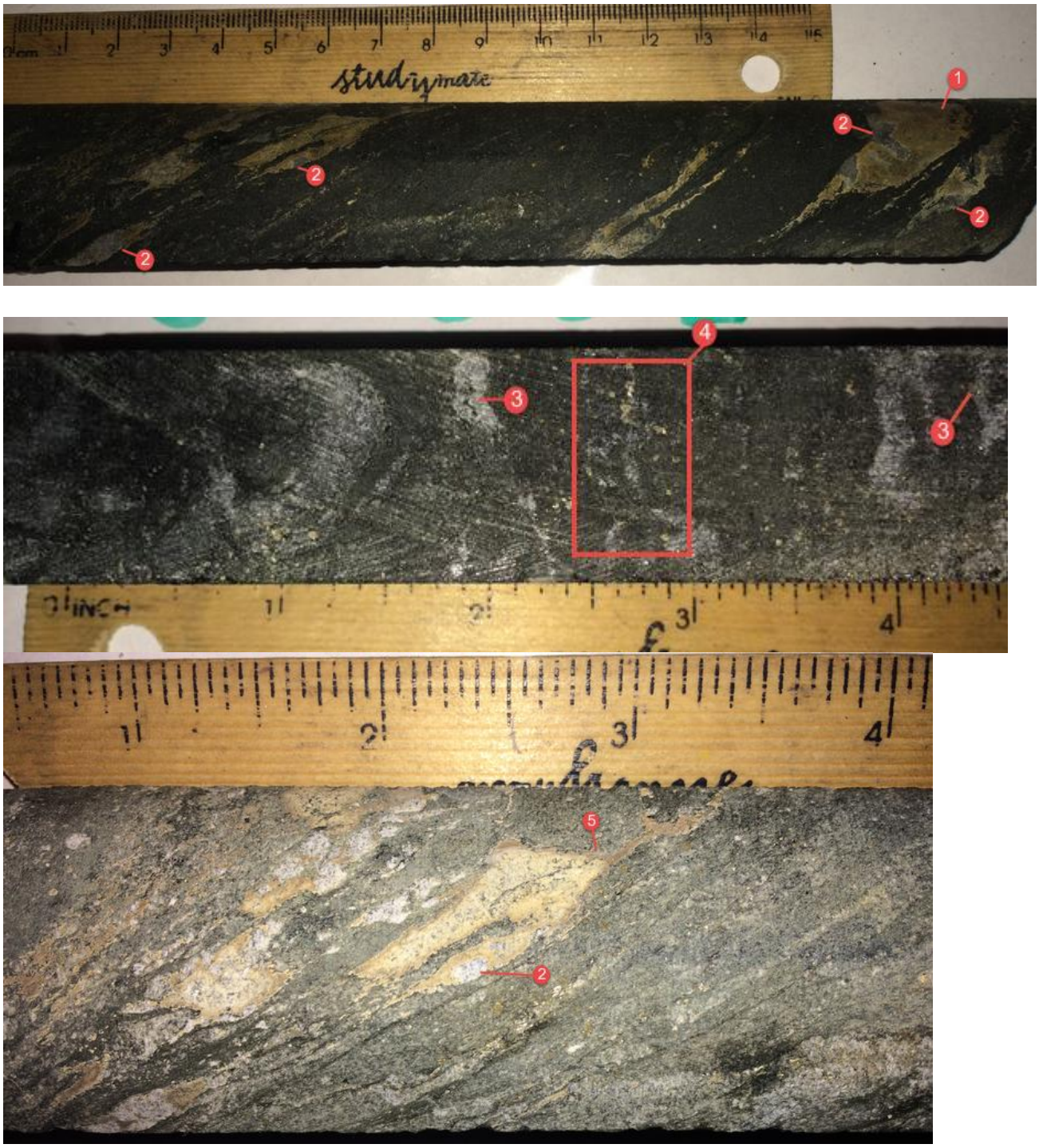

Figure :67Chlorite schist with dolomite and quartz veining

Note: will reduce this to one image in future, all 3 images are annotated so just easier to keep it like this for now

Petrology:

Host rock

The host rock is a well-foliated chlorite-quartz-biotite schist. It is composed of fine-medium (100-200μm) rounded and elongated quartz crystals, and biotite crystals from <50μm to 500μm that have been largely altered to chlorite (~100μm in size). Lenses of calcite +/- sphene run parallel to foliation as an aggregate of course grained crystals 500-800μm in size.

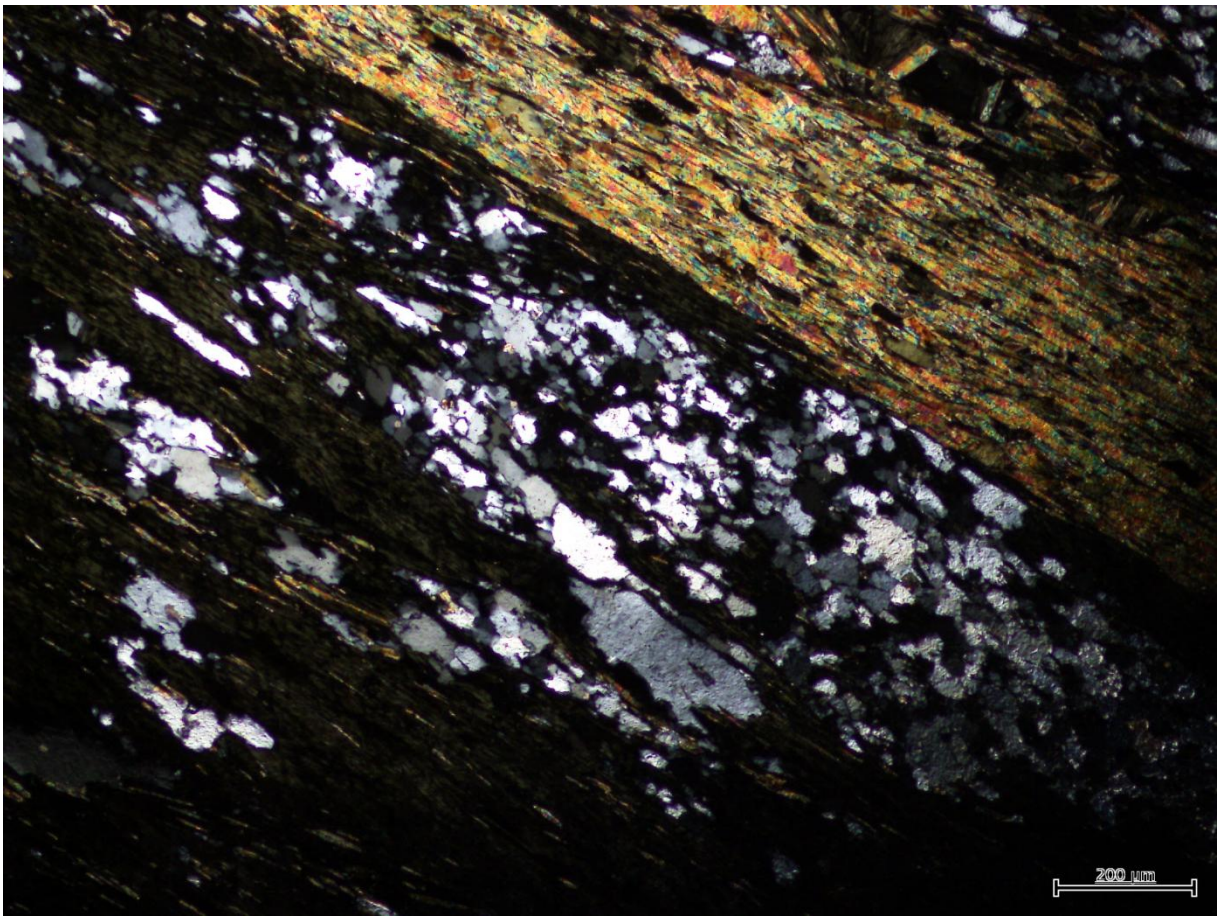

Figure 68: Figure depicting the main constituents of the host rock, quartz-biotite-chlorite schist

Sulphides

Pyrite is present in this sample, occurring as rare, early (deformed in the direction of foliation) crystals that show an association with calcite. Pyrite also shares strong grain contacts with an unidentified mineral that appears dirty possibly due to high degree of internal deformation, in XPL this mineral is brown with no twinning or undulation.

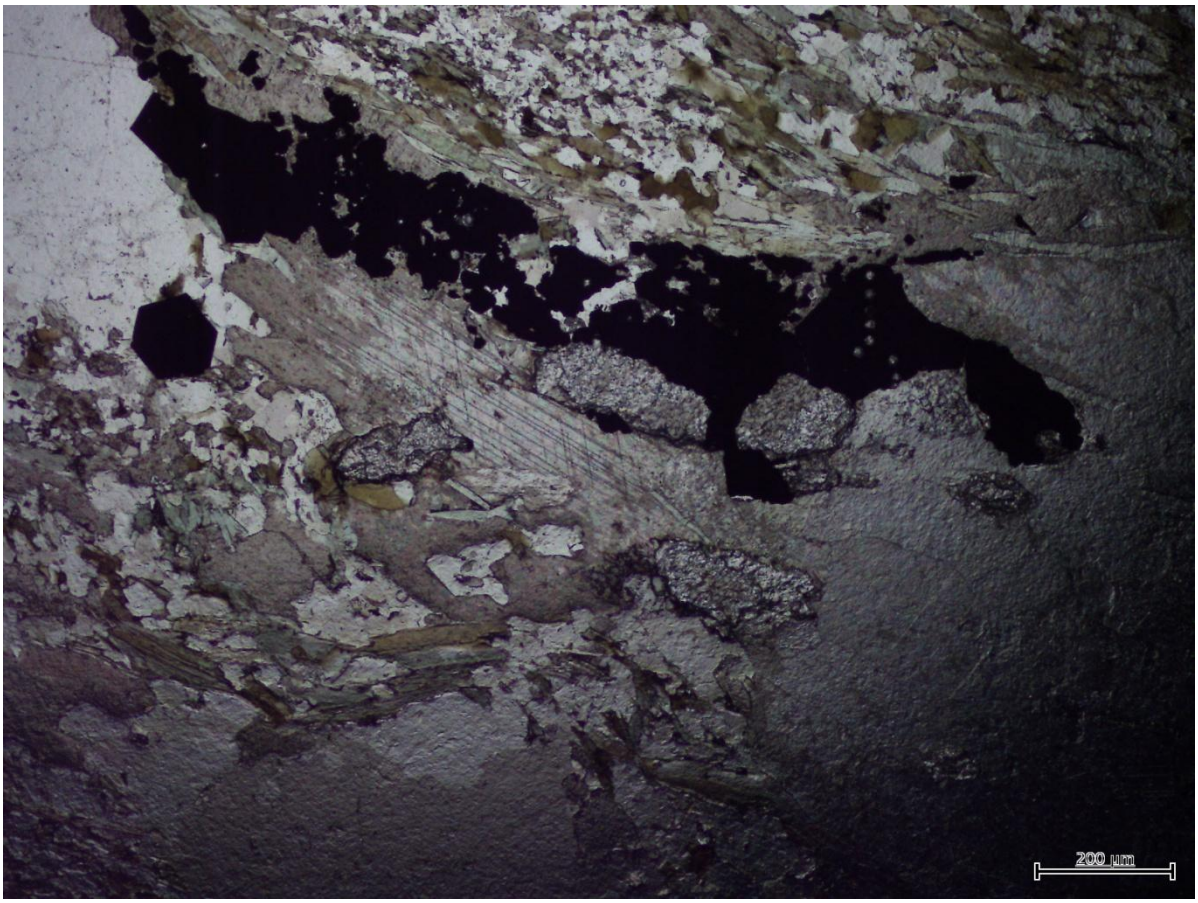

Figure 69: Pyrite forming at the edge of a calcite lense

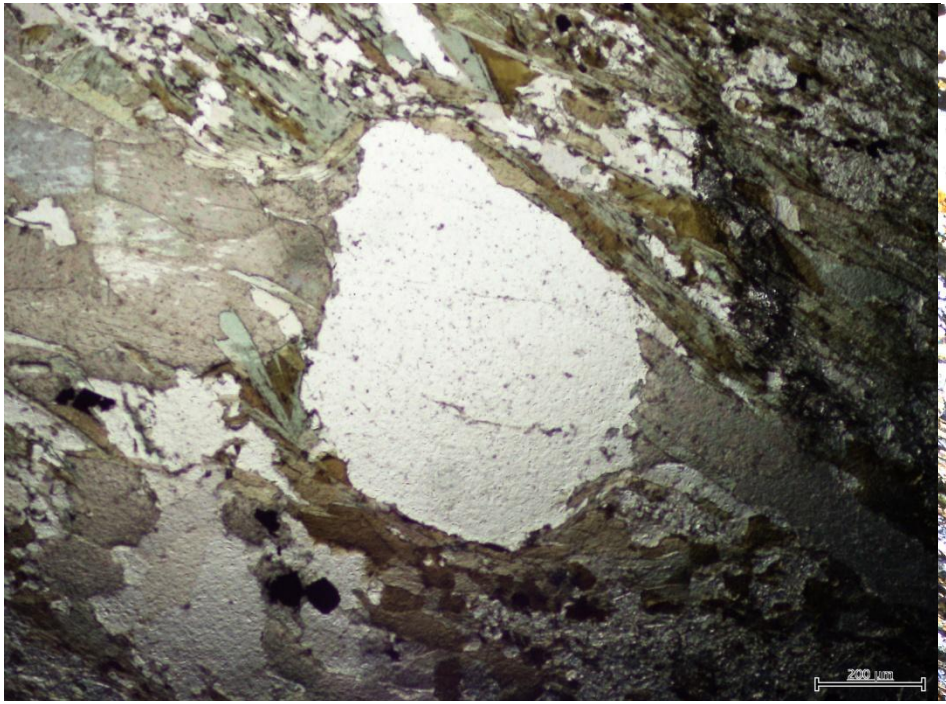
200 µm

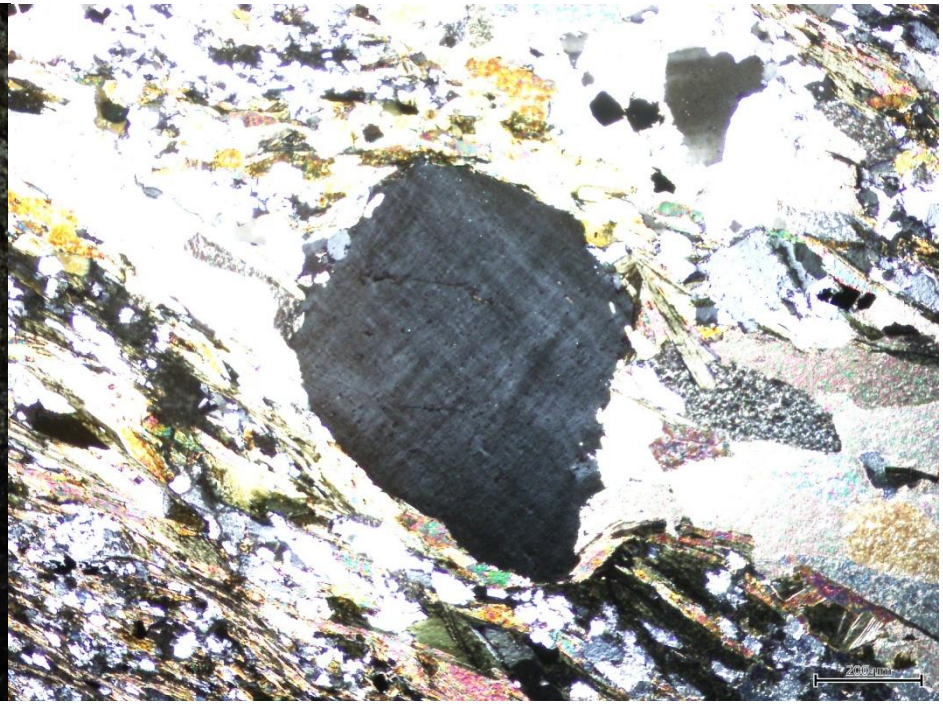
200 µm

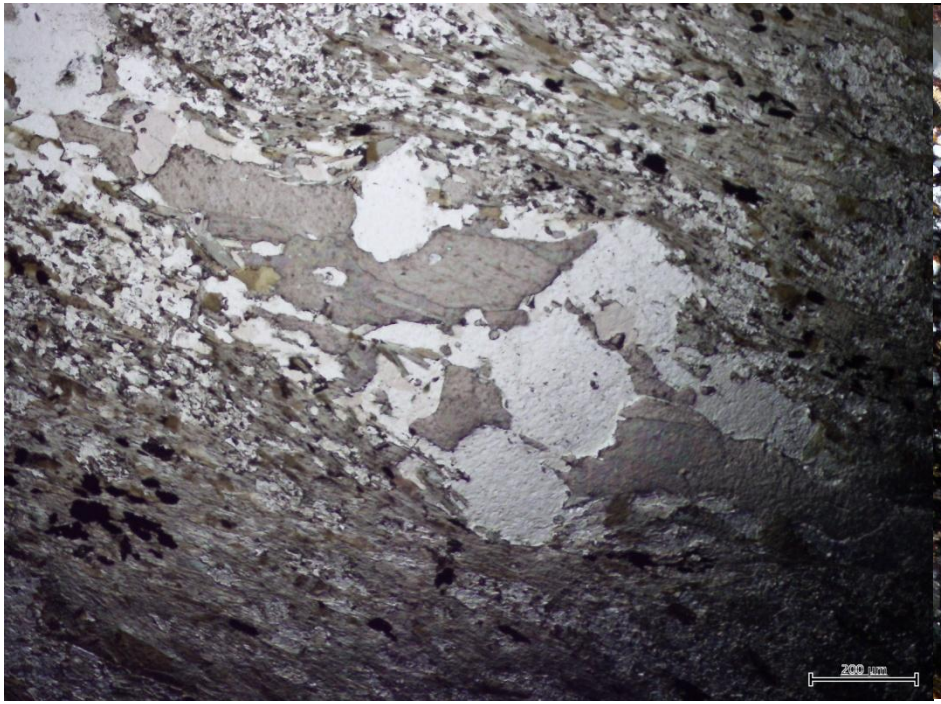
200 µm

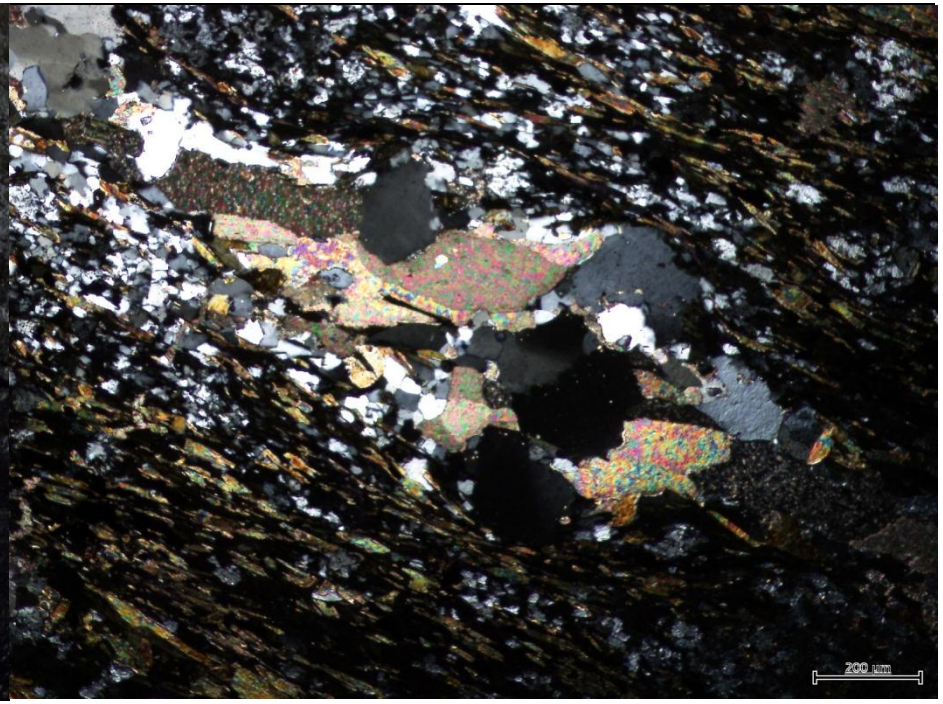
200 µm

Figure 70: Top left: PPL of feldspar with deformed calcite, chlorite and biotite moving around grain. Top right: XPL shows light perthitic texture of feldspar crystal. Bottom left and Bottom right: PPL and XPL (respectively) of calcite infill texture around quartz.

Paragenesis:

feldspar
Quartz
Biotite
Calcite + pyrite + sphene
Chlorite

MC003B.3

Hand Sample

Meterage: unknown (check pictures)
Lithology: chl schist
Description: dolomitisation (1) and silicification (2) overprinting chl schist. Very coarse cu-sulphide (3) overprinting everything (cpy>py (+ something else? (4))) Fine cu-sulphides at edge of dolomite also (5).

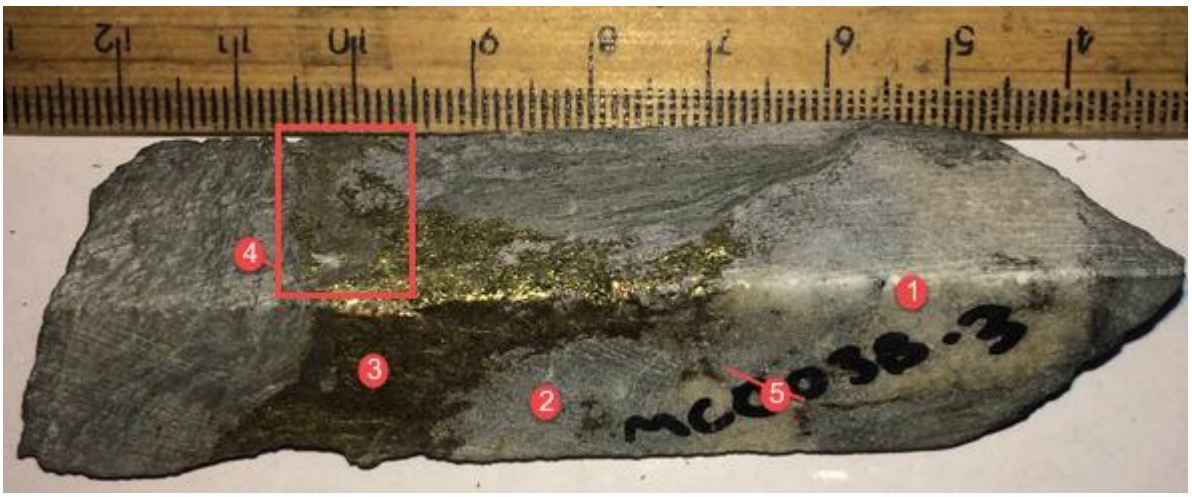

Petrology:

Mineral	Primary/ Alt/Infill	Crystal size (µm)	Modal %	Characteristics
chlorite	alteration	<50	20	green in PPL and in XPL, elongated pencil shape, 1 cleavage
quartz	primary	300-500	30	clear PPL, undulose extinction, 1st order birefringence
biotite	infill	100	5	brown-yellow pleochroism, 2nd order birefringence, 1 cleavage
chalcopyrite	infill	1000-1500	20	straw-yellow in RFL
pyrite	infill	700	10	silver-yellow in RFL
quartz	infill	50	10	clear PPL, undulose extinction, 1st order birefringence
dolomite	infill	500	5	strong grain contact to cpy, lamellar twinning, colourless PPL, 2nd order birefringence

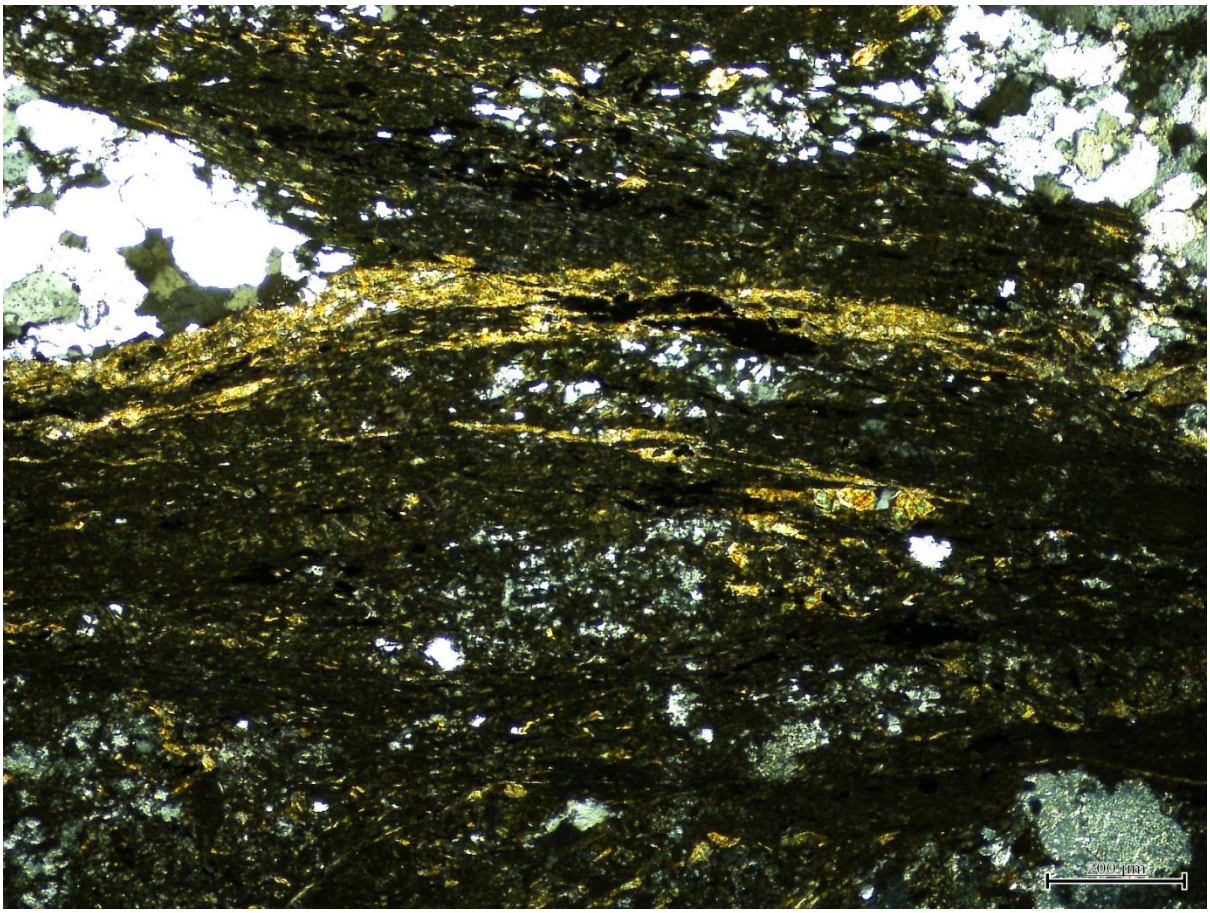

Figure 71: Chlorite + biotite showing foliation, moving around quartz aggregates

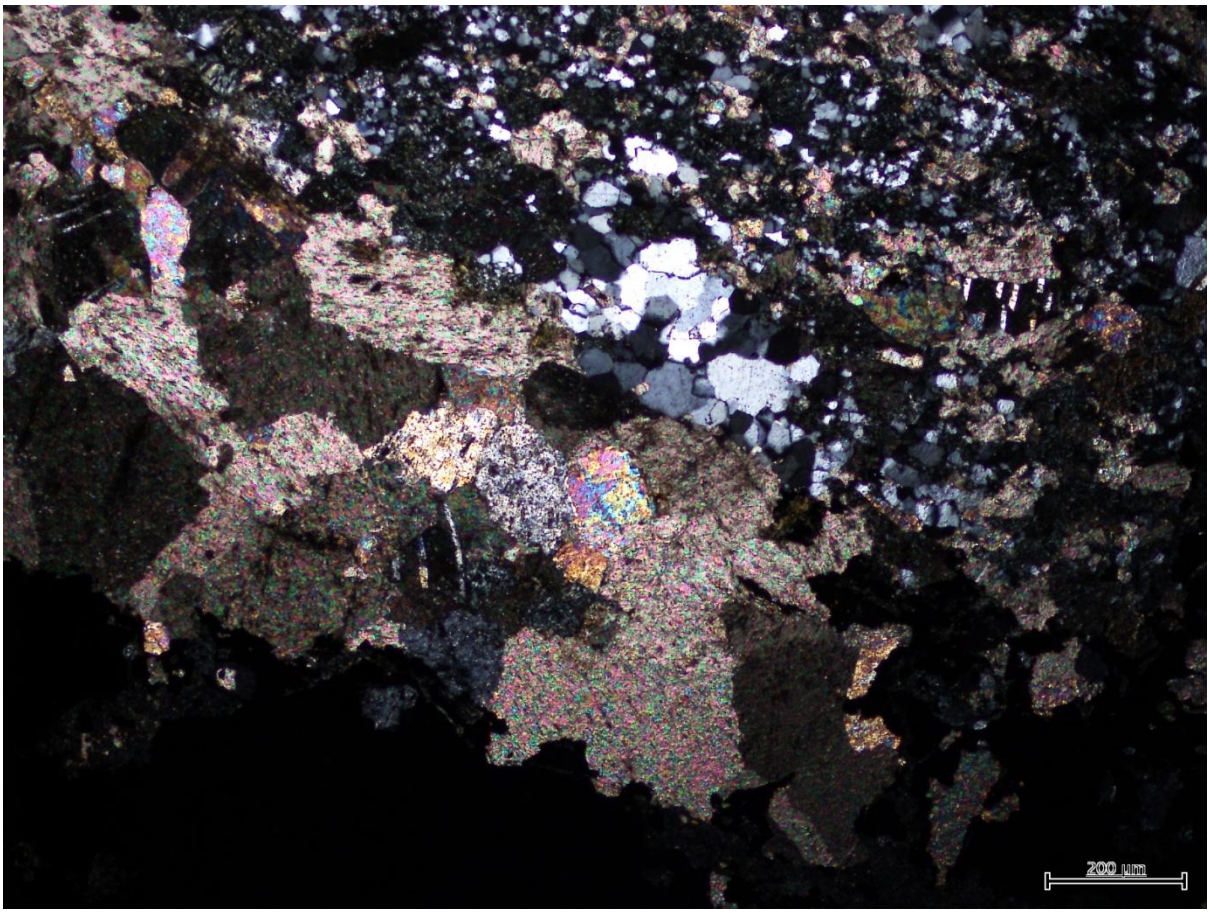

Figure 72: Dolomite in contact with the isotropic chalcopyrite

Host Rock

Due to the altered nature of the rock it is difficult to distinguish the host rock. Fine, dirty chlorite +/- biotite has intruded as fractures spanning 500-600µm between quartz crystals. Due to the altered nature of the sample I have named it an altered chlorite-quartz schist.

Infill and veining

The sulphides + dolomite are only found adjacent to one another with strong grain contacts, with dolomite forming the outer edge around the sulphides. This is taken to be evidence of repeated fracturing of fluid pathways, suggesting that dolomite veining occurred and was subsequently replaced by sulphides. Late stage microscale quartz + chlorite veining is also observed crosscutting primary quartz and the sulphides.

Sulphides

The sulphides have a defined infill texture, with the pyrite forming the core of the sulphide mass, surrounded by a chalcopyrite outer boundary.

Paragenesis

Quartz
Dolomite
Sulphides
Chlorite +/- biotite
quartz +/- chlorite

Hole MC003B, sample #5

Hand Sample

Meterage: 426.1m
Lithology: granite
Description: K-feldspar (1), chlorite in fractures (2), quartz (3) and plagioclase (4)

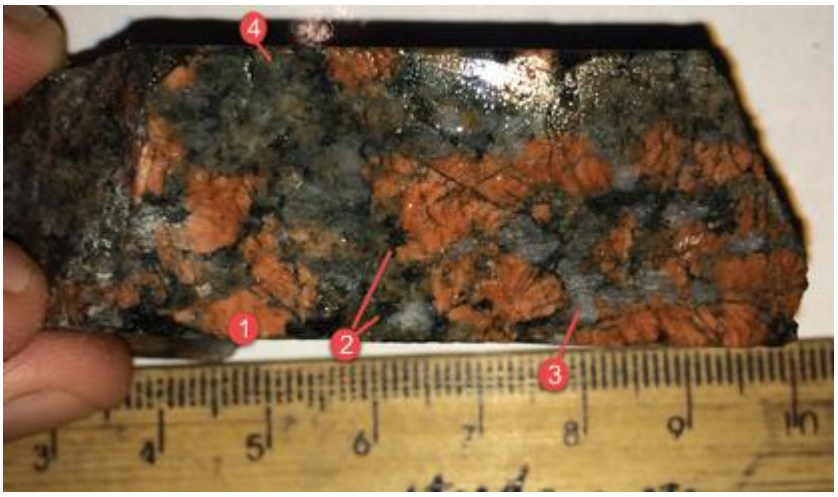

Petrology

Mineral	Primary/Alt /Infill	Crystal size (µm)	Modal%	Characteristics
k-feld (microperthite)	primary	1000	35	plagioclase exsolution features, pink tinge in PPL, 1st order birefringence
k-feld (microcline)	primary	300-500	5	tartan twinning, 1st order birefringence
quartz	primary	500-700	35	clear PPL, undulose extinction, 1st order birefringence
plagioclase	primary	400-600	20	simple and carlsbad twinning, 1st order birefringence
chlorite	Alteration? Infill?	100	5	green in PPL, 1st order birefringence, 1 cleavage

Host rock:

The abundance of quartz and feldspars and the coarseness of the rock suggest this is a granite. Feldspars display microperthitic texture representing albitic exsolution during prolonged cooling of the granite body.

Chlorite - Infill or alteration?

Chlorite appears to have infill texture, it is visible intruding along grain boundaries and precipitates larger crystals where there is a 3 point contact. It may be that these 3 point contacts were originally biotite, and fluid influx through fractures and grain boundaries resulted in alteration to chlorite.

Paragenesis:

k-felspar + quartz + plagioclase
Chlorite

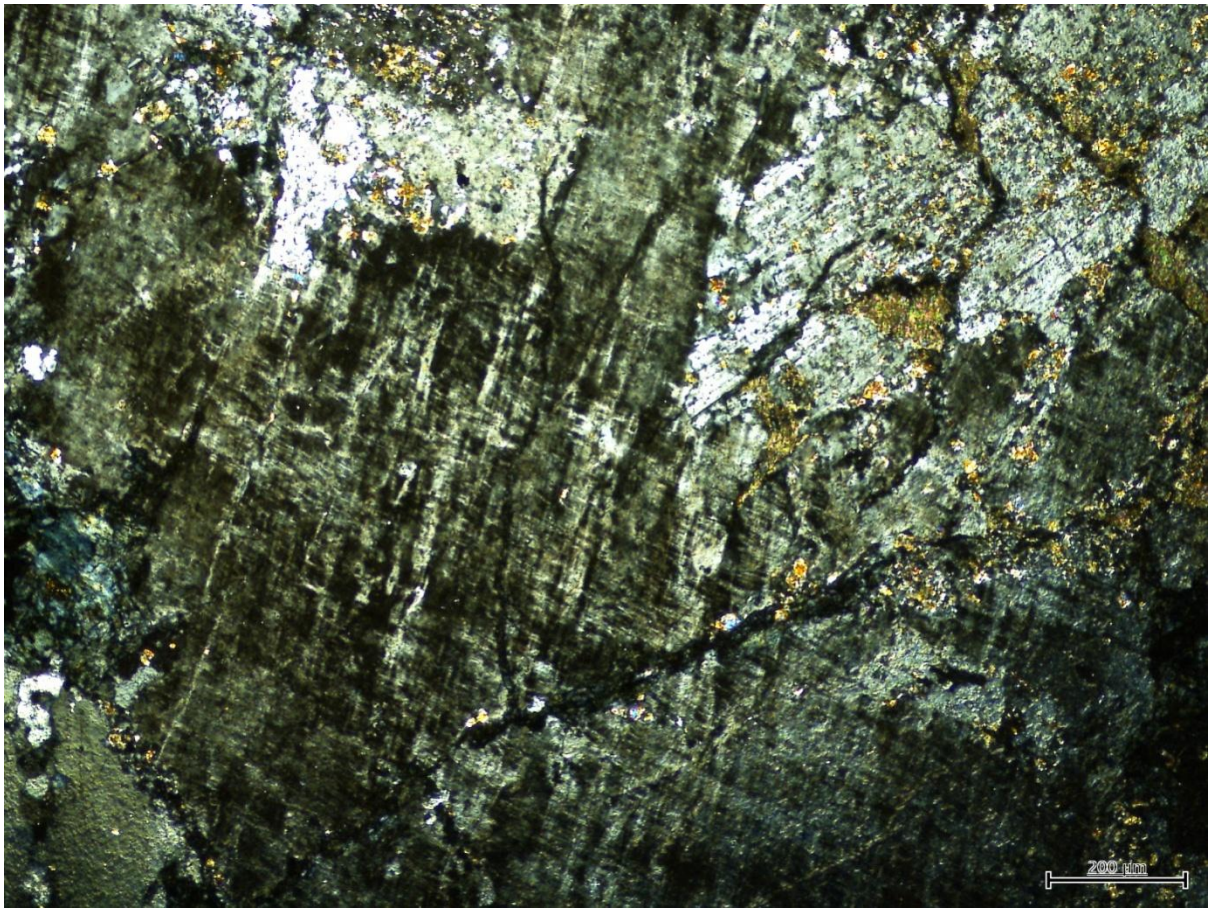

Figure 73: Perthitic texture of k-feldspoar with low birefringence chlorite in fractures